Queen Mary
University of London
Barts and The London
School of Medicine and Dentistry
William Harvey Research Institute

From the bench to the pipeline: testing the immunosuppressive potential of novel therapy targeting Annexin A1

Thesis of

Miss Giuseppa Piras

2014

A thesis submitted to Queen Mary University of London (Barts and the London School of Medicine and Dentistry) in partial fulfilment of the requirements for the degree of Doctor of Philosophy

Centre for Biochemical Pharmacology
William Harvey Research Institute
Queen Mary University of London, Barts and The London School of Medicine and Dentistry

I, Giuseppa Piras, confirm that the research included within this thesis is my own work or that where it has been carried out in collaboration with, or supported by others, that this is duly acknowledged below and my contribution indicated. Previously published material is also acknowledged below.

I attest that I have exercised reasonable care to ensure that the work is original, and does not to the best of my knowledge break any UK law, infringe any third party's copyright or other Intellectual Property Right, or contain any confidential material.

I accept that the College has the right to use plagiarism detection software to check the electronic version of the thesis.

I confirm that this thesis has not been previously submitted for the award of a degree by this or any other university.

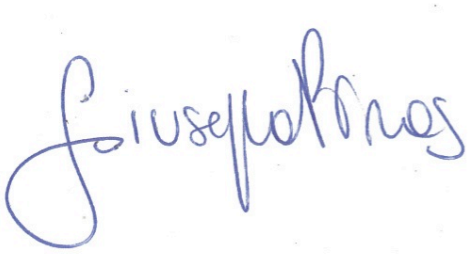

17th of March 2014

Details of collaboration and publications:

Dr Simone Sharma at UCL Genomic facility (http://www.genomics.ucl.ac.uk/) provided the microarray service. The microarray study has been done in collaboration with Dr Masahiro Ono (Department of Infection and Immunity, Institute of Child Health, University College London) who performed the microarray and SPIA analyses. While, behavioural studies were performed in collaboration with Dr Robert Deacon (Department of Experimental Psychology, University of Oxford).

During the PhD, I have been co-author of an original research manuscript, a commentary and a review. I have also published my first-author paper which is only partly included in the results of this thesis.

Acknowledgements

I would like to express my gratitude to the QMUL who sponsored me in these three years and three months. In particular, I am grateful to Dr Fulvio D'Acquisto and Prof. Mauro Perretti who welcomed me in the Department of Biochemical Pharmacology, who supported my scientific research, and who believed in my skills and dedication. I am sincerely thankful for the guidance and lively discussions throughout my PhD work, which had a tremendous impact on both my personal and professional development.

I would also like to thank Dr Eija Jokitalo who inspired me and encouraged my decision to further my scientific carrier with a PhD. A big thanks goes to Dr Lorenza Rattazzi who has been beside me during both the happy and the difficult moments in my professional and personal life. This dissertation would have not been possible without her continuous support. Together with them, I would like to thank all members of the Department of Biochemical Pharmacology, also known as BioPhamily, and in particular Dr Thomas Gobbetti, Dr Donata Federici Canova, Dr Simon McArthur, Dr Suchita Nadkarni, and Dr Ajantha Sinniah for our scientific discussions, useful advice and comments on my research.

I would also like to acknowledge Prof. Roderick Flower for the kind words of encouragement and the interesting scientific conversations during my PhD work.

Last but not least, I would like to thank Maria Popova, Elke Zinniker, Stefania Geraci, Piero Scaturro, Mariangela Tabone, Federico Di Maio, Merja Joensuu and all my friends (including my colleagues already mentioned above) who have been supporting me every step of the way. They have been my source of inspiration and strength throughout my life and I wish to partially dedicate this work to them.

I am grateful to my parents, brothers and close relatives. I dedicate this thesis to them because I would have not been able to achieve all this without their wise advice, continuous support and love.

Abstract

Autoimmune diseases and mood-related disorders are among the major plagues of our modern society, as they impair the normal daily life of patients at both social and physical levels.

Autoimmunity is caused by the loss of immunological tolerance i.e. the inability of immune cells to make a distinction between self and non-self antigens. Intriguingly, patients suffering from autoimmune diseases also show higher rate of "unjustified" mood disorders, such as depression and anxiety. Recent evidence indicates mood disorders as biomarkers for autoimmunity rather than co-morbidities since their occurrence is unrelated to the time of diagnosis of the autoimmune disease or to the degree of disability.

In this thesis I investigated the phenotype of T cell-specific transgenic mice overexpressing Annexin-A1 ($AnxA1^{tg}$): homeostatic immunomodulatory protein with dual opposite functions in the innate and adaptive immune system. Consistent with the previously observed pro-inflammatory role in T cells, $AnxA1^{tg}$ mice showed higher susceptibility to develop autoimmune diseases like multiple sclerosis and systemic lupus erythematosus. Most interestingly, using a battery of behavioural tests, we showed an increased anxious-like behaviour in AnxA1tg mice compared to wild type. This phenotype was associated with a specific gene pattern in the brain and in T cells as shown by microarray analyses. Adoptive transfer of $AnxA1^{tg}$-CD4+ T cells into wild-type mice caused an increased anxiety-like behaviour in the recipient animals thus providing first experimental evidence for emotional dysfunction in autoimmunity-prone animals.

In conclusion, the results of this study provide novel evidences for the strong link between immune system and CNS. More specifically, our findings highlight a novel function of CD4+ T cells as the drivers of mental and physical wellbeing. Future studies will assess the potential of strategies targeting AnxA1 in T cells as new therapeutic tools for the combined treatment for autoimmunity and associated mental disorders.

Table of Contents

List of Figures

Introduction

Materials & Methods

Results

Discussion

List of Tables

Introduction

Materials & Methods

Results

Abbreviations

$^{-/-}$	Knockout
ACTH	Adrenocorticotropin hormone
AICD	Activation induced cell death
AIRE	Autoimmune regulator
AnxA1	Annexin A1
$AnxA1^{tg}$	Transgenic annexin A1
AP-1	Activator protein 1
APC	Antigen presenting cell
APC	Allophycocyanin
BAD	Bcl-2-associated death promoter
BBB	Blood brain barrier
BSA	Bovine serum albumin
CD	Cluster of differentiation
CFA	Complete freund's adjuvant
CIA	Collagen induced arthritis
CNS	Central Nervous System
CRH	Corticotropin releasing hormone
CSF	Cerebrospinal fluid
CTLA-4	Cytotoxic T lymphocyte antigen-4
CXCR5	C-X-C chemokine receptor type 5
DAG	Diacylglycerol
DC	Dendritic cell
DMD	Disease modifying drug
EAE	Experimental autoimmune encephalomyelitis
EDTA	Ethylenediaminetetraacetic acid
ERK	Extracellular *signal*-regulated kinase
FACS	Fluorescence activated cell sorting
FCS	Fetal calf serum
FITC	Fluorescein isothiocyanate
fMLP	N-formyl-methionine-leucine-phenylalanine
Foxp3	Forkhead box P3
FPR	Formyl peptide receptor

FSC	Forward side channel
HPA	Hypothalamic-pituitary-adrenal
GA	Glatiramer acetate
GCs	Glucocorticoids
GM-CSF	Granulocyte-macrophage colony-stimulating factor
hrAnxA1	Human recombinant AnxA1
JAK	Janus kinase
LCK	Lymphocyte specific protein tyrosine kinase
LPS	Lipopolysaccharide
IFNβ	Interferon beta
IFNγ	Interferon gamma
IFNγR	Interferon gamma receptor
IgG	Immunoglobulin G
IL	Interleukin
MAPK	Mitogen-activated protein kinase
MHC	Major Histocompatibility Complex
MFI	Mean Fluorescence Intensity
MOG	Myelin Oligodendrocyte Glycoprotein
MS	Multiple Sclerosis
NFAT	Nuclear factor of activated T cells
NF-κB	Nuclear factor kappa-light-chain-enhancer of activated B cells
PBS	Phosphate buffered Saline
PE	Phycoerythin
PKC	Protein kinase C
PI3K	Phosphoinositide 3-kinase
PLCγ1	Phospholipase C gamma 1
PML	Progressive multifocal leukoencephalopathy
PTX	Pertussis toxin
RA	Rheumatoid arthritis
RORγt	RAR related orphan receptor gamma t
rRIK	Recombinant protein 2610019F03Rik
RSS	Recombination signal sequence

SLE	Systemic lupus erythematous
SSC	Side scatter channel
STAT	Signal transducer and activator of transcription
TCR	T cell receptor
Tfh	Follicular T helper
Th	T helper
TNFα	Tumor necrosis factor alpha
TGFβ	Transforming growth factor beta
Treg	Regulatory T cell
ZY	Zymosan

1. Introduction

1.1 Immune tolerance and autoimmunity

We are healthy if our immune system is healthy. In the course of our lives, when we encounter something that poses a threat to our body, an efficient immune system is able to identify it and eliminate it. The immune cells are the guardians responsible for our defence against foreign insults and they successfully accomplish it by their ability to distinguish body components (self-antigen) and the threats coming from the outside (non-self antigen). Thus, the immune system reacts against non-self components, such as bacteria or viruses, while it ignores our own tissues and organs (1). However, recent studies have also suggested that the immune system is able to react against danger/alarm signals that originate from stressed self-cells (2). The self-non-self discrimination dogma and this more recent danger model are considered the pillars of the sophisticate mechanism by which self-tolerance is established. Through self-tolerance, the immune system prevents the occurrence of inappropriate immune reactions that could potentially cause permanent or deleterious body injuries (3, 4). Break of self-tolerance is thus the leading cause of autoimmunity i.e of an uncontrolled and self-harming reaction against our own tissues and organs.

1.1.1 Self-tolerance of the adaptive immune system

Self-tolerance is pursued in two main forms: central and peripheral tolerance. Central tolerance is established during the development and maturation of immune cells in the primary lymphoid organs. B cells in the bone marrow and T cells in the thymus, respectively, are screened for their ability to discriminate between self and non-self through a receptor-antigen recognition system. In the same way a keyhole matches a

unique key, immune cells expose specific receptors, each of which recognises only one unique antigen (3, 5).

T cell or B cell receptors (TCRs and BCRs, respectively) are generated through similar processes such as somatic gene rearrangement and junctional diversity. TCR and BCR genes exist as separate multiple gene segments called V (for Variable), D (for directional) and J (for junctional). These "segments" are randomly recombined in a single V(D)J sequence in order to have a functional gene. The recombination process is under the control of RAG1/RAG2 proteins whose function is to bind to and cleave a recombination signal sequence (RSS). This introduces double-strand DNA breaks (hairpin structures) in the gene sequences that need to be rearranged. The hairpins are then cleaved and the gene sequences are ligated with the eventual addition of random nucleotides. In this way, several different and new combinations of receptors are created. This is crucial to increase variability in the repertoires of TCRs and BCRs that will be able to recognise a different number of antigens. Considering the continuous and rapid evolutionary changes of pathogens, the high variability of these receptors is beneficial and advantageous for adequate immune protection. However, this can also leads to the formation of potentially self-reactive receptors, which can cause autoimmunity.

The binding of TCR and BCR to their cognate antigen presented in the context of the mayor histocompatibility complex (MHC) molecules is the driving force behind the identification of potential auto-reacting cells. In the case of B cells, the exposure of immature B cells to bone marrow-specific antigens and additional antigens imported by blood circulation in the marrow can lead to B cells apoptosis or to no response

(tolerance). In a similar way, T cells are exposed to a wide variety of self antigens, known to be tissue- and organ-specific (about 3000 genes) – such as insulin – because they are expressed by specialised epithelial cells in the thymus (4).

Upon exposure to self-antigens, T cells undergo two main selection steps named positive and negative selection. The first occurs in the cortex of the thymus and allows T cells that are able to recognise self-antigen-MHC complexes to proceed to maturation, while T cells unable to recognise self-antigen-MHC complexes are deleted by neglect-induced death (3, 6-8). Negative selection occurs in the inner part of the thymus – the medulla. Notoriously, T cells require two signals to be activated and to react; signal one is triggered by the binding of TCRs and antigen-MHC complexes, while signal two is mediated by the binding of CD28 co-receptors to costimulatory molecules. Thus, positively selected T cells are newly exposed to self-antigens and to costimulatory molecules. Those that bind to self-antigens and costimulatory molecules with high affinity are eliminated by apoptosis, while the rest continue maturation and differentiation into either CD4+ or CD8+ T cells. Negative selection is also known as clonal deletion and it is fundamental to ensure the formation of self-tolerant T cells (3, 6, 7, 9). Along clonal deletion, immune tolerance is pursued by clonal diversion. In this case, self-reactive clones are reprogrammed and differentiate in regulatory T cells (Tregs), which are able to suppress auto-reactive T cells (7, 10).

Central tolerance is not able to eliminate all the possible auto-reactive cells. Among the mature immune cells, there are a variable number of auto-reactive cells which are not exposed to their self-antigens in the central lymphoid organ. These cells only

encounter their self-antigens in secondary lymphoid organs. Thus, humans have developed peripheral tolerance mechanisms to peripherally repress potential dangerous immune cells. For instance, peripheral tolerance is maintained by anergy or peripheral deletion of auto-reactive T cells (7, 11). The former is a long-term unresponsiveness state of T cells caused by the activation of TCR in the absence of signal two (12). The latter is a programmed cell death (apoptosis) that can be induced by Fas-death receptor signalling (13). Other possible mechanisms of tolerance induction include the TCR/co-receptor down-regulation (14), immune deviation (15) or secretion of immuno-regulatory cytokines such as IL-10 or TGFβ (16).

In certain conditions, however, immune tolerance towards self-components dramatically fails causing aberrant immune responses, collectively referred to as autoimmunity. The action of autoantibodies and self-reactive T cells against self-components causes a state of chronic inflammation and permanent damage that are features of several autoimmune diseases.

The failure of immune tolerance has no clear origins. Multiple factors seem to contribute to the development of autoimmune diseases. These include genetic, hormones, diet, chemical and/ or exposure to infections (17). Systemic inflammatory conditions show strong associations between autoimmune diseases and specific MHC genes (18). Another example in human is the severe autoimmune polyendocrine syndrome which is caused by aberrations of a single gene, **A**uto**I**mmune **RE**gulator (**AIRE**) gene (19). Genetic susceptibility is not always sufficient to explain the occurrence of autoimmune disorders. The higher prevalence of autoimmune diseases in developed countries suggests a strong influence of

environmental risk factors. Exposure to metal, ultraviolet and infectious agents has been linked to various autoimmune conditions. For example, the Epstein-Barr viral infection might contribute to multiple sclerosis (20, 21) and group A streptococcus can trigger rheumatic heart disease (22). The exact mechanism by which an infection induces a specific autoimmune disease is unknown. It has been proposed that microbial antigens might resemble self-antigen structures and because of this, induce a cross-reactive immune response – a hypothesis referred to as molecular mimicry (23). Increased salt (sodium chloride) concentration has been shown to boost the induction of pathogenic T cells (24); ultraviolet exposure, in contrast, has been identified as a positive factor that prevents from the development of autoimmune diseases (25).

1.1.2 Autoimmune diseases

Autoimmune diseases affect about 3-8% of the world's population. The female/male ratio shows that women are most affected (26). To define a disease as an autoimmune disease, we use direct, indirect and circumstantial evidences. The direct evidence is the transmissibility of the disease by transferring of antibodies or T cells. The indirect evidence is based on the possibility to reproduce the disease in animal models. If direct or indirect evidence is not available, the presence of typical markers, such as high serum level of IgG autoantibodies or infiltration of immune cells in the affected organ or tissue, provides circumstantial evidence. Moreover, family history of the same autoimmune disease or multiple autoimmune diseases in the same patient are also helpful criteria used for the diagnosis of autoimmune disease (27).

Among the autoimmune diseases, we can pedagogically distinguish localized and systemic diseases (3). Multiple sclerosis (MS) and type 1 diabetes are, for example, classified as localized autoimmune diseases since they are restricted to a specific tissue or organ. Diseases like systemic lupus erythematous (SLE) and rheumatoid arthritis (RA), on other hand, are systemic diseases because the autoantibodies can cause multiple organ impairment (3).

A list of the most common autoimmune diseases and their associated self-antigen is reported in the Table 1.1 below.

Table 1.1: Autoimmune diseases

DISEASE	AUTO-ANTIGEN	CONSEQUENCES
Type 1 diabetes mellitus	Insulin	Destruction of pancreatic β cells.
Rheumatoid arthritis	Unknown synovial joint proteins	Joint inflammation and destruction.
Multiple Sclerosis	Myelin associated proteins	Brain inflammation and demyelination.
Graves' disease	Thyroid-stimulating hormone receptor	Hyperthyroidism.
Hashimoto's thyroiditis	Thyroid peroxidase	Hypothyroidism.
Myasthenia gravis	Nicotine acetylcholine receptor	Neuromuscular impairments.
Systemic lupus erythematosus	DNA, histones, ribosomes, protein of the spliceosome complex	Glomerulonephritis, vasculitis, rush.

Sometimes these diseases can be silent for a long period of time before presenting general and/or specific symptoms. Most of them cause fatigue, fever and general ill feeling, such as body pain, muscle weakness, insomnia, loss of appetite, variation of weight and/or loss of coordination. Patients suffering from autoimmune diseases are likely to present psychiatric disorders including depression, anxiety, obsession,

irritability and hallucinations (28). Indeed, autoimmune patients have the highest chances of developing schizophrenia with autoimmune hepatitis being at the highest risk and rheumatoid arthritis at the lowest.

Many studies have shown that patients affected by autoimmune diseases have higher probability to develop other forms of autoimmunity in their lifespan. An example is the case of a 30-year-old woman suffering from myasthenia gravis and hypothyroidism (29). After her thymus was surgically removed, first she developed RA and later SLE (29). The manifestation of two or more autoimmune diseases in the same patient occurs with a rate greater than expected by chance (30). Thus, among patients affected by type 1 diabetes, RA and autoimmune thyroiditis have higher prevalence (31). The coexistence of several autoimmune diseases in the same patient (polyautoimmunity) is referred to as a kaleidoscope of autoimmunity (32). Polyautoimmunity suggests the existence of shared pathological mechanisms among autoimmune diseases and the possibility to have a single therapeutic approach for at least those conditions that are strongly associated with each other. It should be noted that not all autoimmune diseases are positively correlated. For instance, RA and MS seem to have an inverse correlation (30).

1.1.2.1 Therapeutic approaches to autoimmune diseases

The therapeutic treatments of autoimmune diseases are often directed at relieving the symptoms, considering surgical interventions in extreme cases (33). Other approaches aim to help patients by administering either lacking vital products or nutrients that have been affected by the impairment of target organs such as insulin

in the case of type 1 diabetes (34) or vitamin B12 for SLE (28, 35). Anti-inflammatory drugs such as aspirin or glucocorticoids are used to reduce inflammation and pain associated with autoimmunity (36). However, these therapeutic approaches address only the symptoms instead of removing the causes of the disease. For this purpose, immunosuppressive and disease-modifying drugs are employed.

Immunosuppressive drugs reduce the activation and efficacy of the immune system (37). However, their use needs to be limited because they cause several side effects and make the patient more vulnerable to opportunistic infectious (38). A list of the most commonly used immunosuppressive drugs, their mechanisms of action and toxicity are reported in Table 1.2.

Table 1.2: Immunosuppressive drugs

DRUG	ACTION	MAJOR TOXICITY
Cyclophosphamide	Intercalates DNA interfering with cell proliferation	Leukopenia, myeloproliferative disorders, infertility.
Azathioprine	Interferes with purine nucleotide synthesis	Leukopenia, pancreatite, hepatotoxicity.
Mycophenolato	Interferes with de novo guanosine nucleotide synthesis	Gastrointesinal bleeding, lymphopenia, infectious.
Cladribine	Interferes with purine synthesis	Lymphopenia.
Cyclosporine and Tacrolimus	Inhibits calcineurin-mediated production of IL-2 and clonal expansion of T helper cells	Nephrotoxicity, hypertension.

Disease-modifying drugs (DMD) alter the course of disease as well as improve symptoms (37). These drugs are immune modulators that interfere with the pathogenic mechanisms underlying autoimmune diseases. They are also called biologics. Among them there are monoclonal antibodies which have achieved

resounding success in the treatment of RA and MS (39, 40). Their mechanisms of action differ depending on the molecular target. For instance, Rituximab binds to the CD20 antigen on the surface of mature B cells causing their depletion (41). Instead, Natalizumab targets the alpha-4 subunit of integrins on the surface of lymphocytes. This prevents the adhesion of lymphocytes to the vascular walls and their migration from the blood stream into target tissues (42, 43).

Other biologics exert their immune modulating effects by redistributing lymphocytes from the circulation to the secondary lymphoid organs (Fingolimod) (44), preventing T cell costimulation (Abatacept) (45) or interfering with TNF activity (Etanercept) (46). Finally, there are biologics which are used for their known therapeutic effect in autoimmune diseases, although their mechanisms of action are only partially known (47).

Glatiramer acetate (GA), for instance, is a random synthetic polymer of 4 specific amino acids (**G**lutamic acid, **L**ysine, **A**lanine and **T**yrosine) that are naturally present in the myelin basic protein. Despite its wide use and its beneficial effects in MS patients, its mechanism of action has not been fully understood yet (48). Indeed, it has been proposed that GA might interfere with T cell differentiation promoting the formation of anti-inflammatory T helper 2 (Th2) and reducing the pro-inflamamtory Th1 (46). GA might also exert direct neuroprotective effects through the induction *in situ* of neurotrophic factors such as BDNF (48).

Treatments based on biologics have several advantages including high tolerability by the patients and greater selectivity for the target (47). However, they are rarely

curative and are burdened by serious side effects (38). The most adverse side effect is progressive multifocal leukoencephalopathy (PML) (49), which is a viral infection of the brain. Other common side effects include serious infections, headaches, fever, fatigue, bradycardia and paradoxically autoimmunity (38).

A list of the most used DMDs, their action and toxicity is provided below in Table 1.3.

Table 1.3: Biologic drugs

DRUG	DISEASES	ACTION AND PROPOSED MECHANISM	SIDE EFFECTS
Natalizumab	MS, Crohn's disease	Prevents transmigration of lymphocytes: Binds to and blocks α4 integrins exposed on leucocytes	PML, opportunistic infectious, fatigue, hypersensitivity
Rituximab	RA, MS, SLE	Deletion of B cells: binds to CD20 on mature B cells	PML, opportunistic infectious.
Etanercept	RA, psoriasis, ankylosing spondylitis	Neutralize TNF activity: binds soluble and transmembrane TNF and inhibits binding to TNFRs	Serious bacterial and fungal infectious, tuberculosis, malignancies.
Fingolimod	MS, SLE, psoriasis	Lymphatic sequestration of lymphocytes: modulator of sphingosine 1-phosphate receptor	Bradycardia, infectious, macular edema, shingles, skin cancer
Belimumab	SLE, RA	Inhibits BAFF	Severe infectious, hypersensitivity.
Leflunomide (Teriflunomide)	RA, MS	Inhibits de novo pyrimidine synthesis (inhibitor of the DHODH); inhibitor of Jak1 and Jak3	PML, nausea, oral ulcers, alopecia, increased of liver enzymes, infections
Glatiramer Acetate	MS	Induce Th2 and regulatory T cells	Anxiety, rapid heartbeats, tightness in the throat, chest pain, hypersensitivity

TNFRs: TNF receptors; BAFF: B-cell activator factor; DHODH: Dihydroorotate dehydrogenase.

1.1.2.2 Psychiatric health and autoimmune diseases

Patients affected by autoimmune diseases frequently develop psychotic disturbances (28). To some extents, the same correlation has been found in the reverse scenario: people affected by psychotic disorders often show immune imbalance and abnormalities (50, 51). The most common neuropsychiatric symptoms found in autoimmune patients are depression, anxiety and mood disorders. Depression and anxiety have high lifetime prevalence in MS, around 79% and 40% respectively, followed by scleroderma (another chronic multisystem disorder) and SLE (28). Suicide risk reaches 28.6% prevalence in MS (28). This raises questions such as whether the coexistence of psychotic symptoms and autoimmune diseases results from a cause-effect relationship. Epidemiological study of the nature of their comorbidity shows that suicidal intents as well as depression and anxiety do not correlate to the degree of physical disabilities (52). It has also been documented that depression and other psychotic symptoms, such as bipolar disorder, affect patients even before the diagnosis is made and before the development of physical signs of autoimmunity (53), i.e. in one sixth of the cases of MS associated depression is diagnosed prior to the MS diagnosis (54). MS patients have higher prevalence of anxiety or depression compared to patients suffering from other unrelated diseases or healthy controls (55).

Hence, the higher prevalence of depression or anxiety in patients affected by autoimmune diseases might be not only a psychological consequence of general malaise or physical impairments caused by autoimmune reactions. New hypotheses are investigated with the intent to explain such association. Among those, some suggest that mental disorders are a reflection of direct effects of cytokines on the

central nervous system. Others suggest that mental disorders and autoimmune diseases share common pathological pathways or, simply, that mental disorders predispose to the development of chronic physical illness (56).

1.1.2.3 Multiple sclerosis and its experimental models

Multiple Sclerosis (MS) is a neurodegenerative disorder that affects the central nervous system (CNS) and it is a major cause of non-traumatic disability in young adult. Around 2,500,000 people in the world are estimated to suffer from MS, with a prevalence of 1 in 600 in the UK, about 100,000 cases.

MS is characterized by lesions of the white matter in the CNS, often referred to as plaques. These are the result of an inflammatory reaction that causes the degradation of myelin, the fatty sheath of the neuronal axons. The process is known as demyelination and is responsible for the impaired transmission of the electrical signals across the axons. This causes several unpredictable disabilities, including optic neuritis, ataxia, muscle weakness, speech problem, and bowel and sexual dysfunctions.

MS is diagnosed when the first neurological attack lasts for 24 hours and it is followed by subsequent attacks which occur at least 30 days after the previous attack in order to be considered separate events. However, patients manifest different disease courses. About 85% of the patients initially present a relapsing-remitting disease form, in which clearly defined, repeated attack are followed by remissions. Approximately 50% of this might transit into a secondary progressive form in which neurological deficits cumulate without relapse. About 15% of the patients develop a

primary progressive course in which the disease worsens progressively without remission (57).

The current understanding of the pathogenesis of MS comes from direct studies of MS patient lesions, as well as from investigation performed on animal models of encephalomyelitis. EAE (experimental autoimmune encephalomyelitis) is generally accepted as the model that better shares the clinical and pathological features of MS (58). It models the MS disease pattern, i.e. relapses/remissions, as well as its manifestations such as paralysis, ataxia and visual impairment. Both MS and EAE share MHC-linked susceptibility, T cells and antibodies reactive to myelin, demyelination and axonal dystrophy. In addition, studies performed with this model have allowed for the discovery of several effective therapeutics including GA and interferon-β (IFNβ) (59, 60).

T cells play a key role in the development of EAE (61) as it has been shown by the induction of the disease following transfer of purified, activated myelin-specific $CD4^+$ T cells into healthy syngenic animals (62) as well as by the isolation of auto-aggressive T lymphocytes in naïve rats (63). Less clear is the contribution of CD8+ T cells. However, a recent study has shown that CD4+, but not CD8+ T cells are the inducer of the diseases (64).

The EAE can be induced in a wide range of species by immunization with CNS white matter protein (either self or non-self) called encephalitogen. These include myelin basic protein (MBP), proteolipid protein (PLP), myelin oligodendrocyte glycoprotein (MOG), or their peptides ($PLP_{139-151}$ and MOG_{35-55}). Each

encephalitogen and animal species offers different advantages. Rodent models in particular allow for the study of genetically homogeneous population, which reduces disease variability and increases reproducibility. However, the severity of the disease is greatly dependent on the MHC haplotype, the encephalitogen's amino acid sequence and the immunization protocol (58).

Among the murine models, the most commonly used strains are:

- SJL/J (MHC haplotype: H-2(s)). Immunization of these mice with $PLP_{139-151}$ causes the development of an acute EAE, similar to a single relapsing event in MS patients (65);
- Biozzi (H-2dq1) AB/H. Immunization of these mice with spinal cord homogenate or MOG induces a chronic relapsing/remitting EAE that resembles the relapsing/remitting MS in humans (66);
- NOD (H-2(g7)). Immunized mice with MOG_{35-55} display a relapsing/remitting EAE that is followed by a chronic non-remitting phase, resembling a secondary progressive course of MS;
- C57BL/6 (H-2(b)). Immunization of these mice with MOG_{35-55} leads to the development of chronic progressive EAE, which can be a model for the primary progressive MS in human (67).
- 2D2 Mice. TcR transgenic model of MOG-driven EAE on C57BL/6 background. These mice have clonally homogenous MOG-specific CD4 T cells, which make them prone to develop EAE with a suboptimal dose of MOG_{35-55} and around 4% of 2D2 mice develop spontaneous EAE.
- 1C6 Mice. TcR transgenic model of MOG-driven EAE on NOD background. These mice have clonally homogenous MOG-specific CD4 and CD8 T cells.

In all these models, a correlation between behavioural changes and the development of EAE has been described. For instance, Pollak and colleagues showed that the EAE induced in mice is accompanied by sickness behaviour that resembles the symptoms of depression. Indeed, in these mice autoimmunity was associated with anhedonia, social disinterest and cognitive impairment typical of depressive episodes (68, 69). EAE mice also display anxiety-like behaviour measured, for instance, by the reduction of exploratory activity (70). This is clearly observed even before the onset of motor dysfunction (71), therefore both sickness behaviour and anxiety-like behaviour do not correlate temporally to the muscle weakness and are the consequences of independent causes. The hypoactivity of the serotonergic system, the hyper-activation of the hypothalamic-pituitary-adrenal (HPA) axis (72) or the increase of cytokines such as IL1β or TNFα in the CNS, in particular in the striatum and hippocampus, have been described as possible biological alterations responsible for these observations. However, we have recently shown that the migration of T cells into the blood after immunisation is associated with the rise of mood changes in the early stage of the EAE. This would suggest the circulation of effector T cells also has an effect on the induction of anxiety-like behaviour (73).

Although the EAE shows clinical and genetic features of MS, there are serious limitations to its use in translational studies. For instance, several successful therapies for EAE, such as treatment with anti-TNFα, have been proven to worsen the clinical conditions of MS patients (74). However, EAE remains a valid instrument to dissect the pathogenesis of MS and to give insights into the role of T cells in autoimmunity.

1.2 T cells and their role in autoimmunity

T cells are fundamental players in the adaptive immune system. They are responsible for the host defence against a number of pathogens including bacteria, viruses and parasites. As discussed in Section 1.1 Immune tolerance and autoimmunity, immune homeostasis is the result of the balance between the various mechanisms that control immune tolerance and potentially autoreactive T cells (7, 75). In fact, autoreactive T cells can be considered one of the main therapeutic targets for the treatment of several autoimmune diseases.

Next paragraphs provide a brief overview of the life cycle of a T cell, naïve T cell activation, T helper cell differentiation and their plasticity, as well as a description of the main T cell phenotypes associated with autoimmune diseases.

1.2.1 Life cycle of a T cell

The T cell repertoire develops in the thymus, from where functional T cells born α/β or γ/δ TCR are selected and survive. The T cell precursor starts the maturation as a double negative (DN) T cell, which expresses neither CD4 nor CD8. During the maturation, first the functional rearrangement of the β chain and later pre-α/β TCR promote the development of DN to double positive (DP; CD4+ CD8+) T cells (76). Both DN and DP are heterogeneous populations, in which several cell subsets are distinguished according to the expression of cell surface markers. Each cell subset is considered to be a distinct developmental step that a T cell undertakes to mature.

DN T cells are subdivided into at least 4 different subtypes called DN1, DN2, DN3 and DN4. The maturation of DN T cells occurs in 4 stages, from DN1 to DN4, during which CD44+ CD25- DN T cells progressively decrease CD44 and increase CD25 expression. The β selection, i.e. the rearrangement of a functional VDJ TCRβ, occurs during DN1 and DN2 and it is critical for the passage from DN3 to DN4 (77). At this stage, RAG1/2 proteins play a key role in T cell development (see section 1.1.1 Self tolerance of the adaptive immune system) and defective Rag gene expression arrest T cells at DN3 (78). The formation of a functional pre-α/β TCR is critical for the further proliferation and differentiation step that brings CD44- CD25+ DN4 T cells to CD44- CD25- CD3+ DP T cells (77). In 6-8 cell divisions, DP T cells generate the mature α/β TCR which drives the clone selection and lineage commitment (77, 78).

Positive and negative selection allows for the survival and maturation of α/β TCR clones that bind to MHC molecules with low avidity and do not recognise, with some exceptions, self-antigens. Positive selected DP T cells progressively increase the expression of CD69 and CD5, which continue to be highly expressed until the DP T cells become single positive (SP; CD4+ or CD8+) T cells (79, 80). The passage from DP T cells to CD4 or CD8 lineage has been explained using different models of lineage commitment. The *stochastic/selection model* suggests that DP T cells randomly commit to a lineage at the start of the positive selection (78, 81). In contrast, the *instructive model* proposes that the co-engagement of TCR and CD4 or CD8 co-receptor determine specific intracellular signals that influence the progression towards one or the other lineage (78, 81). Engagement of one co-receptor induces transcriptional silencing and thus the progressive loss of the other

co-receptor. A third model, called the *instructive/default model*, suggests that DP T cells are by default committed to the CD4 lineage and can be diverted from their fate by the MHC-class I instructive signal, which commits cells to the CD8 lineage (78, 81). The most recent lineage commitment model is the *strength of signal model*. This suggests that the intensity or duration of signalling direct the development into CD4 or CD8 lineage. In particular, short or weak signal generate CD8 SP T cells, whereas long or intense signal produce CD4 SP T cells (78, 81, 82).

CD4 or CD8 SP T cells populate the lymphoid organs. Upon recognition of the specific antigen, they activate, proliferate and differentiate in different effector T cells. Upon antigen clearance, the expanded T cell population is reduced and rescued as memory T cells (83). In humans and mice, two major memory-T cell subsets have been described: central memory and effector memory T cells, T_{CM} and T_{EM} respectively. T_{CM} constitutively express CCR7 and CD62L, fundamental receptors for the homing into secondary lymphoid organs, which are also typical markers of naïve T cells. They show little effector function, but rapidly proliferate and differentiate to effector cells after antigenic stimulation. T_{EM} express typical receptors for the homing in inflamed tissues where they show rapid effector function (84). Memory T cells ideally can survive for a lifetime. However, their number is limited by a virtual immunologic space in the body where T cells have access to and yet must share limited survival resources such as homeostatic cytokines (83).

1.2.2 Naïve T cells and their activation

Naïve T cells are normally quiescent and low-proliferating cells. To become fully activated they need three different signals (3).

Signal 1 is triggered by the recognition of the antigen-MHC complexes by the TCRs and its co-receptors. Antigen presentation occurs via two main classes of MHC, which are called class I and class II. MHC class I molecules are widely expressed in our body and present mainly cytosolic antigens, while MHC class II molecules are mainly expressed on antigen-presenting cells (APC) and present antigens processed through endocytic pathway (85). The recognition of MHC class I or II is mediated by the CD8 and CD4 co-receptors, respectively (78).

Signal 2 is provided by the binding of costimulatory receptors to costimulatory proteins expressed on APCs. There are several kinds of costimulatory receptors; some induce the T cell activation, such as CD28, whereas others elicit inhibitory signals, such as CTLA-4 (86). CD28-mediated signal 2 integrates signal 1 and it is non-redundantly required for the activation and clonal expansion of T cells; in the absence of CD28 co-stimulation, T cell anergy is observed (87).

Signal 3 is mediated by a variety of cytokines and soluble mediators secreted by APC(s) and the surrounding tissues. These skew T cell differentiation towards a specific phenotype and are important modulators of T cell plasticity. This will be discussed in more details in section 1.2.3.

Once naïve T cells have received all the information for their activation, a complex cascade of intracellular signalling events occurs (88). In summary, engagement of TCR and its co-receptors allows for their clustering followed by activation of the lymphocyte-specific protein tyrosine kinase (Lck), phospholipase C gamma 1 (PLCγ1) and phosphoinositide 3-kinase (PI3K). These signalling pathways generate secondary cell messengers such as diacylglycerol (DAG) and calcium. The former activates mitogen-activated protein kinase (MAPK) pathways and protein kinase C (PKC), upstream the activation of transcription factors such as NF-κB and AP-1. The release of intracellular calcium from the endoplasmic storages induces the activation of calcineurin which in turn activates the transcription factor NFAT. All together NF-κB, AP-1 and NFAT control T cell proliferation, death and differentiation.

The binding of CD28 to costimulatory B7 molecules activates phosphatidylinositol 3 kinase (PI3K)-AKT pathway activating NF-κB and PKC signalling (89). The PI3K-AKT pathway promotes the production of IL-2, expression of IL-2R and cell-cycle progression leading to the survival of T cells (87). Signal 2 has synergic effect to signal 1, thus favouring the setting of the biological threshold for T cell activation. Indeed, TCR signal is strictly dependent on the quality and quantity of T cell-APC interactions (90). Signal 2 is able to potentiate the strength of the TCR signal and influence the potency of the signalling, which is then responsible for quality and magnitude of the T cell response (91).

1.2.3 T helper cells and their differentiation

T helper (Th) cells are CD4+ T cells that recognise bacterial and parasitic antigens presented by MHC class II molecules on the surface of APCs, including macrophages and dendritic cells. Once naïve Th cells recognise the antigen-MHC complexes and receive all the activating signals, they go through clonal expansion and differentiation in effector T cells. Clonally expanded T cells then undergo through clonal contraction and remain as memory Th cells (83). Activated Th cells communicate with a variety of immune cells, such as macrophages and B cells (hence the name "helper cells"), providing instructions for the elimination of the pathogen.

Various effector Th cells exist in our immune system. They contribute to different immune responses through the secretion of specific cytokines, which are used to distinguish and describe each Th subtype. The profile of cytokines associated with each Th subset reflects the activation of different intracellular pathways and relative transcription factors. Table 1.4 summarizes these different features.

Th1 cells express the transcription factor T-bet and release IFNγ; they fight mainly intracellular pathogens. Th2 cells, instead, express GATA-3 and produce IL-4, IL-5, IL-13, which give protection mainly against extracellular parasites (92). Th17 cells express the transcription factor RORγt and high level of IL-17, IL-22, IL-21 and IL-23R. These cytokines are important for the defence against extracellular pathogens and fungi in specialised tissues like skin and gut (93). More recently, Th9, Th22 and Tfh cells have been described. The first two are named after the main cytokine they produce- IL-9 and IL-22- while the latter mostly release IL-6. Similarly to Th2, Th9

cells protect from parasites (94), while Th22 cells are implicated in the defence against microbes in the skin (95). Tfh cells steadily reside in the germinal centres of secondary lymphoid organs due to the continuous expression of the B cell follicle homing receptor CXCR5 and, in turn, regulate antigen-specific B cell activation (96). ThGM-CSF cells have been recently added to the list; they have been identified as T cells expressing RORγt and GM-CSF with crucial pathogenic action in autoimmune neuroinflammation (97).

All effector responses incited by Th cell subtypes can be "tamed" by Treg cells. These subtypes of T cells are generated during T cell development (these are known as naturally occurring Treg) or can be induced in the periphery by exposure of naïve T cell to TGFβ (called induced Treg). In both cases, Treg cells are characterized by the expression of Foxp3 and by the production of anti-inflammatory cytokines such as TGFβ and IL-10 (98).

Table 1.4: Proprieties of T cell helper lineages

	Cytokine(s) signature	Master Regulator	STAT Regulator
Th1	IFNγ	T-bet	STAT1; STAT4
Th2	IL-4; IL-5; IL-13	Gata-3	STAT6
Th9	Il-9	-	-
Th17	IL-17; IL-21; IL-22	RORγt	STAT3
Th22	IL-22	AHR	-
Tfh	IL-6	BCL6	STAT3
Treg	TGFβ	Foxp3	STAT5

As mentioned earlier, the differentiation of naïve CD4+ T cells in one or another subset is determined by quantity and type of antigen (avidity for TCR binding) as well as by specific cytokines that are present in the cell surrounding (Figure 1.1). For example, low-affinity binding between antigen and TCR skews towards Th2 phenotype (91). IFNγ and IL-12 strongly guide the differentiation towards Th1 phenotype, while IL-4 leads to the Th2. TGFβ induces the differentiation of Treg, but the combination of TGFβ and IL-6 skews the differentiation towards Th17 cell type (99).

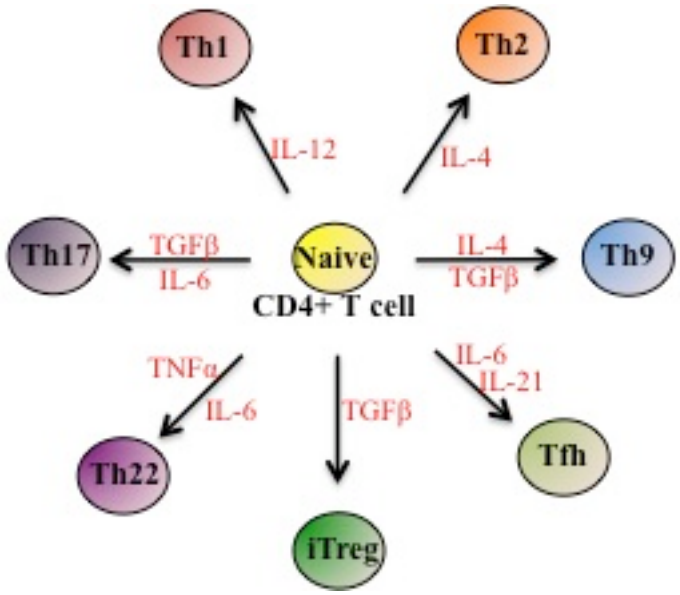

Figure 1.1. Phenotype of CD4+ Th cells. Naïve CD4 T cells can differentiate in several phenotypes depending on the cytokines released in the milieu.

Cytokines transduce their signalling through JAK/STAT pathway (100). STAT proteins are transcription factors that translocate into the nucleus upon homodimerisation and phosphorylation by JAK. There are 7 different STAT proteins which have non-redundant functions in the Th differentiation. STAT1 and STAT4

are required for Th1 cell differentiation, whereas STAT6, STAT3 and STAT5a/b are required for Th2, Th17 and Treg cell differentiation, respectively (see Table 4) (101).

STAT activation regulates gene transcription directly by binding gene promoters and indirectly through epigenetic modifications of the chromatin (102, 103). The latter leads to a variation in chromatin condensation which determines the accessibility of transcription factors to gene regulatory sequences. In this way, epigenetic modifications strongly influence expression and/or repression of specific cytokine loci and thus, the stability of Th phenotypes. For instance, the IFNγ promoter is accessible for the transcription in Th1 cells, while the IL-17 promoter is not. Conversely, the IFNγ promoter show repressive genetic marks in Th17 cells, while the IL-17 promoter becomes accessible to the transcription (102). Thus, cytokines that promote a particular T cell phenotype also influence negatively the differentiation by silencing key factors regulating the others. Another example is the ability of IL-12 to induce the expression of T-bet and the silencing of GATA-3 favouring the skewing towards Th1 phenotype or the capacity of IL-4 to exert the opposite effect thus favouring the development of Th2 cells (92). Hence, the differentiation towards a particular Th subset antagonizes the development of the others.

For many years Th differentiation was considered a terminal commitment to a specific Th lineage. However, recent studies on T cell polarization and on cell-fate mapping have revealed that Th cells show several degrees of flexibility in expressing Th-specific transcription factors in response to extracellular stimuli (99, 104, 105). For instance, signalling through IL-12R induces destabilization of both Th17 and

Th2 subsets, both of which then assume Th1 features, i.e. expression of T-bet and production of IFNγ (106, 107). The conversion of Th17 cells in Th1 has been observed in several animal models of experimental autoimmunity (105, 108). The switching from one T cell phenotype to another has often been detected at the site of chronic inflammation and correlated with the manifestation of signs of disease (105, 109). This is consistent with the previously mentioned concept that it is mainly the local tissue milieu (i.e. signal 3 factors) that dictates the specific effector function of Th cells.

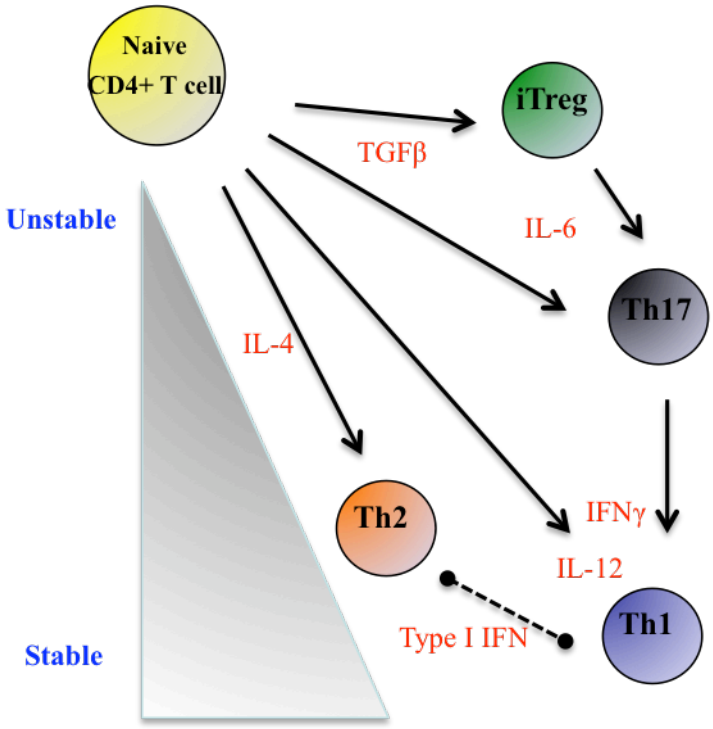

Figure 1.2. Transitions of CD4+ T phenotypes. A hierarchy of stability has been suggested to explain experimental observations of Th phenotype transitions. Naïve CD4+ T cells are placed in higher unstable state followed by iTreg and Th17 cells. Th1 and Th2 cells are considered stable, although a switch from Th2 to Th1/Th2 hybrid phenotype has been shown.

As electrons decay from high energy levels to low energy levels, **$CD4^+$ T cell plasticity** has been defined as a cell transition from an unstable T cell subtype to a more stable phenotype (96) (Figure 1.2). The stability of a specific Th-phenotype has been explored through genome-wide studies of epigenetic modifications i.e. DNA methylation sites which are known to be permissive or recessive marks for gene transcription. These studies showed that some genomic regions present both activating and repressive epigenetic marks (bivalent modifications), which predispose to either the expression or the silencing of that particular region (110). For instance, Th17 cells present bivalent modifications in both T-bet and GATA3 loci. Hence they are preconditioned cells that can be reprogrammed into Th1 or Th2 subtype (111). Thus, Th17 cells are considered an unstable Th subtype. Conversely, Th1 and Th2 cells are classified as stable subtypes since transitions from these phenotypes to Th17 are not observed (96). This finding correlates with the only presence of repressive epigenetic configuration found in IL-17 and RORγ genes in both Th1 and Th2 cells (111).

1.2.4 T helper cells and autoimmune diseases

Dys-regulation of T cell self-tolerance leads to a number of problems including autoimmune diseases. Although we can only speculate on the cause(s) of the breach of immune tolerance, we do know that Th cells have a key role in the pathogenesis of these disorders. One of the main matters of debate currently discussed is whether a single subtype of effector Th has predominant role in the diseases or combination of factors and Th phenotypes contribute to these.

For a long time, Th1 cells and its signature cytokine IFNγ were considered the main pathogenic driving factors of organ-specific autoimmune diseases. IFNγ and other Th1 cytokines are detected at the sites of inflammation in both patients and animal models; for examples, IFNγ is abundant in MS lesions as well as in EAE (112, 113). Furthermore, T-bet and STAT4 knockout animals are protected from developing signs of diseases such as in model of diabetes, EAE or experimental arthritis (CIA) (114-117). However, the incidence and severity of these autoimmune diseases either do not vary or may even increase as reported in animals deficient in IFNγ, IFNγR or STAT1 (114, 118, 119).

This led to the identification of Th17 lineage as an alternative key T cell subset in autoimmunity. Indeed, Th17 cells and IL-17 have been detected in various autoimmune diseases including MS, RA and psoriasis (113, 120). Studies on mice deficient in the IL-23p19 or IL-12p40 indicated that IL-23 is critical in Th17 cell-driven autoimmune response. In this instance, the absence of the IL-23 signal correlates with a reduced number of IL-17-producing Th cells leading, functionally, to a degree of resistance in the development of EAE and CIA models (121).

Conversely, mice knocked out in IL-17 do not show the same resistance proprieties and develop these autoimmune responses (122, 123). Thus, the attention has been recently focused on the IL-23/IL-23R signalling pathway, its downstream signals – both non genomic and genomic – and on how this influences the development of the diseases.

Among the IL-23-induced molecules in Th17 cells, GM-CSF has been shown to be highly pathogenic. In contrast to IFNγ or IL-17 knockout mice, mice knocked out for GM-CSF do not develop EAE and CIA, suggesting the existence of a new pathogenic Th phenotype: ThGM-CSF (97, 124, 125). Neutralizing antibodies against GM-CSF have proven clinical efficacy in RA patients, while this needs to be tested in patients suffering from MS (126).

Studies on Th17 skewing have shown that depending on the polarising conditions, IL-17-producing Th cells can be pathogenic or non-pathogenic upon adoptive transfer. These two Th17 populations differ in the expression of several molecules including key cytokines and transcription factors. For instance, Th17 cells induced by TGFβ3 and IL-6 are pathogenic, whereas differentiation in the presence of TGFβ1 and IL-6 induces non-pathogenic Th17 which can become pathogenic following further IL-23 stimulation (127). Pathogenic Th17 cells express higher levels of several factors such as GM-CSF, T-bet and STAT4 that, as mentioned above, are highly correlated with the development of autoimmune reactions (127). Hence, pathogenic Th17 cells have been suggested to have a hybrid Th17/Th1 phenotype i.e. they express both RORγt and T-bet as well as they release both IL-17 and IFNγ. Consistent with these observations, these two Th17 populations are detected in

human samples and have been associated with the immune response to different pathogens (128).

Other data show that the plasticity of Th17 has an important role in the pathogenesis of autoimmune diseases. Indeed, as mentioned earlier, in target tissues Th17 cells switch to Th1 and this conversion is necessary for the induction of full-blown disease in an experimental model of diabetes (129). Furthermore, hybrid Th17/Th1 cells and Th17-derived Th1 cells have been detected in synovial fluid of juveniles RA patients (130). These and many other observations thus suggest that the two phenotypes are connected with each other and are important in orchestrating the development of autoimmune diseases.

1.3 Annexin protein family

The annexins are a family of 13 proteins that present an evolutionary conserved carboxyl terminal core of four to six homologous repeats and a unique N-terminal segment. The protein core mediates their ability to bind negatively-charged membrane phospholipids in a calcium-dependent manner. The N-terminal segment varies in length and mediates the biological functions of each annexin (131).

Annexins are important for cell membrane scaffolding since they influence cell shape and stabilize membrane lipid rafts. They are also involved in trafficking and organization of vesicles, exocytosis and endocytosis and contribute to control cell growth and ion flux (131). All the annexins are mainly intracellular proteins that can be sequestered at the plasma membrane of the cells; however Anx-A1, -2 and -5 make an exception since they can be secreted extracellularly to elicit biological effects in an autocrine/paracrine manner (132).

1.3.1 Annexin A1

Annexin A1 (AnxA1), also known as lipocortin or lipomodulin, is identified as a glucocorticoid-inducible protein able to inhibit the phospholipaseA_2 activity, thus altering downstream the arachidonic acid cascade (133, 134). AnxA1 is a 37kDa protein constituted by 346 amino acids. In mice, AnxA1 is 355 amino acids long and its gene shares 70% homology with the human gene. AnxA1 has an N-terminal segment of 47 amino acids which mediates, in the presence of high concentration of calcium, its biological activity (135). The N-terminal segment contains a

phosphorylation and a proteolytic cleavage sites that are likely regulatory sites for the activity of the protein (136).

AnxA1 is widely expressed in different cell types and is detectable in almost all the leukocytes. Neutrophils contain the largest amounts of Anx-A1, which is stored predominantly into gelatinase granules (137, 138), followed by monocytes, macrophages, mast cells and dendritic cells. T and B cells have lower levels of AnxA1 comparing to the other leukocytes. However these levels increase in activated T cells (138).

After treatment with glucocorticoids, AnxA1 expression augments in myeloid-derived leukocytes (139). Cell treatment with glucocorticoids has the opposite effect in T cells, with decreased expression and synthesis of AnxA1 (140). In all the cell types, first AnxA1 is mobilised by translocation to the plasma membrane, and then it is released in the extracellular space (141).

AnxA1 and its-derived peptides are ligands of the formyl peptide receptors (FPRs). Three FPRs have been described in humans: FPR1, FPR2/ALX and FPR3. Both FPR1 and FPR2/ALX share about 80% homology with the murine genes. In mice these are known as fpr1 and fpr2, respectively. FPR3 seems to share similarities with fpr2. Additional members of FPR have been identified in mice but they do not have counterparts in humans (142). All these receptors belong to a family of seven G-protein-coupled receptors used by the bacterially-derived product fMLP and an array of endogenous mediators to deliver a wide range of signalling molecules that are important for leukocyte activation and trafficking (143). Full length AnxA1 exerts its

biological functions mainly *via* activation of FPR2/ALX (144). In T cells, both FPR1 and FPR2/ALX are expressed at very low levels with activated and memory cells expressing more than naïve T cells (138). Consistent with this, a study from our group has shown that activation of T cells with anti-CD3 plus anti-CD28 leads to the upregulation and externalisation of FPR2/ALX as quickly as after 30 minutes after stimulation and remained stable for the following 6 hours (145).

1.3.2 Annexin A1 and its dual role in immune responses

AnxA1 has dual actions in the immune response. In the innate immune system, AnxA1 has been shown to reduce the recruitment of leukocytes into inflamed tissues by inhibiting the adhesion and transmigration of leucocytes (146-148). For instance, AnxA1 knockout mice exhibit an exaggerated inflammatory response in the experimental model of zymosan-induced peritonitis – a classical experimental model of inflammation used to study leukocyte migration (149). Multiple cellular and molecular mechanisms have been proposed to be responsible for these effects. These include downregulation of neutrophil transmigration, apoptosis of neutrophils in the sites of inflammation, inhibition of eicosanoid production – such as leukotrienes or prostaglandins – as well as stimulation of phagocytosis by macrophages (132, 150, 151). This wide spectrum of functions reflects the pleiotropic nature of this molecule as well as its cell-specific functions. In addition to this, different effects can be observed if the endogenous molecule or the recombinant protein/peptides are being investigated. In all cases, it is important to highlight that AnxA1 has unique place in the arsenal of anti-inflammatory molecule because of its ability to act as a pro-resolving mediator for innate immune responses.

In the adaptive immune system AnxA1 has been shown to have pro-inflammatory effects on T cells and dendritic cells. Previous studies in our Centre investigated the role of AnxA1 in T cells showing that the human recombinant AnxA1 (hrAnxA1) increases anti-CD3 plus anti-CD28-induced proliferation, IL-2 production and expression of activation markers such as CD69 and CD25 in T cells (145). These T cells also show prolonged anti-CD3 plus anti-CD28-induced ERK and AKT phosphorylation. Naïve T cells exposed to hrAnxA1 differentiate into a Th1 phenotype in both neutral and skewed conditions (145). Furthermore, AnxA1 knockout (AnxA1-/-) T cells display impaired anti-CD3 plus anti-CD28-induced proliferation and activation as well as decreased ERK and AKT phosphorylation. While, T cells from AnxA1-/- mice show a marked Th2 and an impaired Th17 phenotype compared to wild type T cells when differentiated in Th2 or Th17 conditions, respectively (152). This was also confirmed in Weyd *et al*., studies, which show that T cells pre-treated with AnxA1 secrete higher concentration of TNF and IFNγ upon stimulation (153). Conversely, a recent study by Yang *et al*., contradicted these findings and proposed that deficiency of AnxA1 in CD4+ T cells exacerbates T cell–dependent inflammation (154).

These modulatory effects of AnxA1 on T cell activation have also been explored at the level of development. Analysis of AnxA1-/- thymocyte populations at the immature DN stage showed a proportional decrease in the DN1 and an increase in the DN3 subsets compared to control littermates. There were no significant differences in thymocyte numbers or proportions of CD4+ and CD8+ SP populations between Anx1-/- and wild type (AnxA1+/+) mice (155). However, crossing AnxA1-/- mice onto HY-TCR transgenic mice, an increase in DP and CD4 SP cells in male

HY-TCR/AnxA1-/- compared to HY-TCR/AnxA1+/+ was observed. Conversely, female HY-TCR/AnxA1-/- mice showed an increase in DP and a decrease in CD8 SP cells compared to female HY-TCR/AnxA1+/+ (155). Consistent with the effects observed on mature T cells, AnxA1-/- thymocytes showed a decrease in anti-CD3-induced Erk phosphorylation and NFκB activation compared to control littermates (155).

Together these results indicate that the levels of AnxA1 control the threshold of TCR signalling and by doing so, can regulate T cell activation and proliferation. In addition, AnxA1 modulates *T cell functions acting as master switch in Th1/Th2/Th17 differentiation and balance*.

1.3.3 Annexin A1 and autoimmunity

A dys-regulated expression of AnxA1 has been associated to several human pathologies with controversial outcomes. For instance, loss of AnxA1 expression is negatively correlated with breast or gastric cancer, while its upregulation is associated with tumour progression in lung and prostate carcinomas (156). In autoimmune diseases such as RA or SLE, patients have been found positive to auto-antibodies against AnxA1 (157, 158). In some cases, such as SLE, the level of anti-AnxA1-antibodies was found to correlate with the disease activity (158, 159). The biological function of the auto-AnxA1-antibodies is controversial since they could impair the anti-inflammatory or inflammatory activities of AnxA1 and thus might promote pro- and anti-inflammatory downstream effects, respectively (159). Increased levels of AnxA1 protein have been detected in the CNS of MS patients at

the peak of disease (160, 161). This was initially associated with the anti-inflammatory counter-action of AnxA1 on the innate immune response (162). However, comparative expression analyses have shown 10-fold increase of AnxA1 in MS brain lesions at the early stage of inflammation (163). Moreover, AnxA1 was upregulated 1.5 to 2 fold changes in peripheral blood mononuclear cells of patients affected by autoimmune diseases, including MS patients, compared to healthy control volunteers (164-166). RA patients also show higher expression of AnxA1 in CD4+ T cells compared to healthy volunteers (145). Together with these evidences, studies have shown that administration of hrAnxA1 during the immunisation phase of the model exacerbates signs of disease in DBA mice subjected to collagen-induced arthritis (145). In addition, $AnxA1^{-/-}$ mice have been shown to develop a bland EAE compared to wild type mice and this was correlated to a lower number of T cells and macrophages infiltrating the CNS (167).

Last but not least, genome-wide association studies (GWAS) database shows that single point mutation in the AnxA1 gene has been associated with bipolar disorder, as well as with schizophrenia (168). These psychotic disorders have been shown to be associated with alterations of immune homeostasis and accompanying autoimmune diseases – as extensively discussed in section 1.1.2.2 Psychiatric health and autoimmune diseases (169, 170).

1.4 Central Nervous System and T cells crosstalk

The crosstalk between immune system and CNS is fundamental for the homeostasis of the whole body and for the synchronization/integration of human functions. There are substantial evidences that support this connection, some of which also come from daily-life. It is self-evident that systemic inflammation or infections induce behavioural responses mediated by the CNS such as fever, reduction in motor activity, loss of appetite, sleepiness, hyperalgesia, anxiety and depression. These symptoms are often combined under the name of *sickness behaviour* and are mediated by a number of factors including the acute-phase proteins (IL-1, IL-6, IL-8 and TNFα) (171, 172). This is a form of protective and fitness response of our body to cope with adverse health conditions and can be considered a safeguard mechanism that our body has evolved in order to favour healing and repair.

The brain and the spinal cord, referred to as CNS, have been considered immuno-privileged sites of our body thanks to their ability to restrict the access of immune cells and also limit immune functions. The CNS microenvironment is able to induce immunological ignorance as it has been demonstrated by the prolonged survival of tissue grafts in this anatomical site (173, 174).

The blood brain barrier (BBB) plays an important role in separating CNS and the immune system, and in regulating tightly their communication (175). It limits the penetration of antibodies, immune mediators and immune cells from the systemic circulation. However, the BBB is necessary but not sufficient to provide and maintain immune privilege. Indeed, even in case of compromised BBB, the CNS maintains its separation from the immune system. Consistent with this, studies have

shown the injection of an antigen into the CNS is able to induce systemic tolerance as showed by the absence of T cell response against the same antigen once this has been reintroduced into another part of the body (176). Thus, it seems that it concerns active processes able to down-regulate local and systemic inflammation.

As suggested by Britta Engelhardt (University of Bern), the CNS anatomical organization resembles the architecture of a medieval castle, where the castle itself represents the CNS parenchyma. This is protected by two walls separated by a moat (the BBB). Endothelial cells and pericytes resemble the outer castle wall while astrocytes resemble the inner castle wall (173). The cerebrospinal fluid (CSF), subarachnoid space or meningeal spaces could be represented by the moat. In these spaces, the immune surveillance takes place. T cells can cross the outer wall, through the recognition of selectins and adhesion molecules and enter into the moat where they can encounter meningeal myeloid cells such as macrophages and dendritic cells, even if these are less represented (177).

1.4.1 Role of T cells in CNS homeostasis and pathologies

T cells and leukocytes penetrate into the CNS via the choroid plexus or through post-capillary venules. In homeostatic and healthy conditions, they accumulate in the subarachnoid space while are rare in the CNS parenchyma. On average, the leukocytes found in the CSF of normal healthy donors are about 1000–3000 cells/ml. T cells in the non-inflamed CSF are predominantly central memory T cells (CD4+CD45RO+CD27+CD69+) which have been recently activated and expressing high levels of CC chemokine receptor type 7 (CCR7), L-selectin, and P-selectin glycoprotein ligand-1 (PSGL-1) (177). The passage into the CSF is partly regulated

by the binding of α1β4 integrin (or VLA-4) and PSGL-1 expressed onto T cells to their ligands, VCAM-1 and P-selectin, respectively, present onto endothelial cells (175).

The immune surveillance exerted by T cells in the CNS is similar to that performed in other tissues. The activation of MHC class II^+ APCs such as microglial cells or astrocytes by an immunogenic stimulus, however, increases the expression of MHC complexes and co-stimulatory molecules causing an increase of avidity in the interaction of T cells and APCs. Therefore, in this context even low avidity TCRs such as the ones born by self-reactive T cells can be activated and give rise to immune reactions that might result in autoimmunity. This is the case for patients suffering from MS who differ from healthy controls not in term of the frequency of myelin-specific T cells, which are comparable, but in the frequency of high avidity T cells (177).

Besides the regular immune surveillance, T cells have physiological and homeostatic effects on the CNS. Studies have shown the existence of self-reactive T cells that are able to protect the CNS in presence of neuronal injury by reducing secondary degeneration processes and increasing neuronal survival (178-180). Indeed, T cells have an active role in modulating neurogenesis as well as in memory and learning functions (170, 181-185). This was observed in both SCID mice and nude mice (i.e. mice with few or no T cells) which have impaired neurogenesis in response to an appropriate stimulus. While, the defect was corrected following the transfer of spleen cells from normal animals and was not observed if the splenocyte population was

depleted from T cells (182).

Similarly, T cells are able to restore the dysfunctional learning observed in SCID mice or following ablation of adaptive immunity (181). In addition, the reconstitution of SCID mice with T cells or the boosting of T cells by vaccination with myelin specific peptide have been shown to ameliorate and diminish post-traumatic stress disorder (186, 187). In general, cognitive tasks in mice are accompanied by increased number of T cells in the meningeal space (183) and the performance are impaired by treatments that reduce T cell migration into CNS (such as antibody against VLA-4; (43)) or trap T cells in the lymph nodes (such as Fingolimod treatment; (44)) (183). When one considers the different subtypes of T cells, it is interesting to note that using CD4 or CD8 specific antibodies, studies have shown depletion of CD4 T cells but not of CD8 is associated to learning impairment in mice (185). It has been also described that performance of cognitive tasks led particularly to accumulation of IL-4 producing T cells in the meninges. This is consistent with cognitive defects observed in IL-$4^{-/-}$ mice (183).

The absence of IL-4-/- T cells has been shown to cause a shift in the phenotype of meningeal myeloid cells towards a proinflammatory state. This was associated with a rise in IL-1β, IL-12 and TNF-α in the meningeal space which in turn negatively affected CNS functions (188). Yet, depletion of circulating immune cells worsens disease course of neurodegenerative conditions (189). Indeed, T cells with a Th2-like phenotype are associated with upregulation of genes involved in tissue repair, whereas Th1 phenotype are not (190). It has been shown that IL-4 expression in the

CNS is able to upregulate the expression of chemokines (CCL1, CCL17 and CCL22) involved in the recruitment of Treg (191) and of brain-derived neurotrophic factor (BDNF) (183).

BDNF is an essential neurotrophic factor for adult neurogenesis, spatial learning and memory (192). It is classically produced by astrocytes and neurons and it has recently discovered being secreted also by immune cells (193). Interestingly, other neurotrophins and their receptors are produced and act on the immune system (Table 1.5), in particular it has been showed that myelin specific T cells in the brain secrete high amount of BDNF (193, 194).

Table 1.5: Expression of neurotrophic factors by immune cells

	T cells	B cells	Monocytes
NGF	+	+	+
BDNF	+	+	+
NT 3	+	+	+
NT 4/5	+	No data	No data

NGF: Nerve Growth Factor; NT:Neurotrophin.

All together these observations led to the formulation of a new concept termed *protective autoimmunity* by its own author Prof Michael Schwartz (Weizmann Institute of Science, Rehovot, Israel). According to this theory, the adaptive immune response is fundamental for the maintenance of CNS integrity and homeostasis. More specifically, immune cells (mainly CD4+ T cells) are pivotal for CNS neuroprotection and repair. Indeed, CD4+ T cells recognize brain antigens upon

injury to the CNS and this signals the recruitment of the body's defense mechanisms. However, if this response escapes control, its benefit is replaced by a detrimental effect that leads to an inflammatory autoimmune disease. This innovative concept rebuilds the way to interpret immunobiology and has a wide range of therapeutic implications.

1.4.2 Stress, HPA axis and inflammation

CNS and immune system, together with endocrine system, act in a synchronised manner. The co-operations occur through preferential signalling canals that are shared by the three systems.

As mention in the section above, neurotrophins are an example of common factors that CNS and immune cells used for the crosstalk during stressed conditions for the CNS. Interestingly, the presence of both endogenous and exogenous stressors activates sympathetic nervous system and HPA axis, which through the secretion of their final mediators, catecholamines and glucocorticoids (GCs) respectively, regulate many systemic functions such as metabolism, heart rate, thermogenesis and also the immune system (195).

Catecholamines act i.e. in secondary lymphoid organs up-regulating IL-1β and IL-6 expression and release by peripheral macrophages (196). This pro-inflammatory profile is for example observed after social disruption stress or exposure to mild electric foot shock stress (197). In addition, these mice showed splenomegaly and an increase in anxiety- but not depressive-like behaviour (198, 199). Catecholamines further potentiate the production of IL-8 by monocytes of the lung thus contributing

to the recruitment of leukocytes in local inflammation (200). However, if we consider the bigger picture, the systemic effect of catecholamines is to skew T cells towards a Th2 phenotype, thus controlling the production of IL-12 and IL-10 (201). Studies have shown in both in human and mouse that β_2-AR agonists inhibit the production of IFNγ by Th1 cells while β-ARs antagonists causes a substantial increase in LPS-induced TNFα and IL-12 production (195). This is relevant to autoimmune conditions where agonists for β-ARs suppress EAE or CIA development (202, 203).

Cytokines such as IL-1, IL-6 or TNFα are able to penetrate the BBB and stimulate the secretion of corticotropin releasing hormone (CRH) in the hypothalamus (203, 204). CRH in turn stimulates the secretion of adrenocorticotropin hormone (ACTH) in the pituitary and this untimely leads to the increased secretion of GCs in the adrenal cortex (204). GCs suppress the production of TNFα, IL-2 and IFNγ *in vitro* and *in vivo* in both mouse and human (205). High concentration of GCs has inhibiting effects on the secretion of IL-1 and IL-12 by macrophages (201, 206) or on the expression of IL-12 receptor on T cells and NK cells (207). Then, GCs have stimulatory effect on the production of IL-10 by CD4+ T cells (208), which has also been measured in the blood of MS patients after treatment with GCs (209). Circulating GCs act also centrally in the CNS. It has been described two type responses to GCs: early and late effects. The former known also as nongenomic effects occur rapidly within 15-20 min and lead to a rapid adaptation to stress- i.e. they include the increase of locomotion, food intake, aggressive behaviour and the decrease of ACTH secretion (210). The late responses, known as genomic effects, required *de novo* protein synthesis and this implies a latency of days. Paradoxically,

low concentration of GCs locally activates alveolar macrophages and during chronic stress such as autoimmune diseases, characterised by high levels of IL-1, TNFα and IL-6, the CRH is suppressed while ACTH and GCs have inappropriately normal plasma levels.

1.4.2.1 HPA and Annexin A1 interconnection

AnxA1 has been proposed to be one of the factors that mediate the negative feedback between GCs and ACTH (211). Studying pituitary glands obtained from rats, it has been observed that AnxA1 secretion increases in presence of ACTH (212). Treatment of pituitary glands with dexamethasone *ex vivo* inhibits ACTH production (213). This inhibitory effect fails in presence of anti-AnxA1 antibody or antisense oligonucleotide for AnxA1 (214, 215). However, AnxA1 knockout mice do not respond to this mechanism, likely due to compensatory pathways (Prof. Rod Flower personal communication).

The expression of AnxA1 in the CNS is not ubiquitous (216). Looking at the pituitary gland, AnxA1 is highly and specifically expressed by follicular cell localised in the anterior pituitary gland. Then in presence of ACTH, AnxA1 is detected at the intercellular contacts between follicular cells and hormone-secreting cells. This suggested that upon GCs stimulation AnxA1 is released from the cytoplasmic storage of follicular cells using ABC transporters and inhibits the release of ACTH by the hormone-secreting cells through the binding to its receptor (211).

1.4.3 T cells and Emotional disorders

It is evident that immune cells are indispensable messengers in our body. Their products and cell-cell interactions mediate long and short distance communication in the body. It is not yet completely known how this communication is regulated and the mechanisms that prevent likely detrimental effects caused by uncontrolled or dys-regulated immune system.

For instance, activated macrophages and T cells have been proposed as major cause of BBB destabilisation linked to mental disorders. Studies have shown that systemic inflammation can trigger dementia and associated depression or anxiety (169, 217, 218). A very exciting recent study has also shown that treatment of patients suffering major depression with anti-TNF-α resulted in a significant improvement only in those patients that had high level of C-reactive protein (CRP) further suggesting a link between systemic inflammation and mood disorders (219). Consistent with this, increased concentration of inflammatory biomarkers, typical Th1 cell signatures – such us IL-2 and IFNγ – have been detected in the blood of patients with severe clinical depression (220, 221).

High prevalence of anxiety- and depression-related disorders has been recorded in patients suffering from autoimmune diseases (see section 1.1.2.2 Psychiatric health and autoimmune diseases). In a similar way, a high prevalence of autoimmune diseases in patients affected by bipolar disorder (a maniac-depressive illness) or schizophrenia has been reported (50, 222).

Emerging clinic observations on stressed and depressed individuals have shown a reproducible decreased number and percentage of leukocytes including T cells, but higher CD4/CD8 T cell ratio (223). An impaired T cell response has been also described in those patients, in which T cells exhibit accelerated apoptosis (224). In another study on stressed law school students, the authors have shown an association between optimism and high number of CD4+ T cells (225). It is important to highlight that these observations are strictly related to demographic and clinical parameters such as age, sex and severity of mental illness, which should be taken in account (226).

For instance, schizophrenic patients at the early stage of the disease show increased number of CD3+ and CD4+ T cells, among which memory cells are significantly fewer (227), while, at later stage, the CD4+/CD8+ T cell ratio decreases (228). In contrast to this, an increased number of activated CD4+ T cells have been found in patients suffering mood disorders such as patients with treatment-resistant depression (229) or anxiety (230).

To add a further level of complexity to this already variegated scenario, evidences have shown that chronic and acute stresses seem to have different effect on the immune system (231). In the case of acute stress, the immune system and lymphocytes are stimulated as shown by the detectable increase of activation marker expression, proliferation and production of cytokines including IFNγ (232). While chronic stress has been shown to lead to a decreased number and percentage as well as to lower response of lymphocytes to proliferation stimuli (233). However, this is not the case in patients suffering from autoimmune diseases, who exhibit active and

proliferative lymphocytes although under chronic stress. In this last scenario the lack of immunosuppression has been attributed in EAE to the presence of pro-inflammatory T-cell lineages that are resistant to GCs (234).

Lymphocytes share more than 75% of the transcriptome with the brain. They express several receptors including receptor for cytokines, GCs, catecholamine, dopamine and acetylcholine that allow lymphocytes to promptly respond and take part to systemic inflammation as well as fight-or-flight body responses. Thus, CNS alterations in metabolism or cellular functions observed during neuropsychiatric disorders consequently imprint lymphocyte alterations in their metabolism and functions. For this tight connection between CNS and lymphocyte actions, studies have interestingly suggested to use peripheral blood mononuclear cells (PMBCs), in particular lymphocytes, to identify genes associated with CNS diseases including psychiatric disorders or, in general, to investigate alterations in the immune-neuroendocrine system (232, 235).

1.5 Hypothesis of the PhD

The main hypothesis of this PhD project was to demonstrate the proinflammatory effects of AnxA1 in T cells *in vivo* using T cell-specific AnxA1 transgenic mice ($AnxA1^{tg}$). We also tested the hypothesis that agents blocking AnxA1 function (neutralizing antibody, VJ-4B6) could provide an effective new therapy for the treatment of autoimmune diseases.

Serendipitously, while testing these ideas, we observed an abnormal behaviour in $AnxA1^{tg}$ mice characterised by a wide range of manifestations ranging from signs of anxiety to maternal cannibalism. This behavioural phenotype was particularly interesting to us considering the ever-increasing amount of literature describing a connection between mood disorder and autoimmunity.

In light of these findings we formulate another new hypothesis i.e. that AnxA1 overexpression in T cells might represent a predisposing factor for the development of mood disorders in autoimmunity and *vice-versa*.

1.6 Aims of the PhD

The specific aims of this PhD range from wide and macroscopic *in vivo* evaluations to more microscopic cellular and molecular analyses. These are to:

- Study the development of MOG_{33-55}-induced EAE and pristane-induced lupus in $AnxA1^{tg}$ mice;
- Characterize at cellular and molecular levels the phenotype of T cells in the above-mentioned experimental models;
- Characterize the emotional behaviour of $AnxA1^{tg}$ mice;
- Explore molecular mechanisms using microarray gene expression analysis;
- Test the therapeutic potential of a novel AnxA1 neutralizing antibody called VJ-4B6 in mouse model of autoimmunity and mood disorders.

2. Materials & Methods

2.1 AnxA1^{tg} Mice: genotyping, breeding and husbandry

In all the experiments we have used T cell specific Annexin-A1 transgenic mice (AnxA1^{tg}) backcrossed on C57BL/6 background for more than 11 generations. Two AnxA1^{tg} colonies have been generated starting by two separate founders: Bella (female mouse) and Eric (male mouse). These mice were previously generated in our lab using a C terminal FLAG-tagged AnxA1 cDNA construct cloned into the VACD2 cassette. The VACD2 plasmid contains promoter and locus control region (LCR) sequences of the human CD2 gene, which confer T cell specific expression and, integration site independent and copy number dependent expression, respectively (Figure 2.1) (236).

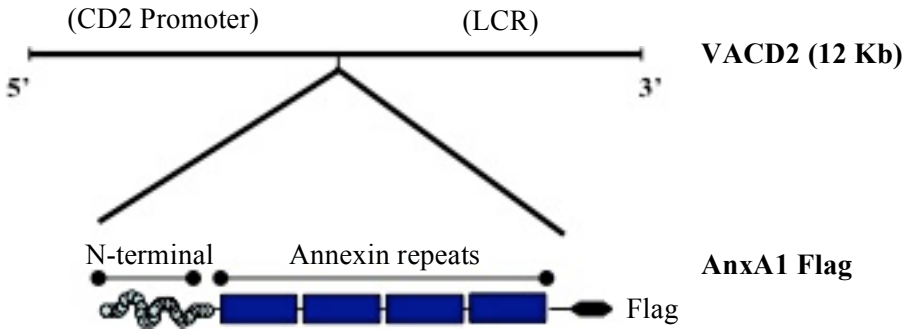

Figure 2.1. AnxA1^{tg}-VACD2 construct used to generate AnxA1^{tg} mice. Scheme of the VACD2 backbone plasmid used for the creation of the transgenic strain. AnxA1^{tg} gene is downstream the CD2 promoter and a schematic representation of AnxA1 protein domains is depicted. The bleu boxes represent the annexin-repeats which follow the unique N-terminus and proceed the FLAG tag.

The AnxA1^{tg} mice were kept inbreeding to maintain the homozygous colony in pathogen-free condition in our animal house. If not alternatively specified, experiments were done using Eric's mouse progeny. Control littermates were used

for a comparison throughout the backcrossing. Most of the experiments described in this thesis have been performed with commercially available C57BL/6 control mice (Charles River Laboratories; Margate, UK) that have been previously shown to have no difference compared to AnxA1^{tg} littermate (Dr D'Acquisto personal communication). Mice were housed for 7 days for their acclimation according to the guidelines given by the local Ethical Committee for the use of Animals. Most of the behavioural data have been generated with C57BL/6 control mice bred in house in order to avoid any interference of the housing condition onto the behavioural tests we have performed. The mice were kept in standard conditions: 12-hour light/dark cycles and 22 ±1ºC. Animal work was performed according to Home Office regulations in UK (Guidance on the Operation of Animals, Scientific Procedures Act, 1986). The animals used in these studies were aged between 5 and 8 weeks.

To genotype the transgenic colony I have used a protocol previously validated in the host lab. Briefly, genomic DNA was extracted from ear clips using REDExtract N-AMP –XNAT kit (Sigma-Aldrich, Dorset, England) as recommended by the manufacturer's instruction. Each tissue clip tissue was incubated in 50µl extraction solution prepared by mixing the tissue preparation and the tissue extraction solutions in a ratio 1:3. The DNA extraction was achieved at 94ºC for 12minutes. Then, the samples were cooled down at 4ºC for 3-5min and 50µl of neutralization solution was added in each one. From each sample, 4ul of genomic DNA was then subjected to PCR with the following specific primers for AnxA1^{tg}: forward primer 5'-GTATGGAATCTCTCTTTGCCAAGC-3'; reverse primer is 5'-ACGGATATGCACATCAGGAGGG-3' (Thermo Scientific, UK). The parameters of the PCR reactions are: initial denaturation at 94ºC for 3min followed by 30 cycles

of denaturation at 94ºC for 45sec, annealing at 60ºC for 45sec and extension time at 72ºC for 15sec, and afterwards a final extension step at 72ºC for 7 min.

a. PCR samples:

4µl of extracted DNA
10 µl of PCR Reaction Mix
0.4µM for each primer*
x µl of H_2O up to 20µl.

* Forward and reverse primers were 1:100 diluted in one solution and 3µl of this mixed solution was used for the PCR reaction.

b. DNA amplification parameters:

	Anx A1tg
Initial denaturation	94ºC 3min
Denaturation	94ºC 45sec
Annealing	60ºC 45sec
Extension time	72ºC 15sec
	(30 cycles)
Final extension time	72ºC 7min

The amplified DNA was loaded onto 2% agarose gel and detected by GelRed Nucleic Acid Gel Stain, 10,000x (Biotium, Hayward, CA) at the transilluminator.

2.2 MOG $_{35-55}$ induced EAE

The MOG_{35-55} induced EAE in C57BL/6 mice is an accepted model to investigate T cell- and macrophage-mediated demyelination (58, 67). Other advantages of this model include an efficient induction rate and the presence of histopathological signs comparable to those found in human lesions (237). This model is induced by the s.c. injection of MOG_{35-55} emulsified to complete Freud's adjuvant (CFA). The CFA contains heat killed *Mycobacterium tuberculosis* (strain H37Ra), which enhances immune responses to the antigen. The immunisation is followed by an i.p. injection of *Bordetella pertussis* toxin (PTX) at day 0 and day 2. The first signs of EAE started to manifest around day 10^{th} -12^{th} from when progressive motor deficits were observed until day 18^{th} -20^{th} (Figure 2.2). The animals were weighed daily to monitor the progression of the disease. Experiments were carried out using $AnxA1^{tg}$ and control C57BL/6 male mice of 6-7 week old.

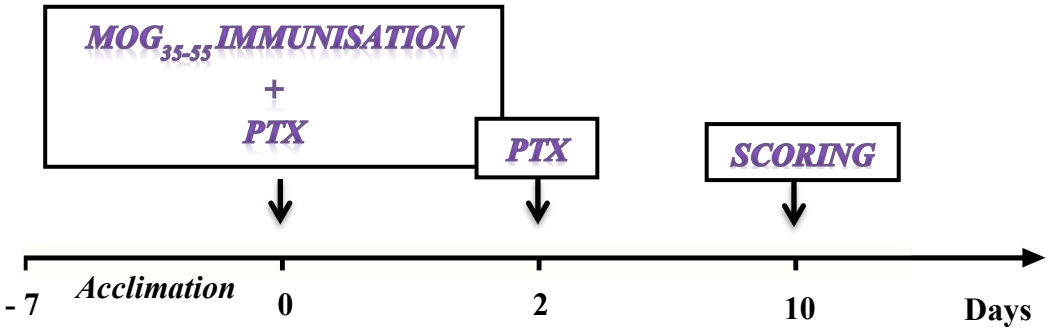

Figure 2.2. Timeline used for the induction of the EAE by MOG_{35-55} immunisation. Animals were let acclimating for a week before the immunisation. At day 0, MOG_{35-55} and PTX were injected. A second PTX injection occurs at day 2. The scoring of the EAE disease signs starts around day 10.

2.2.1 Water-in-oil emulsion preparation and mice immunisation

The immunisation for MOG_{35-55} induced EAE was performed following three main steps.

First, the emulsion for the immunisation was prepared. Each mouse received an emulsion composed of 300µg of MOG_{35-55} peptide (MEVGWYRSPFSRVVHLYRNGK, synthetized by Cambridge Research Biochemicals, UK) dissolved in 150µl of PBS and 150µl of CFA (Complete Freud's Adjuvant, Sigma-Aldrich, Dorset, England). Figure 2.3 shows a flowchart of the procedure to obtain the emulsion of MOG_{35-55} in CFA. First, CFA was placed in a glass flask and second, MOG_{35-55} previously dissolved in PBS was add. It is a rather important aspect that the blades of the homogenizer are completely submerged into the mixture of MOG_{35-55} and CFA in order to obtain a perfect emulsion. Thus the volume of the used glass flask was strictly related to the volume of the emulsion to be done, which was dependent on the number of mice to be immunised. For instance, to immunise 30 mice, 4.5ml of MOG_{35-55} solution were dissolved in 4.5ml of CFA for a total volume of 9ml for which 50ml glass flask was used to homogenise the mixture. To disperse the MOG_{35-55} solution in the CFA oil, a high-pressure homogenizer was used. About 10 minutes were sufficient to obtain the water-in-oil emulsion, which was then transferred into 1ml syringes (BD Luer-Lok™). The filling up of the syringes has been done slowly and without needle (23G). The emulsion was maintained in ice both during the preparation phase and the filling up of the syringes (Figure 2.3).

Second, the PTX solution was prepared. The PTX (Sigma-Aldrich, Dorset, England) arrived as lyophilized powder that was resuspended in 500µl water in order to have 0.1µg/µl concentrated solution, according the manufacture' instructions. For each mouse 500ng of PTX were diluted in 100µl PBS. The i.p. injections were carried out using 500µl tuberculin syringes.

Third, the mice were anesthetized by inhalation of Isoflurane (IsoFlo 100%w/w, Abbott, Illinois, USA) mixed to oxygen and nitrous oxide. Finally, the mice were immunised with i.d injection of 150µl of emulsion in each flank, i.e. each mouse received 300µl total volume of the emulsion, and i.p injection of 100µl of PTX.

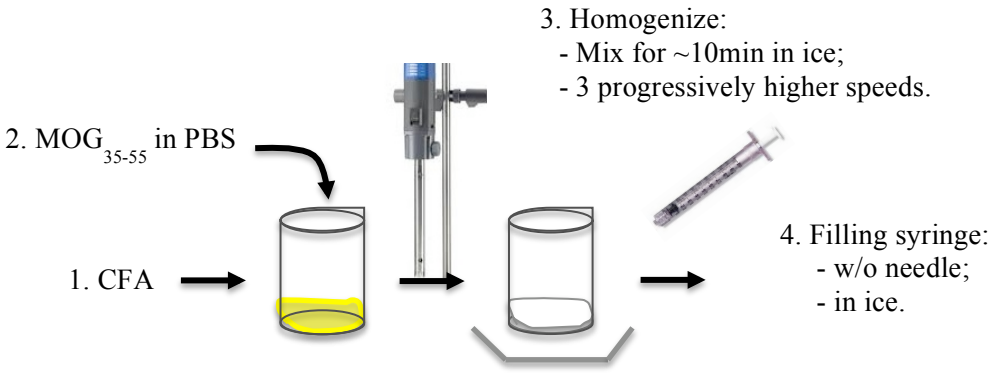

Figure 2.3. Preparation of MOG_{35-55} emulsion in CFA. MOG_{35-55} is diluted in PBS and added to CFA in a glass flask (1:1 volume ratio) in order to prepare a water-in-oil emulsion (**1&2**). The homogenization is carried in ice and increasing progressively the speed (**3**). About after 10 min, the emulsion is ready and is transferred in BD Luer-Lok™ 1ml syringes. Keep the emulsion at 0ºC until the time of injection (**4**).

2.2.2 Scoring system and time course of MOG $_{35-55}$ induced EAE

The signs of disease for the EAE range from weakness of the tail proceeding to full paralysis of hind limbs. A 6-point scale scoring system based on motor deficits was used to represent disease severity: 0- no disease; 1- partial flaccid tail; 2- complete flaccid tail; 3- impaired righting reflex; 4- partial hind limb paralysis; 5- complete hind limbs paralysis; 6- moribund or dead animal (Figure 2.4).

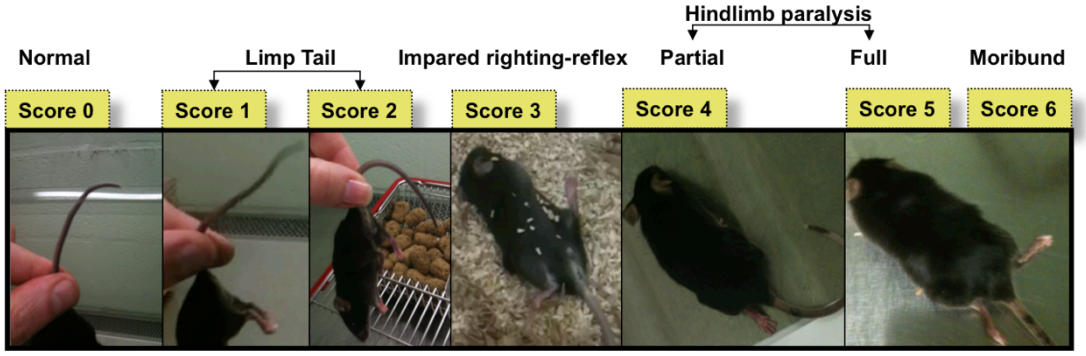

Figure 2.4. The EAE scoring system. The scoring system is based on 6-point scale. The photos depict the observed motor impairment that is conventionally associated to each score.

Generally, in a time course of EAE development it is possible to recognise three different phases: pre-onset, onset and disease (Figure 2.5a). The pre-onset phase starts the day of induction of EAE, when mice are immunized with MOG_{35-55}. During this time the immune system is primed towards MOG_{35-55} and autoreactive T cells expand and transmigrate from the draining lymph nodes to CNS (109, 238, 239).

This apparently quiescent phase is followed by the onset phase when the first signs of disease start to manifest (around day 10^{th} -12^{th}). Here, the inflammatory cascade prompted by T cells has been turned on and has started to cause damage in the CNS. The following third phase, called for convenience the "disease phase", is featured by the progressive motor deficits upon day 18^{th} -20^{th} (Figure 2.4).

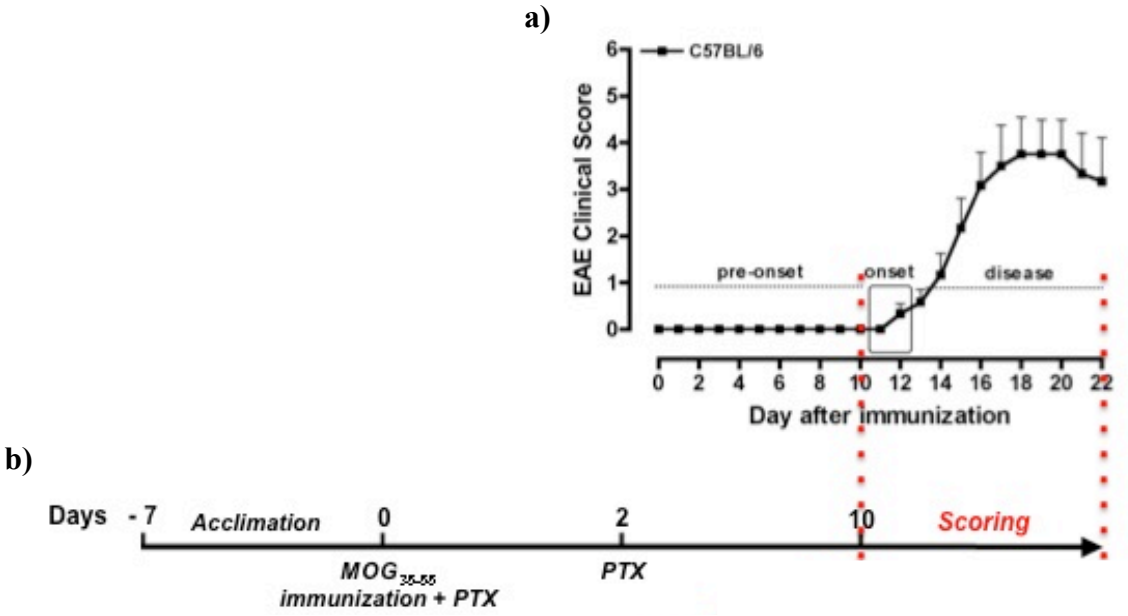

Figure 2.5. MOG_{35-55}-induced EAE. a) MOG_{35-55} induced EAE in C57BL/6 manifests as chronic progressive motor disability. Three phases can be distinguished: pre-onset, onset and disease. **b)** Mice are immunized after 7 days of acclimation by injection of self-antigen MOG_{35-55} (day 0) and PTX (day 0 and 2). The mice are scored for EAE disease signs after 10 days from immunization.

The onset of the disease is a conventionally defined as the time mice manifest a score of 1 or 2. This means that when the mouse is held from the base of its tail, the latter does not respond to stimuli and falls down lacking in tone. As the disease progresses, the mice reach a score of 3 characterised by the loss of righting reflex. This is a

reflex that occurs naturally when the body of an animal is inverted. In mice affected by EAE, such an instinctive reflex is impaired and thus sick mice remain lying on their back when turned. When mice show a score of 4 and 5, it is clearly possible to notice a partial (one leg) and full (both legs) paralysis of hindlimbs, respectively. The development of EAE is not synchronized among the immunised mice, meaning that not all mice affected by EAE manifest same score at the same time. This explains the existence of a standard deviation of the EAE disease score, which becomes higher over time during the disease phase (Figure 2.5a).

2.3 Pristane-induced lupus

Pristane is naturally occurring hydrocarbon oil that induces chronic inflammation when introduced into the peritoneal cavity. After a single i.p. injection mice develop typical characteristic of SLE including production of autoantibodies, immune complex-mediated glomerulonephritis and alveolar haemorrhage. The convenience of this experimental system compared to the other well-known model of SLE is that is strain-independent and chemically induced (thus more reproducible) (240, 241).

AnxA1^{tg} or wild type female mice of about 6-weeks were injected i.p. with 500µl/mouse of pristane (Sigma-Aldrich, Dorset, England). All mice were monitored for their weight for over one month from the injection. Lethality and tissue histology were used to compare the grade of disease in the two groups. T cell phenotype in the model was assessed at day 14 from the day of the injection by intracellular staining of T cells present in the peritoneal exudates (242).

2.3.1 Proteinuria scoring

Proteinuria was measured in a drop of murine urine by using a colorimetric assay strip for albumin (Siemens/ Bayer Albustix; MidMeds, UK), where 0- absence of traces, 1- mild (30mg/dl), 2- moderate (100mg/dl) and 3- severe (>300mg/dl).

2.4 Treatments

VJ-4B6 is a monoclonal antibody with IgG2b isotype that recognizes the AnxA1 in its native tertiary and/or quaternary structure. Therefore the binding of VJ-4B6 to AnxA1 protein has a neutralizing action. VJ-4B6 antibody was generated using the genetic immunization technology developed by Genovac (Aldevron, Freiburg, GE) (Figure 2.6).

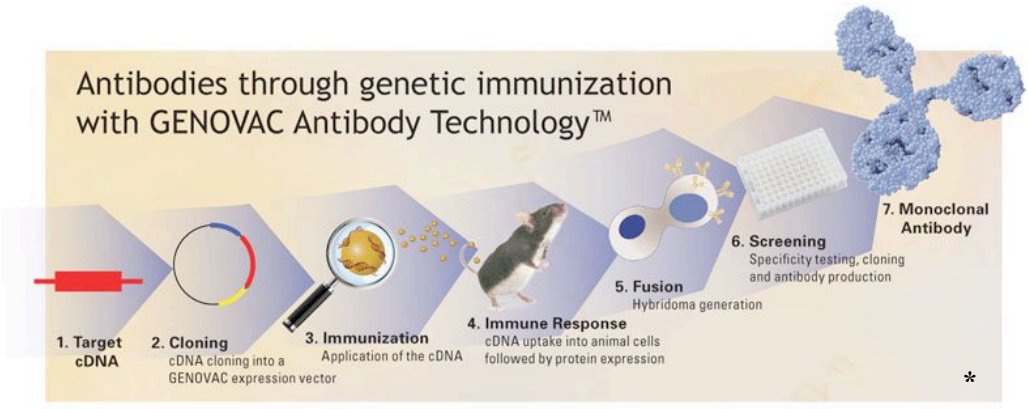

Figure 2.6. Genetic immunisation through GENOVAC antibody technology. The cDNA of an antigen is cloned in a vector, which allows the protein to be expressed in the native conformation at the plasma membrane. The cloned vectors are transferred into mice carried by gold particles. The murine cells engulf the cDNA and express it on their surface leading to the activation of B cells and the production of antibodies against the native structure of the antigen. Then, B cells are purified and fused with myeloma cells to form hybridomas, which are screening for the different antibody clones. ***http://www.aldevron.com/antibody/immunization/geneticimmunization/**

To study the effect of VJ-4B6 on MOG_{35-55} induced EAE, C57BL/6 mice received three different doses of VJ-4B6 (5, 50 and 100ng per mouse) or 50ng per mouse IgG2b (BD-Pharmingen, Oxford, UK) as negative control. The antibodies were diluted in PBS and injected i.p. 100µl per mouse at day 4, 10 and 16 from

immunisation (Figure 2.7a). To test the therapeutic effects of VJ-4B6 in EAE, we administrated i.p. 50ng VJ4B6/mouse soon after the onset of early signs of EAE (score 1 or 2).

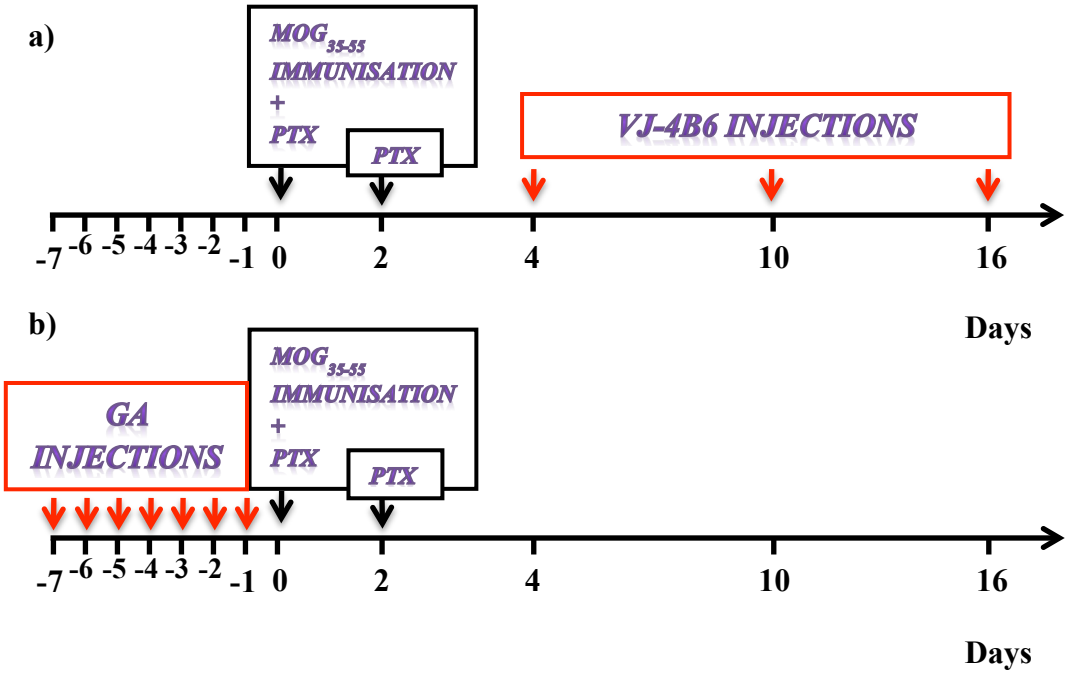

Figure 2.7. Timeline for the different treatments used in EAE model. a) VJ-4B6 was administered at day 4, 10 and 16 from immunisation day; **b)** Glatiramer acetate (GA) was administered for one week before the immunisation for 7 consecutively days.

Glatiramer Acetate (GA) (Poly (Ala, Glu, Lys, Tyr) 6:2:5:1 hydrobromide, Sigma-Aldrich, Dorset, England) exerts a suppressive effect on EAE induced in rodents (243, 244). Thus, this drug was used as positive control. GA (10mg) was solubilized in PBS in order to have a 1.5µg/µl concentrated solution and administered subcutaneously at a dose of 150µg in the mouse back. The administration was

performed daily over 7 days before immunization (Figure 2.7b) and 100µl PBS-vehicle was used as control.

The 2610019F03Rik gene was chosen as candidate gene out of list of genes obtained from the microarray analysis of CD4+ T cells (see section 2.15 and section 3.8.2). This gene codifies for 190aa long protein that has 75% homology with the human protein and unknown function *in vivo*. To test the effect of 2610019F03Rik protein in anxiety, AnxA1^{tg} mice were injected i.p. with 500ng/mouse anti-C8orf42 polyclonal antibody in rabbit (Novus Biologics, Cambridge, UK) or rabbit IgG (Santa Cruz Biotechnology, Inc., Dallas, Texas, US) diluted in 100µl/mouse 1x PBS. Otherwise, wild type mice were injected i.p. with 500ng/mouse purified human recombinant protein C8orf42 (Entrez Gene ID: 157695; OriGene technologies, Inc., Rockville, US), called rRik, or with 500ng/mouse rRik previously denatured at 95ºC for 10 min. Wild type mice injected with 1xPBS were used as control group. Before and after injection, mice were screened for anxiety-like behaviour using the behavioural paradigm described in section 2.17.4.

2.5 Blood and plasma collection

Mice were anaesthetized by vapour of Isoflurane in oxygen gas flow (IsoFlo 100%w/w, Abbott, Illinois, USA). Blood was collected by intra-cardiac punctures using 1ml syringes with 23G needle filled up with at least 200µl of 3.2% p/v sodium citrate ($C_6H_5Na_3O_7$ x $2H_2O$, Sigma-Aldrich, Dorset, England; diluted in distilled water) in order to avoid blood coagulation.

A volume ranged from 0.5 to 1ml of blood was collected in 2ml eppendorf and let to sediment for couple of hours at 4ºC. To separate the plasma from the cellular components, samples were centrifuged at 2.000 rpm for 5 minutes at 4ºC. Plasma was transferred into a new tube and store at -80ºC for further analysis. In some experiments blood cells were processed for flow cytometer analysis (see section 2.11.3).

2.6 Tissue collection and histology

Kidney, lungs, spleen and lymph nodes were collected after injection of pristane, while brain and spinal cord were collected from MOG_{35-55} immunised mice. After collection, tissues were washed in PBS and fixed with 4% PFA for 24h at 4°C before paraffin embedding. The spinal cords were first fixed as described before and then decalcified in 10% formic acid for 3-5 days at 4ºC, then resuspended in 4% PFA once again overnight at 4ºC before paraffin embedding. The Pathology Service (Barts and Cancer Institute, QMUL) performed the embedding in paraffin wax, the cutting and hematoxyline & eosin (H&E) staining in the sections.

Brain collected for gene expression analysis were harvested in 3ml of RNA later to preserve the RNA from degradation and stored at 4ºC for brief time or at -20ºC for longer storage.

2.7 Zymosan peritonitis

Zymosan (ZY) is a component of the yeast wall and it is an inflammatory stimulus once injected into a number of tissue sites. Injection of ZY in the peritoneal cavity of mice causes inflammatory responses known as peritonitis (148). ZY was dissolved in 1x PBS and load in 1ml syringes with 26G needle just before the injection and administered i.p. at 1 mg/ 500ul PBS/ mouse. 4h after the injection, blood and peritoneal lavages were collected.

2.7.1 Peritoneal lavage

Peritoneal lavages were obtained injecting i.p. 2ml of PBS containing 3mM EDTA. Peritoneal fluids were collected through a small cut on the peritoneal membrane using a plastic Pasteur pipette. Lavages were centrifuged at 400G for 10 minutes to separate the cells from the sup. Cell pellets were resuspended in PBS, counted and stained for FACS analysis while sup were stored at -20ºC and used to measure a panel of different inflammatory cytokines.

2.8 Isolation of mononuclear cell from lymphoid organs

The procedure reported here describes how to collect mononuclear cells and lymphocytes from thymus, spleen and lymph nodes. Figure 2.8 shows the anatomical localisation and macroscopic appearance of these tissues. Each organ was collected and smashed through a 70µm mesh cell strainer (Falcon, UK) in RPMI medium (PAA laboratories, Buckinghamshire, UK) supplemented with 100U/ml of penicillin and streptomycin (PAA laboratories, Buckinghamshire, UK).

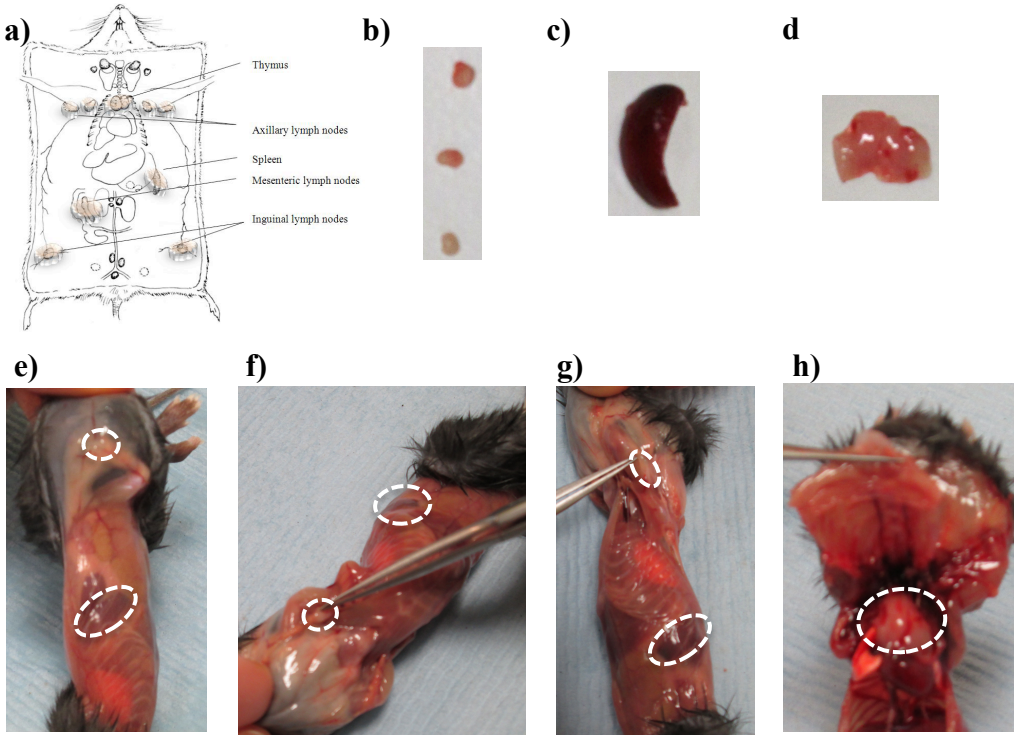

Figure 2.8. Lymphoid organs collected in these studies. a) Anatomy scheme of lymphoid organs in mouse (highlighted in pink shades). (Modified from **http://eulep.pdn.cam.ac.uk/**). **b)** Lymph nodes, **c)** spleen and d) thymus after collection. Circles in **e)** to **g)** highlight the anatomical locations for inguinal and axillary lymph nodes and spleen. In **h)** circle marks the thymus located in the murine chest, on top of the heart.

To isolate mononuclear cells, the cell suspensions were layered onto Histopaque-1077 (Sigma-Aldrich, Dorset, England) in a ratio 3:1. Histopaque-1077 is a density gradient cell separation medium containing Ficoll and sodium diatrizoate. After 10 min centrifugation at 400G, an opaque ring called buffy coat forms at the cell medium/histopaque-1077 interface. The buffy coat is the layer composed by mononuclear cells, while rest of cells such as granulocytes and/or red blood cells pellet at the bottom of the centrifuge tube (Figure 2.9).

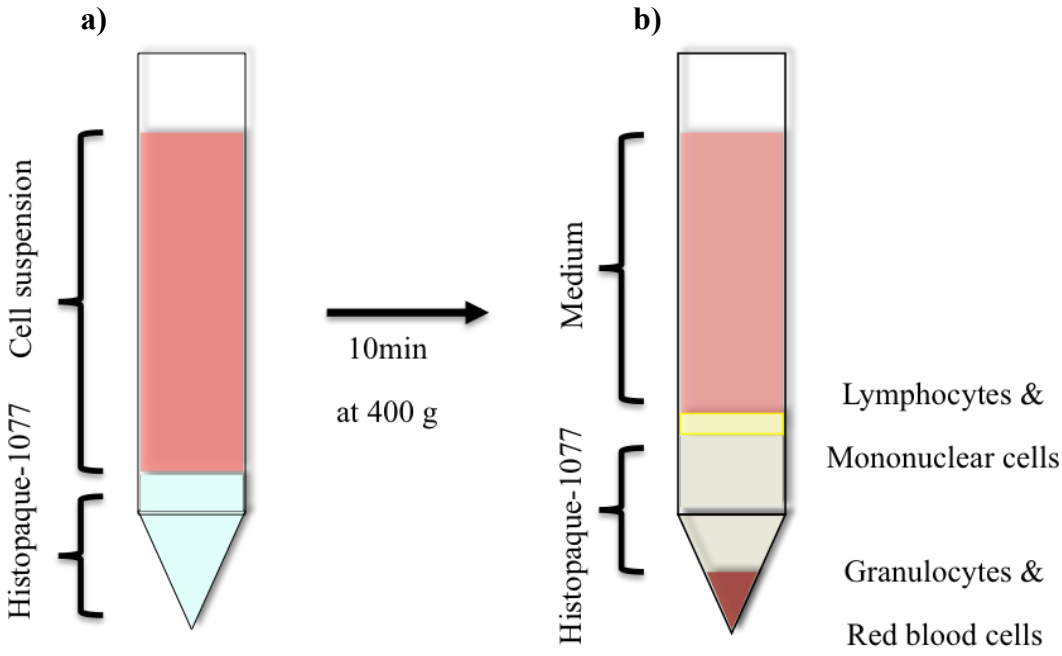

Figure 2.9. Lymphocytes and mononuclear cells separation by density gradient medium of Histopaque-1077. a) The leukocytes were suspended in RPMI medium and then layered onto Histopaque-1077. **b)** During the centrifugation, cells sediment in base on their density giving a typical multilayer sample. The bottom of this is constituted by granulocytes and red blood cells, while lymphocytes and other mononuclear cells compose the interface layer between Histopaque-1077 and medium.

The whole buffy coat was used for cell characterization. Alternatively, the buffy coat was used as source of CD3 positive and CD4 positive T cells.

2.8.1 Isolation of T cells by negative selection

Purification of CD3+ or CD4+ T cells was performed using dynal mouse CD3+ T cell or CD4+ T cell negative isolation kit (Dynal Invitrogen, life technologies, Paisley, UK), respectively (Figure 2.10). The principle of a negative isolation is to isolate the cell target by depletion of other unwanted cells through magnetic selection (Figure 2.10a). More specifically, the unwanted cells are bound to antigen specific antibodies, which are in turn bound to magnetic beads. So when the cell suspension contained in a plastic tube or flask is put in contact to a magnet, the unwanted cells accumulate at the side of the magnet while the cell target remain in the supernatant.

Lymphocytes were suspended $10x10^6$ cells/100µl in PBS (without Ca^{2+} and Mg^{2+}) with 0.1% BSA (bovine serum albumin; Sigma-Aldrich, Dorset, England) and 2mM EDTA (0.5M EDTA, Gibco) at pH 7.4, called *Buffer A*. The cells were incubated with FCS (20µl; Invitrogen, life technologies, Paisley, UK) and antibody mix (20µl) for 20 minutes at 4ºC. After a wash with 2ml of *Buffer A* at 300G for 8 minutes at 4ºC, labelled cells were resuspended in *Buffer A* and incubated with 200µl magnetic bead suspension for 15 minutes at 4ºC with gentle tilting and rotation. As final step, the cell suspension is put in contact with a magnet and the supernatant transferred in a clean tube.

Figure 2.10b and c show an example of the yield of CD3+ T cell (stained for CD4 and CD8) and CD4+ T cells obtained after negative isolation, respectively. In Figure 2.10c, I have also compared the yield and purity of CD4+ T cells obtained after a single (middle panel) or a double (right panel) round of purification.

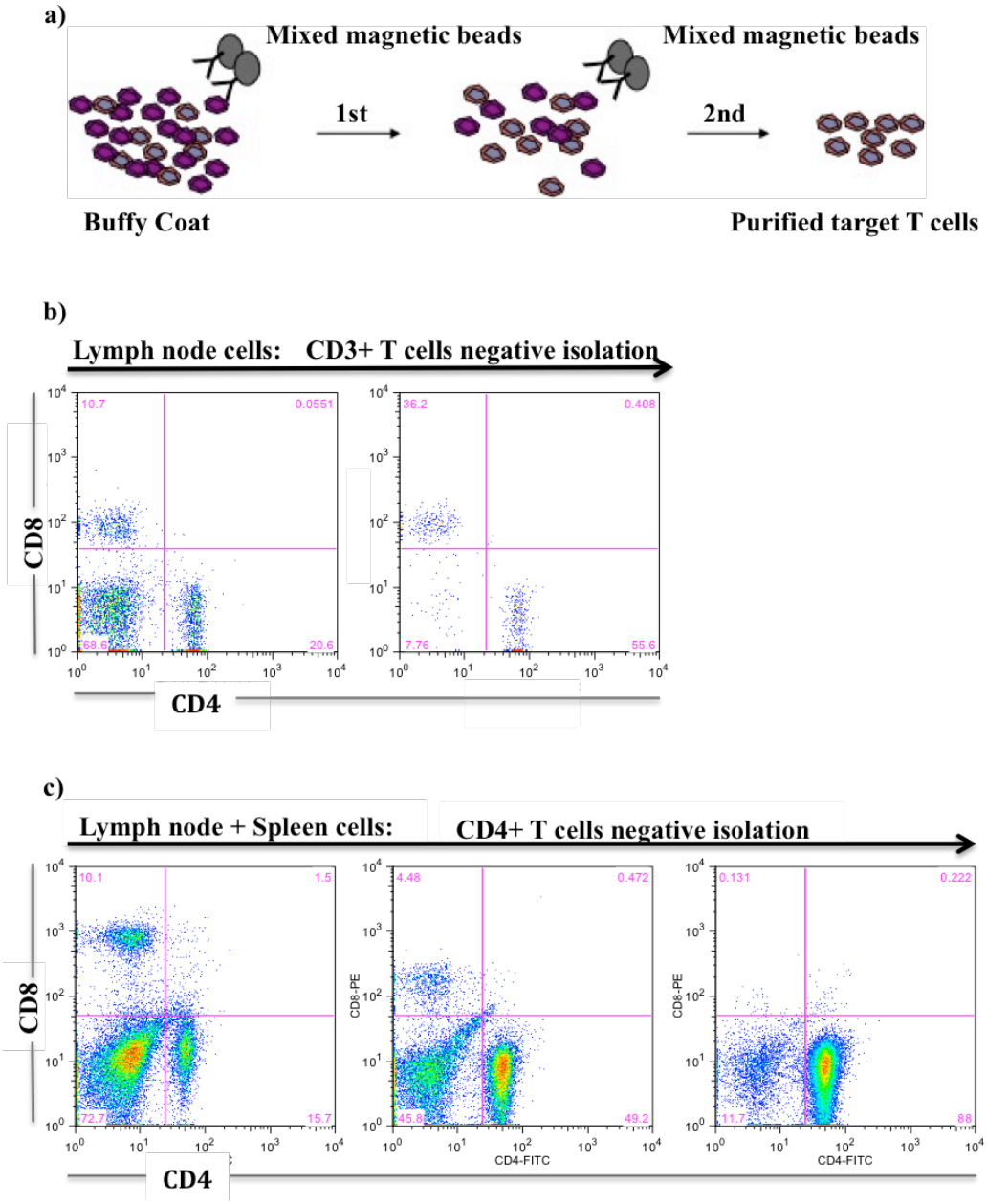

Figure 2.10. T cell negative isolation. a) Enrichment of target T cells after the removal of other cell types by the binding to magnetic specific antibodies and magnetic selection. **b)** The dot plot shows the staining of lymph nodes cells for CD4 and CD8 before and after CD3+ T cell isolation. **c)** Dot plots show the progressively enrichment in CD4+ T cells after double negative isolation from lymphocytes pooled from spleen and lymph nodes.

2.9 Leukocytes isolation from central nervous system

Mononuclear cells were isolated from spinal cord samples after induction of MOG_{35-55} induced EAE, at day 9 and 16 after immunization. Vertebral columns were dissected from the lumbar to the cervical region and washed several times in PBS to remove blood trace. Spinal cords were extracted by hydro pressure in the spinal canal using a 2ml syringe and 19-gauge needle. Subsequently, tissues were torn apart in sterile PBS by mechanical pressure through a 70µm mesh cell strainer (BD-Falcon). Mononuclear cells were isolated by density gradient centrifugation in Percoll (GE Healthcare, Little Chalfont, UK). In detail, cells were pelleted at 400G for 5 min and suspended in a 30% Percoll solution. The 30% Percoll solution was carefully layered onto a 70% Percoll solution in a ratio 1:2 and centrifuged at 500G for 30 min. In this density gradient mononuclear cells sediment at the interface between 30% and 70% Percoll layers. About 2-3ml of interface solution was collected only after the fatty layer at the top of the centrifuge tube was carefully removed. The purified mononuclear cells were washed twice in RPMI supplemented with 100U/ml of penicillin and streptomycin and 10% of FCS.

2.10 Cell counting

Improved Neubauer ruled haemocytometer was used for counting cells. This cell-counting chamber is composed by 4 primary lateral squares delimitated by triple lines and subdivided in 16 smaller secondary squares. Cells located within the primary squares have been considered in the count (Figure 2.11). The average obtained out of the four squares is multiplied by the dilution factor (if cells were

diluted) first and by 10^4 to obtain the number of cells per ml. The formulae used are reported below:

Cells/ml = average of total count x dilution factor x 10^4

Total cells = Cells/ml x volume of original cell suspension

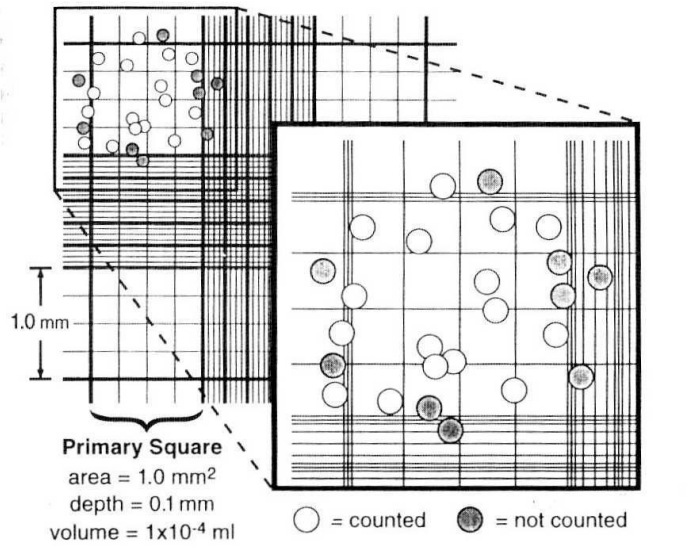

Figure 2.11. Illustration of improved Neubauer ruled haemocytometer. One of the primary squares subdivided in 16 secondary squares is enlarged and an example of counted and not counted cells is given. (http://www.cf.ac.uk/biosi/staffinfo/kille/Methods/Cellculture/HAEMO.html).

2.11 Flow Cytometry

The flow cytometry exploits the light property of interaction with mass to obtain qualitative and quantitative information of cells or particles. In flow cytometry, cell suspension undergoes hydrodynamic focusing to produce a single stream of cells. Single cells pass through a laser beam causing the scattering of the beam in different angles. Typically, the light detected up at 20º angle to the excitation line is called Forward Scatter Channel (FSC), which is an indication of the size of the cell, and at 90º angle to the excitation line is named Side Scatter Channel (SSC), which is a measure of the cell granularity. FSC and SSC allow the interested cells to be identified through their physical characteristics, which are traditionally considered unique for a specific type of cell. Lymphocytes are usually a population of cells with FSC and SSC lower than 400 and 200, respectively, in a linear scale of brightness (Figure 2.12, left panel). After stimulation, they blast and their dimension increases in both FSC and SSC, which eventually are lower than 600 and 300, respectively (Figure 2.12, right panel).

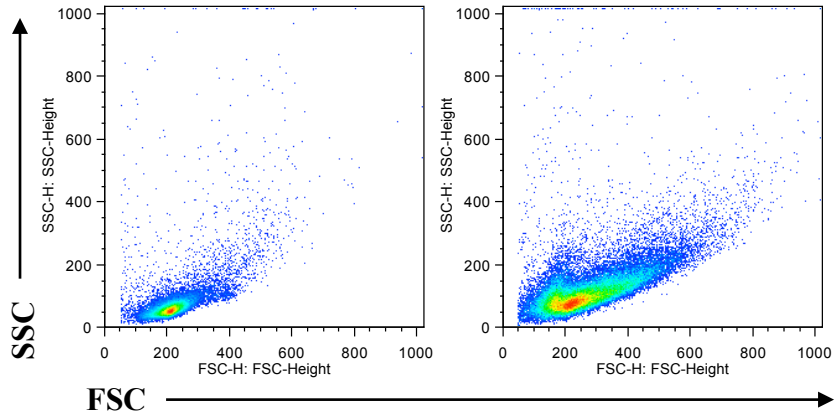

Figure 2.12. Typical lymphocyte population at flow cytometer. Cell size and granularity, FSC and SSC respectively, of freshly isolated (left panel) or anti-CD3/CD28 stimulated (right panel) lymphocytes.

Light interaction also includes light absorbance and light emission of any fluorochrome labelling the cells. The most widely used fluorochromes are FITC (fluorescein isothiocyanate), PE (Phycoerythin) and APC (Allophycocyanin). Each of these absorbs light energy at a certain wavelength and re-emits it at a longer wavelength (see Table 2.1). The emission spectra of different fluorochromes can overlap as for instance it occurs for FITC and PE. In case of overlapping spectra, fluorescence compensation needs to be performed. This consists in subtracting the fluorescence of fluorochrome A that interferes with the channel used to detect the fluorescence of fluorochrome B and *vice versa*. Thus, the true fluorescence emitted by fluorochrome A is for example the detected value diminished by the percentage of fluorescence leaked from fluorochrome B.

Table 2.1: Fluorochrome excitation/emission properties

Dye	Excitation (nm)	Emission (nm)	Fluorescent colour
FITC	488-490	525	green
PE	488-565	578	yellow
APC	633-650	661	purple

Fluorochrome conjugated antibodies are used to obtain information about cell surface proteins or receptors as well as for intracellular molecules such as cytokines. We performed multiple fluorochrome staining of cell suspension (usually up to 4 fluorochromes) to phenotype the cells we obtained.

2.11.1 Cell staining for FACS

Cells were incubated with specific conjugated antibodies (See Table 2.2 for details) diluted in FACS buffer (PBS supplemented with 5% FCS and 0.02% sodium azide) for a minimum of 30 minutes up to a 1-hour at 4ºC and then, washed and resuspended in FACS buffer. Only when the flow cytometer analysis was performed the day after, cells were fixed with 1% PFA (paraformaldehyde; Sigma-Aldrich, Dorset, England). Aliquots of cell suspension were kept unstained and single stained for each used fluorochrome was made to perform compensation.

2.11.2 Intracellular antigen labelling

Intracellular staining (ICS) is a widely used technique that allows the measurement of a wide range of factors (from signalling molecules to cytokines) that are stored inside the cells. In T cell studies, intracellular staining is often used to inform about the Th phenotype(s) of the cells under investigation. Lymphocytes were isolated from MOG_{35-55} immunized mice from peripheral lymphoid organs and spinal cord. Lymphocytes ($10x10^6$ cells/ml) from lymph nodes and spleen were cultured for 72 hours with either medium alone (CTRL) or with anti-CD3 and anti-CD28 antibodies (1µg/ml; plate bound) or with the specific antigen MOG_{35-55} (100µg/ml). At third day, the cells were pelleted and the supernatants stored at -20ºC. Subsequently, the cells were triggered again with concanavalin-A (ConA, 5µg/ml; Sigma-Aldrich, Dorset, England) in presence of protein transport inhibitor Brefeldin-A (1:1000; eBioscience) for 4 hours. Mononuclear cells isolated from the spinal cords instead were directly triggered with ConA and Brefeldin-A after collection. While, $2.5x10^6$ cells/ml cell exudates from peritoneal lavages of mice injected with pristane were plated in RPMI medium supplemented with 10% FCS and 1U P/S in presence of

50ng/ml PMA (Phorbol 12-myristate 13-acetate; Sigma-Aldrich, Dorset, England), 1mM Ionomycin (Sigma-Aldrich, Dorset, England) and 1:1000 Brefeldin-A. They were incubated for 1h and then processed for ICS of IFNy, IL-17 or IL-4, as described below.

In a typical experiment cells were pelleted and then stained for CD4 (1:500) for 30min and fixed with 1% PFA for 10 minutes. Thereafter, cells were permeabilized and stained for 30 min in permeabilization buffer (composed by 0.1% saponin and 0.09% sodium azide in PBS, eBioscience, Hatfield, UK) containing conjugated antibodies for cytokines (dil: 1:250) such as IFNγ, IL-17, GM-CSF and IL-10 (See Table 2.2 for details). Labelled cells were washed and resuspended in FACS buffer plus 1% PFA.

2.11.3 Staining of peripheral blood T cells

We used the following procedure to measure the number of T cell circulating in peripheral blood. Typically, we used 100µl of mouse blood freshly isolated by cardiac puncture (see paragraph 2.5 for blood collection). First, the plasma was removed as described in paragraph 2.5 and the pelleted blood cells were resuspended in 200µl of FACS buffer. Next, antiCD16/32-blocking Fc Ab (1:500; 10/15min in ice) is added to block unspecific binding. Samples were then stained with either antiCD3-APC or antiCD3-APC/antiCD4-PE or antiCD3-APC/antiCD8-PE (1µl of each were added to the samples) for 15 to max 45 minutes on ice. After washing, red blood cells were removed by lysis. To this aim, 400µl of 1x RBC lysis buffer (diluted in distilled H_2O and kept at RT; eBioscience, Hatfield, UK) was added to each sample and incubated for a max of 8

minutes. During the lysis, samples were pipetted up/down. Finally, samples were washed once with PBS/BSA and resuspended in 300µl FACS buffer before the analysis.

2.11.4 CFSE staining

T cell proliferation was analysed by staining cells with carboxyfluorescein succinimidyl ester (CFSE). This is a fluorescent dye that enters into the cells and covalently binds intracellular proteins. Therefore it is retained by cells and diluted during cell division from mother cell to daughter.

Lymphocytes were resuspended at $10x10^6$ cells in 1 ml of 1x PBS. It is important to use 15 ml tubes and to avoid any serum contamination in the cell suspension. CSFE (Invitrogen, life technologies, Paisley, UK) was added to the cells at 3µM final concentration (from a stock solution of 10µM in DMSO). Samples were incubated for 8 min at RT in dark under shacking. Then, the samples were mixed with an equal volume of FCS and topped up with 1x PBS. Cells were spun down and washed twice with 1x PBS. Finally, cells were resuspended in complete medium and plated at $2.5x10^5$ cells in 200µl volume per well in a 96-well plate.

To follow the proliferation, cells were incubated at 37ºC in 5% CO_2 for 48h and 72h. The stimulation conditions tested were: a) 1µg/ml or 0.3 µg/ml of plate-bound anti-CD3; b) 1µg/ml or 0.3µg/ml anti-CD3 plus 1µg/ml anti-CD28 plate-bound; 3) 0.3µg/ml plate-bound anti-CD3 and 1µg/ml anti-CD28 diluted in the medium and 4) 0.3µg/ml anti-CD3 and 1µg/ml anti-CD28 both diluted in the medium. Unstained or stained but not stimulated samples were also carried as controls.

After the stimulation, cells were collected and analysed at FACS Calibur. Data were analysed at FlowJo 9.7.1v for the valuation of the proliferation parameters through the proliferation platform (scheme in Figure 3.12). The considered parameters were:

- **% Divided**: it indicates the percentage of precursor cells that divided in the initial population;
- **Proliferation index** (Prolif. Index): it gives the number of divisions per cell that has divided taking in account only the responding cells;
- **Replication index** (Repl. Index): it indicates the fold increase of the responding cells.

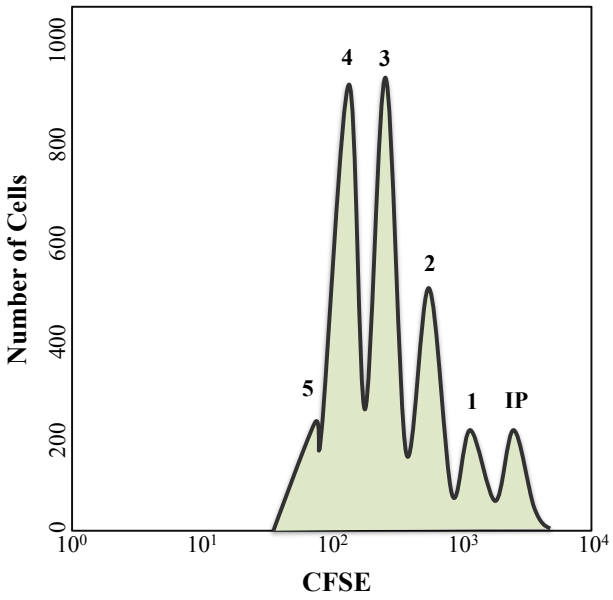

Figure 2.13. Scheme of a flow cytometer analysis of CSFE dilution with cell division. Initial cell population (IP) is the brightest population from which CFSE intensity reduces at every round of cell division (from 1 to 5 peaks). After cell proliferation, IP are the precursor cells that did not divide while the cells in peaks 1 to 5 come from responding cells.

Table 2.2: List of antibodies used in flow cytometry. For each clone, commercial source and working dilution are specified.

Name	Clone	Company	Dilution
Anti mouse CD3e	145-2C11	eBioscience	1:250
Anti mouse CD4	GK1.5	eBioscience	1:500
Anti mouse CD5	53-7.3	eBioscience	1:500
Anti mouse CD8	53-6.7	eBioscience	1:500
Anti mouse CD25	PC61.5	eBioscience	1:500
Anti mouse CD28	37.51	Biolegend	1:400
Anti Human/mouse CD44	IM7	eBioscience	1:500
Anti mouse CD45	30-F11	Biolegend	1:500
Anti mouse CD62L	MEL-14	eBioscience	1:500
Anti mouse CD69	H1.2F3	eBioscience	1:500
Anti mouse CD115	AFS98	eBioscience	1:500
Anti mouse IL-10	JES5-16E3	eBioscience	1:250
Anti mouse IL-17A	eBioTC11-18H10.1	eBioscience	1:250
Anti mouse IFNγ	XMG1.2	eBioscience	1:250
Anti mouse GM-CSF	MP1-22E9	BD Bioscience	1:250
Anti mouse CD11b	M1/70	eBioscience	1:500
Anti mouse Ly6G	RB6-8C5	eBioscience	1:500
Anti mouse F4/80	BM8	eBioscience	1:250
Donkey Anti-Mouse IgG	Polyclonal	eBioscience	1:500
F(ab)2 Donkey Anti-Rabbit IgG	Polyclonal	eBioscience	1:250

2.11.5 Cytometric bead array (CBA)

Cytokine production was measured by bead-based analytic assay in flow cytometry. This assay allows the simultaneous quantification of 20 analytes in a single volume of sample (as little as 25 µl) using the same principle of an ELISA. Basically, it consists of beads that have two different sizes (4 and 5 µm) and are dyed with different intensities of a fluorescent dye (far-red emission, 700nm). The group of beads having particular size and a certain fluorescent intensity recognise one specific analyte thanks to the antibody coating.

We used a Mouse Th1/Th2 10plex and custom-designed Mouse Th1/Th2/ Th17 /Th22 13plex kits (eBioscience, Hatfield, UK). The former contains antibody-bounded beads for GM-CSF, IFNγ, IL-1α, IL-2, IL-4, IL-5 IL-6, IL-10, IL-17 and TNFα, while the latter contains antibody-bounded beads for IFNγ, IL-1α, IL-2, IL-4, IL-5 IL-6, IL-10, IL-13, IL-17, IL-21, IL-22, Il-27 and TNFα and was supplemented with antibody-bounded beads for GM-SCF and IL-23.

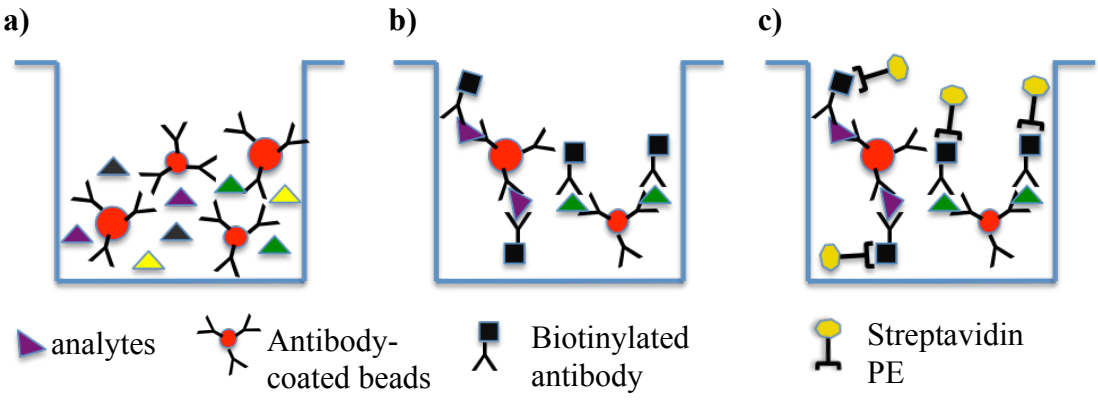

Figure 2.14. Illustration of CBA principles. a) Analytes/cytokines are incubated with the antibody-coated beads, which act as capture antibody. **b)** Captured cytokines are bound to biotinylated antibodies and these **c)** Streptavidin PE, as a sandwich ELISA.

Each sample (25µl of cell culture supernatant) was incubated with 50µl bead mixture and 50µl mix of antibodies conjugated with biotin for 2h. After two washes, streptavidin PE conjugated antibodies was added (Figure 2.14) and samples were left to rock for 1 hour in dark. Finally, samples were washed and stored overnight at 4ºC. Standards diluted 1:3 serially for 7 times were prepared and processed at the same time. Table 2.3. shows the parameters which were used for the analysis at BD LSR Fortessa (BD Bioscience cell analyser).

Table 2.3: BD LSR Fortessa setting for the CBA analysis. Voltage and mode for FSC, SSC, YG-585/15 and R-670/14 filters are specified.

Detector	Voltage	Mode
FSC	444	Lin
SSC	250	Lin
YG-585/15	430	Log
R-670/14	400	Log

During detection, two different populations of beads were distinguished according their size by SSC/ FSC profile (Figure 2.15, left panel). Within each population, the analytes were differentiated by specific internal dye intensity linked to antibody-coated beads in y-axes (Figure 2.15 right panels). Figure 2.15 (bottom panels) shows a typical pattern observed following changes in concentration of each analyte (note the shift of intensity in PE emission on x-axes). The concentration of each analyte was determined through the calibration curves obtained with the standards by using FlowCytomixPro (eBioscience software).

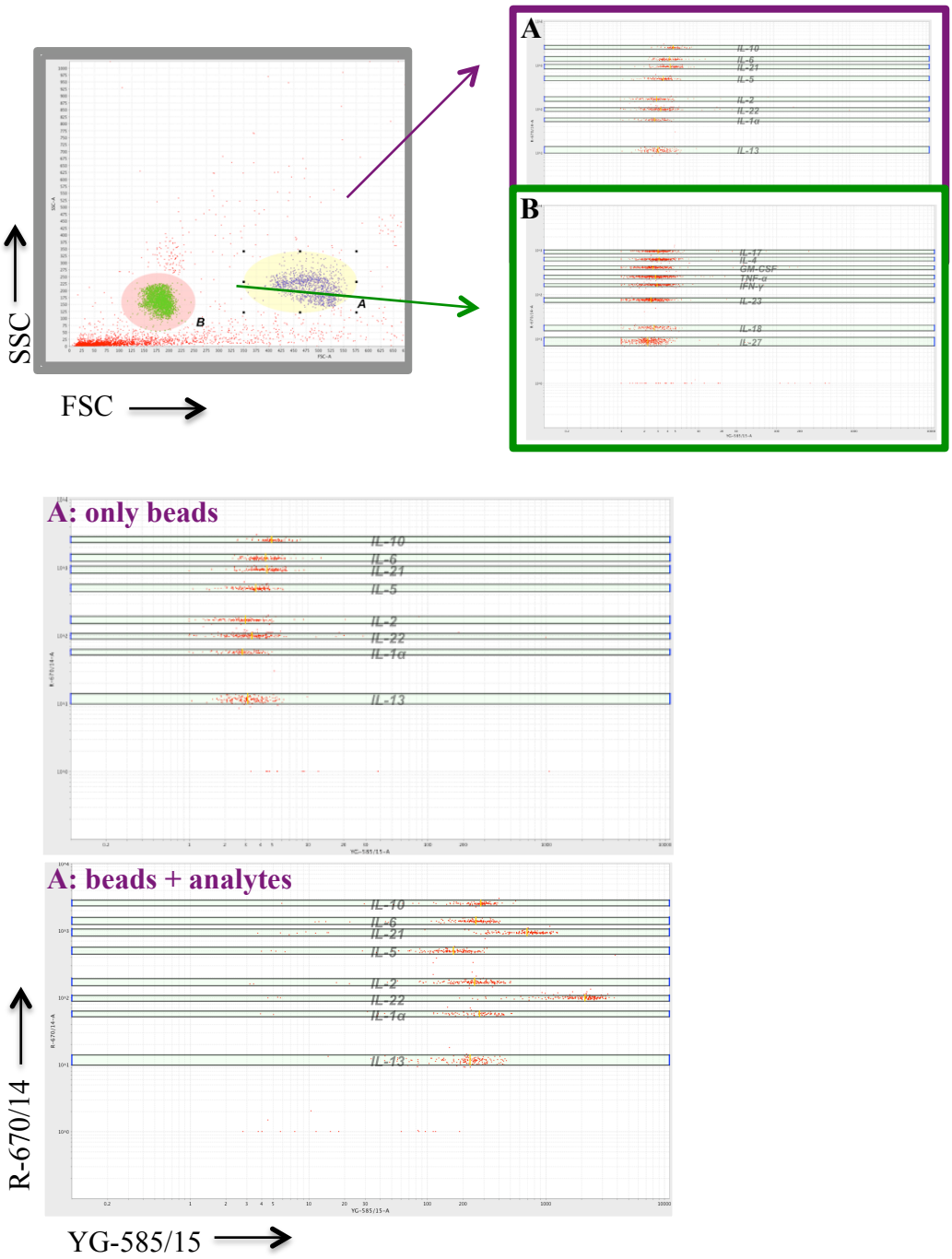

Figure 2.15. CBA flow cytometer analysis. Top-right panel: SSC/FSC dot plot showing two populations (highlighted in violet A or green B) of antibody-coated beads that are distinguishable based on their size. **Top-left panels:** Dot plots of A (top) and B (bottom). The far-red emission is shown in y-axes while the PE emission is shown in x-axes. In the two populations each different cytokine is visualized as a unique red cloud at a specific far-red fluorescent intensity. **Bottom panels:** The presence of analytes shifts the PE signal towards higher intensity indirectly correlated to the analyte concentrations.

2.12 T cell adoptive transfer

T cells were purified from lymph nodes and spleen of wild type or AnxA1^{tg} mice as already described in paragraph 2.8. Wild type mice received i.p. ~6x10^6 of CD3$^+$ or CD4$^+$ T cells in 200µl of PBS either isolated from wild type or AnxA1^{tg} mice. Mice injected i.p. with 200µl PBS-only was carried as further control group. After T cell adoptive transfer, recipient mice were tested for anxiety-like behaviour (see section 2.17.4) and later they were either immunised for MOG_{35-55} EAE or culled for brain collection.

2.13 Purification of total RNA

Purification of total RNA was carried out using RNeasy Mini kit (Qiagen, Manchester, UK) and following the manufacturer's instructions. The adsorption of the RNA to the silica-membrane of RNeasy spin columns is the principle on which the kit is based. Total RNA was purified from wild type and AnxA1^{tg} CD4+ T cells (2.5-5x10^6 cells/ml) after stimulation with anti-CD3/anti-CD28 (1µg/ml; plate bound) overnight. Cells were collected and lysed in RLT buffer supplemented with β–mercaptoethanol and homogenized using syringe fitted with a 19G needle. 70% ethanol was added to adjust the binding condition and samples were loaded in the RNeasy spin columns. Contaminants were removed by serial washes with buffer RW1 and total RNA was eluted with 30µl RNAse free water. Spectrophotometer ND-1000 (NanoD rop, ND-1000) was used to quantify the concentration and the purity (ratio of 260nm absorbance to 280nm absorbance values were between 1.8 to 2.0) of the extracted RNA. A microfluidic analysis using Agilent 2100 Bioanalyzer

was performed to check the integrity of the purified RNA (performed by the microarray facility, see section 2.15), which provides the picture of the RNA degradation on the base of the ideal full-length RNA that show a ratio of 28S to 18S ribosomal RNA bands equal to 2:1.

2.13.1 Preparing Brain tissue for RNA extraction

Whole brains were harvested and stored in RNAlater (Ambion, Applied Biosystems, life technologies, Paisley, UK) at -20C. The RNA extraction for this tissue was performed using a specific RNeasy Lipid Tissue Midi Kit (Qiagen, Manchester, UK) and according to the manufacturer's instructions. Briefly, the whole brain was homogenised in 1ml of Qiazol lysis buffer (Qiagen, Manchester, UK) using 2ml tube containing 1.4mm ceramic (zirconium oxide) beads (Precellys, Stretton, UK). The setting for homogenisation was 4000rpm for 30 sec for 3 cycles. Homogenates were transferred in a new 2ml eppendorf tube and diluted with an extra 1ml of Qiazol lysis buffer. Proteins and membrane were precipitated adding 200µl of chloroform followed by shaking for 15 sec. Samples were then centrifuged at 12000G for 15 min. Only 300µl of the supernatant was used for the RNA purification while the rest was diluted 1:1 with ethanol and stored at -80ºC.

2.14 cDNA synthesis and Real Time PCR

SYBR green quantitative PCR (Q-PCR or Real Time PCR) was used to measure relative or absolute gene expression level. SYBR Green is a dye that fluoresces when it intercalates with double-stranded DNA. During the PCR cycles, the intensity of fluorescence increases in relationship with the exponential amplification of the DNA

amount. The Q-PCR measures the increase of fluorescence during each amplification cycle. Conventionally, we use the threshold cycle (Ct) i.e. the number of cycles needed for the fluorescence signal to overcome the background noise, as value to accurately quantify the amount of a target gene.

A double step protocol was followed, in which first complementary DNA (cDNA) was generated from total RNA samples by reverse transcription PCR (RT-PCR). 5-10µg of total RNA (~10µl) was mixed with 1µl of oligo-dT primer (0.5µg/µl) and RNase free water to bring up the volume to 12µl. Samples were incubated at 70ºC for 10 min and then on ice for 5 min. A master mix solution composed by 1µl RNasin (40U/µl; Promega, Southampton, UK), 1µl dNTPs (10mM), 1µl AMV reverse transcriptase (10U/µl Promega, Southampton, UK), 4µl 5x first strand buffer and 1µl RNase free water was added to each sample. The retro-transcription was carried out at 42ºC for 60 min, followed by incubation at 70ºC for 10 min. cDNA samples were stored at -20ºC and used for Q-PCR.

Every sample was tested in triplicate for the gene expression. To do so, 4µl of cDNA were mixed with 20µl SYBR Green Master Mix (Qiagen's QuantiTek, Manchester, UK), 4µl primers and 12µl dH_2O. From this mix, 10µl were added to 3 wells of a 384 well plate. GAPDH was used as endogenous housekeeping gene. The PCR conditions used were one cycle of 95ºC for 15 min followed by 40 cycles of 94ºC for 15 sec, 55ºC for 30 sec and 72ºC for 30 sec. These steps were then followed by a dissociation step of 95ºC for 15 sec, 60ºC for 15 sec and 95ºC for 15 sec. The ABI prism 7900HT PCR system and SDSv2.4 software (Applied Biosystem Inc., CA, USA) were used for the analysis of single transcripts.

Relative quantification of the transcripts was performed using the comparative Ct method (245). This approach compares the normalised Ct values of the samples of interest (transgenic mice in our case) to a control (wild type mice). Briefly, Ct values of both samples and control were normalised to the GAPDH gene and then the relative normalised values (called ΔCt) compared by difference (termed ΔΔCt). The final fold change was calculated using the $2^{-\Delta\Delta Ct}$ formulas.

2.15 Microarray analysis

Purified RNA was processed by using Ambion WT Expression kit and GeneChip WT Terminal Labeling Kit (Affimetrix, High Wycombe, UK). Whole-transcript expression analysis was performed by using Affimetrix Mouse Gene 1.1 ST array. The microarray service and the relative statistical analysis were provided by UCL Genomic facility (http://www.genomics.ucl.ac.uk/). The data were analysed by Dr Masahiro Ono (Department of Infection and Immunity, Institute of Child Health, University College London).

2.15.1 Preparing RNA samples for Affimetrix analysis

The following procedures and protocol has been provided and performed by Dr Simone Sharma at the UCL Genomic, Cancer Institute and Wolfson Institute for Biomedical Research, University College London. From the total RNA, transcript mRNAs were selected by rRNA reduction procedure. From these samples, double strand of complementary DNAs (cDNA) were synthetized by a double-step reaction

in presence of reverse transcriptase enzyme and primers containing T7 promoter sequence. The cDNA was used as template to synthetize antisense complementary RNA (cRNA) by using T7 RNA polymerase *in vitro* transcription (IVT) technology. The cRNA was cleaned up and used for the synthesis of sense single strand DNA (ss-DNA). During the synthesis, ss-DNA incorporated dUDP so that it can be fragmented in small DNA target. The ss-DNA was fragmented using a combination of uracil DNA glycosylase (UDG) and apurinic/apyrimidinic endonuclease 1 (APE 1), which removes uracil residues and cleaves the phosphodiester backbone where the base is missing. The fragmented DNA targets were labelled using terminal deoxynucleotidyl transferase (TdT) in presence of a biotinylated compound (Biotin Allonamide Triphosphate) and finally, hybridized to the array (Figure 2.16).

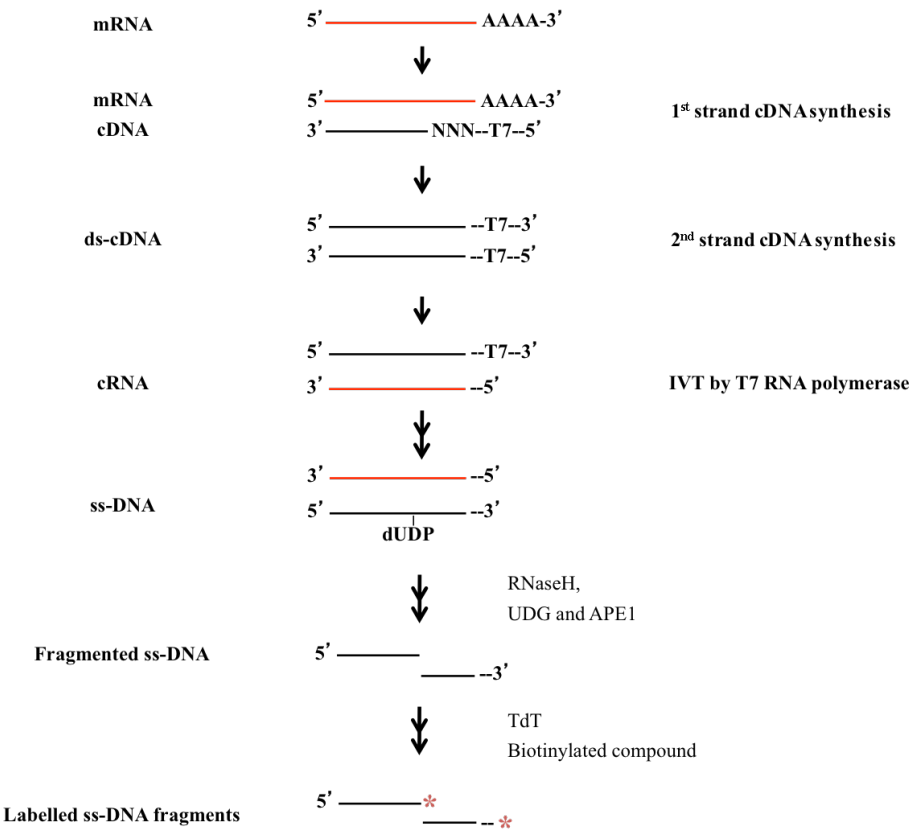

Figure 2.16. Flowchart of microarray sample preparation. Schematic steps for the preparation of samples before microarray analysis is performed.

2.15.2 Microarray

The Affimetrix Mouse Gene 1.1 ST array contains more than 770,000 unique, 25-mer oligonucleotide probes that interrogate more than 28,000 genes. Each gene or transcript is represented by 22 different oligonucleotides fragments (11 matches and 11 mismatches) which are synthetized directly on-chip.

Samples were hybridized to the chip and the excess was removed by washes. The arrays were ultimately stained with streptavidin-PE and processed for the analysis. The hybridization procedures were performed with a GeneChip Fluidics Station 450 while the arrays were scanned using the Affymetrix GeneChip Scanner.

Quality control (QC) was performed using Expression Console first and Bioconductor. The QC for hybridizations within the microarray experiment allows identifying outliers by different quality metrics thus to exclude them from the analysis.

The acquired data were normalized using the RMA normalization algorithm in Expression Console 1.2. RMA is the standard method used for probe summarization (i.e. calculating a transcript signal value from multiple independent probes) and normalization of Affymetrix expression array data.

Probe annotation and ANOVA analysis were performed using Partek software. Based on these tests, a list of genes with differential expression across groups was identified (according to p-values and corrected p-values by multiple hypothesis testing with Benjamini-Hochberg).

2.16 Immunoprecipitation and Western blot analysis

Cell lysis was performed using a lysis buffer containing 20mM Tris-HCl and 200mM NaCl at pH 8, 10µl/ml T-X100 and the following protease inhibitors (TNT buffer): 10mg/ml apotinin (10µg/ml), 200µM Na_3VO_4 (0.2µM; 1µl/ml), 1mg/ml Leupeptin (3µg/ml), 100mM PMSF (0.5mM; 5µl/ml), 1M NaF (1mM; 1µl/ml), 0.5mM PeP (0.5µM; 1µl/ml) and 0.5M EDTA (0.25mM; 0.5µl/ml). Cell pellets were resuspended in a 1:2 volume ratio of lysis buffer in round-bottom microfuge tubes, pipetted up/down several times and kept on ice for at least 5 min. Cell lysates were centrifuged at 13,226G for 10-15 minutes at 4ºC.

The supernatants were collected and analyzed for protein contents using the Bradford protein assay (5x Bio-Rad protein assay dye, Bio-Rad, Hertfordshire,UK) and BSA as standard. Briefly, BSA standard curves were prepared by 1:2 serial dilution of 2µg/µl BSA solution (in dH_2O). To determine the proteins content in the lysates, each sample was diluted in 1:250, 1:500 and 1:1000 in 1:5 Bio-Rad solution. The colorimetric changes were detected at spectrometer by plating 100µl of each sample and the standard curve in 96well plate. Absorbance was blanked against the Bio-Rad solution alone and read at 595nm using Thermo Scientific Multiskan FC machine.

Protein immunoprecipitates (IPs) were obtained incubating 500µl of conditioned medium or 100µl of protein lysate (diluted up to 500µl with TNT) with 1µl of primary antibody in presence of 50µl of mixed bead solution of protein A + G. The incubation was performed overnight at 4ºC under rocking. Each IP was then spun down, washed twice with 500µl TNT buffer and resuspended in 50µl of 6x sample

buffer (4% SDS, 20% glycerol, 10% 2-mercaptoethanol, 0.004% bromphenol blue and 0.125 M Tris-HCl, pH approx. 6.8).

Each sample was denatured at 90ºC for 5 min before loading onto SDS-polyacrylamide gel (10%) (precast high performance gel; NuPAGE SDS-PAGE Gel system, life technologies, Paisley, UK). Proteins were separated at constant voltage of 200V and then transferred onto 0.45μm pore size, hydrophobic, polyvinylidene difluoride Immobilon-P Transfer Membranes (Millipore, Watford, UK) at 4°C for max 2h at 125V.

Membranes were then blocked in 5% non-fat dry milk diluted in Tris-buffer saline solution containing 0.1% Tween 20 (TBST). Thereafter, membranes were incubated with primary antibody diluted in the same blocking solution – in particular: anti-AnxA1 polyclonal antibody in rabbit (Zymed Laboratories, Cambridge, UK; 1:1000 dilution) for 1h at RT under rocking and anti-C8orf42 polyclonal antibody in rabbit (Novus Biologics, Cambridge, UK; 1:1000 dilution) overnight at 4ºC under rocking. Membranes were then washed for 30 min with TBST with the solution being changed at 10-min intervals and incubated with the secondary antibody (HRP-conjugated goat anti-rabbit 1:2000, Dako, Cambridge, UK), for 1h at RT under rocking. Membranes were again abundantly washed with TBST and proteins were then detected using enhanced chemiluminescence (ECL) detection kit or Luminata Forte (Millipore, Watford, UK) and visualized on Hyperfilm (GE Healthcare, Little Chalfont, UK).

2.17 Animal behavioural tests

There are several experimental validated paradigms to test emotion-related behaviour in mice. These are based on the conflict-avoidance approach and exploit the natural tendency of mice to avoid aversive conditions such as brightly lit and open spaces. In this study mice were tested for anxiety- and depressive-like behaviour using the marble-burying test, open field test, climbing test and light/dark box test. These techniques and scoring system were initially mastered under the kind supervision of Dr. Robert Deacon, Department of Experimental Psychology, University of Oxford.

Mice were group-housed in quiet environmental conditions with food and water provided *ad libitum*. Temperature, room lightening and noise level were kept consistent for all the subjects throughout the tests.

2.17.1 Marble-burying test

Marble-burying tests were performed as described in Deacon RM, Nature Protocol 2006 (246). In details, 15 marbles were organized in 3 columns of 5 marbles each on 5-6 cm of lightly pressed sawdust in cages with tall walls (Figure 2.17, left picture). Mice were acclimated for 15-30 min in the room before performing the test. Single mice were observed for a period of 15 min during which several parameters were scored. These are: digging latency (the time elapsed before digging begins), number of bouts, total digging time and number of buried marbles- 2/3 of their depth (Figure 2.17).

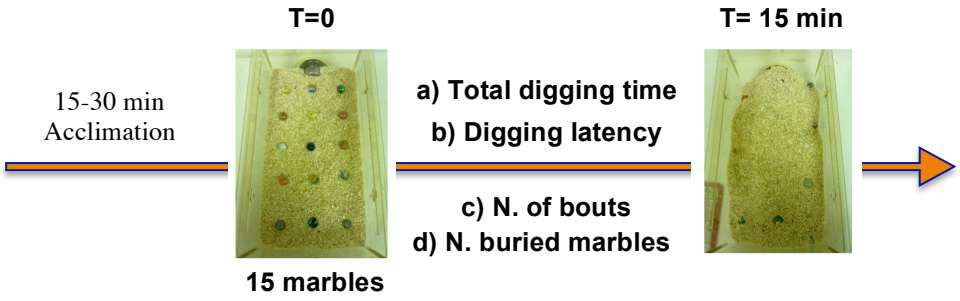

Figure 2.17. Marble-burying test. Mice were tested for anxiety-like behaviour using marble-burying test. It is 15-min test for single mouse in which a) total digging time, b) digging latency, c) number of bouts and d) number of buried marbles are scored.

2.17.2 Open field test

Motility, fear and explorative behaviour were tested through the open field test as described by Deacon (247). Briefly, mice were placed in a white wide arena (50x12x30cm) where a grid of 10cmx10cm squares was drawn (Figure 2.18, left picture). Explorative and emotional behaviours were scored for a time period of 3min measuring three different parameters: rearing latency (the time elapsed before the first rearing), numbers of rearing, numbers of squares crossed, number of passage through central squares and urination/defecation (Figure 2.18). Rearing is considered a natural movement of the mouse to stands up on its hind legs stretching its body up or towards a wall (Figure 2.18, middle picture). Between mice the walls and floor were cleaned with a moist, followed by a dry tissue.

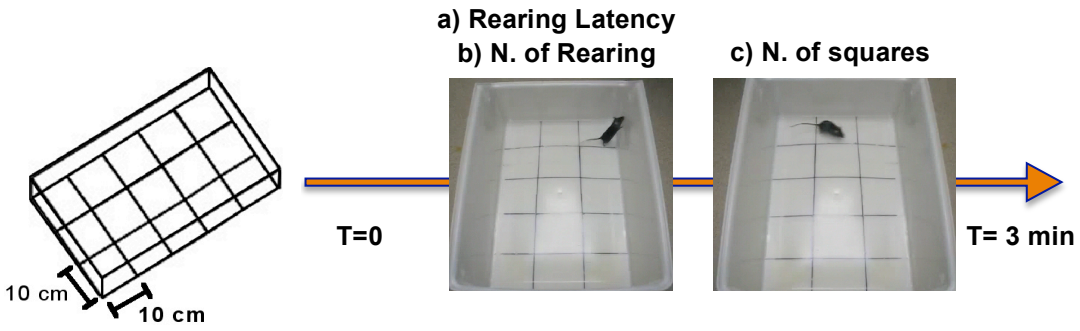

Figure 2.18. Open field test. Mice were tested for fear and explorative behaviour using the open field test. It is 3-min test for single mouse during which a) rearing latency (the time elapsed before the first rearing), b) total number of rearing and c) the number of crossed squares are scored.

2.17.3 Climbing test

The climbing test is a paradigm used to study fear and explorative behaviour in mice. We followed the procedure described in Deacon (personal communication). Single mice were placed inside a cylinder of wire mesh (6mm^2) 60 cm high, 28 cm diameter, closed at the top. The cylinder was placed on flat surface covered with a thin layer (about 0.5cm) of sawdust. Climbing is for a mouse to have all 4 feet on the wire mesh. Mice were recorded for 5 min during which the recorded parameters were latency to the first climbing (the time elapsed before the first climbing), total duration of climbing (the total time spent perched on the wire mesh) and number of climbing (Figure 2.19).

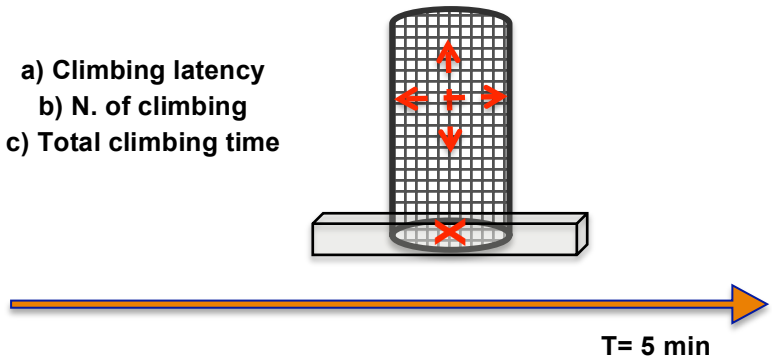

Figure 2.19. Climbing test. Mice were tested for fear and explorative behaviour using the climbing test. It is 5-min test per single mouse in which a) climbing latency, b) total number of climbing and c) the total climbing time are scored. (X= mouse at T_0; red arrows: mouse during the climbing).

2.17.4 Light/Dark box test

The light/dark box test is widely used to study anxiety in rodents and to test classical and new anxiolytic drugs such as benzodiazepines (248). The apparatus consists of an open white compartment 30x20x20 cm joined by a 3x3 cm opening to a dark box (painted black with a lid) 15x20x20 cm. One side of the light box is made transparent by making it from clear plastic, permitting viewing of the mouse from the side (Figure 2.20).

The test was performed as described in Deacon (249). Mice were placed in the middle of the lit side facing away from the opening. The latency to cross (all four feet) to the dark side, the time spent in the lit side (all four feet) and the number of transitions between the two compartments though the opening were measured for the 5 min duration of the test (Figure 2.20). The number of faecal boli and the

presence/absence of urination were also recorded. The cleaning regime between mice was to remove urine and/or faeces and wipe with moist followed by dry tissues the surfaces.

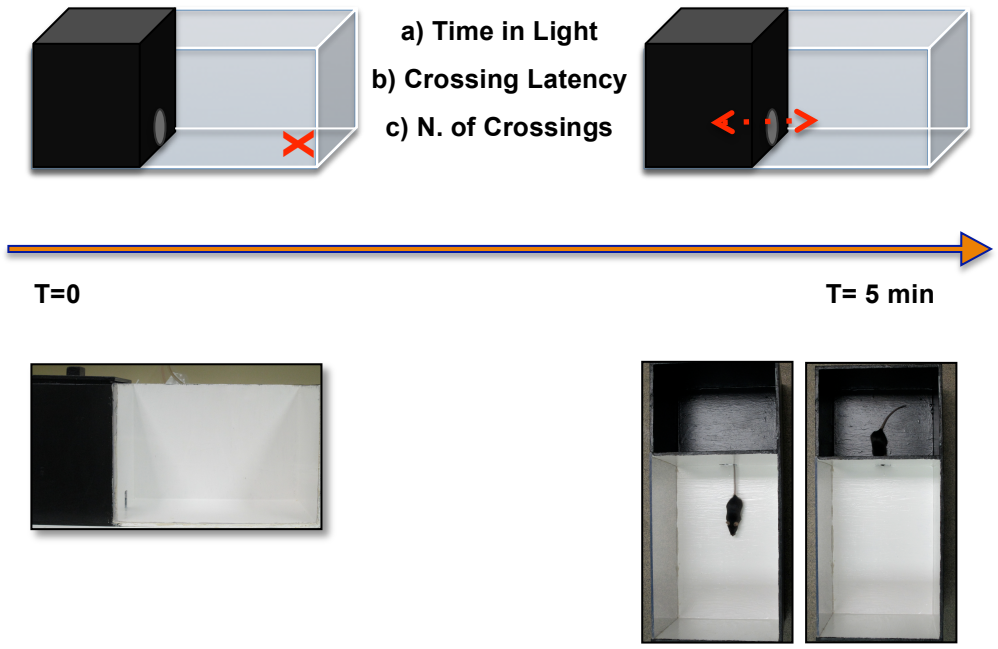

Figure 2.20. Light/Dark box test. Mice were tested for anxiety-like behaviour using the light/dark box test. It is 5-min test per single mouse during which are scored a) total time in light, b) crossing latency and c) the total number of crossings. (X= mouse at T_0, red arrows: crossing direction).

2.18 Statistical analysis

According to the nature of the data, t-test, one-way or two-away ANOVA analyses were used. Behavioural data were analysed with non-parametric tests such as Mann Whitney U test and Kruskal-Wallis method. Time-course observations were analysed with the repeated measures analysis and Boneferroni's post-doc test. All statistical analyses were performed through GraphPad PRISM software (version 4.0c) with the exception of microarray analysis which was performed as described in section 2.15.2. Data were considered significant when p-value was < 0.05.

3. Results

3.1 AnxA1^{tg} mice

The T cell-specific AnxA1^{tg} mice were generated by a previous PhD student in our lab. A detailed analysis of the immune cell repertoire and of thymocytes positive and negative selection was already been performed when I joined the lab. The following sections show part of the analyses that I have performed just at the beginning of my PhD.

3.1.1 Characterization of the T cell repertoire in AnxA1^{tg} mice

During their development in the thymus, thymocytes pass through stages of development defined by expression of cell surface markers. CD4- CD8- double negative (DN) cells differentiate into CD4+ CD8+ double positive (DP) cells that then mature into single positive CD4+ and CD8+ T cells. The DN population can be further subdivided by cell surface expression of CD44 and CD25: the most immature CD44+ CD25- DN cells (DN1) acquire CD25 expression to become CD44+ CD25+ (DN2). CD44 is then downregulated as cells become CD44- CD25+ (DN3), and CD25 is also downregulated as cells become CD44- CD25- (DN4). The DN4 population differentiates to DP cells.

In the thymus, the frequencies of pro-T cells (CD3- CD4- CD8-) divided in the four DN stages showed no significant changes in wild type and AnxA1^{tg} mice (Figure 3.1a). Similarly, there were no significant difference in the percentage of DP (CD4+ CD8+) as well as single positive CD4+ or CD8+ populations between wild type and AnxA1^{tg} mice (Figure 3.1b).

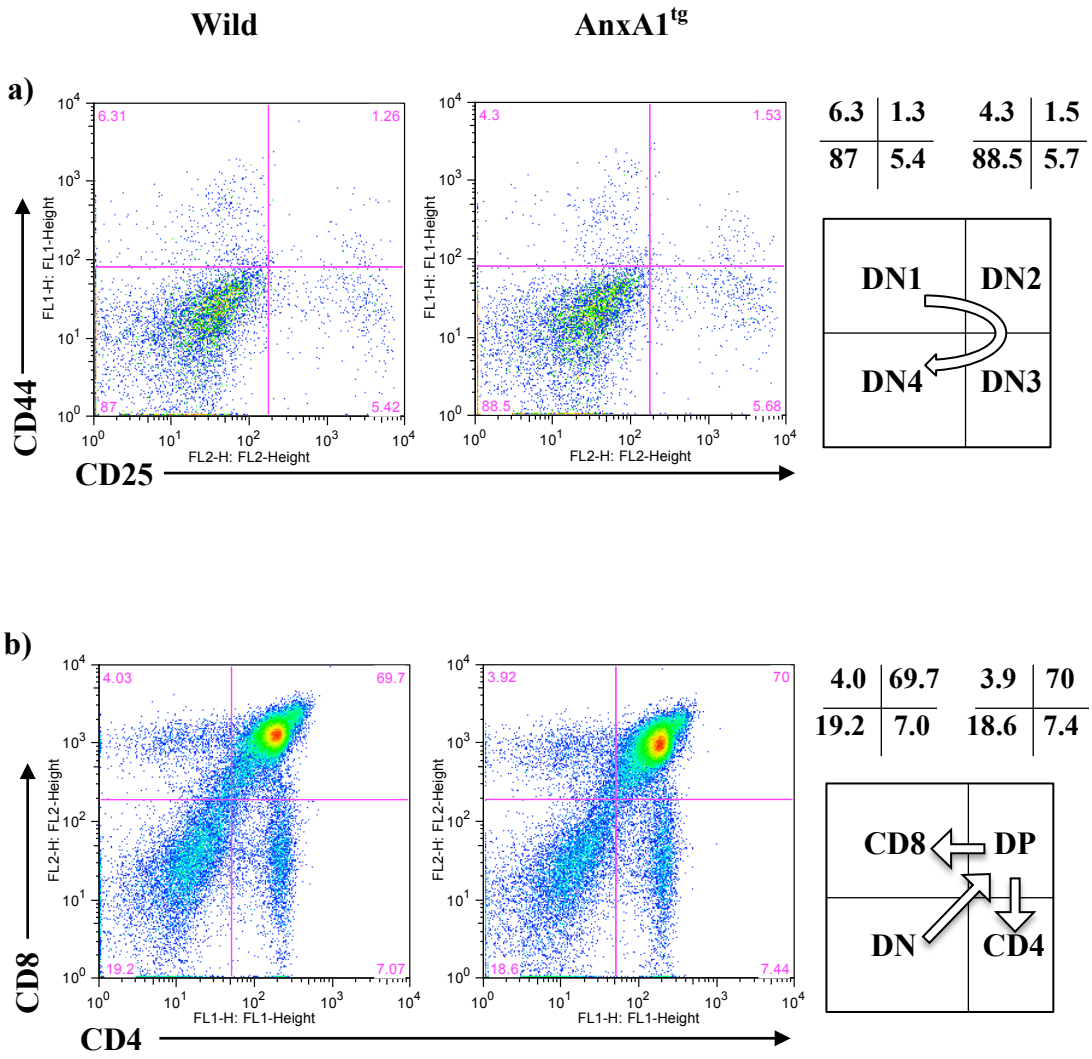

Figure 3.1 Thymocyte profile during T cell development. a) Development from DN1 to DN4 of thymocytes in wild type and AnxA1^{tg} mice using the expression of CD44 and CD25 surface cell markers: CD44+ CD25- (DN1), CD44+CD25+ (DN2), CD44- CD25+ (DN3) and CD44- CD25- (DN4). **b)** Maturation from DN to DP and then single positive CD4 and CD8 T cells in the thymus of wild type and AnxA1^{tg} mice.

The overexpression of AnxA1 does not influence the T cell development. In line with this, total cell counts of thymus are comparable between wild type and AnxA1^{tg} mice. However, total cell counts of lymph nodes, but not spleen show higher cellularity in the AnxA1^{tg} compared to wild type (Figure 3.2).

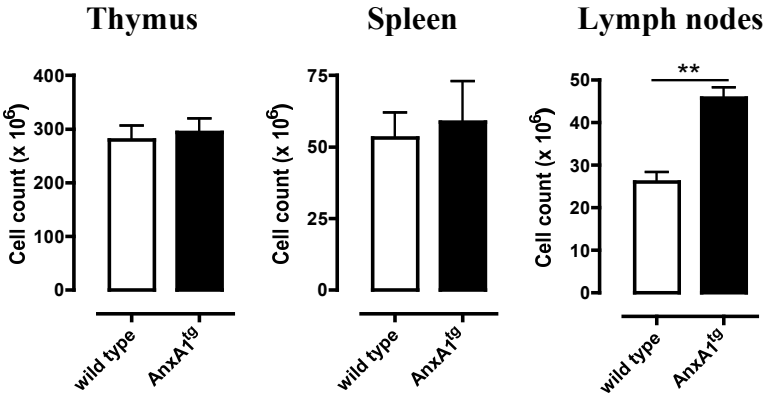

Figure 3.2. AnxA1^{tg} lymphoid organ cellularity. Cell counts of thymus, spleen and lymph nodes of wild type and AnxA1^{tg}, after organ homogenisation and mononuclear cell isolation (**p<0.01, n=4-5 mice per group; representative of N=2 separate experiments).

Lymphocytes were stained for CD3 as well as for CD4 and CD8. Although the percentages of CD3+ T cells do not change in the two groups, the number of CD3+ T cells is higher in the AnxA1^{tg} lymph nodes due to the higher cellularity (Figure 3.3). Then, analysis of the CD4+ and CD8+ T cells showed an increased percentage and number of CD4+CD3+ but not CD8+CD3+ T cells in AnxA1^{tg} compared to wild type (Figure 3.4).

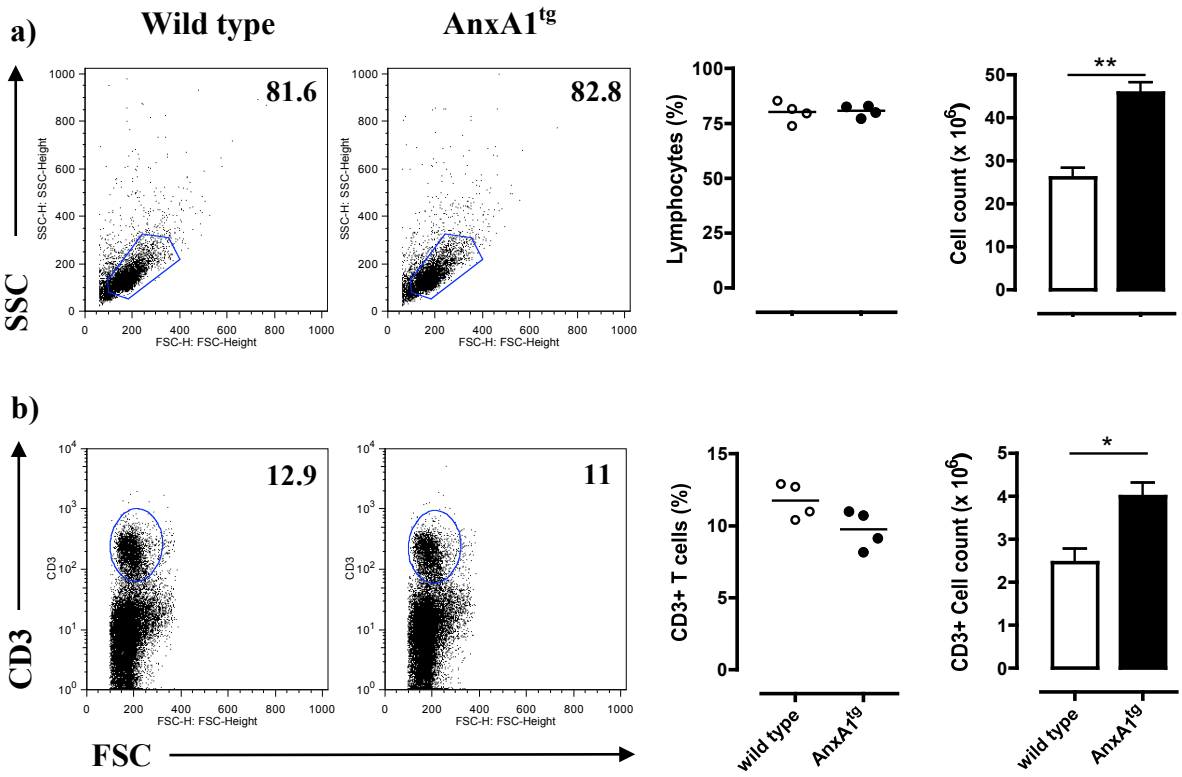

Figure 3.3. Lymphocytes in AnxA1^{tg} mice. a) Typical SSC/FSC dot plots of lymphocytes and **b)** CD3+ T cells collected from wild type and AnxA1^{tg} lymph nodes. Percentage values and total cell counts are reported in the right graphs. (*p<0.05; **p<0.01; representative of N=2 experiments of n=4-5 mice per group).

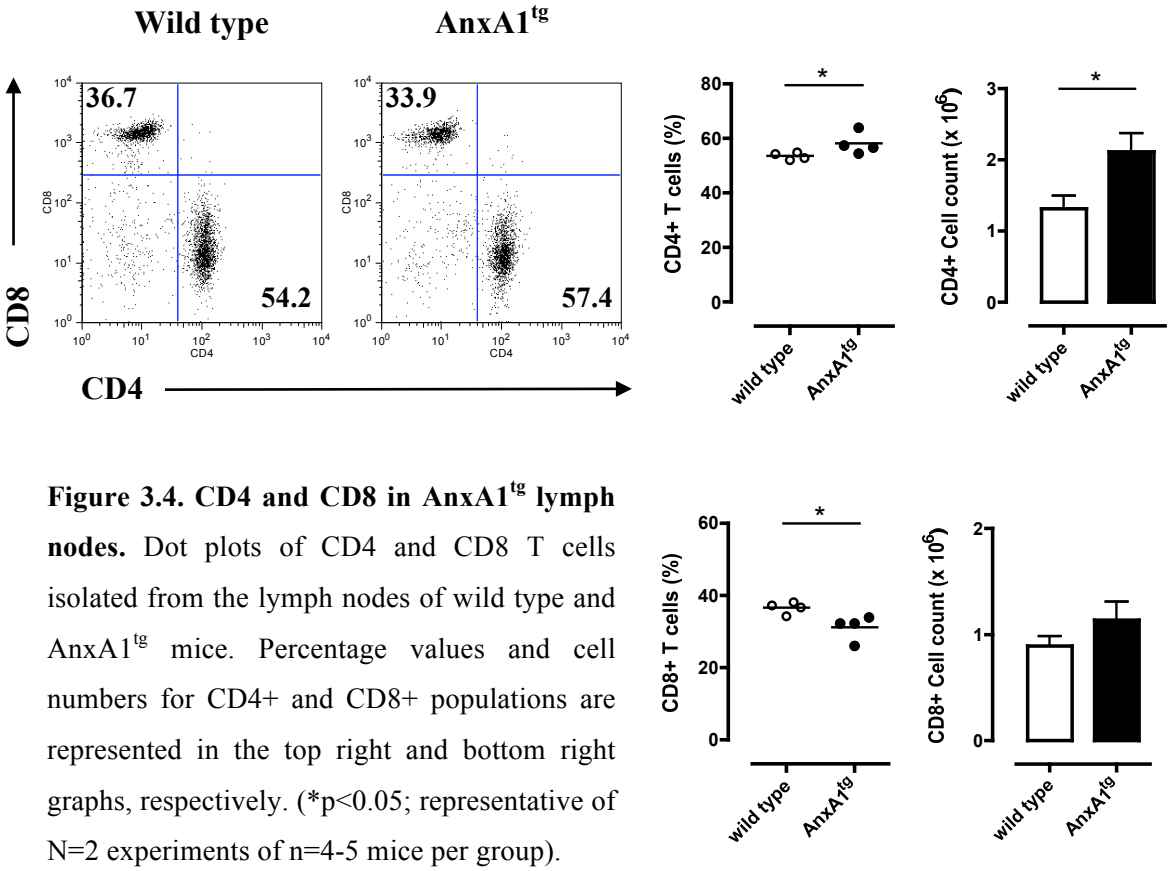

Figure 3.4. CD4 and CD8 in AnxA1^{tg} lymph nodes. Dot plots of CD4 and CD8 T cells isolated from the lymph nodes of wild type and AnxA1^{tg} mice. Percentage values and cell numbers for CD4+ and CD8+ populations are represented in the top right and bottom right graphs, respectively. (*$p<0.05$; representative of N=2 experiments of n=4-5 mice per group).

3.3.2 T cell proliferation

CD4+ T cells were tested for proliferation by CFSE dye dilution. Lymphocytes were stimulated using several conditions: a) plate-bound anti-CD3 (1 and 0.3 µg/ml); b) plate-bound anti-CD3 (1 and 0.3µg/ml) plus plate-bound anti-CD28 (1µg/ml); 3) plate-bound anti-CD3 (0.3µg/ml) plus soluble anti-CD28 (1µg/ml) and 4) soluble anti-CD3 (0.3µg/ml) plus soluble anti-CD28 (1µg/ml).

Stimulation with plate-bound anti-CD3 did not elicit the expected proliferative response that one should see based on a number of evidence in the literature. Both wild type and AnxA1^{tg} CD4+ T cells did not show a concentration-dependent response to anti-CD3 stimulation. The proliferation indexes were comparable to the non-stimulated condition in both wild type and AnxA1^{tg} T cells. However, these results in the Table 3.1 show that AnxA1^{tg} T cells has higher basal proliferation index. 86% of AnxA1^{tg} CD4+ T cells went through cell division against 69% of wild type and in addition these performed higher number of cell cycles compared to wild type as indicated by the replication indexes (Rep Index: 4.5 and 2.9, respectively) (Table 3.1; N=1 experiment).

Table 3.1: Proliferation analyses after plate-bound anti-CD3 stimulation

CD4+ T cells	Anti-CD3 (µg/ml)	% Divided	Prolif. Index	Rep. Index	Time
Wild type	-	68.5	1.33	2.9	72h
	0.3	85	1.24	2.7	72h
	1	75	1.3	2.9	72h
AnxA1^{tg}	-	86	2	4.45	72h
	0.3	84.3	2	4.5	72h
	1	78.4	2	4.7	72h

Wild type and AnxA1^{tg} CD4+ T cells also showed similar proliferation rate (Prolif. Index) upon plate-bound stimulation with anti-CD3/CD28 (Table 3.2). Interestingly, AnxA1^{tg} CD4+ T cells showed greater proliferation responses compared to wild type when stimulated with the lower concentration of anti-CD3 either plate-bound or in solution in the presence of soluble anti-CD28. This is indicated by the higher proliferation index, replication index and percentage of CD4 + cells going in cell division of AnxA1^{tg} compared to wild type T cells (Table 3.2; N=1 experiment). The Figure 3.5 and 3.6 show the proliferative response of wild type and AnxA1^{tg} lymphocytes, respectively, in absence of stimulation (left panel) and after plate-bound or soluble anti-CD3/CD28 stimulation. In particular, Figure 3.35b and 3.36b show the percentages of CD4+ T cells that have been through cell division i.e. positive for CFSE of wild type and AnxA1^{tg}. The CFSE profiles of these cells are shown in Figure 3.35c and 3.36c, which indicate the proliferation profile of wild type and AnxA1^{tg} CD4+ T cells, respectively.

Table 3.2: Proliferation upon anti-CD3/CD28 stimulation

CD4+ T cells	Anti-CD3 (0.3µg/ml)	Anti-CD28 (1µg/ml)	% Divided	Prolif. Index	Rep. Index
Wild type	Plate-bound	Plate-bound	72.6	1.35	3
	Plate-bound	Soluble	68.7	1.6	4
	Soluble	Soluble	**79.5**	**2**	**6.5**
AnxA1^{tg}	Plate-bound	Plate-bound	81.9	1.3	2.7
	Plate-bound	Soluble	75	1.9	5
	Soluble	Soluble	**85.5**	**2.4**	**8.4**

These are values obtained from one independent experiment

Anti-CD3	**-**	plate-bound	plate-bound	soluble
Anti-CD28	**-**	plate-bound	soluble	soluble

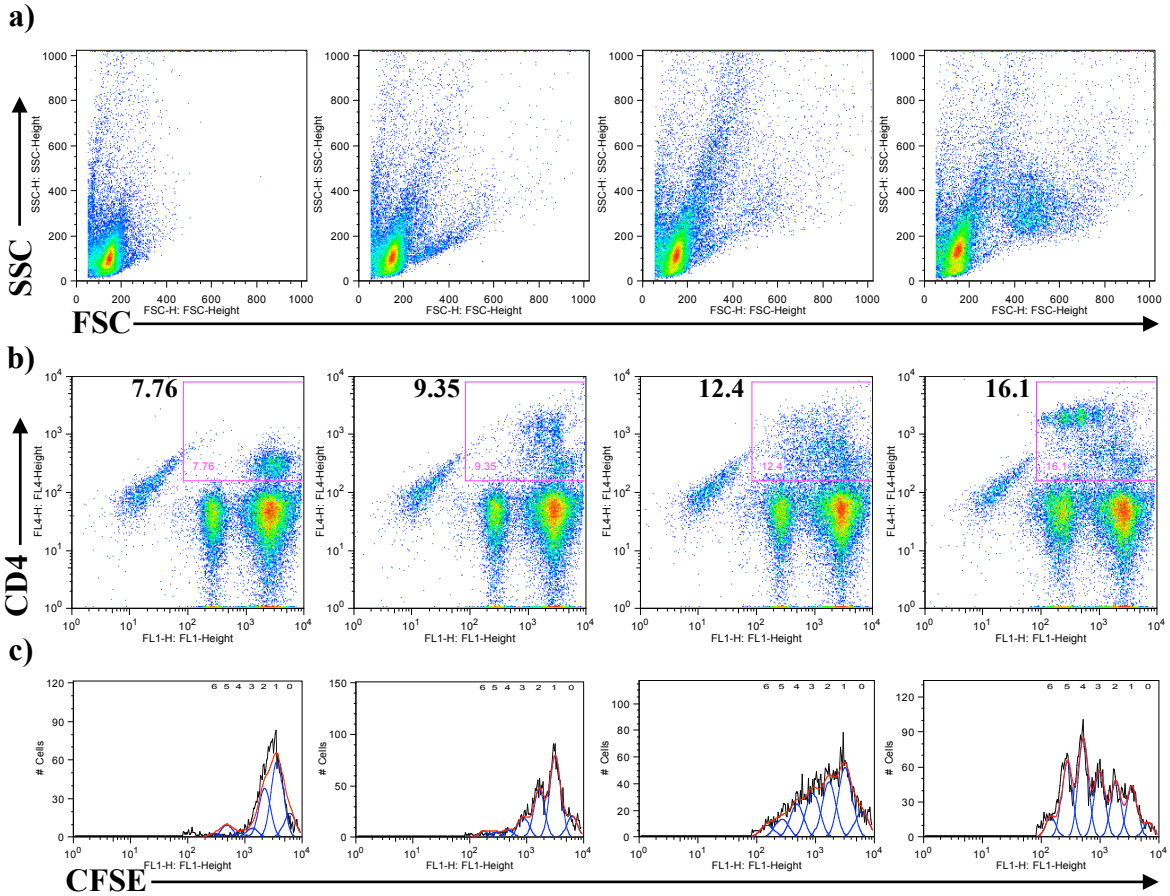

Figure 3.5. Wild type CD4+ T cell proliferation upon anti-CD3/CD28 stimulation. **a)** SSC/FSC and **b)** CD4+/CFSE dot plots of AnxA1^{tg} T cells without stimulation (left panel) or stimulated with anti-CD3 (0.3µg/ml) and anti-CD28 (1µg/ml) either plate-bound or soluble. **c)** CFSE fluorescence intensity in cell generations after proliferation calculated for CD4+ T cells gated in panel b.

Anti-CD3	-	plate-bound	plate-bound	soluble
Anti-CD28	-	plate-bound	soluble	soluble

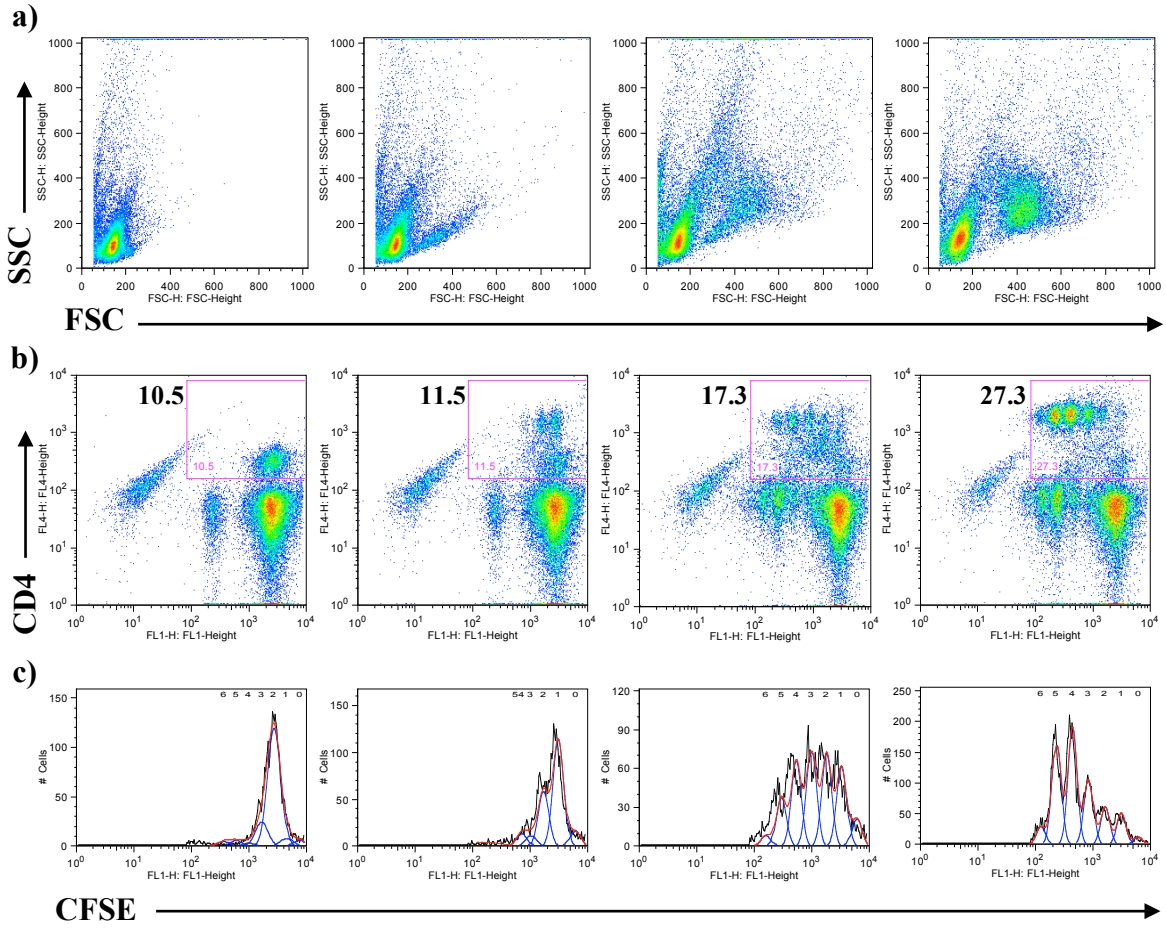

Figure 3.6. AnxA1^{tg} CD4+ T cell proliferation upon anti-CD3/CD28 stimulation. **a)** SSC/FSC and **b)** CD4+/CFSE dot plots of AnxA1^{tg} T cells without stimulation (left panel) or stimulated with anti-CD3 (0.3µg/ml) and anti-CD28 (1µg/ml) either plate-bound or soluble. **c)** CFSE fluorescence dilution in cell generations after proliferation calculated for CD4+ T cells gated in panel b.

3.2 Development of MOG_{35-55}-induced EAE and pristane-induced lupus in $AnxA1^{tg}$ mice

The sections below describe in details the parameters we have used to compare the development of autoimmune diseases in $Anxa1^{tg}$ to wild type mice. The experimental models we have used were the MOG_{35-55}-induced EAE as model of multiple sclerosis and the pristane-induced lupus as model of systemic lupus erythematosus.

3.2.1 Weight loss

The averaged weight of a healthy 6-7 week old C57BL/6 male mouse is about 19-22g and it typically increases over time as shown in Figure 3.7a. Body weight of wild type mice was tracked daily for a period of 20 days and the percentage of gain/loss weight was plotted over time. The mice gradually increased their body weight, which rises on average of 10%. On the contrary, MOG_{35-55}-immunised mice reduce their body weight over an equal period.

The weight of MOG_{35-55}-immunised mice was tracked for 20 days. In figure 3.7b, the percentages of the weight variation are plotted. These mice showed a biphasic change of body weight: first they gained gradually 10% weight in less than 10 days, and then rapidly lost a double amount of their weight increase in the following 5 days. Finally, in the last period of 5 days they gained again weight but they never recovered the initial body weight.

The dramatic weight drop occurs simultaneously to the onset phase of EAE. The weight loss starts even before the clinical signs of EAE were visible as is highlighted by the yellow box in Figure 3.7c. Thus, the body weight was used as parameter to monitor health and/or illness in mice.

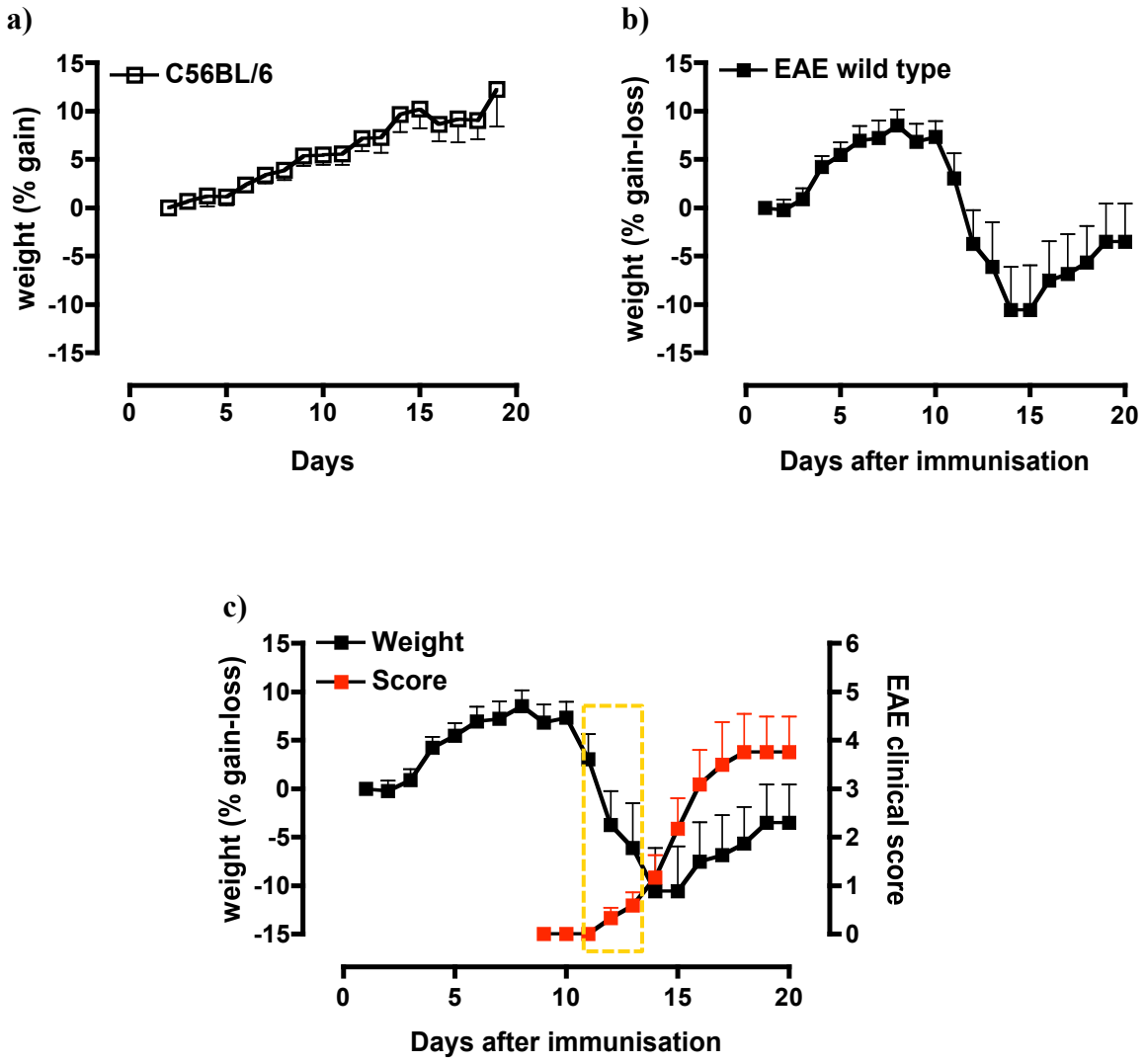

Figure 3.7. Weight variation as disease biomarker. a) Typical daily variation of weight in 6-7 week old male control mice (n= 3). **b)** Typical weight loss in MOG_{35-55}-immunised mice (n=6). The graph in **c)** shows an overlay of the weight loss and the EAE clinical scores. The appearance of disease signs occurs simultaneously to weight sinking (yellow square-dot box).

3.2.2 MOG_{35-55} induced EAE in $AnxA1^{tg}$ mice

Weight loss is one of the parameter that can be used to assess and track the development of the EAE, as mentioned above. As shown in Figure 3.8a, $AnxA1^{tg}$ mice displayed a more pronounced body weight loss compared to wild type as the disease developed. The reduction of body weight for $AnxA1^{tg}$ mice started at day 10 and reached about 15% at day 20. Conversely, for wild type mice the weight loss started at day 13 and never reached more than 5% in the following days.

When we considered the percentage of incidence of disease it was interesting to notice that $AnxA1^{tg}$ showed a reduced number of diseases animals (about 20%) compared to wild type (about 70%) at day 12. However, these differences quickly levelled off in the following 2 days and remained comparable from day 14 onwards (Figure 3.8b).

Although the incidence of disease progressed and reached the same levels in wild type and $AnxA1^{tg}$ mice, the severity of the clinical score were remarkably different from day 16^{th} onwards. The EAE in $AnxA1^{tg}$ mice showed a progressive linear increase in clinical score that reached a maximum of 4-5 at the later stages (day 17^{th} onwards). Conversely, wild type mice showed a maximum score of 2-3 at day 16^{th} and remained at this level till the end of the experiment. The difference between the two EAE clinical score curves is statistically significant and independent of the experiment size ($p<0.0001$ calculated by two-way ANOVA test, Figure 3.8c).

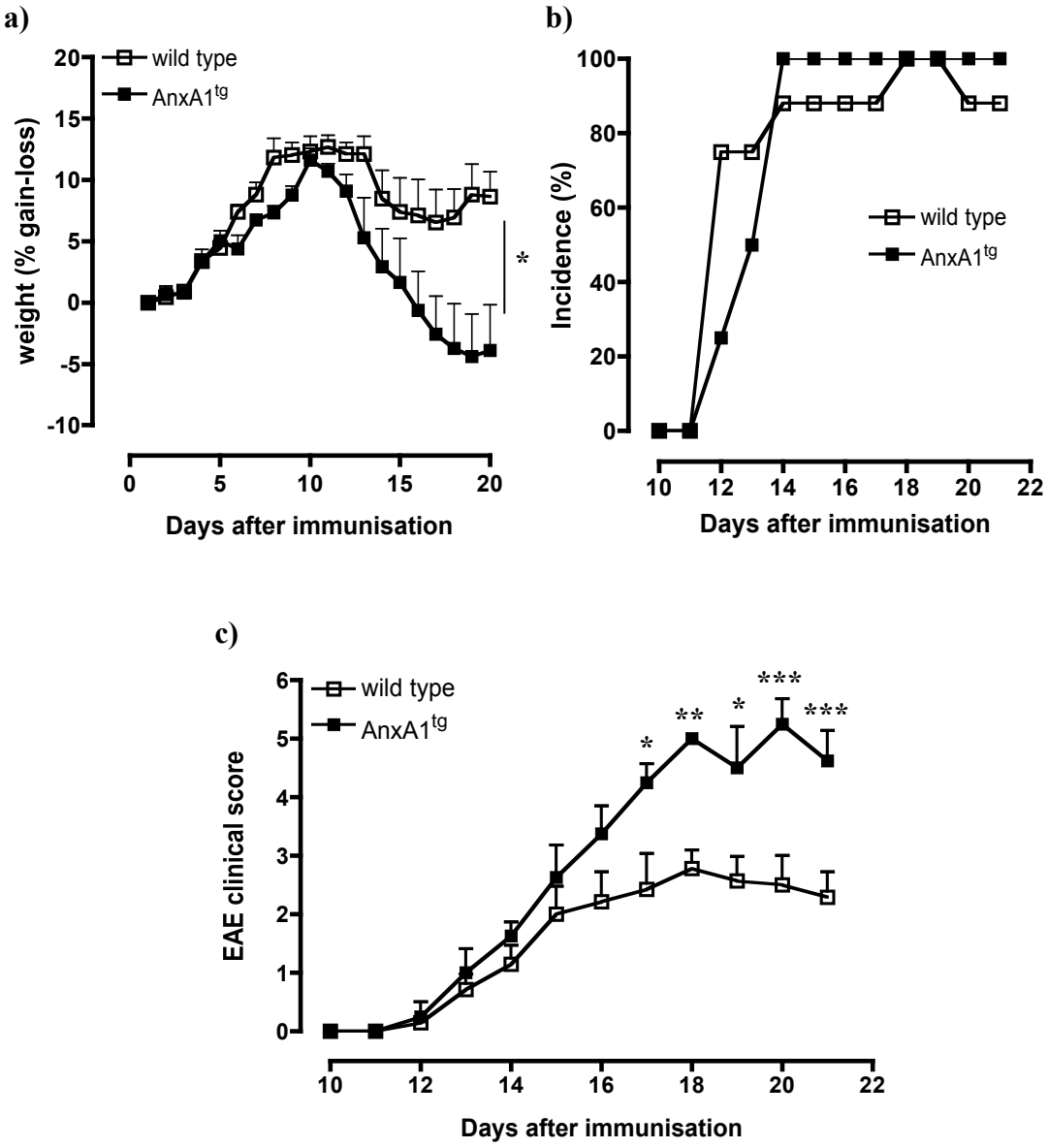

Figure 3.8. MOG_{35-55} induced EAE in wild type and $AnxA1^{tg}$ mice. a) Percentage of weight gain-loss, **b)** incidence of disease and **c)** EAE clinical score of wild type and $AnxA1^{tg}$ mice, respectively (Two-way repeated measure ANOVA, Bonferroni post-test, *p<0.05, **p<0.01, ***p<0.001; n=8; representative experiment of N=3).

Consistent with these results, analysis of the H&E staining of the spinal cord sections obtained at day 14 showed fewer areas of leukocytes infiltration and tissue damages in the wild type compared to AnxA1^{tg} (Figure 3.9).

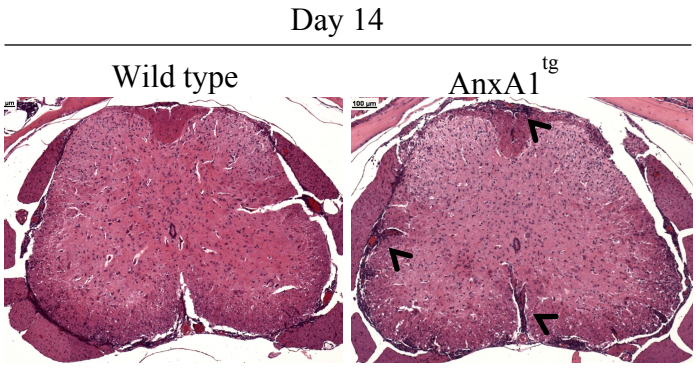

Figure 3.9. Spinal cord sections at 14th day of MOG$_{35-55}$ induced EAE. H&E staining of lumbar sections of spinal cords collected from wild type (left panel) and AnxA1^{tg} (right panel) mice at day 14th after immunisation with MOG$_{35-55}$. Arrowheads highlight areas of leukocytes infiltrations.

The exacerbated development of disease in AnxA1^{tg} mice was most evident when wild type control mice showed middle to mild signs of disease. Indeed, we could not observe any significant difference in experiments where control mice reached that maximum score of disease. The Table 3.3 shows the analysis of disease incidence and area under the curve (AUC) between wild type and AnxA1^{tg} mice in two typical experiments with different disease severity. The autoimmune-prone phenotype of AnxA1 is better revealed in the experiment #2 where the severity of the disease of the control is lower compared to that obtained in the experiment #1.

Table 3.3: Difference in disease development between wild type and AnxA1tg mice.

Exp	Mice	Incidence	AUC	% of AUC increase
#1	Wild type	90% (9/10)	20.5 ± 3.4	
	$AnxA1^{tg}$	90% (9/10)	25± 4.8	22%
#2	Wild type	87.5% (7/8)	16 ± 3.0	
	$AnxA1^{tg}$	100% (8/8)	26.3± 4.0	62%

Data are from two independent experiments with n=8-10 mice per group.

These results suggest that AnxA1 overexpression in T cells acts as a catalyser and amplifier of disease development and are consistent with previous observations obtained *in vitro* that suggested AnxA1 as a homeostatic modulator of strength of TCR signalling (145).

3.2.3 Pristane-induced lupus in AnxA1^{tg} mice

As for the EAE, monitoring weight gain/loss during the development of pristane-induced lupus provides a very useful indication of the severity of the disease. Similar to what we observed with the EAE model, pristane-challenged AnxA1^{tg} mice showed a dramatic weight loss compared to wild type especially during the first two weeks of assessment (Figure 3.10a). These early signs of disease were associated to a progressive reduction in survival that started as early as 7 days from the challenge and reached 70% after 3 weeks (Figure 3.10b).

a)

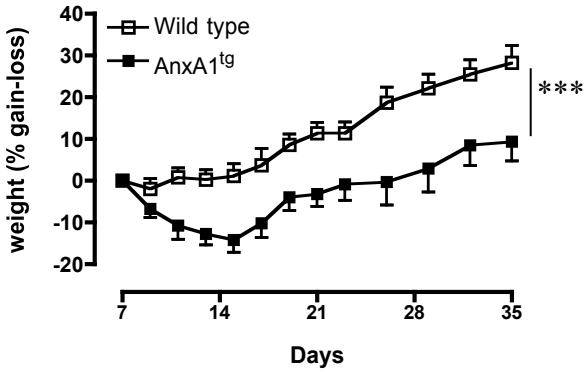

b)

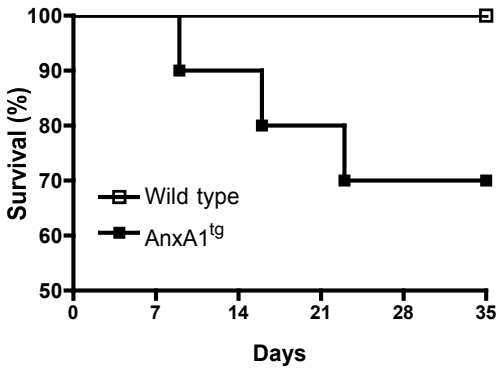

c)

	Live	**Dead**	total
Wild type	8	0	8
AnxA1^{tg}	7	3	10
total	15	3	18

Figure 3.10. Pristane-induced lupus in wild type and AnxA1^{tg} mice. a) Percentage of weight gain-loss and **b)** Kaplan-Meier survival curve of wild type and AnxA1^{tg} mice. **c)** Number of mice alive or dead per group at day 35; contingency table used for Fisher's exact test. (Two-way repeated measure ANOVA, Bonferroni post-test, ***p<0.001; n=8-10 per group).

This increased lethality was matched by more severe signs of tissue inflammation as evidenced by the histological analysis of the target organs such as the spleen and the lungs. Macroscopically, the spleens of AnxA1^{tg} mice were twice the size of those of wild type, with clear differences in colour with the AnxA1^{tg} being of a much lighter red colour compared to the wild type (Figure 3.11a, left panels). The lungs of AnxA1^{tg} mice also showed a very different outlook with peculiar dark-dots spotted parenchyma (an indication of haemorrhagic areas) compared to the classical clear pink colour of the control parenchyma (Figure 3.11b, left panels).

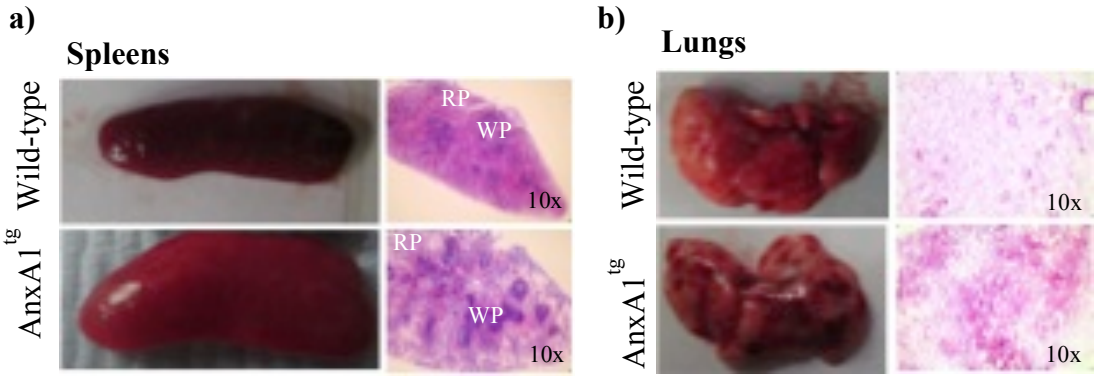

Figure 3.11. Macroscopical and microscopical difference of the spleens and lungs of pristane-challenged AnxA1^{tg} and wild-type mice. a) Spleen of wild type (top left panel) and AnxA1^{tg} (bottom left panel) mice one month after the challenge. On the right panels, the related sections after H&E staining (10x). RP: red pulp; WP: white pulp. **b)** Right lung of wild type (top left panel) and AnxA1^{tg} (bottom left panel) mice one month after the challenge and the related H&E staining of histology sections (right panels; 10x).

H&E staining of the same tissues showed a clear accumulation of white material in in the spleen and dense area of inflammation and cell infiltration in the lung of AnxA1^{tg} mice compared to wild type (Figure 11a and b, bottom right panel).

3.3 Investigate the nature of AnxA1^{tg} T cells in EAE

The results showed so far in two models of autoimmune diseases support the hypothesis of AnxA1^{tg} mice being an autoimmune-prone phenotype. To further investigate mechanisms responsible for the *in vivo* effects, we performed quantitative and qualitative analyses of the T cell phenotype developed during the progression of the EAE in AnxA1^{tg} and wild type mice.

As I have discussed in the Introduction (section *1.2.4 T helper cells and autoimmune diseases*), current views on the role of effector Th cells in autoimmune diseases have recognised the importance of T cell plasticity in determining the pathogenic function of these cells in these diseases. To assess the impact of AnxA1 overexpression on T cell plasticity I have performed the analyses of the Th phenotype at two time points: at day 9 and day 16.

Day 9 is a time preceding the development of signs of disease and has thus been chosen to identify differences in events like T cell priming and activation that occur in the peripheral lymphoid organs at the early stage of the disease. Day 16 is the time the disease is fully developed and thus has been chosen to investigate the phenotype of the T cells infiltrated in the target organ i.e. in the spinal cord in this case. These tests has allowed us to investigate how the overexpression of AnxA1 in T cells would influence the "plastic" adaptation that Th cells experience once they are in the target organ i.e. spinal cords and hence indirectly, the effect of AnxA1 on T cell plasticity (Figure 3.12).

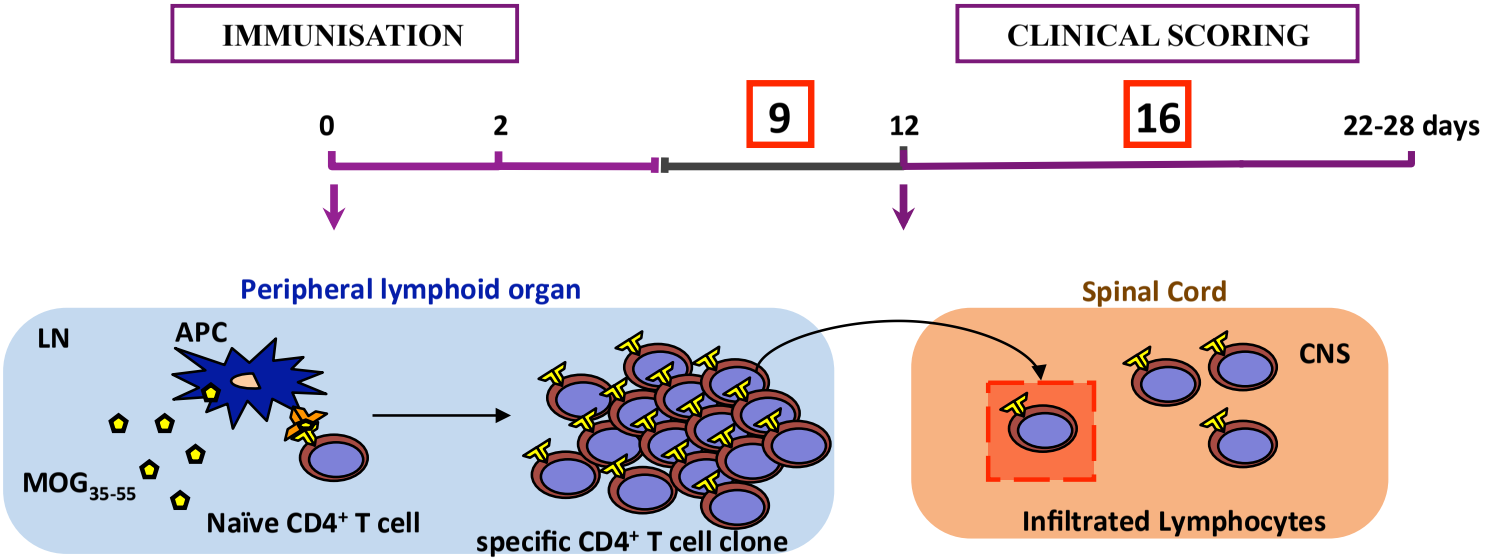

Figure 3.12. Scheme of the experimental strategy used to study Th phenotype during EAE. CD4+ T cell phenotypes were studied at two time points of the EAE: day 9 and 16 after immunisation. The 9th day was chosen to investigate the differences of T cell priming and activation occurring in the peripheral lymphoid organs (lymph nodes and spleen), while the 16th day was used to study the plasticity of T cell phenotype occurring in the target organ (spinal cord).

3.3.1 Influence of AnxA1 on T cell priming and differentiation *in vivo*

Analysis of the total cell count of lymph node and spleen cells harvest from AnxA1^{tg} and wild type mice at 9 day after the immunisation showed no significant differences. To investigate possible differences in T cell phenotypes, cells were stimulated with MOG_{35-55} (100µg/ml) or anti-CD3 and anti-CD28 (5µg/ml) for 72h and then analysed by intracellular staining.

Gated CD4+ T cells from wild type (top panels) and AnxA1^{tg} (bottom panels) from control un-stimulated conditions showed no difference in the profile of IFNγ and IL-17 or GM-CSF and IL-17 production (Figure 3.13 and 3.14, respectively). Stimulation with either MOG_{35-55} or anti-CD3/anti-CD28 showed higher percentages of IFNγ+ or GM-CSF+ CD4+ T cells in AnxA1^{tg} cultures compared to wild type. However, analysis of the cumulative data performed on a number of experiments showed no significant difference in the percentages of CD4+ T cells producing IFNγ, GM-CSF or IL-17 between the two groups (Figure 3.15).

Analysis of the cell supernatants at the end of their differentiation by CBA confirmed these findings and showed no significant difference in the levels of IFNγ and IL-17 whereas GM-CSF was found to be significantly higher in the AnxA1^{tg} than the wild type ($p=0.029$) (Figure 3.16).

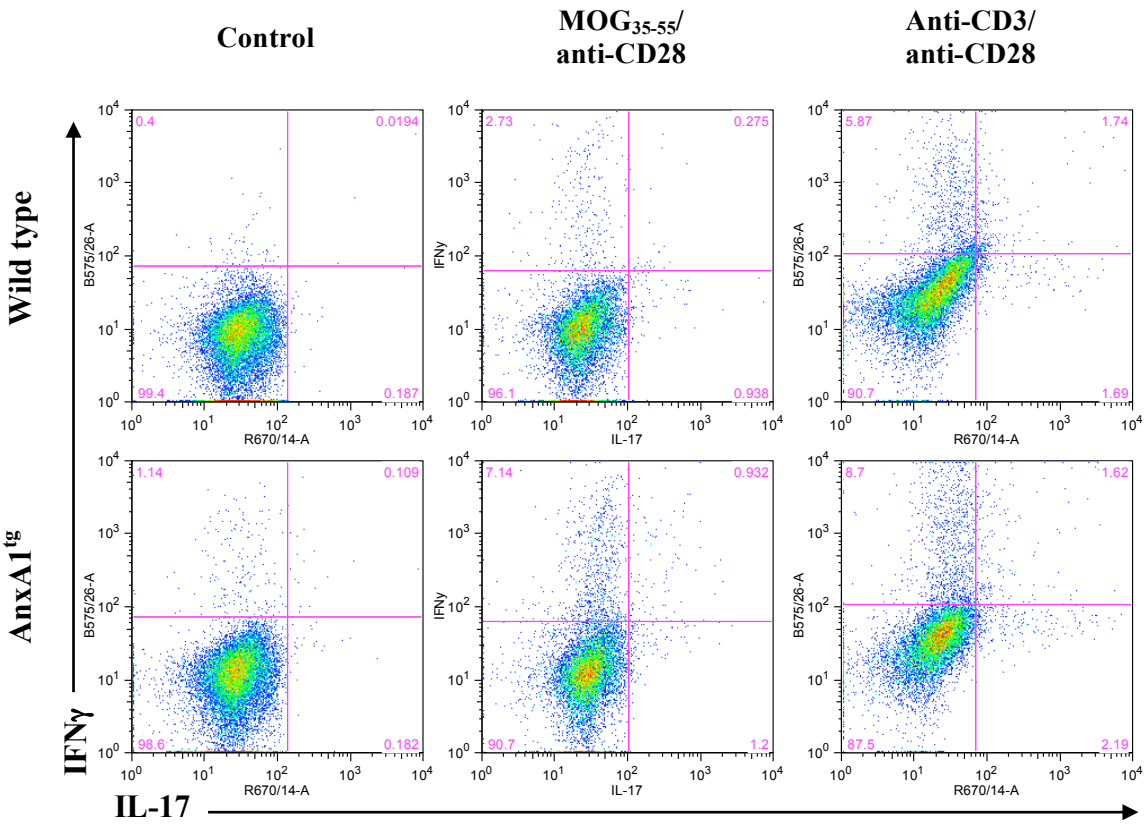

Figure 3.13. IFNγ and IL-17 expression in CD4+ T cells from wild type and AnxA1^{tg} mice at day 9 of EAE. Lymphocytes from peripheral lymphoid organs were cultured in only medium (Control, left panels), in presence of MOG_{35-55}/anti-CD28 (middle panels) or anti-CD3/antiCD28 (right panels) for 72h.

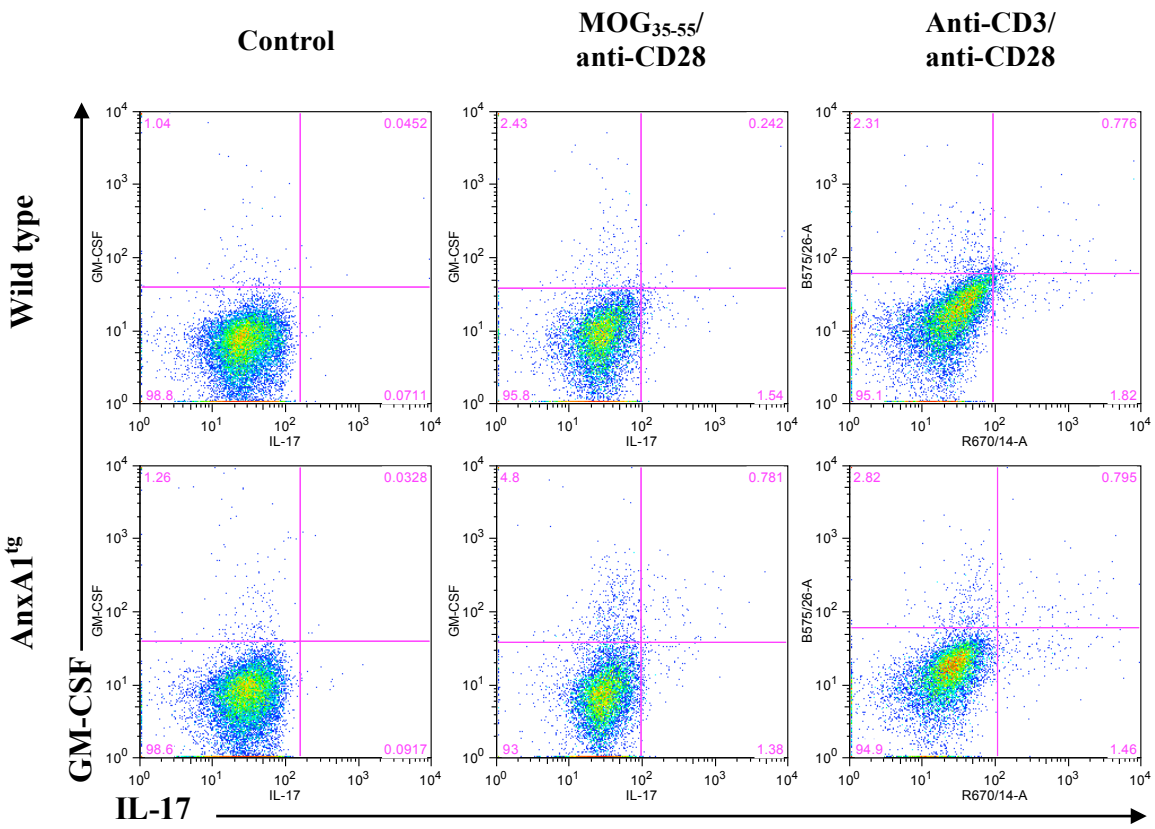

Figure 3.14. GM-CSF and IL-17 expression in CD4+ T cells from wild type and AnxA1^{tg} mice at day 9 of EAE. Lymphocytes from peripheral lymphoid organs were cultured in only medium (Control, left panels), in presence of MOG_{35-55}/anti-CD28 (middle panels) or anti-CD3/anti-CD28 (right panels) for 72h.

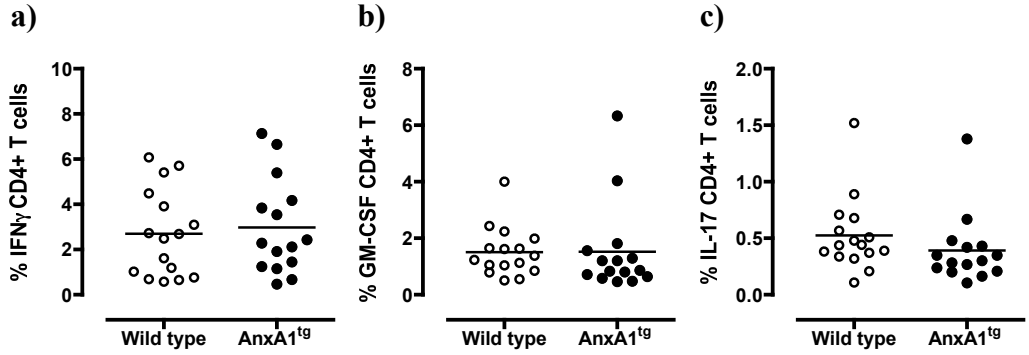

Figure 3.15. Cytokines expression of CD4+ T cells from peripheral lymphoid organs after restimulation with MOG_{35-55}/anti-CD28. Percentagees of **a)** IFNγ+, **b)** GM-CSF+ and **c)** IL-17+ CD4+ T cells in wild type and $AnxA1^{tg}$ lymphocytes collected at day 9 of EAE and restimulated in vitro with MOG_{35-55}/anti-CD28 (unpaired t-test; cumulative data of N=4 experiments with n=4-5 mice).

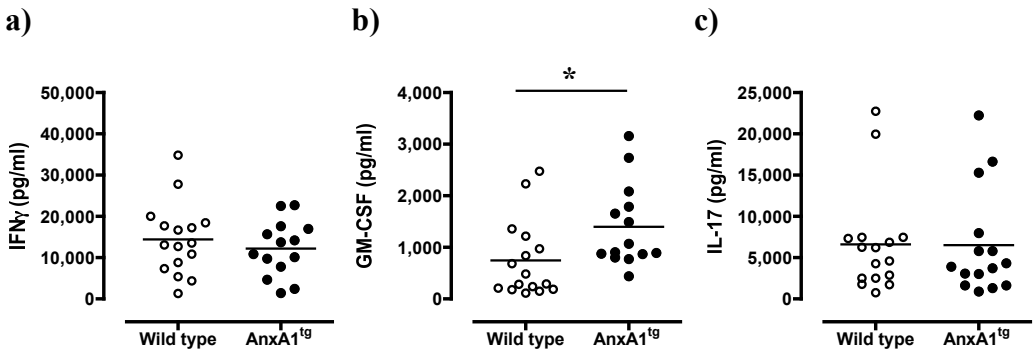

Figure 3.16. Cytokine production by lymphocytes from peripheral lymphoid organs after restimulation with MOG_{35-55}/anti-CD28. CBA quantification of **a)** IFNγ, **b)** GM-CSF and **c)** IL-17 released by wild type and $AnxA1^{tg}$ lymph node cells and splenotytes after restimulation for 72h (p=0.029, unpaired t-test; cumulative data of N=4 experiments with n=4-5 mice).

3.3.2 Influence of AnxA1 on T cell plasticity *in vivo*

Total cell counts as well as pecentages of CD4+ and CD8+ T cells did not change in the spinal cord at day 9 of EAE (Figure 3.17a, top panels, and 3.17b), and hence it was not technically possible for us appreciate potential differences in phenotype between wild type and AnxA1^{tg} mice.

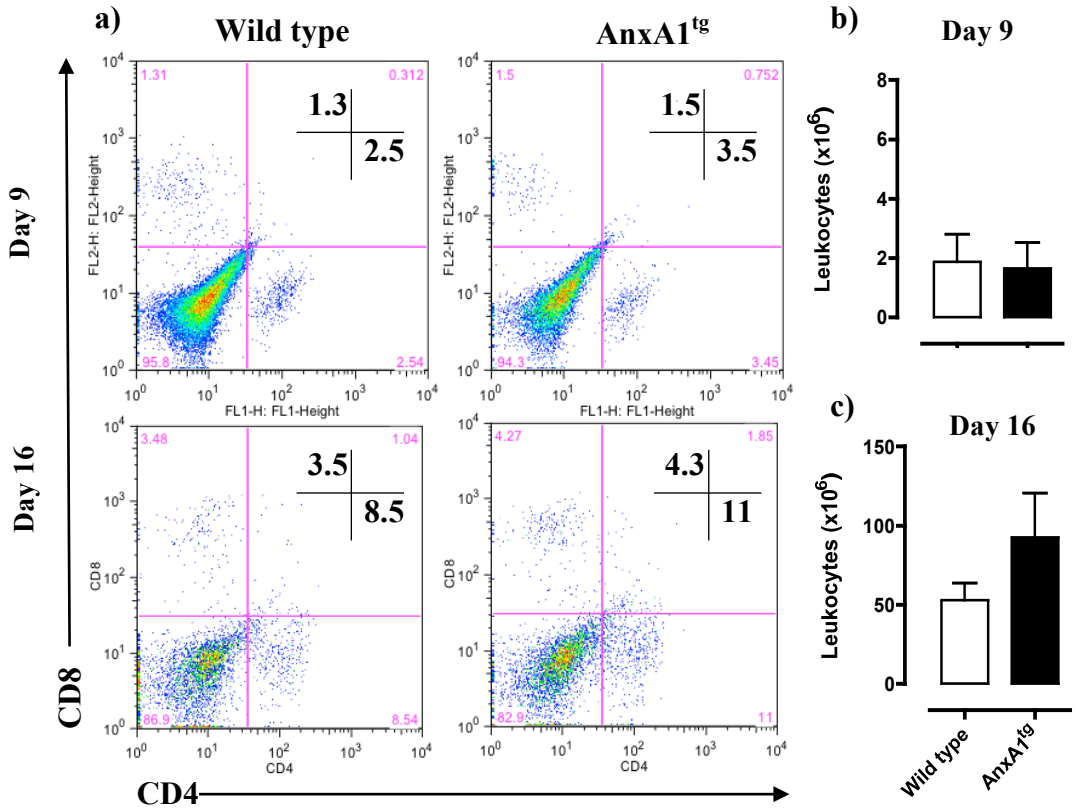

Figure 3.17. T cells infiltrated in the spinal cord of wild type and AnxA1^{tg} mice at day 9 and 16 of EAE. a) CD4+ and CD8+ T cells infiltrated in the spinal cord of wild type and AnxA1^{tg} mice at day 9 (top panels) and day 16 (bottom panels). Total cell counts of leukocytes purified **b)** at day 9 and **c)** at day 16 from the spinal cord of wild type and AnxA1^{tg} mice (unpaired t-test, n=4-5 per group of N=2 experiments).

Conversely, analysis of the total cell count of T cells infiltrated into the spinal cord of immunised mice at day 16 showed a larger population of infiltrated CD4+ and CD8+ T cells in AnxA1^{tg} mice compared to wild type (Figure 3.17a, bottom panels and 3.17c). Both cell number and percentages of CD4+ T cells were almost doubled in AnxA1^{tg} compared to wild type (Figure 3.18).

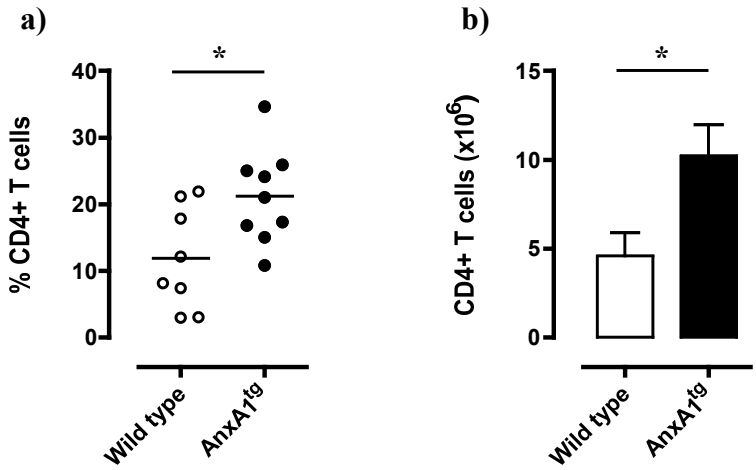

Figure 3.18. CD4 T cells in the spinal cord on day 16 of EAE. a) Percentage and **b)** number of CD4+ T cells purified from the spinal cord of wild type and AnxA1^{tg} mice at day 16 (*$p<0.05$, unpaired t-test; n=4-5 mice per group of N=2 experiments).

When we next investigated IFNγ, GM-CSF and IL-17 production by ICS, we observed an increased percentage of IL-17 producing T cells in the infiltrates of AnxA1^{tg} mice; both as single defined IL-17+ populations and as double positive populations for IL-17 and IFNγ or GM-CSF (Figure 3.19a and 3.19b, top- and bottom- right gates in each dot plot). The pronounced Th17 phenotype of AnxA1^{tg} mice was also associated with a reduction of a single IFNγ producing CD4+ T cell population when compared to wild type mice (top left gates in Figure 3.19a).

The graphs in Figure 3.20 represent the cumulative data of two independent experiments and confirmed the increased percentage of IL-17+/IFNγ and IL-17+/GM-CS CD4+ T cells in the spinal cord infiltrates of AnxA1^{tg} mice compared to wild type.

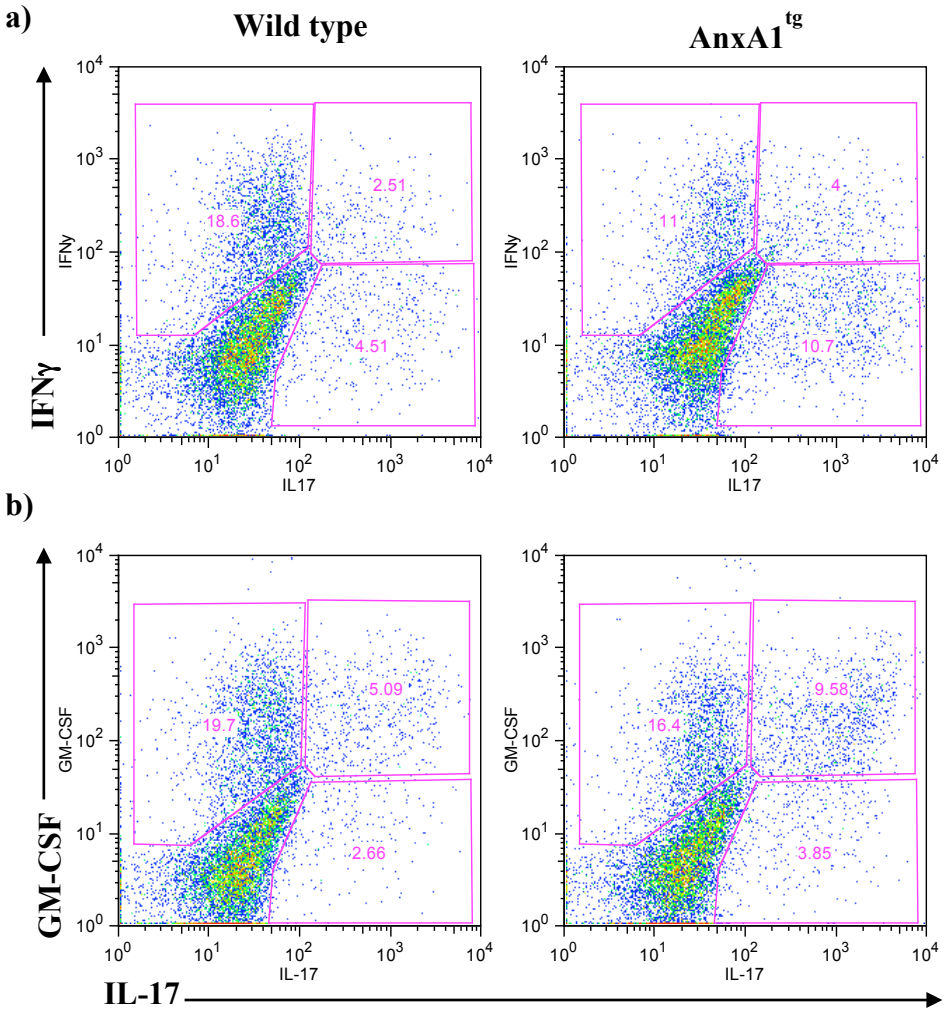

Figure 3.19. CD4+ T cell subsets in spinal cord infiltrate on day 16. a) IFNγ (top-left gate), IL-17 (bottom-right gate) and IFNγ/IL-17 (top-right gate) expressing CD4+ T cells in wild type and AnxA1^{tg} mice. **b)** GM-CSF (top-left gate), IL-17 (bottom-right gate) and GM-CSF/IL-17 (top-right gate) expressing CD4+ T cells in wild type and AnxA1^{tg} mice.

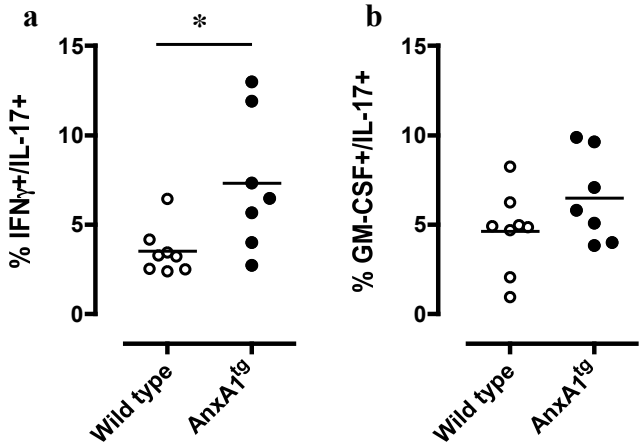

Figure 3.20. Pathogenic phenotype of CD4+ T cells purified from spinal cord at day 16. Percentages of **a)** IFNγ+/IL-17+ and **b)** GM-CSF+/IL-17+ CD4+ T cells purified from the spinal cord of wild type and AnxA1^{tg} at day 16 of the EAE (*p=0.02, unpaired t-test; cumulative data of N=2 independent experiments with n=3-5 mice).

3.4 AnxA1^{tg} T cells in pristane-induced lupus

To investigate the phenotype of CD4+ T cells in pristane-induced lupus, we used the day 14 peritoneal lavage fluids of pristane-challenged mice. AnxA1^{tg} mice show lower percentages and number of CD4+ T cells compared to wild type most likely because of the exacerbated severity of the disease of the former compared to the latter (Figure 3.21). The paucity of recovered cells has made the analysis of the CD4+ T cell phenotype by ICS very difficult. Figure 3.22 shows the percentages of of CD4+ and IFNγ, IL-17 or IL-4 positive T cells found.

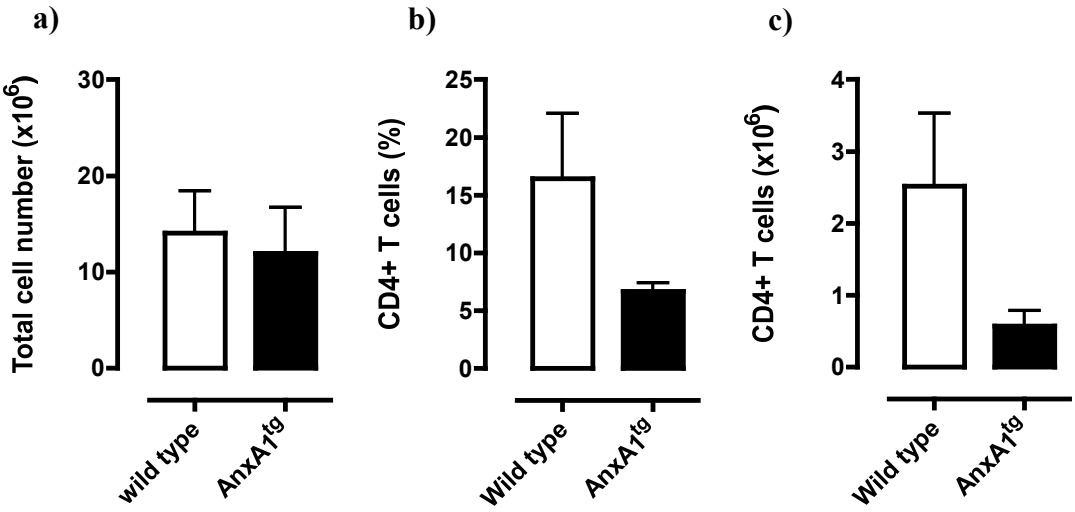

Figure 3.21. T cells in peritoneal fluid of pristane injected mice. a) Total cell number in peritoneal fluid of wild type and AnxA1^{tg} mice. **b)** Percentages and **c)** number of CD4+ T cells recovered in the peritoneal lavage of wild type and AnxA1^{tg} 14 days after the challenge with pristane (N=1 experiment with 4-5 mice per group).

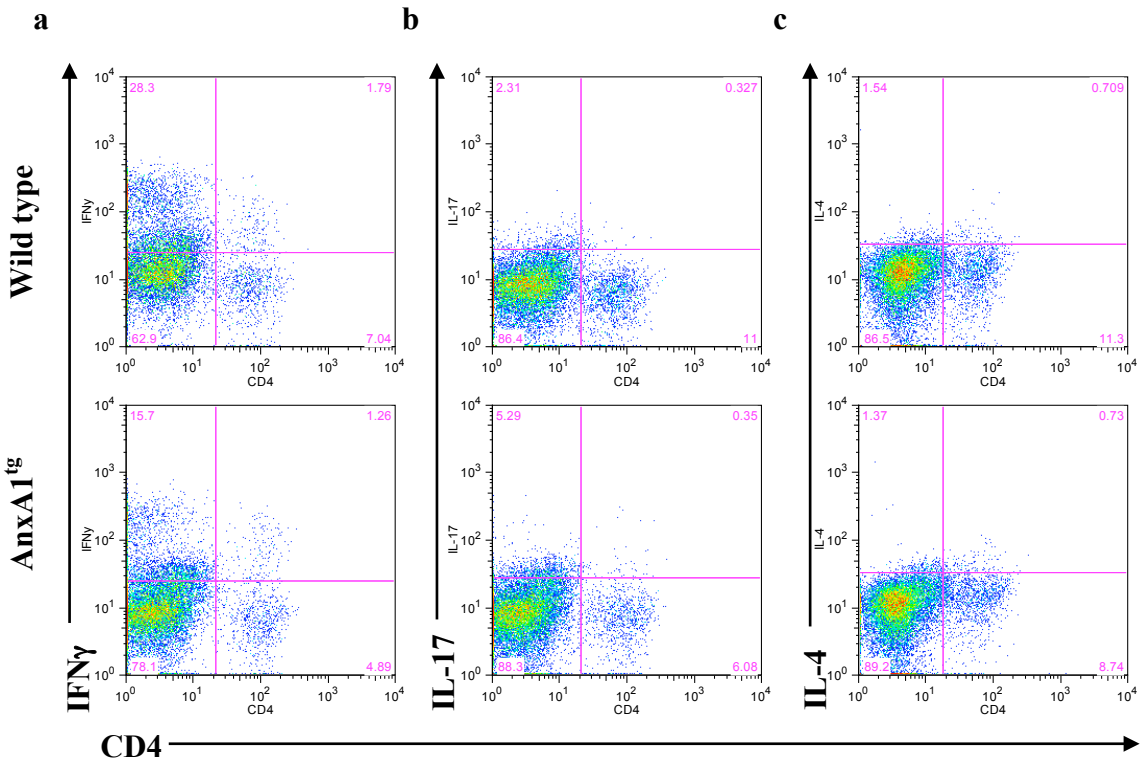

Figure 3.22. ICS of exudates from peritoneal fluid of pristane injected mice. Percentages of CD4+ T cells and **a)** IFNγ+, **b)** IL-17+ and **c)** IL-4+ cells isolated from the peritoneal lavage of wild type and AnxA1^{tg} mice 14 days after the pristane injection.

Analysis of cytokine levels in the peritoneal lavages of these mice showed no significant difference between wild type and AnxA1^{tg} most likely because of the advanced status of disease of the AnxA1^{tg} and the consequent high variability of the samples (Figure 3.23).

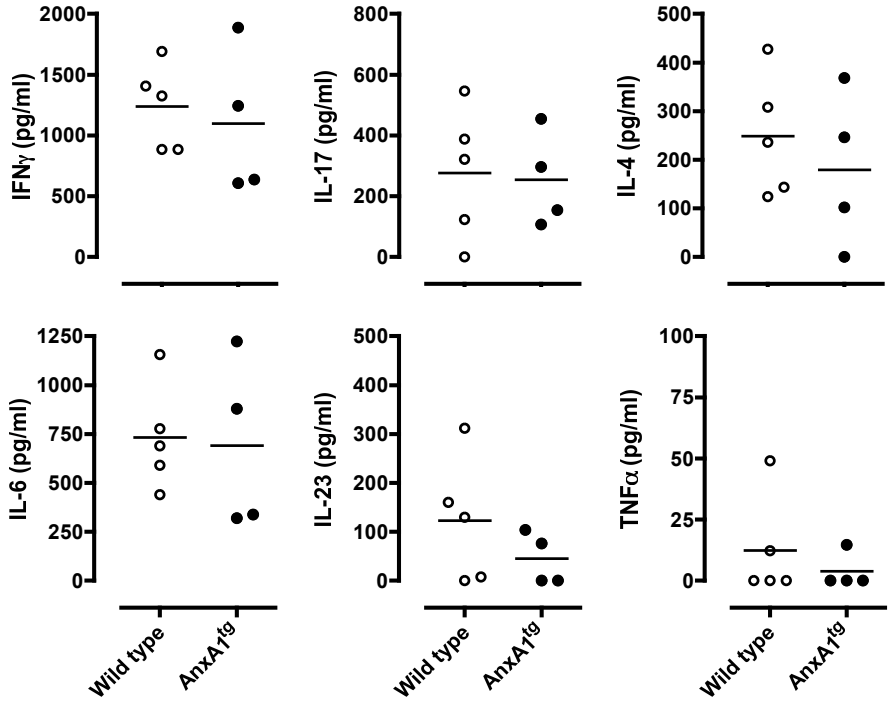

Figure 3.23. Cytokines in the peritoneal fluid of pristane injected mice. Concentrations of IFNγ, IL-17 and IL-4 (top panels) as well as of IL-6, Il-23 and TNFa (bottom panels) measured in the peritoneal lavages of wild type and AnxA1^{tg} mice 14 days after the pristane injection (N=1 experiment with n=4-5 per each group).

3.5 Altered emotional behaviour in AnxA1^{tg}

Surprisingly, AnxA1^{tg} mice showed signs of mood disorders. Both the two strain founders developed either maternal cannibalism or anxiety-like behaviour with the establishment of the homozygous genotype.

3.5.1 AnxA1^{tg}: maternal cannibalism

The AnxA1 transgenic colony coming from the female founder showed cannibal behaviour towards the offspring (Figure 3.24). This phenomenon was not observed with heterozygous mice obtained during the background crosses. Few sporadic events of missed pups were noticed for one breeding pair (G-12; data not shown). G-12 offspring were used for future breeding (Trio H-13 and -14). From this point onwards, pups were found dead, missing or eaten soon after their delivery. Both H-13 and H-14 showed a "fully developed" cannibalism phenotype (Fig 3.25).

Removing male breeders from the cage before the delivery of the newborn did not interfere with this phenomenon thus suggesting maternal driven cannibalism. Interestingly, the cannibal behaviour of the mothers was very specific towards their own progenies since it did not manifest with litter of different breeding pairs of the same backgrounds (C57BL/6).

To overcome the risk of loosing the colony, offspring were fostered with wild type mothers. Of all the pups that were obtained we managed to save one fostered female from H-13 whose first litters were all female that also showed cannibalism (Figure 3.25). In addition to this, other impaired and aggressive behaviour started to

manifest. As an example, a group of female littermates showed clear signs of excessive barberism as evidenced by the absence of whiskers and missing fur on the back of some subjects (Figure 3.26).

The cannibal behaviour was conserved notwithstanding the fostering of the pups. However, and more intriguingly, the continuous fostering over generations seemed to "mellow" the cannibal attitude of these mice since we have been able to save and retrieve more male and female pups (data not shown). These are currently exploited to maintain the colony.

Besides fostering, we tried to rescue the pups administering perphenazine (0.5 or 0.025 mg/ml in drinking water) to pregnant cannibal mothers (Trio L- 15 and 16). This pharmacological treatment was unsuccessful.

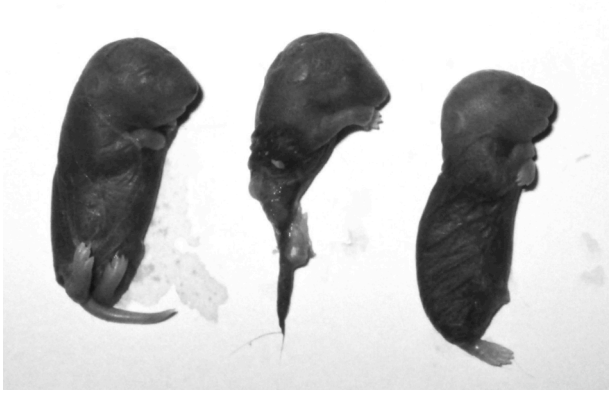

Figure 3.24. Offspring found dead. Three pups found dead post-partum in AnxA1^{tg} mice. Clear signs of cannibalism can be observed in the pup in the middle, while the other two showed missed limp.

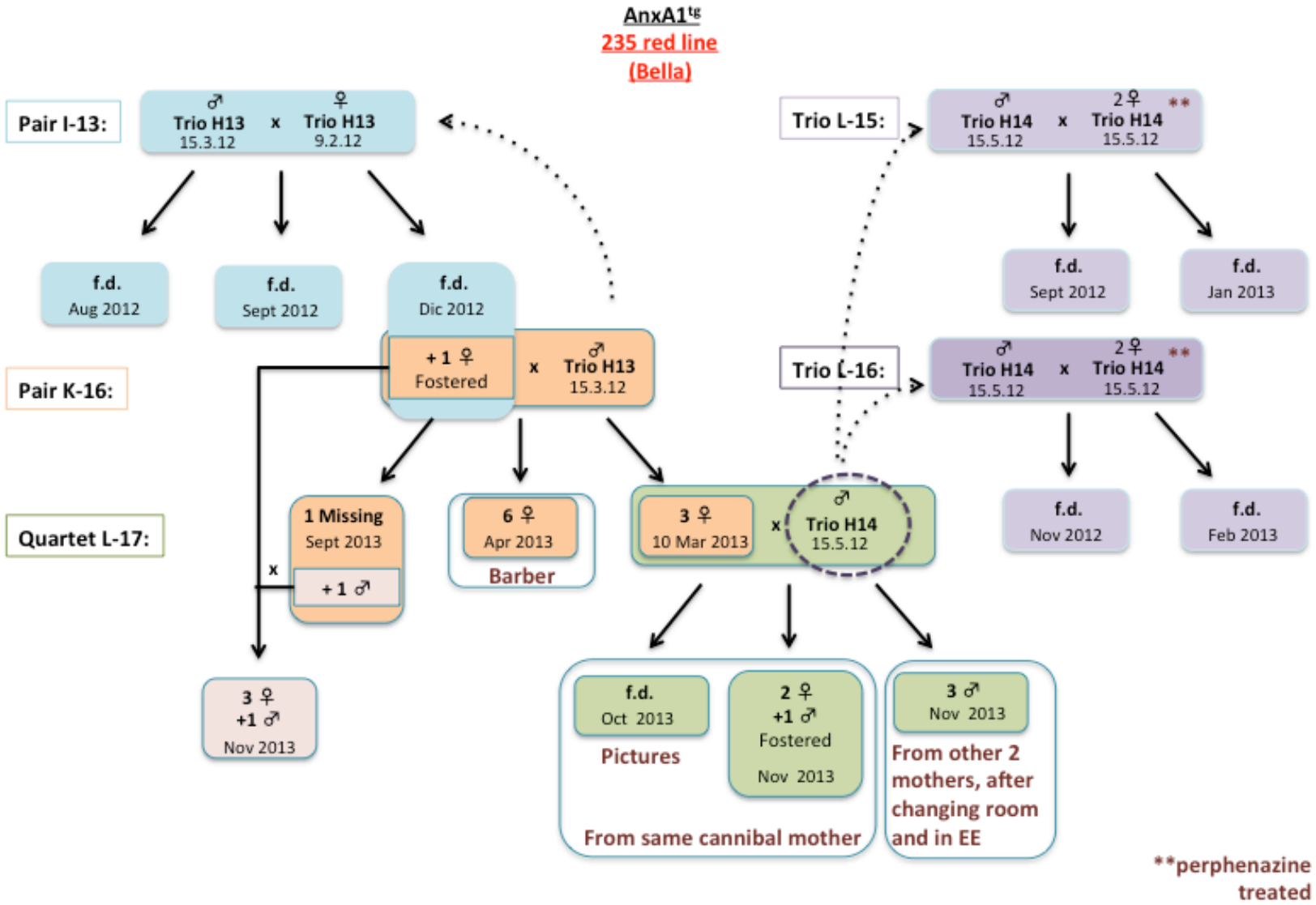
AnxA1tg
235 red line
(Bella)
Pair I-13:
♂ Trio H13 15.3.12 x ♀ Trio H13 9.2.12
f.d. Aug 2012
f.d. Sept 2012
f.d. Dic 2012
Pair K-16:
+1 ♀ Fostered
x
♂ Trio H13 15.3.12
Quartet L-17:
1 Missing Sept 2013
+1 ♂
x
3 ♀ +1 ♂ Nov 2013
6 ♀ Apr 2013
Barber
3 ♀ 10 Mar 2013
x
♂ Trio H14 15.5.12
f.d. Oct 2013
Pictures
2 ♀ +1 ♂ Fostered Nov 2013
From same cannibal mother
3 ♂ Nov 2013
From other 2 mothers, after changing room and in EE
Trio L-15:
♂ Trio H14 15.5.12 x 2 ♀ Trio H14 15.5.12 **
f.d. Sept 2012
f.d. Jan 2013
Trio L-16:
♂ Trio H14 15.5.12 x 2 ♀ Trio H14 15.5.12 **
f.d. Nov 2012
f.d. Feb 2013
**perphenazine treated

Figure 3.25. Maternal cannibalism flow chart. *AnxA1^{tg} progeny coming from the Bella founder*. In the chart breeding Pair I-13, Trio L-15 and 16 were the first breeding to fully show the cannibal phenotype. Pair K-16 and Quartet L-17 were the next generation breeding obtained thanks to mother fostering. Each breeding and related progeny are highlighted with a specific colour. Male breeders were interchanged at least between two different breeding as shown by the dashed arrows. A group of 6 female mice at the second filial generation showed barberism. f.d.: pups found dead; EE: enriched environment.

Figure 3.26. Barberism in AnxA1^{tg}. The barber (top panels) is the mouse that overgrooms other littermates causing patches on their coat and missing whiskers (bottom panels).

3.5.2 The anxious phenotype of AnxA1^{tg}

AnxA1^{tg} mice coming from the male founder did not showed cannibal phenotype, however they showed a different behaviour compared to wild type; they frenetically digged and moved in their home cage once the lid had been open. We decide to investigate the behavioural phenotype of these mice compared to wild type, and so we collaborated with Dr Robert Deacon, who is an expert murine behaviourist. With the help of Dr Deacon, we performed a battery of behavioural tests to define explorative behaviour and motility in mice. We then exploited the approach-avoidance conflict of these tests to describe and interpret the anxiety-like or fear-related behaviour in mice.

3.5.2.1 Marble-burying test

The marble-burying test gives a measurement of anxiety provoking obsessions in mice. It is a good test to measure and thus compare the obsessive digging activity that was readily observable by the naked eye. This test showed that AnxA1^{tg} mice start to dig earlier than wild type mice (Figure 2.27a). Although the absolute number of bouts was similar between the two groups, AnxA1^{tg} mice spent more time digging and buried more marbles compared to wild type (Figure 2.27b-d).

3.5.2.2 Open field test

The open field test assesses simultaneously environmental exploration, locomotor activity and anxiety-related behaviour in mice. AnxA1^{tg} mice show equal explorative and locomotor activity compared to wild type as indicated by the number of rearing

and total square crossed (Figure 3.28b and 3.28c). In addition to this, AnxA1^{tg} mice showed a reduced lag time to rear compared to wild type (Figure 3.28a).

3.5.2.3 Climbing test

The climbing test assesses vertical environmental exploration that has been correlated to dopaminergic activity in mice (250). AnxA1^{tg} mice show an overall decrease in climbing activity compared to wild type. This effect was accompanied by increased latency and decreased number and duration of climbing (Figure 3.29a-c).

3.5.2.4 Light/Dark box test

The light/dark box test assesses the anxiety-like behaviour prompted by a novel and bright environment. Mice were placed in the lit area of the box at the start of the test. AnxA1^{tg} mice showed a very peculiar behaviour in the lit area characterised by freezing and a general appearance of "feeling lost" that was difficult to measure or describe. Similar to the other tests, we could observe an increased lag time in finding the opening and hence to the first crossing (Figure 3.30a). Once the first crossing occurred, the AnxA1^{tg} mice spent about 11% of the time in the light area (35s out of 300s) while the wild type mice about 30% (90s out of 300s) (Figure 3.30b). This difference was also accompanied by reduced number of transitions for AnxA1^{tg} mice compared to wild type (Figure 3.30c).

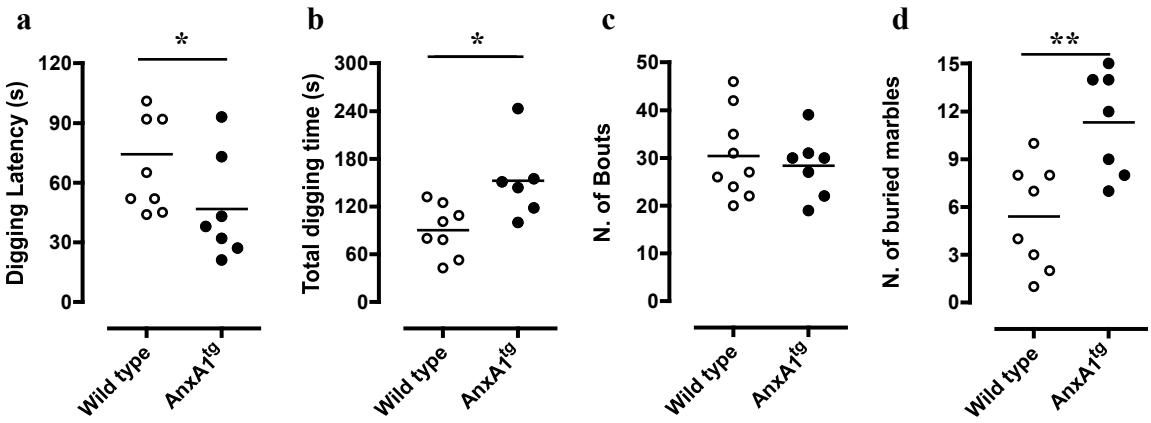

Figure 3.27. Marble-burying test. AnxA1^{tg} and wild type mice were tested for anxiety-like behaviour with the marble-burying test. **a)** Digging latency, **b)** total digging time, **c)** number of bouts and **d)** number of buried marbles are representative of four independent experiments. (*p<0.05, **p<0.01, Mann-Witney test; n=5-9 per each group).

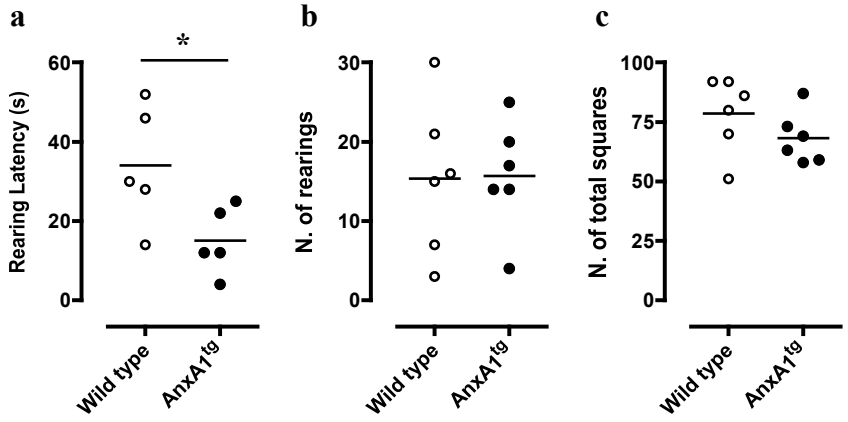

Figure 3.28. Open field test. AnxA1^{tg} and wild type mice were tested for explorative activity and anxiety-like behaviour with the open field test. **a)** Rearing latency, **b)** number of rearing and **c)** number of total squares crossed are representative of three independent experiments. (*p<0.05, Mann-Witney test; n=4-6 per each group).

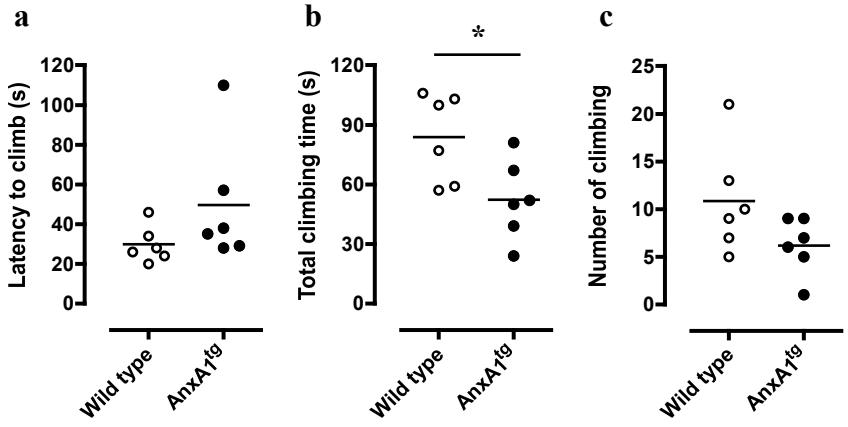

Figure 3.29. Climbing test. AnxA1^{tg} and wild type mice were tested for vertical explorative activity with the climbing test. **a)** Latency to climb, **b)** total climbing time and **c)** number of climbing are representative of two independent experiments. (*p<0.05, Mann-Witney test; n=6-8 per each group).

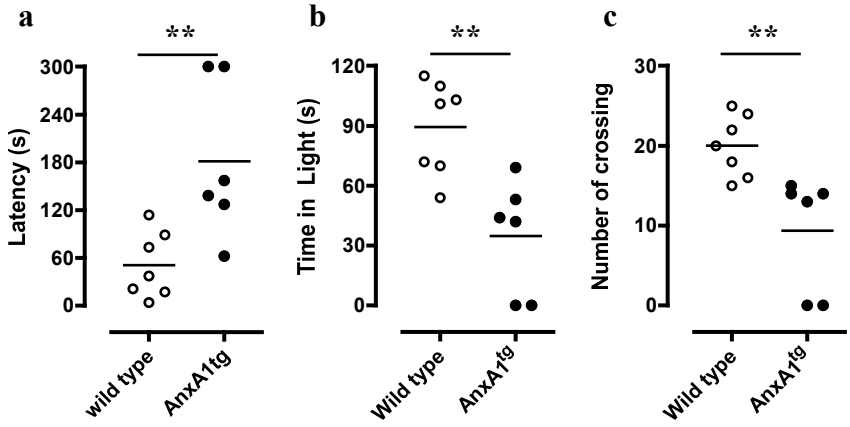

Figure 3.30. Light/dark box test. AnxA1^{tg} and wild type mice were tested for anxiety-like behaviour with the light/dark box test. **a)** Latency to the first crossing, **b)** time in light after the first crossing and **c)** number of crossing are representative of three independent experiments. (**p<0.01, Mann-Witney test; n=6-8 per each group).

3.6 T cells and mood change in early EAE

AnxA1^{tg} mice show a hyper-reactive T cell phenotype, higher susceptibility to develop autoimmune diseases and an interesting "emotional dysfunction". Several evidences in the clinic show that patients suffering from autoimmunity have higher prevalence of anxiety or depression compared to patients suffering from other unrelated diseases or healthy controls. Most interestingly browsing through their clinical history it is often possible to find emotional issues at time earlier than the first manifestation of autoimmune disease. To address whether the emotional changes of AnxA1^{tg} mice were conducive to the exacerbated signs of EAE, we took a step back and investigated if the same emotional changes observed in the clinic could be measured in our experimental system. To this aim, we performed a systematic assessment of the emotional changes at early stage of EAE i.e. soon after the immunisation with MOG_{35-55}. We used the open filed and marble-burying test and assessed changes in behaviour over 10 days, every other day from the day of immunisation.

Immunised mice took more time to start to rear compared to control non-immunised mice (Figure 3.31a) while the number of rearing was similar (Figure 3.31b). Same effect was observed on the marble-burying test: immunised mice showed higher latency to dig while the number of buried marbles was comparable between the two groups (Figure 3.31c and 3.31d).

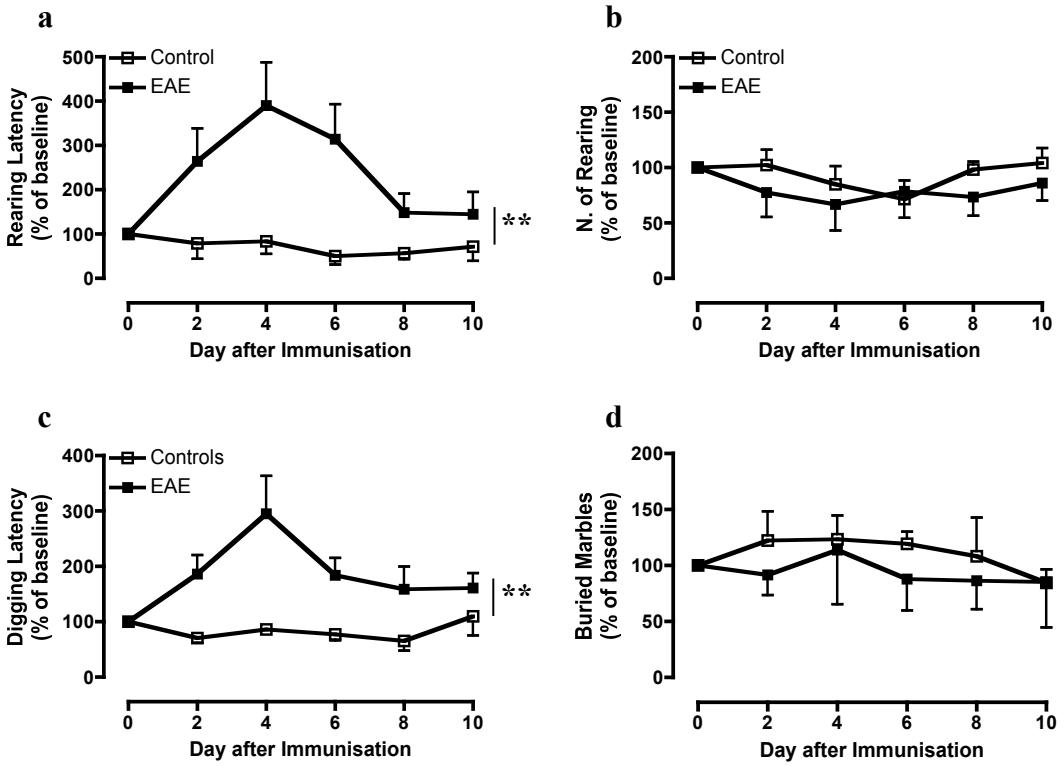

Figure 3.31. Emotional changes in MOG_{35-55}-induced EAE. Time course for **a)** rearing latency and **b)** number of rearing during the open field of wild type mice immunised with MOG_{35-55} (EAE) and littermates not immunised (control). In **c)** and **d)** are represented the time course for digging latency and the number of buried marbles, respectively. Values are plotted as percentage from the baseline for each single mouse. (**$p<0.01$, repeated measure two-way ANOVA; cumulative plots of N=5 separate experiments with n=4-6 -per group).

To correlate these behavioural changes to T cell function at these time points, we next tracked the movement of these cells in and out of circulation. As shown in Figure 3.32a and 3.32b, we observed that CD3+ T cells varied in number both in spleen and blood of the immunised mice. More specifically, the number of CD3+ T cells increases up to day 4 after immunisation mirroring the trend of the behaviour changes we observed.

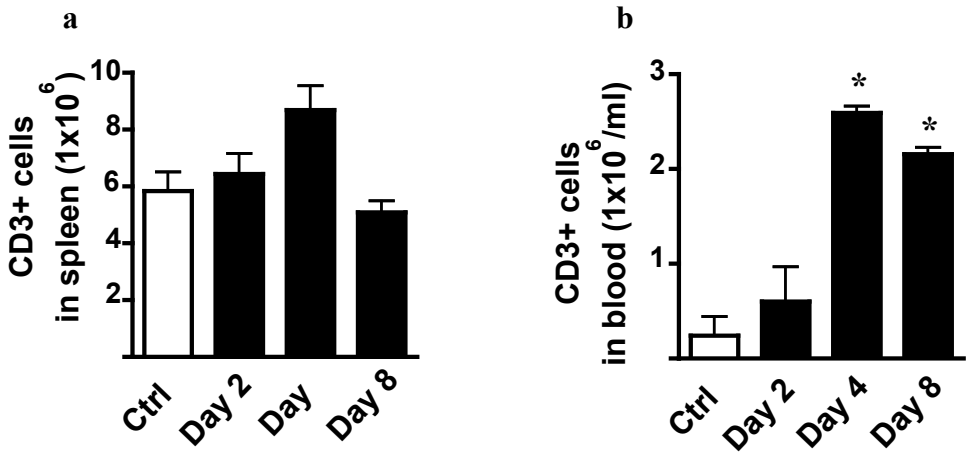

Figure 3.32. CD3+ T cells of mice subjected to MOG_{35-55}-induced EAE. Number of CD3+ T cells **a)** in the spleen and **b)** in blood of control or immunised mice at different time points, in particular at day 2, 4 and 8 after immunisation with MOG35-55. (*$p<0.05$, un-paired t-test; n=3 per time point).

No difference in blood cytokines was detected in those mice. The association between behavioural changes and the increase of CD3+ T cells number in the blood was also observed in mice immunised with $OVA_{323-339}$ plus CFA, but not only CFA (data not shown). In addition, the treatment with GA prevented the behavioural

changed observed in MOG_{35-55} immunised mice and interestingly increased the number of T cells in peripheral lymphoid organs (Figure 3.33a and 3.33b).

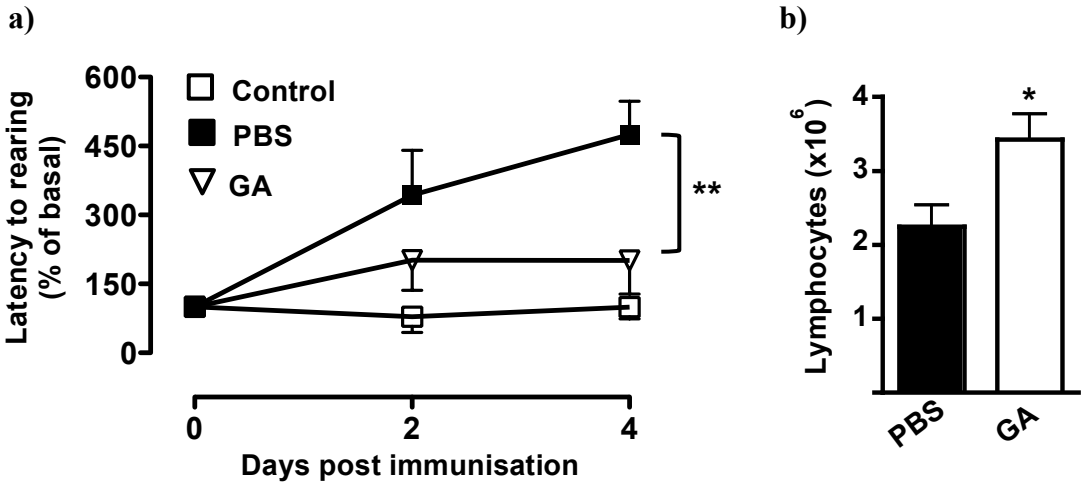

Figure 3.33. GA treatment inhibits the emotional changes observed in MOG_{35-55}-induced EAE. a) Percentages of rearing latency in the open field test of no-immunised (control) and vehicle (PBS) or GA treated mice after immunisation. **b)** Total T cell number in the draining lymph nodes of vehicle or GA treated mice at the 4 of EAE. (**p<0.01, repeated measure two-way ANOVA; representative of N=2 experiments with n=6-8 per group).

Thus, we were able to shown that activation and mobilisation of T cells into the blood correlated in time with the changes in emotional behaviour. These data have been published and a copy of this article has been attached at the appendix of this thesis.

3.7 AnxA1^{tg} T cells adoptive transfer

AnxA1^{tg} mice show anxiety-like behaviour and they are prone to develop autoimmune diseases. These two distinct but intertwined observations rose the question whether the AnxA1^{tg} T cells induce anxiety as well as lead to exacerbated outcomes in the autoimmune models. To address this point, we performed T cell adoptive transfer experiments of AnxA1^{tg} T cells in wild type mice. These chimeric mice were tested for their behaviour using the light/dark box test as read-out and thereafter were immunised with MOG_{35-55} to study the development of the EAE. Alongside T cells, sera from the same donor mice were adoptively transferred into wild type mice.

3.7.1 CD3+ T cell transfer, anxiety test and EAE induction

In a first series of experiments we adoptively transferred the whole CD3+ T cell population isolated from wild type and AnxA1^{tg}. Host mice were tested before the injection (Day -1) and at different time points (day 1, 4, 7, 14 and 21) after the adoptive transfer.

As shown in Figure 3.34a and 3.34b, the behaviour of mice that received CD3+ T cells from wild type or AnxA1^{tg} mice did not significantly changed throughout the experiment till day 14. At this time point, the time spent in light and the number of crossing drastically halved in both groups. Administration of serum from wild type animals increased the time spent in light and the number of transitions at about day 7 (Figure 3.34c and 3.34d) and this did not occur in mice receiving the AnxA1^{tg} mice sera.

At day 21, mice were immunised with MOG_{35-55}. Figure 3.35 shows that the transfer of CD3+ T cells or serum in wild type mice leads to different outcomes: mice receiving wild type CD3+ T cells showed an earlier onset of disease (at day 7) and developed severe EAE (Figure 3.33a and 3.35b). Conversely, mice that received $AnxA1^{tg}$ CD3+ T cells showed milder EAE whose onset was around day 10. The pattern of EAE development of mice receiving $AnxA1^{tg}$ T cells almost overlapped that of control PBS-injected immunised mice (Figure 3.35c and 3.35d).

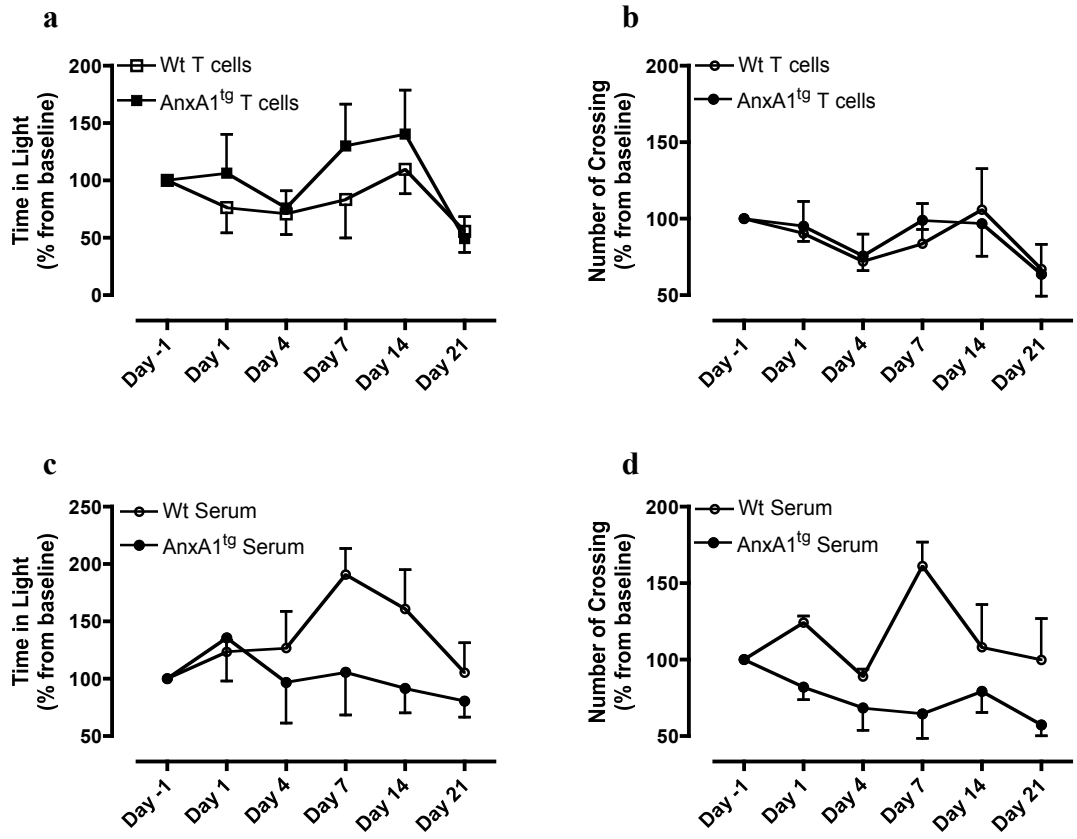

Figure 3.34. Light/dark box test after T cell or serum adoptive transfer. Wild type mice were tested for their basal activity at the light/dark box test (Day -1). Then, they received either CD3+ T cells or sera from wild type (empty square) and AnxA1^{tg} mice (full square). Percentage from the baseline of **a)** time spent in light and **b)** number of crossing after CD3+ T cells or of **c)** time spent in light and **d)** number of crossing after sera transfer are shown for 5 different time points. (Repeated measure two-way ANOVA, n=4 per each group).

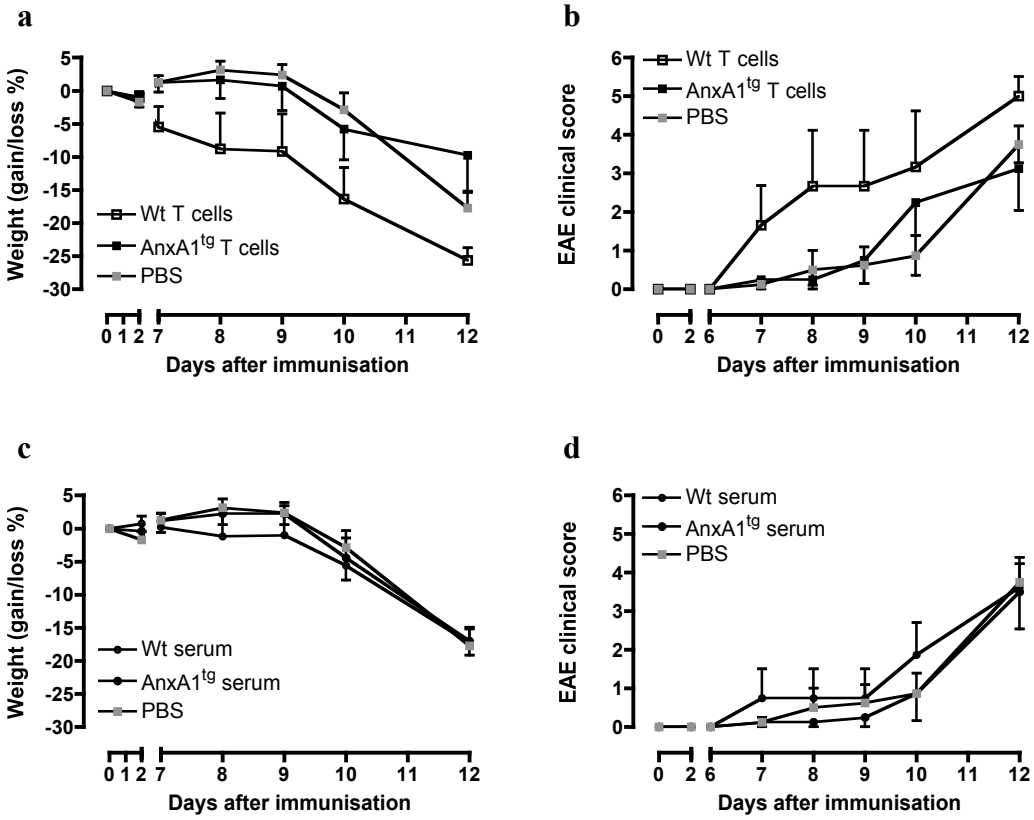

Figure 3.35. MOG_{35-55}-induced EAE after T cell or serum adoptive transfer. a) Weight gain/loss and **b)** EAE clinical score of wild type mice that received either wild type or $AnxA1^{tg}$ CD3+ T cells (empty and full black squares, respectively) or PBS (full grey square). **c)** Weight gain/loss and **d)** EAE clinical score of wild type mice that received either wild type or $AnxA1^{tg}$ sera or PBS. Mice were adoptively transferred 21 days before the MOG_{35-55} immunisation (n=4 per each group).

3.7.2 CD4+ T cells transfer, anxiety test and EAE induction

In a second set of experiments we adoptively transferred CD4+ T cells. Chimeric mice were tested as described above.

Mice that received wild type CD4+ T cells spent more time in the light compared to their basal and the same increase was observed in those injected with PBS vehicle. Conversely, those that received AnxA1^{tg} CD4+ T cells spent more time in the dark compared to the other two groups (Figure 3.36a). In line with this, AnxA1^{tg} CD4+ T cell recipient mice performed a lower number of crossing compared to both PBS and wild type CD4+ T cell recipient mice (Figure 3.36b).

CD4+ T cell recipient mice were tested for the EAE. The overall severity of the disease was mild compared to the ones we routinely run with the onset falling four days later than the expected one i.e. at day 16 rather than day 10-12 and the clinical score reaching a maximum of 1.5 (Figure 3.37). Intriguingly, AnxA1^{tg} CD4+ T cell recipients developed signs of disease earlier (Figure 3.37).

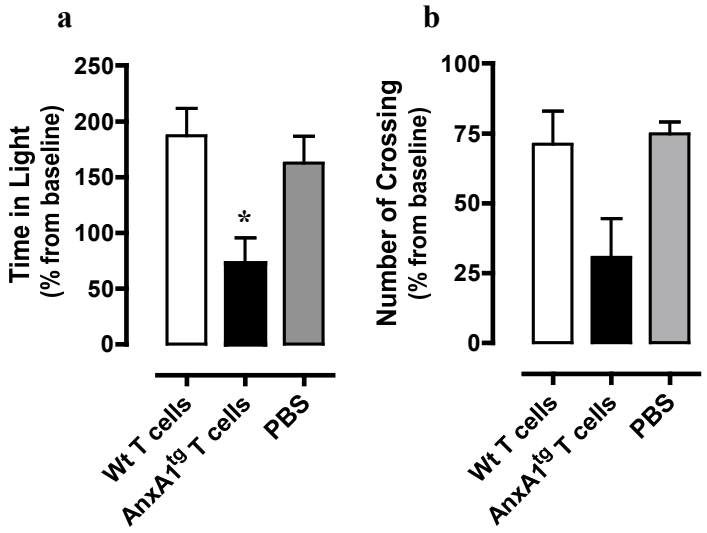

Figure 3.36. Light/dark box test after CD4+ T cell adoptive transfer. a) Time in light and **b)** number of crossing of wild type mice that received either wild type or AnxA1^{tg} CD4+ T cells or PBS. (*p<0.05, Kruskal-Wallis test; representative of N=2 experiments with n=4 per each group).

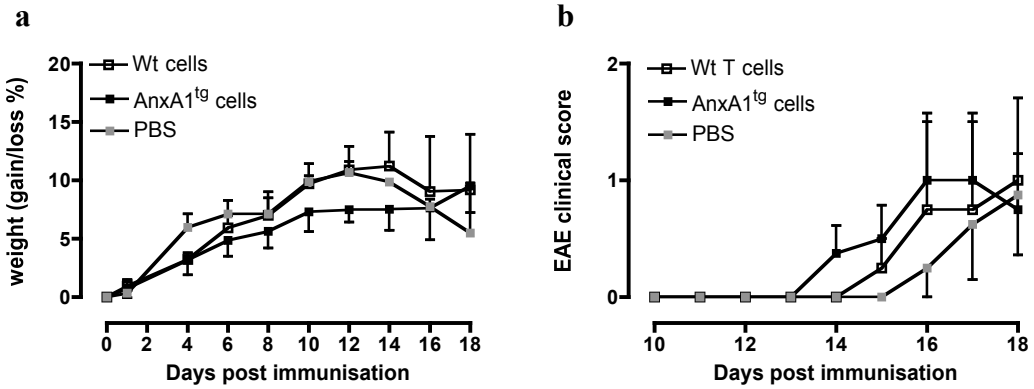

Figure 3.37. MOG$_{35-55}$-induced EAE after CD4+ T cell adoptive transfer. a) Weight gain/loss and **b)** EAE clinical score of wild type mice that received either wild type or AnxA1^{tg} CD4+ T cells (empty and full black squares, respectively) or PBS (full grey square). (n=4 per each group).

3.8 Microarray analysis of AnxA1^{tg} brain and CD4+ T cells

AnxA1^{tg} mice show signs of anxiety-like behaviour and develop severe signs of disease in autoimmune models. To study the mechanism(s) behind these observations *in vivo*, we decided to perform microarray analyses on brain or CD4+ T cells of AnxA1^{tg} and wild type mice.

3.8.1 AnxA1^{tg} brain gene fingerprint

Whole brains were used to study gene expression profile in wild type and AnxA1^{tg} CNS. The gene expression analysis showed a short list of genes (36 out of 23,307 interrogated genes) that have significant different expression in AnxA1^{tg} compared to wild type brain (Figure 3.38).

The most pronounced differences of fold changes were observed for genes found downregulated in AnxA1^{tg} brain. Among these genes, Snca was almost 16 times, while Mageb16 was almost 8 times less expressed in AnxA1^{tg} brain (Table 3.4).

To fully appreciate the meaning of these data, the Signaling Pathway Impact Analysis *(SPIA)* was performed to identify the most relevant signalling pathways modulated in the AnxA1^{tg} mice. This functional analysis identified several GO hits (pathways) for the downregulated genes, but not for the upregulated genes. All the identified signalling pathways resulted inhibited in the AnxA1^{tg} mice compared to wild type mice. However, the adjusted p-values for each pathway were higher than 0.05 (Table 3.5).

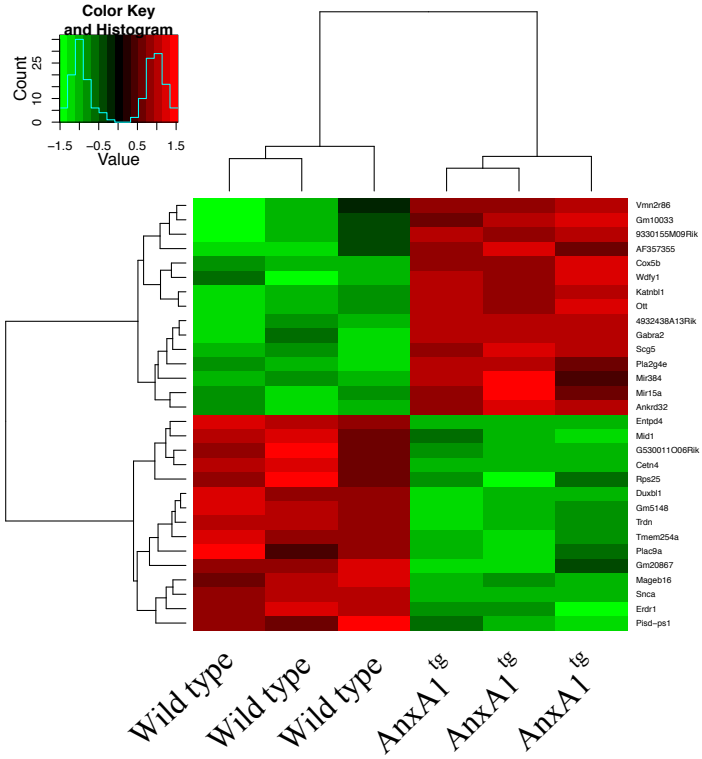

Figure 3.38. Heat-map for the microarray of wild type and AnxA1^{tg} brains. Gene expression of three different brains of both wild type and AnxA1^{tg} represented in colour scale going from the most downregulated (bright green) to the most upregulated (bright red).

Table 3.4: Differential expressed genes in AnxA1^{tg} brain

I.D.	Fold change	Adj p-value
Snca	-3.995	0
Mageb16	-2.81	0.000194
Gm5148	-1.512	0.000152
G530011O06Rik	-1.351	0.002523
Tmem254a	-1.317	0.001787
Mid1	-0.986	0.003069
Gm20867	-0.975	0.020271
Rps25	-0.937	0.01628
Cetn4	-0.926	0.043414
Erdr1	-0.881	0.003186
Duxbl1	-0.878	0.001844
Trdn	-0.855	0.002523
Plac9a	-0.821	0.022588
Pisd-ps1	-0.695	0.033088
Entpd4	-0.689	0.003159
Trdn	-0.643	0.006034
Cetn4	-0.64	0.006392
Mageb16	-0.612	0.008714
Adal	0.507	0.020271
Mir421	0.509	0.020271
4932438A13Rik	0.537	0.029653
Fut9	0.537	0.041221
Cox5b	0.615	0.005176
Mir15a	0.618	0.016149
Katnbl1	0.619	0.004552
9330155M09Rik	0.623	0.029653
Gm10033	0.628	0.041221
Ankrd32	0.659	0.005176
Scg5	0.69	0.003186
AF357355	0.698	0.035643
Vmn2r86	0.704	0.041221
Wdfy1	0.813	0.004544
Mir384	0.854	0.011995
Pla2g4e	0.946	0.001862
Gabra2	0.955	0.001088
Ott	0.997	0.000739

Table 3.5: SPIA on differential expressed genes in AnxA1^{tg} brain

	KEGG pathway	pNDE	pPERT	pGFWER	STATUS
1	Parkinson's disease	2	0	0.569100693	Inhibited
2	Alzheimer's disease	2	0	0.569100693	Inhibited
3	Long-term depression	1	0	0.569100693	Inhibited
4	VEGF signaling pathway	1	0	0.569100693	Inhibited
5	Fc epsilon RI signaling pathway	1	0	0.569100693	Inhibited
6	GABAergic synapse	1	0	0.569100693	Inhibited
7	Morphine addiction	1	0	0.569100693	Inhibited
8	Fc gamma R-mediated phagocytosis	1	0	0.569100693	Inhibited
9	GnRH signaling pathway	1	0	0.569100693	Inhibited
10	Retrograde endocannabinoid signaling	1	0	0.569100693	Inhibited
11	Pancreatic secretion	1	0	0.569100693	Inhibited
12	Lysosome	1	0	0.569100693	Inhibited
13	Vascular smooth muscle contraction	1	0	0.569100693	Inhibited
14	Glutamatergic synapse	1	0	0.569100693	Inhibited
15	Toxoplasmosis	1	0	0.569100693	Inhibited
16	Serotonergic synapse	1	0	0.569100693	Inhibited
17	Huntington's disease	1	0	0.613054537	Inhibited
18	MAPK signaling pathway	1	0	0.690539103	Inhibited
19	Neuroactive ligand-receptor interaction	1	0	0.690539103	Inhibited

** KEGG (Kyoto Encyclopedia of Genes and Genomes); pNDE, pPERT and pGFWER: probability values.*

3.8.2 AnxA1^{tg} CD4+ T cells gene fingerprint

The microarray analyses performed on wild type and AnxA1^{tg} CD4+ T cells showed a long list of genes differentially expressed. Among 35,556 genes that have been interrogated, a total of 2,487 genes were differentially expressed of which 1,746 were upregulated and 741 were downregulated in AnxA1^{tg} CD4+ T cells compared to wild type CD4+ T cells. Table 3.6 shows a list of 77 upregulated genes (red numbers; fold change >0.5) and 60 downregulated genes (green numbers; fold change <-0.5). Genes with a p value <0.05 AND fold change >1.5 were clustered and represented in heat-map (Figure 3.39).

The most upregulated gene in AnxA1^{tg} CD4+ T cells was AnxA1, which was 8 times higher than wild type. Many known genes were found differently regulated such as IL12rb1 *(Interleukin 12 receptor, beta 1)*, Nmnat1 (*Nicotinamide mononucleotide adenylyltransferase 1)*, Hmgb1 (*High mobility group protein 1),* Ccr8 *(Chemokine C-C motif receptor 8)* or Ccl22 *(Chemokine C-C motif ligand 22)*. However, we selectively focused our attention on unknown modulated genes such as 2610019F03Rik.

The Signaling Pathway Impact Analysis *(SPIA)* identified several signalling pathways that are altered in the CD4+ T cells of AnxA1^{tg}. The most significantly modified pathways are listed in Table 3.7.

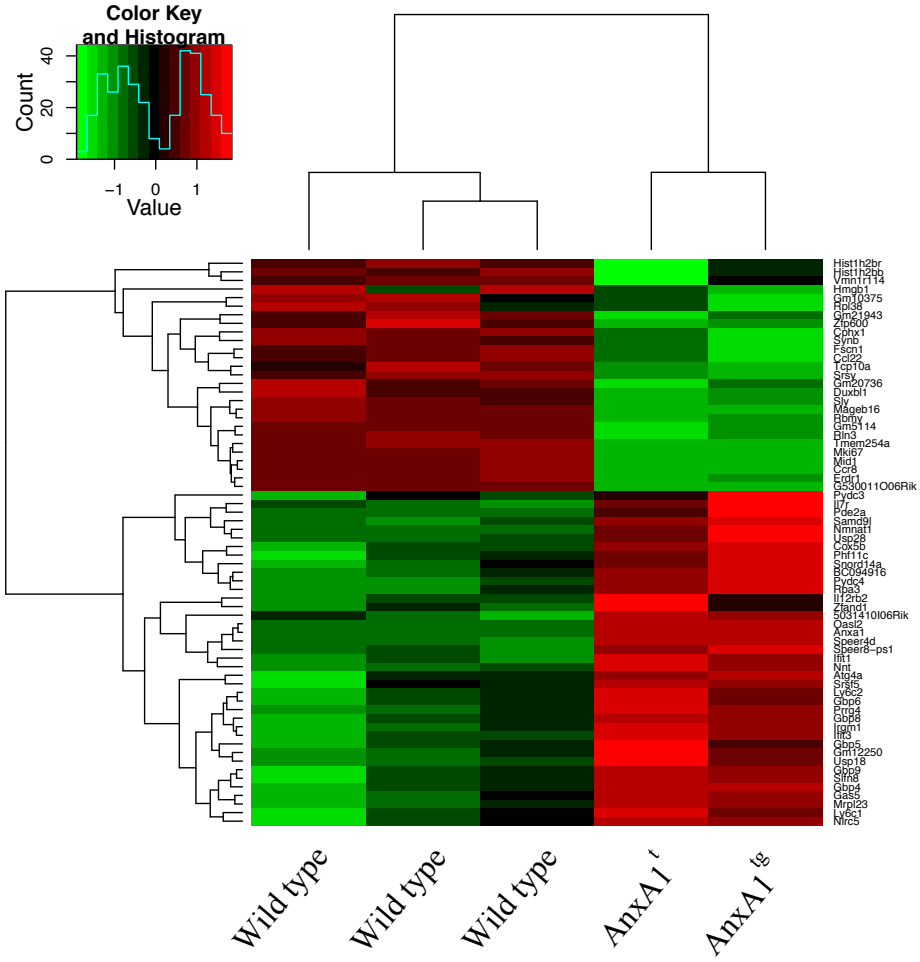

Figure 3.39. Heat-map for the microarray of wild type and AnxA1^{tg} CD4+ T cells. Gene expression of CD4+ T cells from wild type and AnxA1^{tg} represented in colour scale going from the most downregulated (bright green) to the most upregulated (bright red). Genes with $p<0.05$ AND fold change >1.5 are represented.

Table 3.6: Differential expressed genes in AnxA1^{tg} CD4+ T cells

	ID	Fold change	Adj p-value
1	Anxa1	2.978	0
2	Speer4d	1.108	4.00E-06
3	Il12rb2	0.997	0.012621
4	Nmnat1	0.99	0.000434
5	Ifit3	0.982	0.000678
6	Gas5	0.928	0.002568
7	Il7r	0.866	0.001596
8	Speer4d	0.818	0.000157
9	Pydc4	0.804	0.000456
10	Atg4a	0.765	0.012388
11	Pydc3	0.744	0.022645
12	Oasl2	0.741	5.20E-05
13	Gm12250	0.71	0.004814
14	Rpa3	0.706	0.001792
15	Gbp8	0.697	0.002842
16	Pde2a	0.695	0.006101
17	Slfn8	0.691	0.005709
18	Gbp9	0.685	0.004982
19	Gbp4	0.683	0.002126
20	5031410I06Rik	0.667	0.001792
21	Irgm1	0.662	0.001885
22	Zfand1	0.662	0.024261
23	Ly6c1	0.651	0.014999
24	Usp28	0.648	0.002507
25	BC094916	0.639	0.001792
26	Speer8-ps1	0.636	0.000437
27	Srsf5	0.635	0.018716
28	Snord14a	0.63	0.007099
29	Nlrc5	0.627	0.011906
30	Usp18	0.624	0.003771
31	Samd9l	0.621	0.000939
32	Phf11c	0.621	0.007725
33	Mrpl23	0.605	0.004471
34	Gbp5	0.605	0.012632
35	Ly6c2	0.6	0.006604
36	Gbp6	0.595	0.006362
37	Nnt	0.591	0.000939
38	Ifit1	0.591	0.001655
39	Prrg4	0.588	0.002663
40	Cox5b	0.585	0.002877
41	Irgm2	0.58	0.004982
42	Psenen	0.573	0.013998
43	Atp8b4	0.571	0.004982
44	Dennd2d	0.571	0.035523
45	Lgr4	0.569	0.007959
46	Timm21	0.566	0.001331
47	Parp14	0.566	0.004982
48	Ccl1	0.564	0.007422
49	Ifit2	0.562	0.002507
50	Snhg1	0.561	0.002663
51	2210404J11Rik	0.56	0.000827
52	Irf1	0.555	0.006959
53	Snord16a	0.553	0.009438
54	Rpl12	0.55	0.007026
55	Snora69	0.546	0.018716
56	Gbp7	0.541	0.002732
57	Iigp1	0.539	0.010244
58	Irf7	0.534	0.001001
59	Rtp4	0.528	0.010244
60	Nlrc5	0.518	0.016305
61	Atm	0.517	0.009637
62	Srp54b	0.516	0.004814
63	Atpbd4	0.514	0.003672
64	Nlrc5	0.512	0.014385
65	Snora28	0.511	0.004788
66	Snord42b	0.511	0.014652
67	Snord37	0.509	0.018516
68	Nlrc5	0.507	0.021578
69	Ppp2r3c	0.506	0.001945
70	Snhg1	0.502	0.011906
71	Rnf213	0.501	0.006326
72	Dapl1	0.498	0.0194
73	Tk2	0.497	0.004814
74	Fnip1	0.496	0.005709
75	Nlrc5	0.493	0.014559
76	2610019F03Rik	0.492	0.002842
77	9330175E14Rik	0.49	0.004982

	ID	Fold change	Adj p-value
1	Mageb16	-2.774	0
2	Cphx1	-1.528	0.000305
3	Rbmy	-1.321	7.00E-06
4	Rbmy	-1.234	5.00E-06
5	G530011O06Rik	-1.205	1.00E-06
6	Hmgb1	-1.163	0.028011
7	Fscn1	-1.065	0.000434
8	Mid1	-0.969	5.00E-06
9	Ccr8	-0.958	7.00E-06
10	Duxbl1	-0.925	0.001596
11	Erdr1	-0.913	9.00E-06
12	Gm10375	-0.902	0.024667
13	Tmem254a	-0.891	1.20E-05
14	Tcp10a	-0.868	0.000678
15	Sly	-0.867	0.000827
16	Gm20736	-0.844	0.041444
17	Zfp600	-0.84	0.002332
18	Duxbl1	-0.829	0.000717
19	Gm5114	-0.8	0.000142
20	Ccl22	-0.771	0.001655
21	Hist1h2br	-0.768	0.011906
22	Rpl38	-0.763	0.016424
23	Synb	-0.737	0.000823
24	Sly	-0.735	0.000305
25	Vmn1r114	-0.683	0.025858
26	Mki67	-0.679	0.000117
27	Gm20736	-0.673	0.017194
28	Gm10375	-0.651	0.020606
29	Rln3	-0.649	0.000366
30	Gm21943	-0.641	0.00214
31	Cphx1	-0.633	0.000802
32	Gm20736	-0.633	0.002605
33	Hist1h2bb	-0.593	0.013642
34	Srsy	-0.59	0.001223
35	2810417H13Rik	-0.584	0.000802
36	Gm13271	-0.569	0.004739
37	Gm7609	-0.56	0.00871
38	Gm20815	-0.554	0.013851
39	D830030K20Rik	-0.55	0.049643
40	Pros1	-0.547	0.013262
41	Ccna2	-0.545	0.001585
42	Defa20	-0.543	0.011564
43	Defa5	-0.542	0.010244
44	Mir713	-0.537	0.011763
45	Sprr2a1	-0.529	0.002663
46	Gm3696	-0.527	0.006326
47	Olfr538	-0.526	0.005027
48	Ccnb2	-0.522	0.006659
49	Hist1h2br	-0.522	0.007099
50	Gm10058	-0.521	0.001945
51	Il23r	-0.521	0.003995
52	Mup2	-0.521	0.011416
53	Arhgap20	-0.518	0.001655
54	Cd80	-0.517	0.001494
55	Mageb16	-0.516	0.002507
56	Hist1h3f	-0.515	0.015734
57	Hist1h2an	-0.514	0.03121
58	Plk1	-0.498	0.001792
59	Ssty2	-0.498	0.002605
60	Ccl17	-0.498	0.004471

Table 3.7: SPIA of differential expressed genes in AnxA1^{tg} CD4+ T cells

	KEGG pathway	pNDE	pPERT	pGFWER	STATUS
1	Herpes simplex infection	1.06E-09	0.619	1.89E-06	*Activated*
2	RIG-I-like receptor signaling pathway	4.56E-07	0.36	0.000354732	*Activated*
3	Influenza A	9.33E-07	0.574	0.001075025	*Activated*
4	Epstein-Barr virus infection	3.44E-05	0.071	0.004420838	*Activated*
5	Hepatitis C	3.62E-06	0.863	0.005552269	*Activated*
6	Cytosolic DNA-sensing pathway	1.29E-05	0.66	0.014060477	*Activated*
7	Systemic lupus erythematosus	1.30E-05	0.752	0.015888115	Inhibited
8	Toll-like receptor signaling pathway	4.07E-05	0.78	0.046831327	*Activated*
9	Autoimmune thyroid disease	0.000184486	0.261	0.068487394	Inhibited
10	Allograft rejection	0.000328624	0.296	0.129463911	Inhibited
11	Jak-STAT signaling pathway	0.000396472	0.444	0.220716176	Inhibited
12	Cytokine-cytokine receptor interaction	0.001468527	0.149	0.268163061	Inhibited
13	Cell cycle	0.000955963	0.241	0.280806633	*Activated*
14	RNA transport	0.000541036	0.468	0.30550975	*Activated*
15	NF-kappa B signaling pathway	0.000446669	0.85	0.438102725	Inhibited
16	Adipocytokine signaling pathway	0.003217325	0.13	0.477361906	Inhibited
17	Type I diabetes mellitus	0.003340756	0.205	0.737739117	Inhibited

3.9 A candidate gene: 2610019F03Rik

2610019F03Rik is a gene coding for a relatively short protein of 31KDa and has more than 75% of homology with the human gene C8orf42 (or Trdp- testis development related protein). The mRNA expression analysis by Real Time PCR confirmed the increased levels of 2610019F03Rik gene in CD4+ T cells of AnxA1^{tg} compared to wild type (Figure 3.40).

To confirm the expression of 2610019F03Rik at the protein level, we used lymphocytes freshly isolated or stimulated with plate-bound anti-CD3/CD28 (1µg/ml) overnight. We observed that higher number of AnxA1^{tg} CD4+ T cells produced more 2610019F03Rik protein at basal condition compared to wild type (Figure 3.41a, left panel). This difference was maintained after stimulation, although the production of 2610019F03Rik protein increased in both AnxA1^{tg} and wild type CD4+ T cells (Figure 3.41a, right panel).

In addition, we measured the released of 2610019F03Rik protein in the conditioned media of AnxA1^{tg} and wild type lymphocytes by western blot analysis. We found higher amount of 2610019F03Rik protein in the media of no-stimulated AnxA1^{tg} cells compared to wild type. The 2610019F03Rik protein level decreased in both conditioned media after stimulation (Figure 3.41b).

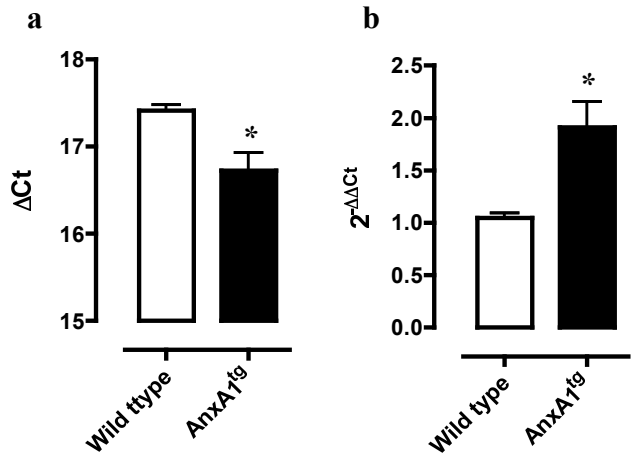

Figure 3.40. 2610019F03Rik expression in CD4+ T cells. 2610019F03Rik mRNA in CD4+ T cells of wild type and AnxA1^{tg} were detected by Sybr green based Q-PCR. **a)** Number of cycles normalised to GAPDH and **b)** fold increase of 2610019F03Rik expression in AnxA1^{tg} compared to wild type. (*$p<0.05$, unpaired t-test; n=3 mice per group).

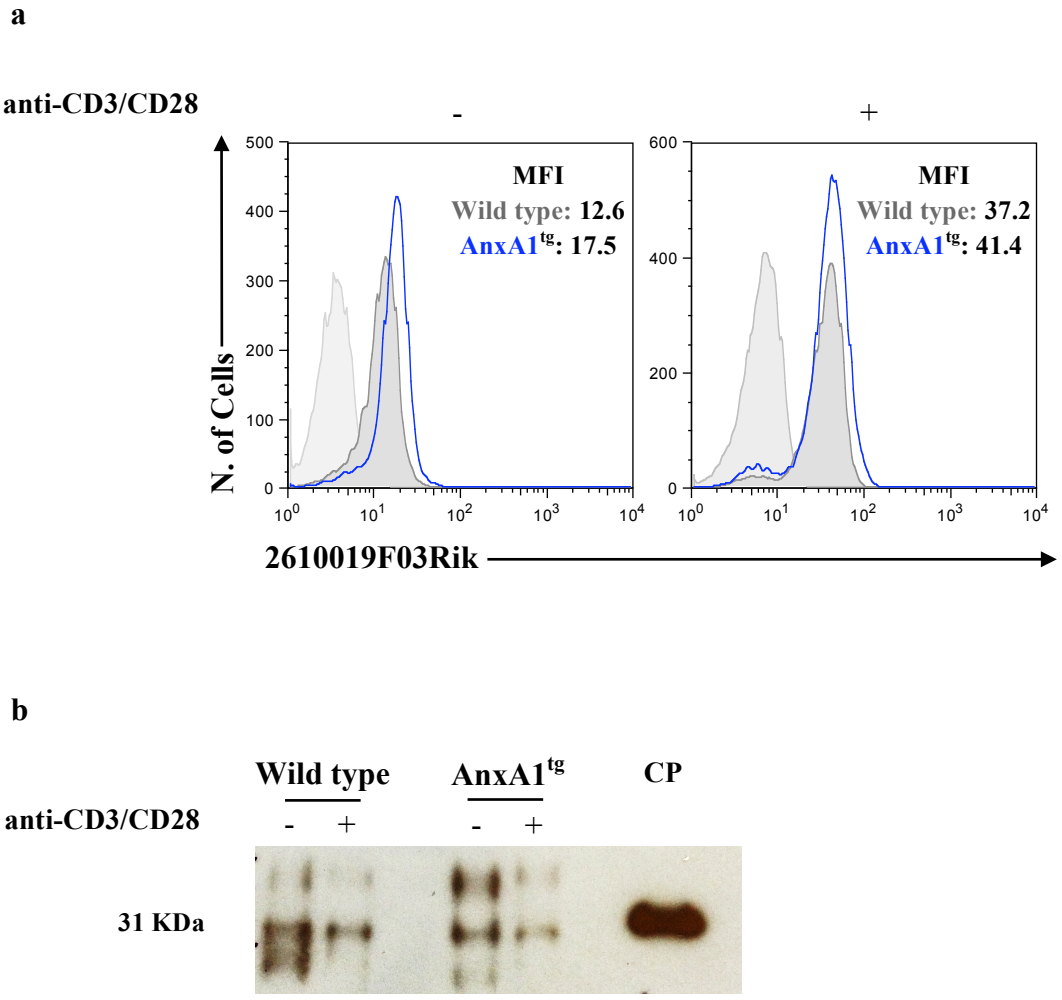

Figure 3.41. 2610019F03Rik protein in CD4+ T cells. a) 2610019F03Rik expression in CD4+ T cells freshly isolated (left panel) or simulated with anti-CD3/CD28 (1µg/ml) overnight (right panel) of wild type (dark grey) or AnxA1^{tg} (blue) mice. Isotype control is in light grey. **b)** Immunoprecipitates of 2610019F03Rik from conditioned media of wild type and AnxA1^{tg} lymphocytes. CP= positive control (human recombinant homologue of 2610019F03Rik).

3.9.1 The 2610019F03Rik as modulator of anxiety

We next tested whether 2610019F03Rik would mediate the anxiety-like behavior of the AnxA1^{tg} CD4+ T cells. To this aim, we used two different approaches: 1) administration of a polyclonal anti-2610019F03Rik antibodies to AnxA1^{tg} mice; 20 administration of human recombinant 2610019F03Rik to wild type mice.

AnxA1^{tg} mice were tested with the light/dark box test before the administration of the antibodies to record their basal levels (Day 0) and then at day 2, 4 and 7. Mice injected with the IgG isotype were used as control. Care was taken in using AnxA1^{tg} mice with similar levels of anxiety in the light and dark test (Figure 3.42). Mice treated with anti-Rik showed a significant increase in the time spent in light compared to IgG control. This effect was particularly evident and statistically significant at day 7 (Figure 3.42a). No changes in the number of crossing were observed (Figure 3.42b).

Administration of recombinant 2610019F03Rik (rRik) to wild type mice significantly decreased the time spent in the light compared to mice treated with vehicle (PBS). These effects became evident at day 4 and were absent at day 2. These effects were not observed in mice receiving heat-denatured rRik (d-rRik) (Figure 3.43).

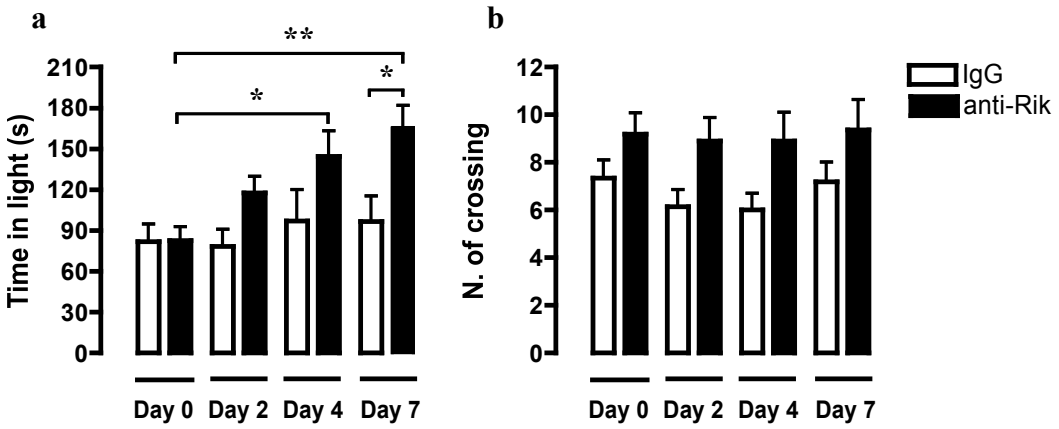

Figure 3.42. Light/dark box test after treatment with anti-2610019F03Rik antibody. AnxA1^{tg} mice were tested at day 0 and then treated with polyclonal anti-2610019F03Rik antibody (500ng/mouse; black bars) or IgG isotype (500ng/mouse; white bars). The treatment was a single i.p. injection at day 0. **a)** Time spent in light after the first crossing and **b)** number of crossing performed by the two groups after 2, 4 and 7 days from the treatment. (*p<0.05, **p<0.01, Kruskal-Wallis test followed by Dunn's multiple comparison test; cumulative data of N=2 separated experiments with n=3-6 mice per group).

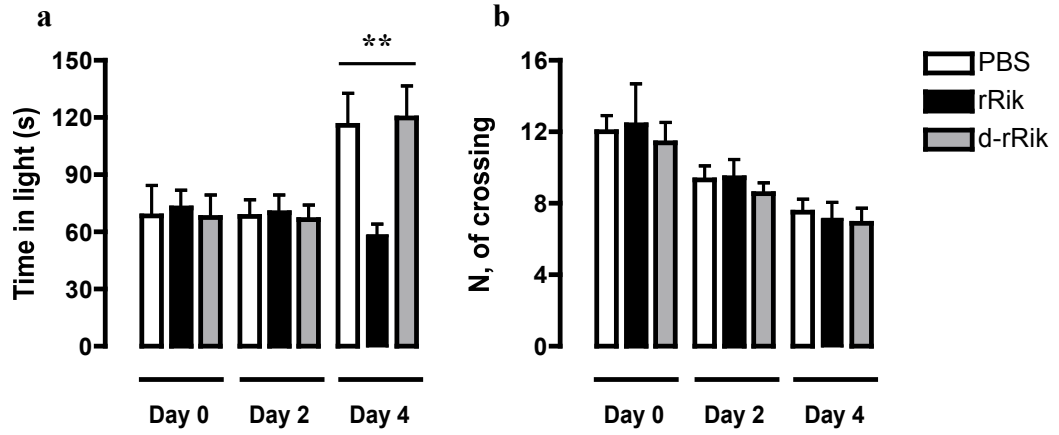

Figure 3.43. Light/dark box test after injection of 2610019F03Rik recombinant protein. Wild type mice were tested at day 0 and then treated with 2610019F03Rik recombinant protein (rRik; 500ng/mouse; black bars), its denatured form (d-rRik; 500ng/mouse; grey bars) or PBS (white bars). **a)** Time spent in light after the first crossing and **b)** number of crossing performed by the three groups after 2 and 4 days from the injection. (**p<0.01, Kruskal-Wallis test followed by Dunn's multiple comparison test; cumulative data of N=2 with n=5 per group).

3.10 VJ-4B6 as treatment in autoimmune diseases

Given the therapeutic potentials of targeting AnxA1, we tested the AnxA1 neutralizing antibody VJ-4B6. Firstly, we tested the toxicity or side effects of VJ-4B6 in wild type mice. Secondly, we tested the effect of VJ-4B6 in a model of acute inflammation such as zymosan-induced peritonitis. Finally, VJ-4B6 was tested in MOG_{35-55} induced EAE.

3.10.1 VJ-4B6 effects in vivo

We first tested potential toxic or side effect of VJ-4B6 in vivo. To this aim, we collected thymus, spleen and lymph nodes of C57BL/6 3 days after the treatment with VJ-4B6 (50ng/mouse i.p.).

No gross differences were found in thymi (data no shown) or secondary lymphoid organs. The percentages of CD4+ and CD8+ T cells in both lymph nodes and spleen of VJ-4B6 treated mice were comparable to those of the vehicle treated ones (Figure 3.44a and 3.44c). Interestingly, total cell number was found triplicated in the spleen of VJ-4B6 treated mice compared to wild type (Figure 3.44d).

The treatment with VJ-4B6 did not affect either the percentages of B cells or granulocytes in the same tissues. Indeed, the percentages of CD11b- CD19+ as well as Ly6G+CD115low cells were comparable between lymph nodes and spleens of vehicle and VJ-4B6 treated mice (Table 3.8).

Lymph nodes

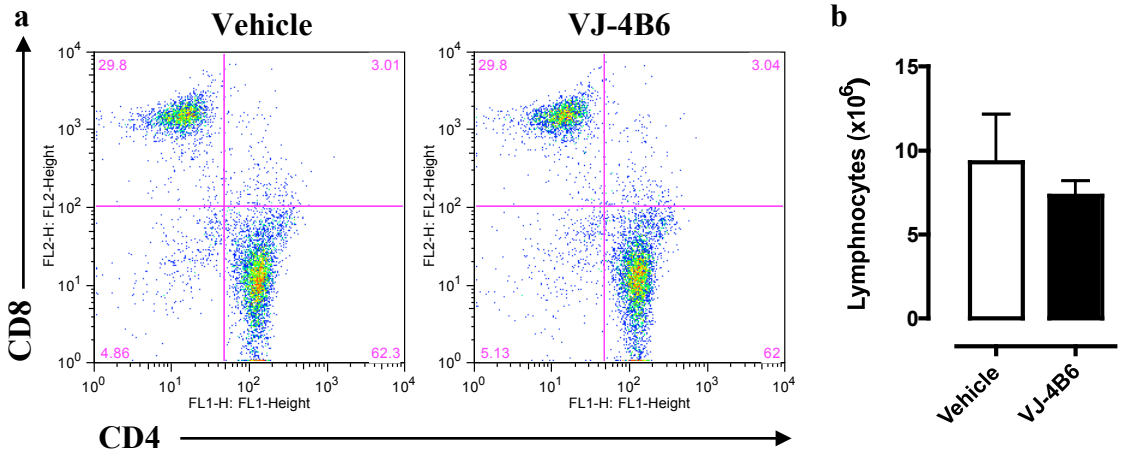

Spleen

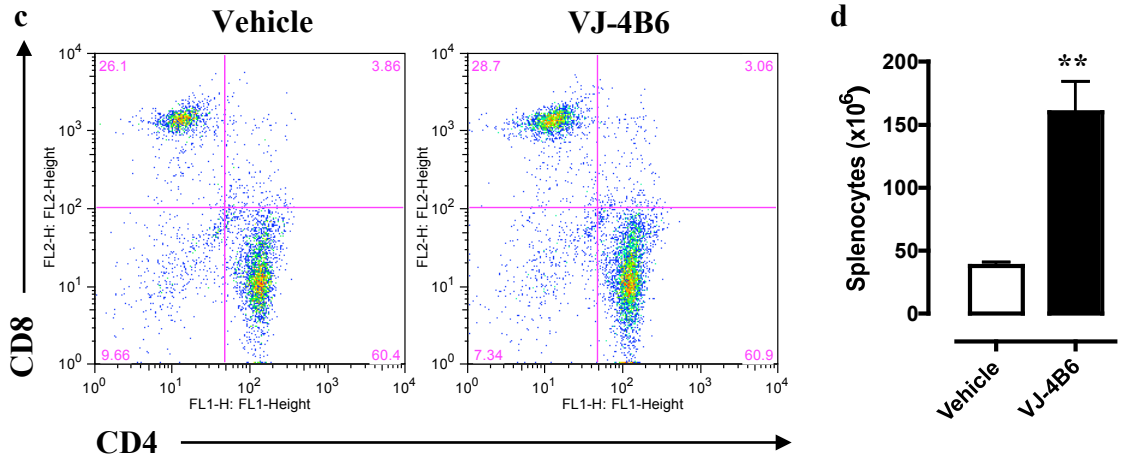

Figure 3.44. Effects of VJ-4B6 on CD4 and CD8 T cells in lymph nodes and spleens. CD4 and CD8 dotplots of **a)** lymph node cells and **c)** splenocytes of vehicle and VJ-4B6 treated mice. Total cell counts of **b)** lymph nodes and **d)** spleens from the two studied groups. (**p<0.01, unpaired t-test; n=4 mice per group).

Table 3.8: FACS staining of leucocytes in peripheral lymphoid organs

		% CD11b-/CD19+	% Ly6G+/CD115^{low}
Lymph nodes	Wild type	53±11.8	5.3±0.14
	VJ-4B6	47±12.0	5.2±0.16
Spleen	Wild type	54±2.34	4.3±0.19
	VJ-4B6	47±3.92	4.0±0.16

Data show the mean values ± SEM of percentage of B cells or granulocytes.

3.10.2 VJ-4B6 effects in zymosan-induced peritonitis

To study the possible influence of VJ-4B6 on leukocyte recruitment, C57BL/6 mice were injected with 50ng/mouse of VJ-4B6 or IgG2b (isotype antibody) and after 24h were challenged with zymosan (1mg/mouse). The peritoneal lavages were collected 4h after the injection to quantify the number of PMNs and monocytes in the peritoneal cavity.

As shown in Figure 3.45, there was no difference in the total cell count as well as in the number of PMN or monocyte between VJ-4B6 and isotype control-treated mice. A blind experiment, done by a colleague in the department, confirmed this result (data not shown).

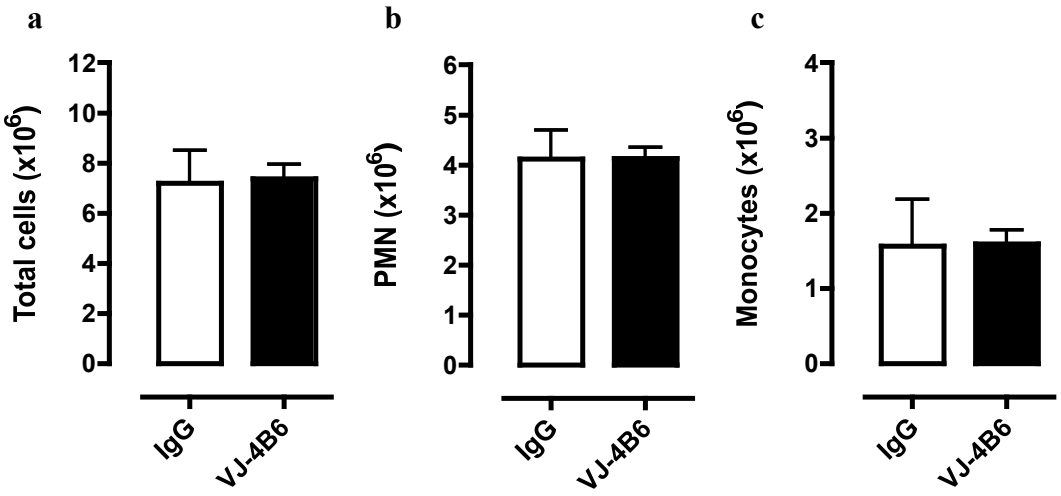

Figure 3.45. Effects of VJ-4B6 in zymosan –induced peritonitis. a) Total cell count, b) PMN and **c)** monocyte number of peritoneal lavages of IgG2b or VJ-4B6 treated mice at 4h of zymosan challenge (unpaired t-test; n=5 mice per group).

3.10.3 MOG_{35-55} induced EAE in VJ-4B6 treated mice

C57BL/6 mice were treated with different doses of VJ-4B6 antibody (5, 50 and 100ng/mouse). IgG2b (100ng/mouse) was administered as negative control. Mice treated with VJ-4B6 showed lower percentages of weight loss compared to control mice from day 10 onwards (Figure 3.46). The 50ng/mouse VJ-4B6 treatment resulted to be the best dose compared to 5 and 100ng (Figure.3.46c).

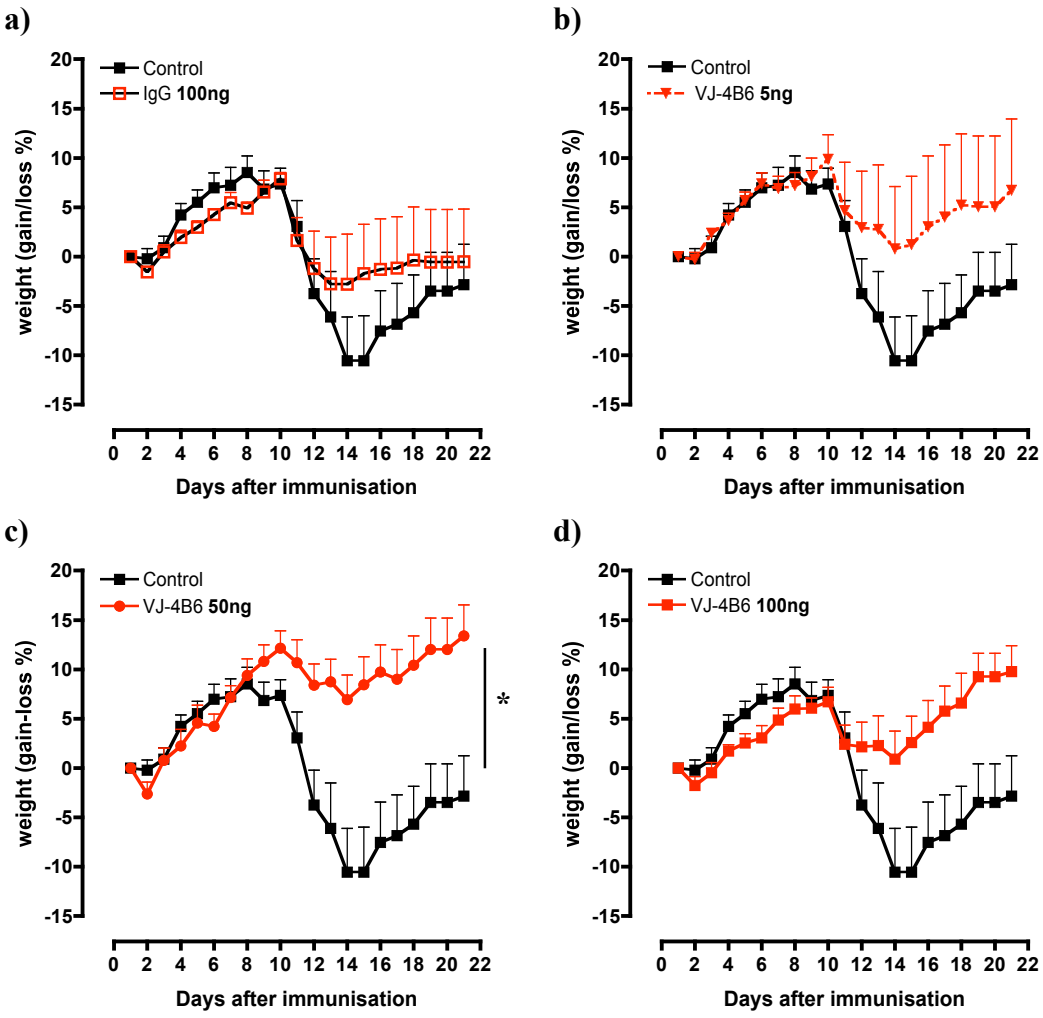

Figure 3.46. Change of weight of VJ-4B6 treated mice on MOG_{35-55} induced EAE. Percentages of weight gain or loss of MOG_{35-55} immunised mice treated with **a)** 100ng IgG2b or **b)** 5ng, **c)** 50ng and **d)** 100ng of VJ-4B6. All the treatments were given i.p. (*$p<0.05$, repeated measure two-way ANOVA; representative of N=2 with n=6-8 mice per group).

The VJ-4B6 reduced the incidence of EAE compared to control and IgG treated groups. Indeed, about 50-60% of VJ-4B6 treated mice manifested signs of EAE compared to 100% in the other two groups (Figure 3.47).

a)

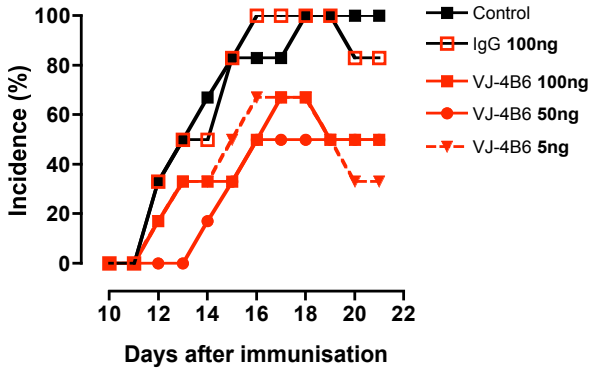

b)

Day 18	No-Disease	Disease	total
Control	0	6	6
IgG 100ng	0	6	6
VJ-4B6 100ng	2	4	6
VJ-4B6 50ng	3	3	6
VJ-4B6 5ng	2	4	6
total	7	23	30

$\chi^2=4.56, p<0.05$

Figure 3.47. Incidence of MOG_{35-55} induced EAE in VJ-4B6 treated mice. a) Percentages of mice that show signs of EAE per day of control and treated group with IgG2b (100ng) or VJ-4B6 (5, 10 and 100ng). All the treatments were given i.p. **b)** Distribution of number of mice per each group showing or not signs of disease at day 18. (*p<0.05, Chi-square (χ^2) trend test; representative of N=2 experiments with n=6-8 mice per group).

Within the VJ-4B6 treated group, those that developed EAE only showed mild signs of disease. In Figure 3.48, the development of EAE is compared for control and treated mice. The averaged score in control mice was of 3.5-4 (Figure 3.48a). This is reduced by VJ-4B6 in dose dependent manner. Indeed, the averaged EAE score was of 2 in mice treated with 5ng VJ-4B6 while it reached score of 1-1.5 in the 50 and 100ng VJ-4B6-treated mice (Figure 3.48b-d).

The AUC values are significantly reduced with 50ng and 100ng VJ-4B6 treatment ($p<0.05$, Figure 3.48c and 3.48d), and no much difference is observed between these two doses. At the contrary, the IgG2b treatment does not exert effect in the EAE development (Figure 3.48a). Thus, the therapeutic effect of VJ-4B6 is specific and it is mediated by the neutralization action on AnxA1 during the EAE. These results were confirmed by independent experiments with 6-8 mice per group each.

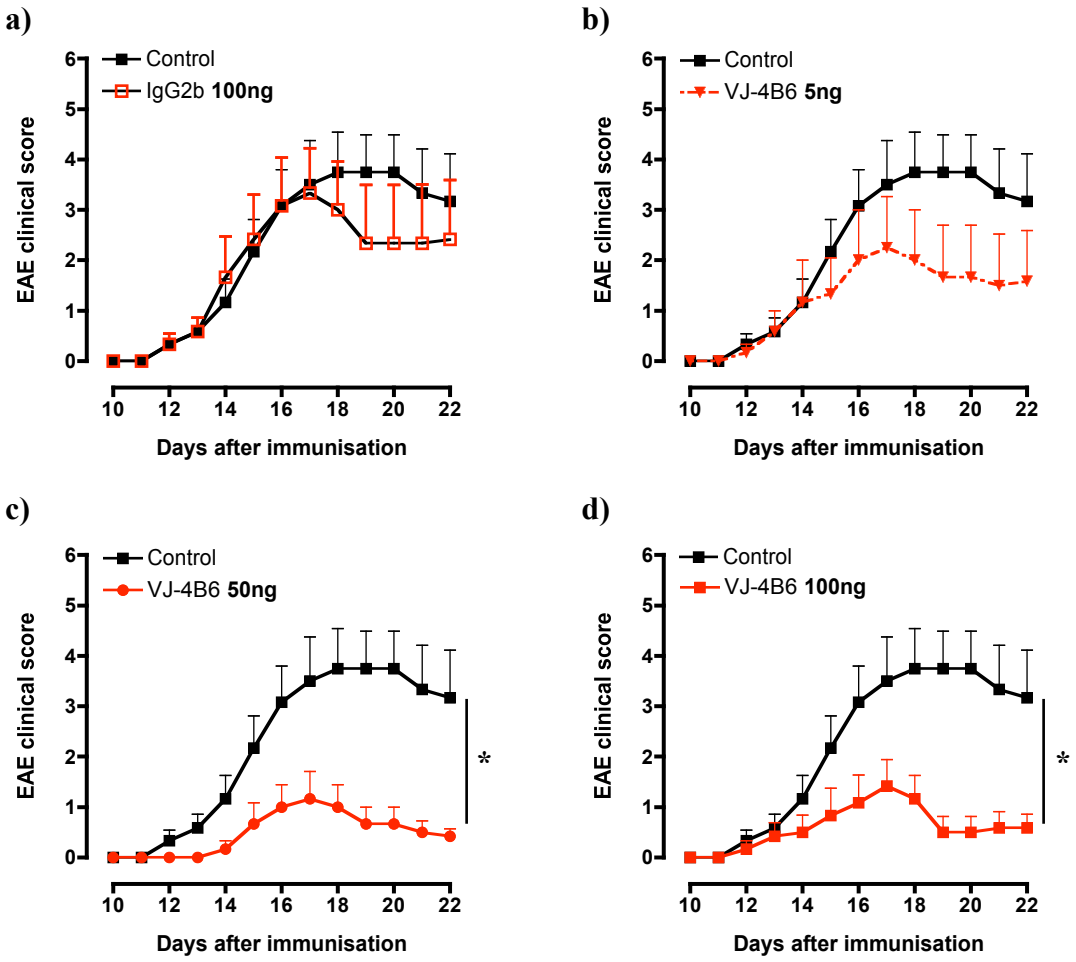

Figure 3.48. Effect of VJ-4B6 on MOG_{35-55} induced EAE. EAE development in mice treated with **a)** 100ng IgG2b or **b)** 5ng, **c)** 50ng and **d)** 100ng of VJ-4B6. All the treatments were given i.p (*p<0.05, repeated measure two-way ANOVA; representative of N=2 experiments with n=6-8 mice per group).

We also tested the therapeutic effect of VJ-4B6 administering the drug post onset of disease. Thus, mice showing first signs of disease (about score of 1 or 2) were clustered for VJ-4B6 (50ng/mouse) or vehicle treatment.

Similar to the previous results, the treatment with VJ-4B6 improved the EAE outcome as shown by the reduced weight loss and lower clinical scores compared to not treated mice (Figure 3.49).

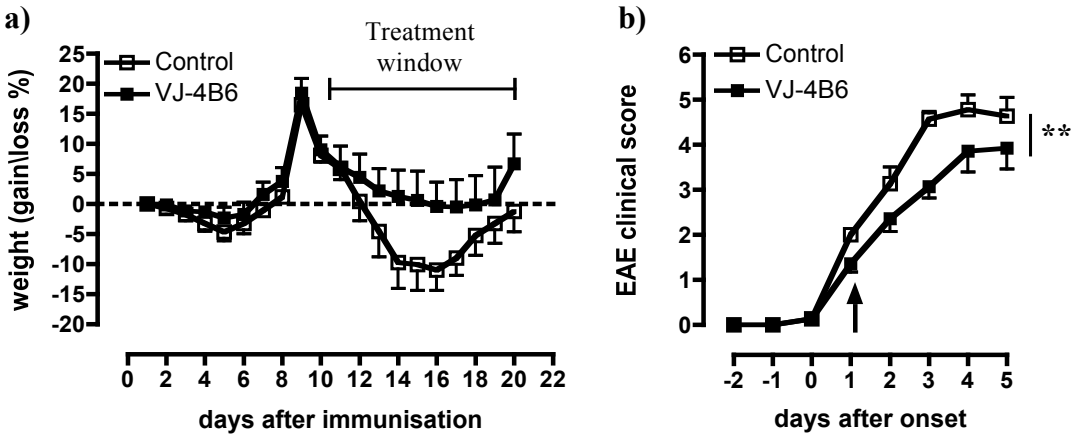

Figure 3.49. VJ-4B6 as post-onset treatment of MOG_{35-55} induced EAE. a) Percentages of gain/loss of body weight and **b)** EAE clinical score of wild type mice immunised and treated with vehicle or 50ng VJ-4B6 after EAE onset (treatment window and black arrow). All the treatments were given i.p. (**p<0.05, repeated measure two-way ANOVA; N=1 experiment with n=8 mice per group).

Glatiramer acetate (GA, 150µg/mouse) used as standard treatment for the EAE was administered subcutaneously for 6 days before the day of immunisation. Control mice received PBS vehicle. Mice treated with GA showed similar weight variation as control mice, albeit delayed by 2-3 days (Figure 3.50a). Similarly, GA delayed the

onset of diseases and slowed down the development of EAE compared to control ($p<0.05$; Figure 3.50b).

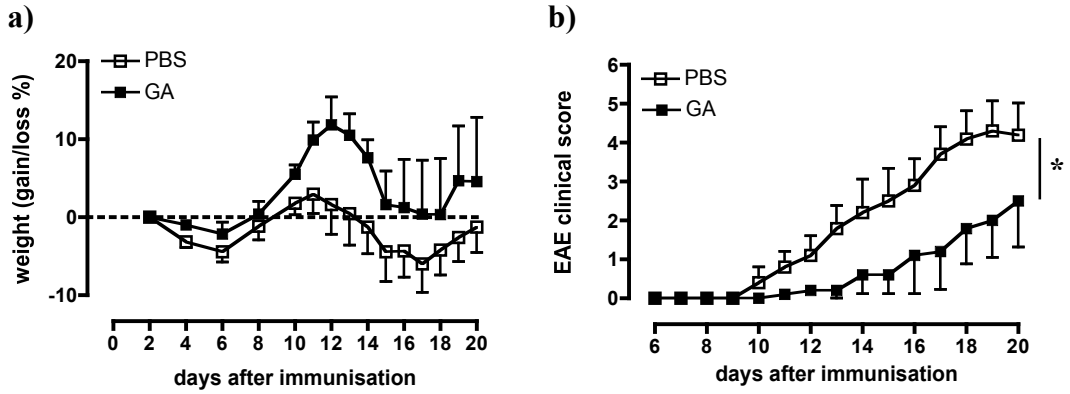

Figure 3.50. Effect of glatiramer acetate on MOG_{35-55} induced EAE. a) Percentages of gain/loss of body weight and **b)** EAE clinical score of untreated (PBS) and GA treated mice. ($p<0.05$, repeated measure two-way ANOVA; 8 mice per group).

3.10.4 T cell phenotype in VJ-4B6 treated mice

We next investigated the effects of VJ-4B6 treatment on T cell phenotypes at day 9 from EAE. The treatment with VJ-4B6 did not affect the frequencies of either CD4+ or CD8+ T cells (Figure 3.51a and 3.51c). However, total cell counts in the lymph nodes and spleens increased by 50% after the treatment. The number of CD4+ and CD8+ T cells in turns doubled compared to control (Figure 3.51b and 3.51d).

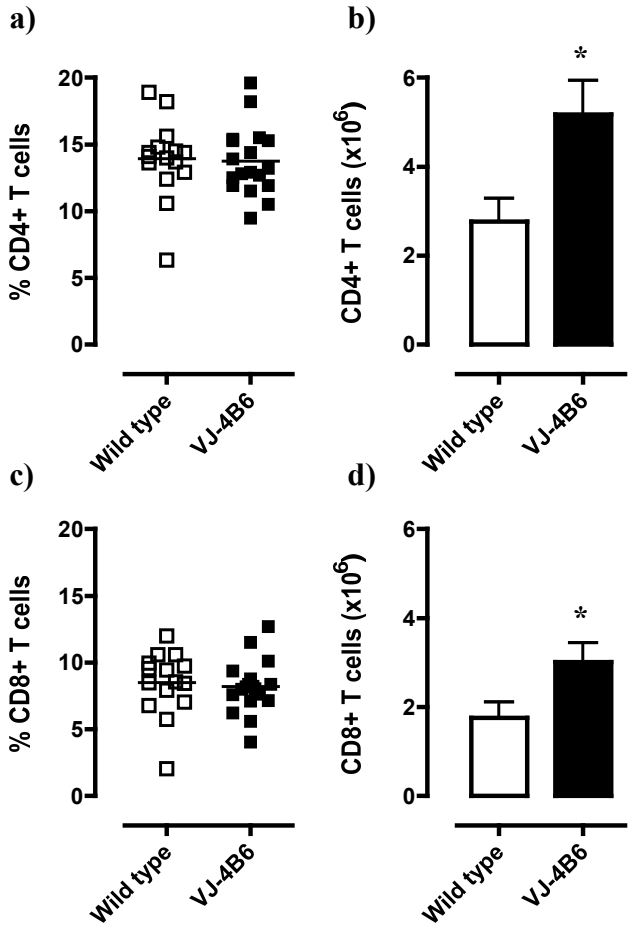

Figure 3.51. Characterisation of T cells of VJ-4B6 treated mice at day 9 of EAE. CD4+ **a)** percentages and **b)** T cell number, and CD8+ **c)** percentages and **d)** T cell number in peripheral lymphoid organs of wild type or VJ-4B6 treated mice after 9 days from EAE immunisation. (*$p<0.05$, unpaired t-test; cumulative data of N=5 experiments with n=4-5 mice per group).

Analysis of CD4+ T cell phenotypes by ICS showed an increase in IFNγ+ and GM-CSF+ cells in VJ-4B6 treated mice compared to wild type (Figure 3.52a and Figure 3.52b). Instead, IL-17 producing CD4+ T cells were comparable between the two groups (Figure 3.52c).

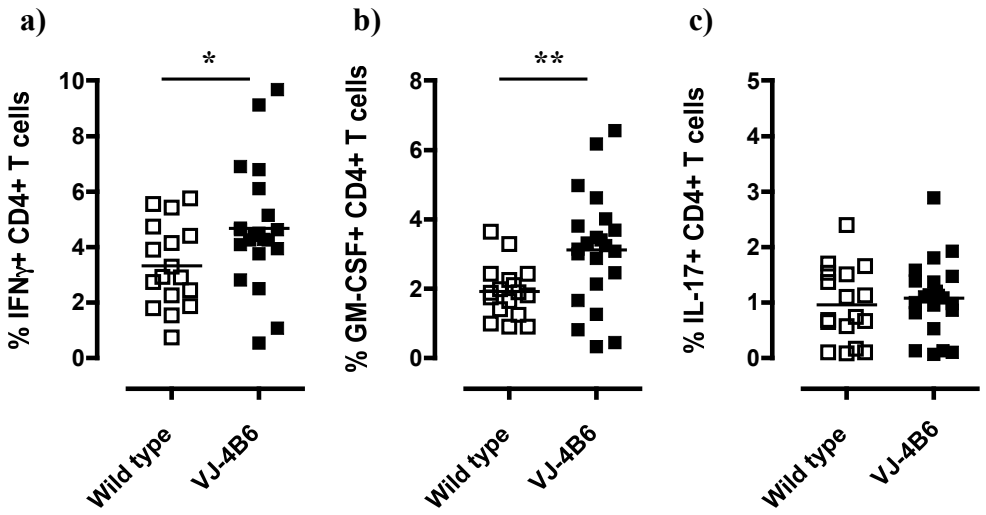

Figure 3.52. ICS of CD4+ T cells of VJ-4B6 treated mice. Percentages of **a)** IFNγ, **b)** GM-CSF and **c)** IL-17 CD4+ T cells of wild type or VJ-4B6 treated mice. ICS was performed after stimulation with MOG_{35-55} and anti-CD28 in vitro for 48h. (*p<0.05, **p<0.01, unpaired t-test; cumulative data of N=3 experiments with n=4-5 mice per group).

Thereafter, we sought to investigate the T cells in the spinal cord at day 16. Infiltrated T cells were counted and stained for CD4 and CD8 (Figure 3.53a and 3.53b). VJ-4B6 treatment clearly influenced the percentage and cell number of CD4+ T cells – halved number of CD4+T cells infiltrated the spinal cord – compared to wild type (Figure 3.53c and 3.53d). In addition, CD8+ T cells also showed decrease in both percentage and cell number after VJ-4B6 treatment (Figure 3.53e and 3.53f).

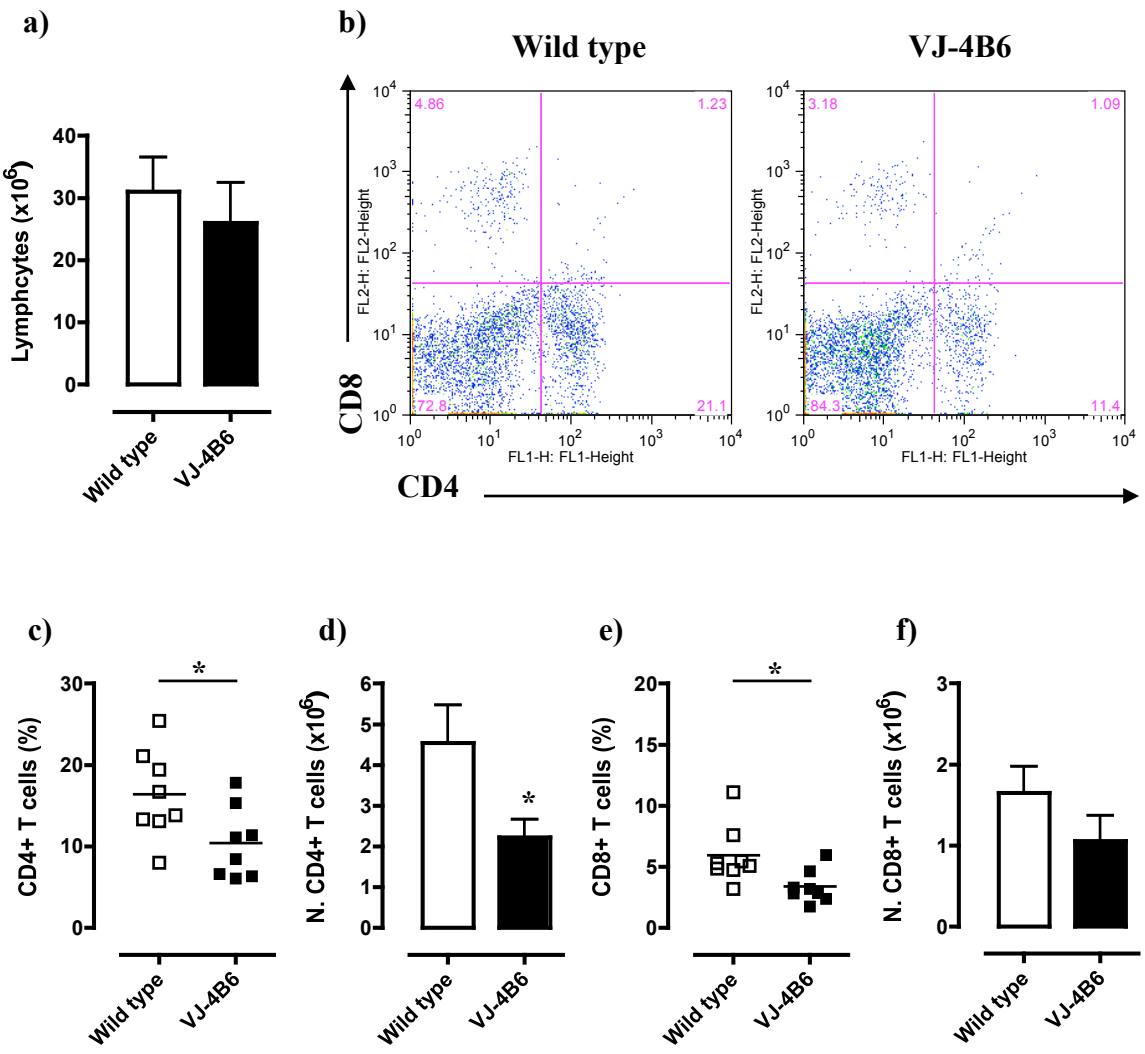

Figure 3.53. Characterisation of T cells in the spinal cord of VJ-4B6 treated mice at day 16. a) Total cell count and **b)** dot plots of CD4+ and CD8+ T cells infiltrated in the spinal cords of wild type and VJ-4B6 treated mice after 16 days from the immunisation. CD4+ **c)** percentages and **d)** T cell number, and CD8+ **e)** percentages and **f)** T cell number of wild type and VJ-4B6 treated mice. (*p<0.05, unpaired t-test; cumulative data of N=2 experiments with n=4 mice per group).

4. Discussion

4.1 Discussion

One of the most interesting aspects of AnxA1 biology is the powerful and broad range of effects in inflammation (251). On one hand, it is able to contribute to the resolution of inflammation modulating the migration and activation of innate immune cells such as neutrophils and macrophages into the inflamed tissue (132, 141, 147, 151). On the other hand, in the context of adaptive immunity it contributes to T cell proliferation and activation hence fostering chronic and autoimmune inflammatory reactions (140, 145, 152, 164, 167).

The main aim of this PhD was to investigate the pro-inflammatory role of AnxA1 in T cells and the potential therapeutic effect of AnxA1 neutralisation in the context of autoimmune diseases. Unexpectedly, we observed that the AnxA1 overexpression in T cells influenced mouse behaviour. This brought us to a novel area of research and propelled the exploration of the fascinating link between "pro-inflamed T cell phenotype" and emotional dysfunctions. T cells have been the subject (and target) of many studies focused on the pathogenesis and treatments of autoimmune diseases. Recent investigations have, however, revealed a key role of these cells in CNS development and function (170, 180, 182, 189, 252). The rather surprising picture emerging from the literature and from the results of this PhD thesis suggests that mental disorders and autoimmune diseases are indeed tightly connected and have common cellular and molecular pathways. This might help to define causes and new therapeutic actions for these pathologies.

4.1.1 AnxA1^{tg} mice and autoimmunity

To investigate the contribution of T cell-AnxA1 in the pathogenesis of autoimmune diseases, we studied the development of MOG_{35-55} induced EAE and the progression of pristane-induced lupus in AnxA1^{tg} mice compared to wild type. MOG_{35-55} induced EAE is a model of demyelination mainly driven by T cells and macrophages (58, 237), although the involvement of B cells in this disease has been recently discussed (253). Pristane-induced lupus is a chemical-induced model of SLE, which develops after the administration in the peritoneum of a hydrocarbon causing typical pathological organ failures – such as lungs, spleen and kidney – that are observed in SLE (241).

Striking differences were observed in the development of EAE between AnxA1^{tg} and wild type mice. The results showed that AnxA1^{tg} mice are prone to develop more severe EAE compared to wild type mice. Indeed, AnxA1^{tg} mice had greater body weight loss compared to wild type mice, conceivably reflecting a major status of general malaise. This was accompanied by higher susceptibility to EAE development and higher scoring of disease. These results were reproducible in independent experiments and consistent with previous studies showing reduced development of MOG_{35-55} induced EAE in AnxA1-/- mice (167).

Similarly, AnxA1^{tg} mice showed exacerbated signs of sickness, such as weight loss and lethality, compared to wild type mice following pristane challenge. The prompt manifestation of these signs and hence the relative short time used for the observation of this model has not given us the possibility to score proteinuria or autoantibodies, which are robust markers at longer time points (254). However, we

were able to associate the increased sickness of the AnxA1^{tg} mice with severe splenomegaly and heavy inflammatory infiltration in their lungs, which are typical of this model (240).

4.1.2 AnxA1^{tg} T cells and immune disorders

At basal conditions, the T cell repertoire of AnxA1^{tg} mice did not show gross differences in T cell development in the thymus compared to wild type mice. This is in agreement with the idea that AnxA1 exerts an action on T cells mostly during activation processes, as previously shown by *in vitro* studies with recombinant AnxA1 (145) or by studies with AnxA1-/- mice (155). In the lymph nodes, conversely, we found an increase in the total cell number of CD4+ T cells. This difference was not observed in the spleen.

To understand how AnxA1 overexpression in T cells influences autoimmune disease progression *in vivo*, we analysed the Th phenotypes of AnxA1^{tg} and wild type mice. For pristane-induced lupus, peritoneal fluid has been reported as suitable sources of lymphocytes to study the T cell phenotypes at early stage of this model (242). Analysis of CD4+ T cells in the peritoneal cavity revealed a reduced number of these cells in AnxA1^{tg} compared to wild type mice with no qualitative changes in their effector phenotype. We can speculate that T cells from AnxA1^{tg} might have a faster priming/activation and thus already be in the target organs, as suggested by the accelerate disease course of AnxA1^{tg} compared to wild type mice. Interestingly, the cytokines measured in the peritoneal lavages have similar concentration in AnxA1^{tg} and wild type mice.

The MOG_{35-55} induced EAE provided us with more insightful results and this might be because this model is more suited to study T cell effector functions and plasticity or, in more general terms, to evaluate the contribution of T cells to the pathogenesis of autoimmune conditions like MS. Through these studies, we were able to study the biologic influence that AnxA1 has in T cell priming and activation in pathological setting.

For decades, IFNγ producing Th1 cells have been considered the only effector T cells able to induce EAE. This conclusion was supported by several evidences including presence of high levels of IFNγ in the inflammatory lesion in the CNS and/or the induction of EAE by adoptive transfer of T clone with a Th1 phenotype (112, 113). In addition, knocking out key molecules involved in the production of IFNγ, in particular T-bet and STAT-4, has been shown an increased resistance to the development of EAE (114, 115). Paradoxically, mice knocked out for either IFNγ or IFNγ-receptor could still develop EAE (118).

IL-12 knockout mice showed the opposite outcomes depending on which of the two subunits of IL-12 was genetically ablated. In particular, the resistance to EAE was associated with deletion of the IL-12p40 subunit, which later was discovered to be the common subunit of IL12 and IL-23. The fact that even the absence of IL-23p19, the second subunit of IL-23, abrogated the EAE let to the conclusion that IL-23 is indispensable for development of this disease (121).

The discovery of IL-23 paved the way to the identification of Th17 cells. Indeed, IL-23-induced Th17 cells were shown to be stronger inducer of EAE upon adoptive transfer compared to Th1 cells (255). On the other hand, Th1 cells were shown to be more potent or even facilitate the entry of Th17 in the CNS (256). Interestingly, the absence of IL-17 in mice merely reduced, but not abrogate the signs of EAE (122). Thus, the role of Th17 cells in EAE and autoimmunity is still controversial and currently a very hot topic in the field.

Studies on adoptive transfer of Th1- and Th17-polarized myelin-specific T cells showed that both Th phenotypes were able to induce EAE; their pathogenic effects was potentiated when transferred in combination (257). However, IL-12-polarized IFNγ-deficient T cells transferred in IL-17-receptor knockout mice were still encephalitogenic (124). This study led to the conclusion that there is a new type of IFNγ- and IL-17-independent T cells that are crucial for the development of EAE: these are the recently identified GM-CSF producing T cells (ThGM-CSF cells). Consistent with this, treatment of mice with GM-CSF neutralising antibodies as well as GM-CSF knocked out mice showed a complete protection against EAE (97, 124).

In light of all these findings, we have given particular attention to Th1, Th17 and ThGM-CSF phenotypes to investigate the potential differences between AnxA1^{tg} and wild type mice during EAE. In particular, we carefully analysed the effects of AnxA1 on T cell plasticity investigating the phenotype of Th cells both before (day 9) and after (day 16) the onset of EAE.

At day 9, we observed that neither the total cell number nor the percentage of CD4+ T cells in the periphery was different between AnxA1^{tg} and wild type mice. However, the percentages of CD4+ T cells were significantly higher in AnxA1^{tg} compared to wild type upon antigen re-challenge *in vitro* suggesting an increased capability for clonal expansion and survival of AnxA1^{tg} T cells. The percentages of IFNγ, GM-CSF and IL-17 producing CD4+ T cells consistently increased in concert with the type of stimulation in both AnxA1^{tg} and wild type. We also observed a hierarchy in the cytokine production with higher percentage of IFNγ+ CD4+ T cells followed by GM-CSF+ and IL-17+ CD4+ T cells. This holds true in both wild type and AnxA1^{tg} mice and did not change over a number of experiments.

Higher concentrations of GM-CSF were detectable in the culture medium of AnxA1^{tg} lymphocytes after antigen specific stimulation. This increased production was not matched by the results obtained with the intracellular staining and are likely due to either reduced sensitiveness of ICS technique (it measures cytokines produced intracellularly at a single time point rather than their accumulation in the medium) in revealing differences in GM-CSF producing Th cells or due to the detection of GM-CSF produced by other T cells rather than only CD4+ T cells. This could be indeed the case for IL-17 which has been shown to be also highly expressed in γδ T cell population (105).

We observed some degree of variability within each single experiment. This is a common effect and it might be explained by the lack of "synchronization" in T cell activation *in vivo* (not all animals develop disease at the same time and to an

equivalent extent) and/or by the somehow not fully defined effector phenotypes during the pre-onset phase of EAE. In line with this, Korn *et al*. showed that effector Th cells in the peripheral lymphoid organs as well as in the circulation do not show great variation in their phenotype during the development of EAE, while those infiltrated in the CNS do (238). Hence, we investigated T cells migrated from the periphery to the CNS.

The development of EAE in AnxA1^{tg} and wild type mice appears to run in a similar way from the onset of disease till the clinical score reaches a value between 2 and 3. However, at later stage (roughly from day 16), these mice progressed differently showing exacerbated signs of disease in AnxA1^{tg} mice only. Previous studies on the same EAE model showed that the frequency of Th secreting IL-17 or IFNγ changes over time in both periphery and CNS, with particular pattern moving from IL-17 single positive to double positive IL-17/ IFNγ and IFNγ single positive T cells. Then, Hirota *et al*. were able to show that the committed Th17 phenotype progressively changes their phenotype in Th1-like at the site of chronic inflammation. Indeed, Th17 cells reduce the expression of IL-17 while increasing IFNγ once they move from the lymph nodes to the spinal cord (105, 109).

Lately, the existence of two main Th17 populations has been proposed: non-pathogenic and pathogenic Th17 cells. The latter differentiate under either IL-1β- or TGFβ- plus IL-6-skewing conditions and subsequently expand under IL-23-mediated signalling. These cells express high levels of T-bet, STAT4 and GM-CSF as well as reduced IL-10 and IL-10- related genes. Thus, pathogenic Th17 cells are considered

to be those cells that acquire a Th1-like phenotype in the CNS during the EAE pathogenesis (127).

In our studies we observed an increase in the total cell number and CD4+ T cells infiltrating the CNS in AnxA1^{tg} mice compared to wild type. Infiltrated AnxA1^{tg} T cells expressed less or equivalent amount of IFNγ and GM-CSF, whereas higher IL-17 levels compared to wild type cells. More intriguingly, higher presence of GM-CSF or IFNγ and IL-17 double positive T cells was quantifiable in AnxA1^{tg} comparing to wild type mice.

Th17 is considered an unstable Th subtype that, as mentioned earlier, during the course of chronic inflammatory conditions, such as EAE, loses IL-17 expression to switch on producing IFNγ. Our data suggest that AnxA1^{tg} Th17 cells maintain the pathogenic phenotype of co-producing IL-17 and IFNγ or GM-CSF for longer time compared to wild type. The increased percentage of Th17/ThGM-CSF as well as of Th17/Th1 populations in AnxA1^{tg} mice might explain the higher severity of EAE signs in these mice compared to wild type mice.

Thus, the influence of AnxA1 in the Th17 plasticity ultimately reduces the number of IFNγ producing T cells. It might seem a contradiction, but the Th1 phenotype has been shown to be more susceptible than Th17 to the suppressive actions of Treg cells (238). Thus, the conversion from Th17 to Th1 might be an important mechanism for the resolution of the disease. In this way, we can speculate that AnxA1 interfere with a biological protective phenomenon by impairing Th17 plasticity.

4.1.3 AnxA1^{tg} T cells and mental disorders

Rodents have "emotions and personalities" and their behaviour can be studied and used for investigating pathways and thus screening a variety of experimental conditions mimicking CNS pathologies. Serendipitously, we observed a difference in behaviour between AnxA1^{tg} and wild type mice. Under the supervision of Dr Robert Deacon, an expert behaviourist from the University of Oxford, we explored potential changes in emotional behaviour using several paradigms. Many of these create an adverse situation for the animal, which tent to avoid it for natural fear; as cats do not like water, mice are wary of bright and lit open areas (258). The systems we used were the marble-burying, the open field, the climbing, and the light/dark box tests.

All these tests allow evaluation of several parameters that are used to score and interpret fear-related or anxiety-like state in mice (246, 248, 259, 260). The reactions that mice have in the new adverse condition share analogous, if not homologous, mechanisms of defence with anxiety disorders in human (259, 261). Hence, behavioural studies in rodents have been long used for either improve our knowledge on the etiopathogenesis of these diseases or for drug testing.

From these behavioural studies, we observed that AnxA1^{tg} mice have an overall increased marble-burying activity – they start to dig earlier and their total digging time is longer than wild type mice showing also by a higher number of buried marbles. In addition, we observed reduced time spent in light and number of crossing in the light/dark box test of AnxA1^{tg} compared to wild type mice. These behaviours have been duly associated to anxious-like behaviour as well as the hesitation – expressed by the latency to rear – for the exploration of the open field. In the

climbing test, AnxA1^{tg} mice spent less time climbing compared to wild type. However, AnxA1^{tg} mice showed equivalent number of bouts in the marble-burying test as equivalent number of rearing and total squares crossed in the open field. All together this behaviour profile highlights a divergence in "emotionality" of AnxA1^{tg} compared to wild type rather than an explorative or motile impairment of these mice (262, 263).

The most interesting part of these behavioural studies is the consideration that AnxA1^{tg} mice derived from a genetic modification in lymphoid cells. These findings have prompted us to focus and investigate how T cells influence the emotional response (a topic that we are currently studying in our group). With great surprise we found support in literature suggesting the importance of T lymphocytes in the regulation of a number of functions including cognition, memory and even trauma (170, 179-185, 264). Among this, Prof Schwartz (Weizmann Institute of Science, Rehovot, Israel) and Prof Kipnis (Center for Brain Immunology and Glia, University of Virginia, Charlottesville, Virginia, USA) also proposes a beneficial action and purpose for CNS-auto-reactive T cells for neurofunctions since they are necessary for cognitive functions – such as memory and spatial learning (170, 181-183). Other findings suggest that active, mostly Th2-skewed CD4+ T cells are critically involved in cognitive functions (183) and elegantly show that they bear a CNS antigen specific TCR (264). Hence the hypothesis of a positive autoimmunity, currently questioned concept in the field since it undermines the historical dogma of CNS as immunoprivileged organ. This novel view considers the CNS as any other tissue and organ in the body so it is as well patrolled by the immune system. The immune response brought about by auto-reactive T cells bearing CNS antigen-specific TCR is

fundamental to restore the homeostasis in the tissue after an insult or stimulus, such as tissue damage or cognitive input.

Our studies suggest that overexpression of AnxA1 in T cells increases the anxiety-like behaviour of C57BL/6 mice providing a novel mechanism by which T cells control emotions. Intriguingly, we observed that T cell priming against either a CNS-specific or an irrelevant antigen (MOG_{35-55} and $OVA_{323-339}$, respectively) followed by T cell mobilisation into the blood stream are sufficient to cause an emotional disorder in mice (73). This might suggest that $AnxA1^{tg}$ T cells might be correlated to emotional disorders because of their hyper-reactive phenotype. Another hypothesis could be that the presence of $AnxA1^{tg}$ T cells in circulation might influence neurogenesis as mice develop. Indeed, we now know that emotional abnormalities observed in immunodeficient mice are restored to the level of wild type in those born with CD4+, but not CD8+, T cell population. Most strikingly, we found that the presence or absence of T cells in circulation could influence the pattern of gene expression in the brain (252). This suggested to us that T cells per se exert a homeostatic control on brain function and consequent emotional response.

We thus sought to better understand how AnxA1 overexpression in T cells influence the emotional response and to do so we explored three main approaches:

a) Adoptively transfer of $AnxA1^{tg}$ T cells into wild type C57BL/6 mice;

b) Investigate the gene expression profiles of $AnxA1^{tg}$ CD4+ T cells;

c) Investigate the gene expression profiles of $AnxA1^{tg}$ whole brain.

Transfer of control or AnxA1^{tg} CD3+ T cell population (CD4 plus CD8) into C57BL/6 mice affected similarly the anxiety-like behaviour of the recipients. In both cases, we observed a reduced time spent in light and reduced number of crossing in the light/dark box test three weeks after the T cell transfer, thus suggesting a relationship between T cells and emotional behaviour.

We observed remarkable differences when we transfer CD4+ T cells. Indeed, the transfer of CD4+ T cells from AnxA1^{tg} T cells into C57BL/6 mice induced an increased anxiety-like behaviour compared to wild type donors and PBS control group. This suggests that AnxA1^{tg} CD4+ T cells were able to induce and transfer anxiety-like behaviour. Interestingly, no significant changes in anxiety-like behaviour were observed in mice receiving sera isolated from the same groups of donors ruling out the possible contribution of inflammatory cytokines or antibody in the behavioural response we observed.

AnxA1 is well known as one of the second messengers of GCs action (133). It has been well described its function of paracrine/juxtacrine mediator in the neuroendocrine system and in particular to be responsible of the negative feedback action exerted by GCs on the HPA axis (211-215). This might raise the query whether the changes in emotional behaviour are due to an alteration of HPA axis in AnxA1^{tg} mice. However, this is a very unlikely mechanism for a number of reasons. First, the transgenic mouse is tissue specific (T cells only) and not a general transgenic. Second, we measured the levels of corticosterone in the plasma of wild type and AnxA1^{tg} mice, and the concentrations were similar (31.6 ± 5, and 34 ± 7.8 ng/ml, n=5 male mice per group). Last but not least, the “extra” amount of AnxA1

produced by T cells in the AnxA1^{tg} mice would not influence the amount of AnxA1 that is present in circulation in view of the relatively low content compared to myeloid cells.

Microarray analysis of CD4+ T cells revealed that AnxA1 has 3-fold increase in expression in transgenic compared wild type. However, this increase of AnxA1 is paltry to justify any direct effect of AnxA1 on the behaviour. Indeed, the amount of AnxA1 in CD4+ T cells remains much lower – even after such boost – than the quantity expressed in the innate immune cells, which physiologically express 25-fold more AnxA1 than CD3+ T cells (138).

In AnxA1^{tg} T cells many interesting cell pathways are altered compared to wild type. Just to mention some, cell cycle, Jak-STAT, and NF-κB signalling pathways which are known to be relevant for T cell proliferation (88, 89, 101, 265) and lineage commitment (78, 92, 101). This might further explain the effects of AnxA1 on the Th phenotype in the transgenic mice. Indeed, we found higher number of T cells populating the lymph nodes of AnxA1^{tg} mice, and AnxA1^{tg} CD4+ T cells have a higher proliferating rate as well as lower threshold of TCR signaling (data not shown) compared to wild type mice. Other interesting altered pathways are related to autoimmune diseases and viral infectious, such as Herpes simplex, Influenza A, and Epstein-Barr virus. This is intriguing since many studies claim a strong association among infectious diseases, autoimmune diseases and mood disorders (169). It has been reported that the risk to develop mood disordered increase by 62% and 45% after infection and autoimmune disease diagnosis, respectively, and this percentage further increase if they co-occur in patients, suggesting a negative synergistic effect

(169). All together this might explain the autoimmune-prone phenotype of AnxA1^{tg} mice, however does not fully explain how the overexpression of AnxA1 in T cells leads to anxiety-like behaviour.

In humans, several clinical studies have described the role of T cells in mood disorders in conflicting ways. On one hand, the decreased number of T cells contributes to establish depression (226) while increased T cell number is associated to optimism (225). In line with these findings, stress conditions and anxiety increase levels of GCs which suppress activation, proliferation and trafficking of immune cells, including T cells (266). On the other hand, psychotic disorders, patients with treatment-resistant depression and anxiety disorders showed elevated number of total white blood cell and helper T cell count (230, 232). Hence, neuroendocrine variations cause changes in leukocytes including lymphocytes. Thus, microarray analysis of T lymphocytes has been proposed as a powerful technique to study CNS abnormalities such as psychiatric disorders (235). Indeed, T cells might promptly reflect changes in CNS homeostasis through their complex communication network made of neurotransmitters, neurotrophic factors and cytokines.

In line with this, to explore how CD4+ T cells could elicit the observed anxiety-like behaviour in AnxA1^{tg} mice we used the microarray analysis. Out of 2,487 genes that were modulated we focused our attention to the new ones and in particular on 2610019F03Rik [http://www.ebi.ac.uk; query: 2610019F03Rik]. This is a yet to be identified protein that is highly inducible upon T cell activation and is expressed at higher levels in AnxA1^{tg} T cells, at both mRNA and protein level. The 2610019F03Rik is evolutionary conserved gene in vertebrates expressing a short

amino acid sequence (190aa) with unknown *in vivo* function and 75% homology with the human protein [http://blast.ncbi.nlm.nih.gov/Blast.cgi]. In our studies, the blocking of 2610019F03Rik by polyclonal antibody or the injection of 2610019F03Rik recombinant protein caused an anxiolytic and anxiogenic effect, respectively. Several other genes, including the vasopressin or cathepsine B gene, have been described to exert a role in anxiety-like phenotype in rodents. Those, however, have been identified in the microarray analysis of brain regions within the limbic area (267). To the best of my knowledge, no gene expressed in lymphocytes has been so far linked to mood disorders. Hence, the 2610019F03Rik might be one of the first factors that is expressed in T cells and might be able to influence anxiety disorders.

All of these results become even more interesting after we compared the gene expression profile of the whole brain of AnxA1^{tg} and wild type mice. The results of this analysis revealed less than 40 genes differentially expressed. The restricted numbers of genes we found provided us with restricted and focused field to research. SPIA analysis of these genes suggested many as being related to neurodegenerative diseases (they include Parkinson's, Alzheimer's or Huntington's diseases, which share highly inflammatory features) or to signalling pathways described in mental disorders i.e. glutamatergic or serotonergic synapses.

4.2 Clinical relevance and AnxA1 therapeutic potential

Several lines of evidence suggest that changes in AnxA1 expression are associated with the development of autoimmune diseases. Biochemical analysis of post-mortem CNS tissues of MS patients revealed co-localization of high level of AnxA1 and expression of CD3 in the white matter plaques (161). Similarly, CD4+ T cells isolated from RA patients show higher expression of AnxA1 at both mRNA and protein levels comparing to CD4+ T cells isolated from healthy volunteers (145, 164). Finally, CD4+ T cells isolated from patients suffering from SLE or MS show higher expression of AnxA1 compared to healthy controls (166, 268).

To explore the therapeutic potential of the findings obtained with $AnxA1^{tg}$ mice, we tested the effects of an AnxA1 neutralizing antibody, VJ-4B6, on the development of MOG_{35-55} induced EAE. Mice treated with VJ-4B6 were significantly protected from EAE since 50% manifested signs of disease and these were in addition mild and stable over time. Similarly, the administration of VJ-4B6 after EAE onset slowed down the EAE development. Overall the therapeutic effects were specific i.e. IgG-isotype antibody was ineffective, and promising when compared to the efficacy of the GA treatment used as positive therapeutic control.

Preliminary experiments investigating the effect of VJ-4B6 *in vivo* showed no toxic effects. The treatment did not cause any changes in the total cell count in thymus or in lymph node. The CD4+/CD8+ T cell ratio was comparable to control mice in the peripheral lymphoid organs, as well as no difference was found in B cell or monocyte number. Interestingly, we observed a surprisingly increased cell number in the spleen.

Likewise, we found increased total cell number and CD4+ or CD8+ T cells, although they show similar frequencies, in peripheral lymphoid organs of VJ-4B6 treated mice at 9 day from EAE immunisation. Interestingly, the phenotype of the CD4+ T cells was highly positive for IFNγ and GM-CSF in VJ-4B6 treated compared to wild type. This suggests that VJ-4B6 might protect from autoimmune diseases by trapping T cells, including the most pathogenic ones, in peripheral lymphoid organs – similarly to the mechanism of action described for the Fingolimod. This hypothesis is indeed supported by our microarray analysis that has shown an increased expression of sphingosine 1- phosphate (S1P) receptor in CD4+ T cells stimulated overnight in presence of VJ-4B6 (data not shown). Consistently, the spinal cord infiltrates at day 16 showed a decreased number of CD4+ as well as CD8+ T cells in VJ-4B6 treated mice. Further studies are needed to investigate if these effects are due a dual action of VJ-4B6 on T cells as well as on APCs including DCs. This might be relevant considering the previously observed tolerogenic properties of AnxA1-/- bone marrow-derived dendritic cells (269).

Our experimental observations are consistent with clinical data reporting higher prevalence of anxiety and depression in patients suffering from autoimmune diseases (28, 52, 53, 55). It was interesting to observe that the adoptive transfer of CD3+ T cells anticipated the onset of EAE (of about three days) and exacerbated clinical signs, and similar outcomes occurred after CD4+ T cell adoptive transfer. More impressive in my view was the association between the anxious profile displayed by the mice and the severe outcome of diseases after the transfer of T cells. This might suggest a cause-effect relationship between number and/or activation state of T cells,

and anxiety-like behaviour. A recent article by Harpaz *et al*., showed that stress negatively affected Treg but not effector T cells, which increase in number and polarise towards Th1-Th17 phenotype. Mice under stress showed, indeed, exacerbations in EAE, which were prevented by a glucocorticoid antagonist (234). Thus, the chronic activation of the HPA axis causes desensitization towards the immunosuppressive effects of glucocorticoid (270) and consequently increases susceptibility to autoimmune diseases. Clinically, periods of high stress have been correlated with relapses of multiple sclerosis or psoriasis (271, 272). Looking at a bigger picture, we could describe this as a physiologic circuit where mood, emotion and mental health induce changing in the peripheral physiology including the state of T cells, and these in turn influence brain functions shaping emotion and cognition according to their state or phenotype.

4.4 Conclusion and future experimental approaches

The AnxA1^{tg} mice revealed to be anxious-like *per se* and when appropriately challenged it was severely susceptible to autoimmune diseases. AnxA1 overexpression in T cells is the only connector between these two phenotypes. The variegated experimental approaches and studies showed in this thesis reveal the complexity of neuro-immune interactions and in particular the connection between autoimmune diseases and mood disorders – such as such anxiety, depression and psychosis. Most importantly, we underline the importance and ability of hyper-reactive CD4+ T cells to affect emotional behaviour. Indeed, the overexpression of AnxA1 in T cells makes T cells highly responsive to proliferative and activation stimuli, and imprints an anxiogenic phenotype (Figure 4.1). In addition to this,

AnxA1 seems to have a strong influence on the plasticity of Th cells and their pathogenic effects.

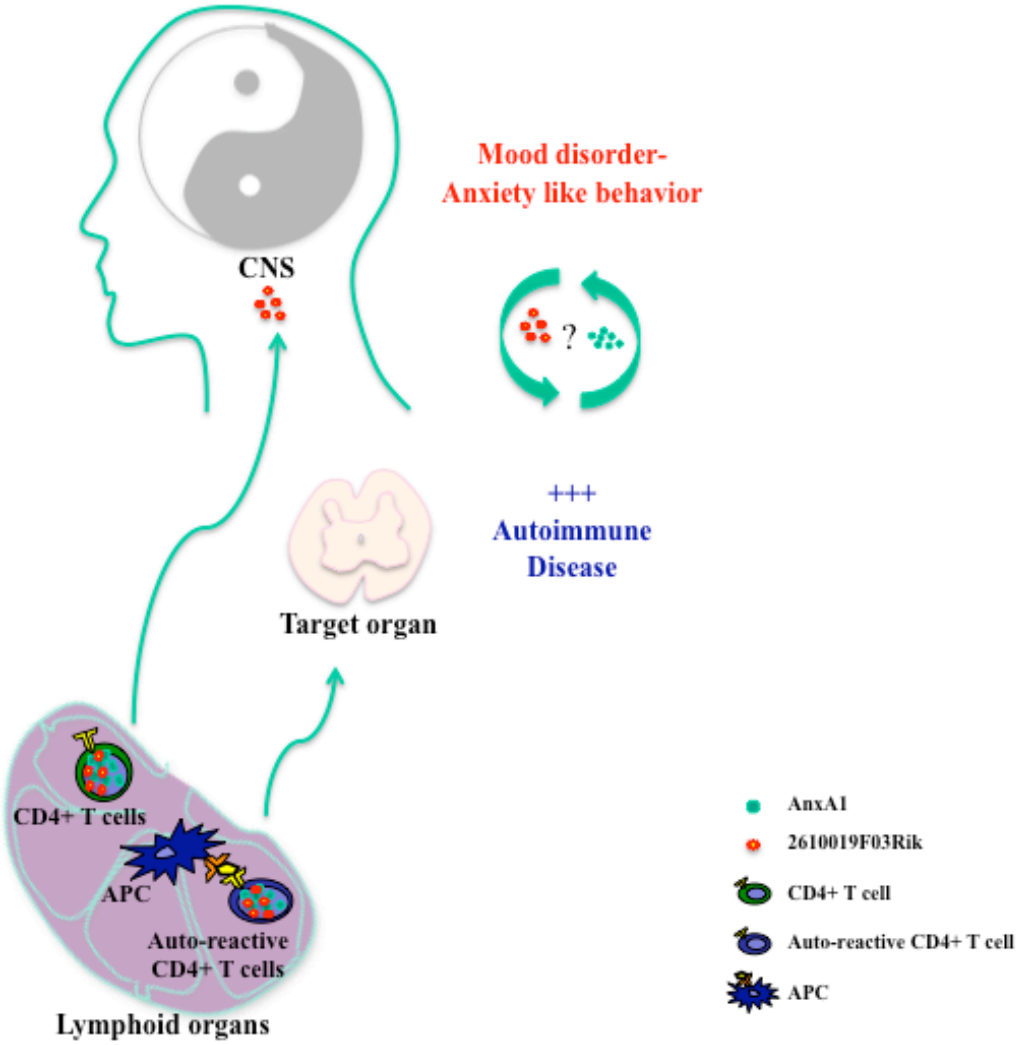

Figure 4.1. Effects of AnxA1^{tg} T cells in mental and body homeostasis. Depicted are the major discoveries made out of the studentship. **1)** CD4+ T cells overexpressing AnxA1 induce alterations in the mental health homeostasis causing an anxiety-like behaviour. **2)** This effect is mediated by a poorly characterised gene product termed protein 2610019F03Rik: this protein is overexpressed in AnxA1^{tg} CD4+ T cells. **3)** In the context of autoimmunity, AnxA1^{tg} CD4+ T cells promote severe development of experimental autoimmune encephalomyelitis. Altogether these novel findings indicate that the AnxA1^{tg} mouse is a viable model for studying the reciprocal influence and shared pathways between mood disorders and autoimmune diseases.

All together these results bring to the conclusion that AnxA1 is an optimal biomarker as well as candidate to therapeutically intervene in both autoimmune diseases and emotional disorders. We also identified 2610019F03Rik protein as mediator that is released by AnxA1^{tg} CD4+ T cells and might be targeted for the treatment of anxiety disorders (Figure 4.1). The results of this thesis provide first evidence for a protective and therapeutic effect of neutralizing antibodies against AnxA1 in a model of MS. Preliminary studies have been done to test the potential therapeutic action of VJ-4B6 in depression and anxiety. Recently, humanised forms of VJ-4B6 antibody have been generated and are currently being tested to confirm the therapeutic potential of targeting AnxA1 in models of autoimmune diseases. Ideally, one of these will be soon selected for future tests assessing efficacy and safety in clinical trials.

Many questions still remain unaddressed. How does anxiety-like behaviour transferred by AnxA1^{tg} CD4+ T cells ensue? We know that the 2610019F03Rik protein might be responsible for the anxiogenic effect of AnxA1^{tg} CD4+ T cells. In addition, the systemic administration of 2610019F03Rik as recombinant protein as well as the administration of a polyclonal antibody against it caused significant modulation of anxiety-like behaviour. However, it remains to establish whether the release of this mediator in the periphery is sufficient to alter the behaviour or whether it is necessary that AnxA1^{tg} CD4+ T cells enter and release their factor into CNS. Consistent with the latter hypothesis, we observed a consistent time lapse between the T cell adoptive transfer and the onset of anxiety – about a delay of at least 14 days – making the tracking of the transferred T cells *in vivo* over time a very interesting next step to explore. In addition, it remains to be explained if the action of

2610019F03Rik is broad and this is affecting other physiological processes or whether it is delineated and specific for brain and/or T cells.

I think it is also worth getting up deep analyses for the understanding of the tight link between anxiety-like status and the susceptibility to the development of autoimmune diseases. Is this something that we are able to manipulate? Removing the cause of the anxiety-like status, are we able to reduce the susceptibility to autoimmune diseases? For instance, if we block AnxA1 and/or 2610019F03Rik in the transgenic CD4+ T cells, are we able to rescue both detrimental phenotypes (autoimmunity and mood disorders)? It would be revolutionary to simultaneously treat patients suffering from mood disorders and autoimmune diseases through the manipulation of T cell phenotype.

These results open new research questions as well. If emotions as well as cognition are dramatically influenced by the presence, amount and type of T cells, is the inverse equation valid too? We already are familiar with the outbreak of opportunistic infections, cold and/or cold sores coinciding with stress periods. However, how do positive feelings and/or general psychological wellbeing influence the immune defences? Are psychotherapy, aromatherapy, meditation, or any positive mood boosting activity able to educate the immune system? AnxA1^{tg} mice represent a unique valuable mouse model to explore all these research questions.

5. References

1. Burnet FM. The Nobel Lectures in Immunology. The Nobel Prize for Physiology or Medicine, 1960. Immunologic recognition of self. Scand J Immunol. 1991;33(1):3-13.
2. Matzinger P. The danger model: a renewed sense of self. Science. 2002;296(5566):301-5.
3. Murphy KP, Travers P, Walport M, Janeway C. Janeway's immunobiology. 7th ed. / Kenneth Murphy, Paul Travers, Mark Walport ; with contributions by Michael Ehrenstein ... [et al.]. ed. New York: Garland Science ; London : Taylor & Francis [distributor]. xxi, 887 p. p.
4. Kyewski B, Derbinski J. Self-representation in the thymus: an extended view. Nat Rev Immunol. 2004;4(9):688-98.
5. Goodnow CC, Sprent J, Fazekas de St Groth B, Vinuesa CG. Cellular and genetic mechanisms of self tolerance and autoimmunity. Nature. 2005;435(7042):590-7.
6. Hogquist KA, Baldwin TA, Jameson SC. Central tolerance: learning self-control in the thymus. Nat Rev Immunol. 2005;5(10):772-82.
7. Xing Y, Hogquist KA. T-cell tolerance: central and peripheral. Cold Spring Harb Perspect Biol. 2012;4(6).
8. Drakopoulou E, Outram SV, Rowbotham NJ, Ross SE, Furmanski AL, Saldana JI, et al. Non-redundant role for the transcription factor Gli1 at multiple stages of thymocyte development. Cell Cycle. 2010;9(20):4144-52.
9. Hager-Theodorides AL, Furmanski AL, Ross SE, Outram SV, Rowbotham NJ, Crompton T. The Gli3 transcription factor expressed in the thymus stroma controls thymocyte negative selection via Hedgehog-dependent and -independent mechanisms. J Immunol. 2009;183(5):3023-32.
10. Flores-Borja F, Mauri C, Ehrenstein MR. Restoring the balance: harnessing regulatory T cells for therapy in rheumatoid arthritis. Eur J Immunol. 2008;38(4):934-7.
11. Liblau RS, Tisch R, Shokat K, Yang X, Dumont N, Goodnow CC, et al. Intravenous injection of soluble antigen induces thymic and peripheral T-cells apoptosis. Proc Natl Acad Sci U S A. 1996;93(7):3031-6.
12. Schwartz RH. T cell anergy. Annu Rev Immunol. 2003;21:305-34.
13. Sobek V, Balkow S, Körner H, Simon MM. Antigen-induced cell death of T effector cells in vitro proceeds via the Fas pathway, requires endogenous interferon-gamma and is independent of perforin and granzymes. Eur J Immunol. 2002;32(9):2490-9.
14. Schönrich G, Kalinke U, Momburg F, Malissen M, Schmitt-Verhulst AM, Malissen B, et al. Down-regulation of T cell receptors on

self-reactive T cells as a novel mechanism for extrathymic tolerance induction. Cell. 1991;65(2):293-304.
15. Guery JC, Galbiati F, Smiroldo S, Adorini L. Selective development of T helper (Th)2 cells induced by continuous administration of low dose soluble proteins to normal and beta(2)-microglobulin-deficient BALB/c mice. J Exp Med. 1996;183(2):485-97.
16. Gabrysová L, Nicolson KS, Streeter HB, Verhagen J, Sabatos-Peyton CA, Morgan DJ, et al. Negative feedback control of the autoimmune response through antigen-induced differentiation of IL-10-secreting Th1 cells. J Exp Med. 2009;206(8):1755-67.
17. Kuchroo VK, Ohashi PS, Sartor RB, Vinuesa CG. Dysregulation of immune homeostasis in autoimmune diseases. Nat Med. 2012;18(1):42-7.
18. Rioux JD, Goyette P, Vyse TJ, Hammarström L, Fernando MM, Green T, et al. Mapping of multiple susceptibility variants within the MHC region for 7 immune-mediated diseases. Proc Natl Acad Sci U S A. 2009;106(44):18680-5.
19. Johanna Aaltone PB, Jaakko Perheentup, Nina Horelli–Kuitunen, Aarno Palotie, Leena Peltonen, Yeon Su Lee, Fiona Francis, Steffen Henning, Cora Thiel, Hans Leharach & Marie–Laure Yaspo. An autoimmune disease, APECED, caused by mutations in a novel gene featuring two PHD-type zinc-finger domains. *Nature Genetics*. 1997(17):399 - 403.
20. Serafini B, Rosicarelli B, Franciotta D, Magliozzi R, Reynolds R, Cinque P, et al. Dysregulated Epstein-Barr virus infection in the multiple sclerosis brain. J Exp Med. 2007;204(12):2899-912.
21. Giovannoni G. Epstein-Barr Virus and MS. Int MS J. 2011;17(2):44-9.
22. Parks T, Smeesters PR, Steer AC. Streptococcal skin infection and rheumatic heart disease. Curr Opin Infect Dis. 2012;25(2):145-53.
23. Karlsen AE, Dyrberg T. Molecular mimicry between non-self, modified self and self in autoimmunity. Semin Immunol. 1998;10(1):25-34.
24. Kleinewietfeld M, Manzel A, Titze J, Kvakan H, Yosef N, Linker RA, et al. Sodium chloride drives autoimmune disease by the induction of pathogenic TH17 cells. Nature. 2013;496(7446):518-22.
25. Correale J, Ysrraelit MC, Gaitán MI. Vitamin D-mediated immune regulation in multiple sclerosis. J Neurol Sci. 2011;311(1-2):23-31.
26. Cooper GS, Bynum ML, Somers EC. Recent insights in the epidemiology of autoimmune diseases: improved prevalence estimates and understanding of clustering of diseases. J Autoimmun. 2009;33(3-4):197-207.

27. Rose NR, Bona C. Defining criteria for autoimmune diseases (Witebsky's postulates revisited). Immunol Today. 1993;14(9):426-30.
28. Weiss DB, Dyrud J, House RM, Beresford TP. Psychiatric manifestations of autoimmune disorders. Curr Treat Options Neurol. 2005;7(5):413-7.
29. Zonana MF, Reyes E, Weisman AK. Coexistence of four autoimmune diseases in one patient: the kaleidoscope of autoimmunity. J Clin Rheumatol. 2002;8(6):322-5.
30. Somers EC, Thomas SL, Smeeth L, Hall AJ. Are individuals with an autoimmune disease at higher risk of a second autoimmune disorder? Am J Epidemiol. 2009;169(6):749-55.
31. Somers EC, Thomas SL, Smeeth L, Hall AJ. Autoimmune diseases co-occurring within individuals and within families: a systematic review. Epidemiology. 2006;17(2):202-17.
32. Anaya JM, Corena R, Castiblanco J, Rojas-Villarraga A, Shoenfeld Y. The kaleidoscope of autoimmunity: multiple autoimmune syndromes and familial autoimmunity. Expert Rev Clin Immunol. 2007;3(4):623-35.
33. Richman DP, Agius MA. Treatment of autoimmune myasthenia gravis. Neurology. 2003;61(12):1652-61.
34. Bolli GB. Insulin treatment in type 1 diabetes. Endocr Pract. 2006;12 Suppl 1:105-9.
35. Segal R, Baumoehl Y, Elkayam O, Levartovsky D, Litinsky I, Paran D, et al. Anemia, serum vitamin B12, and folic acid in patients with rheumatoid arthritis, psoriatic arthritis, and systemic lupus erythematosus. Rheumatol Int. 2004;24(1):14-9.
36. Flammer JR, Rogatsky I. Minireview: Glucocorticoids in autoimmunity: unexpected targets and mechanisms. Mol Endocrinol. 2011;25(7):1075-86.
37. Rang HP, Dale MM. Rang and Dale's pharmacology. 7th ed. ed. Edinburgh: Elsevier Churchill Livingstone; 2012.
38. Lallana EC, Fadul CE. Toxicities of immunosuppressive treatment of autoimmune neurologic diseases. Curr Neuropharmacol. 2011;9(3):468-77.
39. Edwards JC, Szczepanski L, Szechinski J, Filipowicz-Sosnowska A, Emery P, Close DR, et al. Efficacy of B-cell-targeted therapy with rituximab in patients with rheumatoid arthritis. N Engl J Med. 2004;350(25):2572-81.
40. Gensicke H, Leppert D, Yaldizli Ö, Lindberg RL, Mehling M, Kappos L, et al. Monoclonal antibodies and recombinant immunoglobulins for the treatment of multiple sclerosis. CNS Drugs. 2012;26(1):11-37.

41. Reff ME, Carner K, Chambers KS, Chinn PC, Leonard JE, Raab R, et al. Depletion of B cells in vivo by a chimeric mouse human monoclonal antibody to CD20. Blood. 1994;83(2):435-45.
42. Rice GP, Hartung HP, Calabresi PA. Anti-alpha4 integrin therapy for multiple sclerosis: mechanisms and rationale. Neurology. 2005;64(8):1336-42.
43. Yednock TA, Cannon C, Fritz LC, Sanchez-Madrid F, Steinman L, Karin N. Prevention of experimental autoimmune encephalomyelitis by antibodies against alpha 4 beta 1 integrin. Nature. 1992;356(6364):63-6.
44. Rosen H, Sanna G, Alfonso C. Egress: a receptor-regulated step in lymphocyte trafficking. Immunol Rev. 2003;195:160-77.
45. Kremer JM, Westhovens R, Leon M, Di Giorgio E, Alten R, Steinfeld S, et al. Treatment of rheumatoid arthritis by selective inhibition of T-cell activation with fusion protein CTLA4Ig. N Engl J Med. 2003;349(20):1907-15.
46. Neuhaus O, Farina C, Yassouridis A, Wiendl H, Then Bergh F, Dose T, et al. Multiple sclerosis: comparison of copolymer-1- reactive T cell lines from treated and untreated subjects reveals cytokine shift from T helper 1 to T helper 2 cells. Proc Natl Acad Sci U S A. 2000;97(13):7452-7.
47. Chan AC, Carter PJ. Therapeutic antibodies for autoimmunity and inflammation. Nat Rev Immunol. 2010;10(5):301-16.
48. Aharoni R. The mechanism of action of glatiramer acetate in multiple sclerosis and beyond. Autoimmun Rev. 2012.
49. Kleinschmidt-DeMasters BK, Tyler KL. Progressive multifocal leukoencephalopathy complicating treatment with natalizumab and interferon beta-1a for multiple sclerosis. N Engl J Med. 2005;353(4):369-74.
50. Jones AL, Mowry BJ, Pender MP, Greer JM. Immune dysregulation and self-reactivity in schizophrenia: do some cases of schizophrenia have an autoimmune basis? Immunol Cell Biol. 2005;83(1):9-17.
51. Dhabhar FS, Saul AN, Holmes TH, Daugherty C, Neri E, Tillie JM, et al. High-anxious individuals show increased chronic stress burden, decreased protective immunity, and increased cancer progression in a mouse model of squamous cell carcinoma. PLoS One. 2012;7(4):e33069.
52. Chwastiak LA, Ehde DM. Psychiatric issues in multiple sclerosis. Psychiatr Clin North Am. 2007;30(4):803-17.
53. Balon R. Mood, anxiety, and physical illness: body and mind, or mind and body? Depress Anxiety. 2006;23(6):377-87.

54. Byatt N, Rothschild AJ, Riskind P, Ionete C, Hunt AT. Relationships between multiple sclerosis and depression. J Neuropsychiatry Clin Neurosci. 2011;23(2):198-200.
55. Schiffer RB, Babigian HM. Behavioral disorders in multiple sclerosis, temporal lobe epilepsy, and amyotrophic lateral sclerosis. An epidemiologic study. Arch Neurol. 1984;41(10):1067-9.
56. Leonard B. Stress, depression and the activation of the immune system. World J Biol Psychiatry. 2000;1(1):17-25.
57. Lublin FD, Reingold SC. Defining the clinical course of multiple sclerosis: results of an international survey. National Multiple Sclerosis Society (USA) Advisory Committee on Clinical Trials of New Agents in Multiple Sclerosis. Neurology. 1996;46(4):907-11.
58. Gold R, Linington C, Lassmann H. Understanding pathogenesis and therapy of multiple sclerosis via animal models: 70 years of merits and culprits in experimental autoimmune encephalomyelitis research. Brain. 2006;129(Pt 8):1953-71.
59. Teitelbaum D, Arnon R, Sela M, Abramsky O. [Clinical trial of copolymer 1 in multiple sclerosis]. Harefuah. 1989;116(9):453-6.
60. Interferon beta-1b is effective in relapsing-remitting multiple sclerosis. I. Clinical results of a multicenter, randomized, double-blind, placebo-controlled trial. The IFNB Multiple Sclerosis Study Group. Neurology. 1993;43(4):655-61.
61. Montero E, Nussbaum G, Kaye JF, Perez R, Lage A, Ben-Nun A, et al. Regulation of experimental autoimmune encephalomyelitis by CD4+, CD25+ and CD8+ T cells: analysis using depleting antibodies. J Autoimmun. 2004;23(1):1-7.
62. Ben-Nun A, Wekerle H, Cohen IR. The rapid isolation of clonable antigen-specific T lymphocyte lines capable of mediating autoimmune encephalomyelitis. Eur J Immunol. 1981;11(3):195-9.
63. Schluesener HJ, Wekerle H. Autoaggressive T lymphocyte lines recognizing the encephalitogenic region of myelin basic protein: in vitro selection from unprimed rat T lymphocyte populations. J Immunol. 1985;135(5):3128-33.
64. Leuenberger T, Paterka M, Reuter E, Herz J, Niesner RA, Radbruch H, et al. The role of CD8+ T cells and their local interaction with CD4+ T cells in myelin oligodendrocyte glycoprotein35-55-induced experimental autoimmune encephalomyelitis. J Immunol. 2013;191(10):4960-8.
65. Sobel RA, Tuohy VK, Lu ZJ, Laursen RA, Lees MB. Acute experimental allergic encephalomyelitis in SJL/J mice induced by a synthetic peptide of myelin proteolipid protein. J Neuropathol Exp Neurol. 1990;49(5):468-79.

66. Baker D, O'Neill JK, Gschmeissner SE, Wilcox CE, Butter C, Turk JL. Induction of chronic relapsing experimental allergic encephalomyelitis in Biozzi mice. J Neuroimmunol. 1990;28(3):261-70.
67. Mendel I, Kerlero de Rosbo N, Ben-Nun A. A myelin oligodendrocyte glycoprotein peptide induces typical chronic experimental autoimmune encephalomyelitis in H-2b mice: fine specificity and T cell receptor V beta expression of encephalitogenic T cells. Eur J Immunol. 1995;25(7):1951-9.
68. Pollak Y, Orion E, Goshen I, Ovadia H, Yirmiya R. Experimental autoimmune encephalomyelitis-associated behavioral syndrome as a model of 'depression due to multiple sclerosis'. Brain Behav Immun. 2002;16(5):533-43.
69. Pollak Y, Ovadia H, Orion E, Yirmiya R. The EAE-associated behavioral syndrome: II. Modulation by anti-inflammatory treatments. J Neuroimmunol. 2003;137(1-2):100-8.
70. Peruga I, Hartwig S, Thöne J, Hovemann B, Gold R, Juckel G, et al. Inflammation modulates anxiety in an animal model of multiple sclerosis. Behav Brain Res. 2011;220(1):20-9.
71. Haji N, Mandolesi G, Gentile A, Sacchetti L, Fresegna D, Rossi S, et al. TNF-α-mediated anxiety in a mouse model of multiple sclerosis. Exp Neurol. 2012;237(2):296-303.
72. Erkut ZA, Hofman MA, Ravid R, Swaab DF. Increased activity of hypothalamic corticotropin-releasing hormone neurons in multiple sclerosis. J Neuroimmunol. 1995;62(1):27-33.
73. Piras G, Rattazzi L, McDermott A, Deacon R, D'Acquisto F. Emotional change-associated T cell mobilization at the early stage of a mouse model of multiple sclerosis. Front Immunol. 2013;4:400.
74. van Oosten BW, Barkhof F, Truyen L, Boringa JB, Bertelsmann FW, von Blomberg BM, et al. Increased MRI activity and immune activation in two multiple sclerosis patients treated with the monoclonal anti-tumor necrosis factor antibody cA2. Neurology. 1996;47(6):1531-4.
75. Danke NA, Koelle DM, Yee C, Beheray S, Kwok WW. Autoreactive T cells in healthy individuals. J Immunol. 2004;172(10):5967-72.
76. Voll RE, Jimi E, Phillips RJ, Barber DF, Rincon M, Hayday AC, et al. NF-kappa B activation by the pre-T cell receptor serves as a selective survival signal in T lymphocyte development. Immunity. 2000;13(5):677-89.
77. Ceredig R, Rolink T. A positive look at double-negative thymocytes. Nat Rev Immunol. 2002;2(11):888-97.
78. Germain RN. T-cell development and the CD4-CD8 lineage decision. Nat Rev Immunol. 2002;2(5):309-22.

79. Sinclair C, Bains I, Yates AJ, Seddon B. Asymmetric thymocyte death underlies the CD4:CD8 T-cell ratio in the adaptive immune system. Proc Natl Acad Sci U S A. 2013;110(31):E2905-14.
80. Yamashita I, Nagata T, Tada T, Nakayama T. CD69 cell surface expression identifies developing thymocytes which audition for T cell antigen receptor-mediated positive selection. Int Immunol. 1993;5(9):1139-50.
81. Singer A. New perspectives on a developmental dilemma: the kinetic signaling model and the importance of signal duration for the CD4/CD8 lineage decision. Curr Opin Immunol. 2002;14(2):207-15.
82. Crompton T, Outram SV, Hager-Theodorides AL. Sonic hedgehog signalling in T-cell development and activation. Nat Rev Immunol. 2007;7(9):726-35.
83. Lanzavecchia A, Sallusto F. Understanding the generation and function of memory T cell subsets. Curr Opin Immunol. 2005;17(3):326-32.
84. Sallusto F, Geginat J, Lanzavecchia A. Central memory and effector memory T cell subsets: function, generation, and maintenance. Annu Rev Immunol. 2004;22:745-63.
85. Watts C. Capture and processing of exogenous antigens for presentation on MHC molecules. Annu Rev Immunol. 1997;15:821-50.
86. Sansom DM. CD28, CTLA-4 and their ligands: who does what and to whom? Immunology. 2000;101(2):169-77.
87. Acuto O, Michel F. CD28-mediated co-stimulation: a quantitative support for TCR signalling. Nat Rev Immunol. 2003;3(12):939-51.
88. Smith-Garvin JE, Koretzky GA, Jordan MS. T cell activation. Annu Rev Immunol. 2009;27:591-619.
89. Schmitz ML, Bacher S, Dienz O. NF-kappaB activation pathways induced by T cell costimulation. FASEB J. 2003;17(15):2187-93.
90. Corse E, Gottschalk RA, Allison JP. Strength of TCR-peptide/MHC interactions and in vivo T cell responses. J Immunol. 2011;186(9):5039-45.
91. Brogdon JL, Leitenberg D, Bottomly K. The potency of TCR signaling differentially regulates NFATc/p activity and early IL-4 transcription in naive CD4+ T cells. J Immunol. 2002;168(8):3825-32.
92. Murphy KM, Reiner SL. The lineage decisions of helper T cells. Nat Rev Immunol. 2002;2(12):933-44.
93. Bettelli E, Korn T, Kuchroo VK. Th17: the third member of the effector T cell trilogy. Curr Opin Immunol. 2007;19(6):652-7.
94. Licona-Limón P, Henao-Mejia J, Temann AU, Gagliani N, Licona-Limón I, Ishigame H, et al. Th9 Cells Drive Host Immunity against Gastrointestinal Worm Infection. Immunity. 2013;39(4):744-57.

95. Basu R, O'Quinn DB, Silberger DJ, Schoeb TR, Fouser L, Ouyang W, et al. Th22 cells are an important source of IL-22 for host protection against enteropathogenic bacteria. Immunity. 2012;37(6):1061-75.
96. Murphy KM, Stockinger B. Effector T cell plasticity: flexibility in the face of changing circumstances. Nat Immunol. 2010;11(8):674-80.
97. Codarri L, Gyülvészi G, Tosevski V, Hesske L, Fontana A, Magnenat L, et al. RORγt drives production of the cytokine GM-CSF in helper T cells, which is essential for the effector phase of autoimmune neuroinflammation. Nat Immunol. 2011;12(6):560-7.
98. Shevach EM. From vanilla to 28 flavors: multiple varieties of T regulatory cells. Immunity. 2006;25(2):195-201.
99. Bettelli E, Carrier Y, Gao W, Korn T, Strom TB, Oukka M, et al. Reciprocal developmental pathways for the generation of pathogenic effector TH17 and regulatory T cells. Nature. 2006;441(7090):235-8.
100. O'Shea JJ, Gadina M, Kanno Y. Cytokine signaling: birth of a pathway. J Immunol. 2011;187(11):5475-8.
101. Zhu J, Paul WE. CD4 T cells: fates, functions, and faults. Blood. 2008;112(5):1557-69.
102. Hirahara K, Vahedi G, Ghoreschi K, Yang XP, Nakayamada S, Kanno Y, et al. Helper T-cell differentiation and plasticity: insights from epigenetics. Immunology. 2011;134(3):235-45.
103. Kanno Y, Vahedi G, Hirahara K, Singleton K, O'Shea JJ. Transcriptional and epigenetic control of T helper cell specification: molecular mechanisms underlying commitment and plasticity. Annu Rev Immunol. 2012;30:707-31.
104. Zhou L, Lopes JE, Chong MM, Ivanov II, Min R, Victora GD, et al. TGF-beta-induced Foxp3 inhibits T(H)17 cell differentiation by antagonizing RORgammat function. Nature. 2008;453(7192):236-40.
105. Hirota K, Duarte JH, Veldhoen M, Hornsby E, Li Y, Cua DJ, et al. Fate mapping of IL-17-producing T cells in inflammatory responses. Nat Immunol. 2011;12(3):255-63.
106. Hegazy AN, Peine M, Helmstetter C, Panse I, Fröhlich A, Bergthaler A, et al. Interferons direct Th2 cell reprogramming to generate a stable GATA-3(+)T-bet(+) cell subset with combined Th2 and Th1 cell functions. Immunity. 2010;32(1):116-28.
107. Yun Kyung Lee HT, Craig L. Maynard, James R. Oliver, Dongquan Chen,, Charles O. Elson aCTW. Late Developmental Plasticity in the T Helper 17 Lineage. Immunity. 2009;30(1):92–107.
108. Bending D, De la Peña H, Veldhoen M, Phillips JM, Uyttenhove C, Stockinger B, et al. Highly purified Th17 cells from BDC2.5NOD mice convert into Th1-like cells in NOD/SCID recipient mice. J Clin Invest. 2009;119(3):565-72.

109. Murphy AC, Lalor SJ, Lynch MA, Mills KH. Infiltration of Th1 and Th17 cells and activation of microglia in the CNS during the course of experimental autoimmune encephalomyelitis. Brain Behav Immun. 2010;24(4):641-51.
110. Zhou L, Chong MM, Littman DR. Plasticity of CD4+ T cell lineage differentiation. Immunity. 2009;30(5):646-55.
111. Wei G, Wei L, Zhu J, Zang C, Hu-Li J, Yao Z, et al. Global mapping of H3K4me3 and H3K27me3 reveals specificity and plasticity in lineage fate determination of differentiating CD4+ T cells. Immunity. 2009;30(1):155-67.
112. Dardalhon V, Korn T, Kuchroo VK, Anderson AC. Role of Th1 and Th17 cells in organ-specific autoimmunity. J Autoimmun. 2008;31(3):252-6.
113. Damsker JM, Hansen AM, Caspi RR. Th1 and Th17 cells: adversaries and collaborators. Ann N Y Acad Sci. 2010;1183:211-21.
114. Bettelli E, Sullivan B, Szabo SJ, Sobel RA, Glimcher LH, Kuchroo VK. Loss of T-bet, but not STAT1, prevents the development of experimental autoimmune encephalomyelitis. J Exp Med. 2004;200(1):79-87.
115. Boyton RJ, Davies S, Marden C, Fantino C, Reynolds C, Portugal K, et al. Stat4-null non-obese diabetic mice: protection from diabetes and experimental allergic encephalomyelitis, but with concomitant epitope spread. Int Immunol. 2005;17(9):1157-65.
116. Esensten JH, Lee MR, Glimcher LH, Bluestone JA. T-bet-deficient NOD mice are protected from diabetes due to defects in both T cell and innate immune system function. J Immunol. 2009;183(1):75-82.
117. Wang J, Fathman JW, Lugo-Villarino G, Scimone L, von Andrian U, Dorfman DM, et al. Transcription factor T-bet regulates inflammatory arthritis through its function in dendritic cells. J Clin Invest. 2006;116(2):414-21.
118. Lee E, Chanamara S, Pleasure D, Soulika AM. IFN-gamma signaling in the central nervous system controls the course of experimental autoimmune encephalomyelitis independently of the localization and composition of inflammatory foci. J Neuroinflammation. 2012;9:7.
119. Vermeire K, Heremans H, Vandeputte M, Huang S, Billiau A, Matthys P. Accelerated collagen-induced arthritis in IFN-gamma receptor-deficient mice. J Immunol. 1997;158(11):5507-13.
120. Kuchroo VK, Awasthi A. Emerging new roles of Th17 cells. Eur J Immunol. 2012;42(9):2211-4.
121. Cua DJ, Sherlock J, Chen Y, Murphy CA, Joyce B, Seymour B, et al. Interleukin-23 rather than interleukin-12 is the critical cytokine for autoimmune inflammation of the brain. Nature. 2003;421(6924):744-8.

122. Haak S, Croxford AL, Kreymborg K, Heppner FL, Pouly S, Becher B, et al. IL-17A and IL-17F do not contribute vitally to autoimmune neuro-inflammation in mice. J Clin Invest. 2009;119(1):61-9.
123. Nakae S, Nambu A, Sudo K, Iwakura Y. Suppression of immune induction of collagen-induced arthritis in IL-17-deficient mice. J Immunol. 2003;171(11):6173-7.
124. Kroenke MA, Chensue SW, Segal BM. EAE mediated by a non-IFN-γ/non-IL-17 pathway. Eur J Immunol. 2010;40(8):2340-8.
125. Campbell IK, Rich MJ, Bischof RJ, Dunn AR, Grail D, Hamilton JA. Protection from collagen-induced arthritis in granulocyte-macrophage colony-stimulating factor-deficient mice. J Immunol. 1998;161(7):3639-44.
126. Nair JR, Edwards SW, Moots RJ. Mavrilimumab , a human monoclonal GM-CSF receptor-α antibody for the management of rheumatoid arthritis: a novel approach to therapy. Expert Opin Biol Ther. 2012;12(12):1661-8.
127. Lee Y, Awasthi A, Yosef N, Quintana FJ, Xiao S, Peters A, et al. Induction and molecular signature of pathogenic TH17 cells. Nat Immunol. 2012;13(10):991-9.
128. Sallusto F, Zielinski CE, Lanzavecchia A. Human Th17 subsets. Eur J Immunol. 2012;42(9):2215-20.
129. Martin-Orozco N, Chung Y, Chang SH, Wang YH, Dong C. Th17 cells promote pancreatic inflammation but only induce diabetes efficiently in lymphopenic hosts after conversion into Th1 cells. Eur J Immunol. 2009;39(1):216-24.
130. Cosmi L, Cimaz R, Maggi L, Santarlasci V, Capone M, Borriello F, et al. Evidence of the transient nature of the Th17 phenotype of CD4+CD161+ T cells in the synovial fluid of patients with juvenile idiopathic arthritis. Arthritis Rheum. 2011;63(8):2504-15.
131. Gerke V, Moss SE. Annexins and membrane dynamics. Biochim Biophys Acta. 1997;1357(2):129-54.
132. Gerke V, Moss SE. Annexins: from structure to function. Physiol Rev. 2002;82(2):331-71.
133. Blackwell GJ, Carnuccio R, Di Rosa M, Flower RJ, Langham CS, Parente L, et al. Glucocorticoids induce the formation and release of anti-inflammatory and anti-phospholipase proteins into the peritoneal cavity of the rat. Br J Pharmacol. 1982;76(1):185-94.
134. Peers SH, Smillie F, Elderfield AJ, Flower RJ. Glucocorticoid-and non-glucocorticoid induction of lipocortins (annexins) 1 and 2 in rat peritoneal leucocytes in vivo. Br J Pharmacol. 1993;108(1):66-72.

135. Cirino G, Cicala C, Sorrentino L, Ciliberto G, Arpaia G, Perretti M, et al. Anti-inflammatory actions of an N-terminal peptide from human lipocortin 1. Br J Pharmacol. 1993;108(3):573-4.
136. Vong L, D'Acquisto F, Pederzoli-Ribeil M, Lavagno L, Flower RJ, Witko-Sarsat V, et al. Annexin 1 cleavage in activated neutrophils: a pivotal role for proteinase 3. J Biol Chem. 2007;282(41):29998-30004.
137. Perretti M, Christian H, Wheller SK, Aiello I, Mugridge KG, Morris JF, et al. Annexin I is stored within gelatinase granules of human neutrophil and mobilized on the cell surface upon adhesion but not phagocytosis. Cell Biol Int. 2000;24(3):163-74.
138. Spurr L, Nadkarni S, Pederzoli-Ribeil M, Goulding NJ, Perretti M, D'Acquisto F. Comparative analysis of Annexin A1-formyl peptide receptor 2/ALX expression in human leukocyte subsets. Int Immunopharmacol. 2011;11(1):55-66.
139. Goulding NJ, Godolphin JL, Sampson MB, Maddison PJ, Flower RJ. Hydrocortisone induces lipocortin 1 production by peripheral blood mononuclear cells in vivo in man. Biochem Soc Trans. 1990;18(2):306-7.
140. D'Acquisto F, Paschalidis N, Raza K, Buckley CD, Flower RJ, Perretti M. Glucocorticoid treatment inhibits annexin-1 expression in rheumatoid arthritis CD4+ T cells. Rheumatology (Oxford). 2008;47(5):636-9.
141. Perretti M, Flower RJ. Measurement of lipocortin 1 levels in murine peripheral blood leukocytes by flow cytometry: modulation by glucocorticoids and inflammation. Br J Pharmacol. 1996;118(3):605-10.
142. Dufton N, Perretti M. Therapeutic anti-inflammatory potential of formyl-peptide receptor agonists. Pharmacol Ther. 2010;127(2):175-88.
143. Le Y, Murphy PM, Wang JM. Formyl-peptide receptors revisited. Trends Immunol. 2002;23(11):541-8.
144. Bena S, Brancaleone V, Wang JM, Perretti M, Flower RJ. Annexin A1 interaction with the FPR2/ALX receptor: identification of distinct domains and downstream associated signaling. J Biol Chem. 2012;287(29):24690-7.
145. D'Acquisto F, Merghani A, Lecona E, Rosignoli G, Raza K, Buckley CD, et al. Annexin-1 modulates T-cell activation and differentiation. Blood. 2007;109(3):1095-102.
146. Harris JG, Flower RJ, Perretti M. Alteration of neutrophil trafficking by a lipocortin 1 N-terminus peptide. Eur J Pharmacol. 1995;279(2-3):149-57.
147. Perretti M, Croxtall JD, Wheller SK, Goulding NJ, Hannon R, Flower RJ. Mobilizing lipocortin 1 in adherent human leukocytes downregulates their transmigration. Nat Med. 1996;2(11):1259-62.

148. Getting SJ, Flower RJ, Perretti M. Inhibition of neutrophil and monocyte recruitment by endogenous and exogenous lipocortin 1. Br J Pharmacol. 1997;120(6):1075-82.
149. Hannon R, Croxtall JD, Getting SJ, Roviezzo F, Yona S, Paul-Clark MJ, et al. Aberrant inflammation and resistance to glucocorticoids in annexin 1-/- mouse. FASEB J. 2003;17(2):253-5.
150. Solito E, Kamal A, Russo-Marie F, Buckingham JC, Marullo S, Perretti M. A novel calcium-dependent proapoptotic effect of annexin 1 on human neutrophils. FASEB J. 2003;17(11):1544-6.
151. Perretti M, Gavins FN. Annexin 1: an endogenous anti-inflammatory protein. News Physiol Sci. 2003;18:60-4.
152. D'Acquisto F, Paschalidis N, Sampaio AL, Merghani A, Flower RJ, Perretti M. Impaired T cell activation and increased Th2 lineage commitment in Annexin-1-deficient T cells. Eur J Immunol. 2007;37(11):3131-42.
153. Weyd H, Abeler-Dörner L, Linke B, Mahr A, Jahndel V, Pfrang S, et al. Annexin A1 on the surface of early apoptotic cells suppresses CD8+ T cell immunity. PLoS One. 2013;8(4):e62449.
154. Yang YH, Song W, Deane JA, Kao W, Ooi JD, Ngo D, et al. Deficiency of annexin A1 in CD4+ T cells exacerbates T cell-dependent inflammation. J Immunol. 2013;190(3):997-1007.
155. Paschalidis N, Huggins A, Rowbotham NJ, Furmanski AL, Crompton T, Flower RJ, et al. Role of endogenous annexin-A1 in the regulation of thymocyte positive and negative selection. Cell Cycle. 2010;9(4):784-93.
156. Flavia Cristina Rodrigues-Lisoni TH, Eloiza Helena Tajara. ANXA1 (annexin A1). Atlas Genet Cytogenet Oncol Haematol. http://AtlasGeneticsOncology.org/Genes/ANXA1ID653ch9q21.htmlMay 2010.
157. Hirata F, del Carmine R, Nelson CA, Axelrod J, Schiffmann E, Warabi A, et al. Presence of autoantibody for phospholipase inhibitory protein, lipomodulin, in patients with rheumatic diseases. Proc Natl Acad Sci U S A. 1981;78(5):3190-4.
158. Goulding NJ, Podgorski MR, Hall ND, Flower RJ, Browning JL, Pepinsky RB, et al. Autoantibodies to recombinant lipocortin-1 in rheumatoid arthritis and systemic lupus erythematosus. Ann Rheum Dis. 1989;48(10):843-50.
159. Iaccarino L, Ghirardello A, Canova M, Zen M, Bettio S, Nalotto L, et al. Anti-annexins autoantibodies: their role as biomarkers of autoimmune diseases. Autoimmun Rev. 2011;10(9):553-8.
160. Probst-Cousin S, Kowolik D, Kuchelmeister K, Kayser C, Neundörfer B, Heuss D. Expression of annexin-1 in multiple sclerosis plaques. Neuropathol Appl Neurobiol. 2002;28(4):292-300.

161. Elderfield AJ, Newcombe J, Bolton C, Flower RJ. Lipocortins (annexins) 1, 2, 4 and 5 are increased in the central nervous system in multiple sclerosis. J Neuroimmunol. 1992;39(1-2):91-100.
162. Gold R, Pepinsky RB, Zettl UK, Toyka KV, Hartung HP. Lipocortin-1 (annexin-1) suppresses activation of autoimmune T cell lines in the Lewis rat. J Neuroimmunol. 1996;69(1-2):157-64.
163. Han MH, Lundgren DH, Jaiswal S, Chao M, Graham KL, Garris CS, et al. Janus-like opposing roles of CD47 in autoimmune brain inflammation in humans and mice. J Exp Med. 2012;209(7):1325-34.
164. Teixeira VH, Olaso R, Martin-Magniette ML, Lasbleiz S, Jacq L, Oliveira CR, et al. Transcriptome analysis describing new immunity and defense genes in peripheral blood mononuclear cells of rheumatoid arthritis patients. PLoS One. 2009;4(8):e6803.
165. Corvol JC, Pelletier D, Henry RG, Caillier SJ, Wang J, Pappas D, et al. Abrogation of T cell quiescence characterizes patients at high risk for multiple sclerosis after the initial neurological event. Proc Natl Acad Sci U S A. 2008;105(33):11839-44.
166. Li QZ, Karp DR, Quan J, Branch VK, Zhou J, Lian Y, et al. Risk factors for ANA positivity in healthy persons. Arthritis Res Ther. 2011;13(2):R38.
167. Paschalidis N, Iqbal AJ, Maione F, Wood EG, Perretti M, Flower RJ, et al. Modulation of experimental autoimmune encephalomyelitis by endogenous annexin A1. J Neuroinflammation. 2009;6:33.
168. Huang J, Perlis RH, Lee PH, Rush AJ, Fava M, Sachs GS, et al. Cross-disorder genomewide analysis of schizophrenia, bipolar disorder, and depression. Am J Psychiatry. 2010;167(10):1254-63.
169. Benros ME, Waltoft BL, Nordentoft M, Ostergaard SD, Eaton WW, Krogh J, et al. Autoimmune diseases and severe infections as risk factors for mood disorders: a nationwide study. JAMA Psychiatry. 2013;70(8):812-20.
170. Kipnis J, Cohen H, Cardon M, Ziv Y, Schwartz M. T cell deficiency leads to cognitive dysfunction: implications for therapeutic vaccination for schizophrenia and other psychiatric conditions. Proc Natl Acad Sci U S A. 2004;101(21):8180-5.
171. Critchley HD, Harrison NA. Visceral influences on brain and behavior. Neuron. 2013;77(4):624-38.
172. Harrison NA, Brydon L, Walker C, Gray MA, Steptoe A, Critchley HD. Inflammation causes mood changes through alterations in subgenual cingulate activity and mesolimbic connectivity. Biol Psychiatry. 2009;66(5):407-14.
173. Muldoon LL, Alvarez JI, Begley DJ, Boado RJ, Del Zoppo GJ, Doolittle ND, et al. Immunologic privilege in the central nervous system

and the blood-brain barrier. J Cereb Blood Flow Metab. 2013;33(1):13-21.
174. Hong S, Van Kaer L. Immune privilege: keeping an eye on natural killer T cells. J Exp Med. 1999;190(9):1197-200.
175. Engelhardt B, Sorokin L. The blood-brain and the blood-cerebrospinal fluid barriers: function and dysfunction. Semin Immunopathol. 2009;31(4):497-511.
176. Wenkel H, Streilein JW, Young MJ. Systemic immune deviation in the brain that does not depend on the integrity of the blood-brain barrier. J Immunol. 2000;164(10):5125-31.
177. Goverman J. Autoimmune T cell responses in the central nervous system. Nat Rev Immunol. 2009;9(6):393-407.
178. Rook GA, Lowry CA, Raison CL. Lymphocytes in neuroprotection, cognition and emotion: is intolerance really the answer? Brain Behav Immun. 2011;25(4):591-601.
179. Yoles E, Hauben E, Palgi O, Agranov E, Gothilf A, Cohen A, et al. Protective autoimmunity is a physiological response to CNS trauma. J Neurosci. 2001;21(11):3740-8.
180. Kipnis J, Mizrahi T, Yoles E, Ben-Nun A, Schwartz M, Ben-Nur A. Myelin specific Th1 cells are necessary for post-traumatic protective autoimmunity. J Neuroimmunol. 2002;130(1-2):78-85.
181. Brynskikh A, Warren T, Zhu J, Kipnis J. Adaptive immunity affects learning behavior in mice. Brain Behav Immun. 2008;22(6):861-9.
182. Ziv Y, Ron N, Butovsky O, Landa G, Sudai E, Greenberg N, et al. Immune cells contribute to the maintenance of neurogenesis and spatial learning abilities in adulthood. Nat Neurosci. 2006;9(2):268-75.
183. Derecki NC, Cardani AN, Yang CH, Quinnies KM, Crihfield A, Lynch KR, et al. Regulation of learning and memory by meningeal immunity: a key role for IL-4. J Exp Med. 2010;207(5):1067-80.
184. Wolf SA, Steiner B, Wengner A, Lipp M, Kammertoens T, Kempermann G. Adaptive peripheral immune response increases proliferation of neural precursor cells in the adult hippocampus. FASEB J. 2009;23(9):3121-8.
185. Wolf SA, Steiner B, Akpinarli A, Kammertoens T, Nassenstein C, Braun A, et al. CD4-positive T lymphocytes provide a neuroimmunological link in the control of adult hippocampal neurogenesis. J Immunol. 2009;182(7):3979-84.
186. Lewitus GM, Wilf-Yarkoni A, Ziv Y, Shabat-Simon M, Gersner R, Zangen A, et al. Vaccination as a novel approach for treating depressive behavior. Biol Psychiatry. 2009;65(4):283-8.
187. Lewitus GM, Cohen H, Schwartz M. Reducing post-traumatic anxiety by immunization. Brain Behav Immun. 2008;22(7):1108-14.

188. Dantzer R, O'Connor JC, Freund GG, Johnson RW, Kelley KW. From inflammation to sickness and depression: when the immune system subjugates the brain. Nat Rev Neurosci. 2008;9(1):46-56.
189. Schwartz M, Shechter R. Systemic inflammatory cells fight off neurodegenerative disease. Nat Rev Neurol. 2010;6(7):405-10.
190. Sandler NG, Mentink-Kane MM, Cheever AW, Wynn TA. Global gene expression profiles during acute pathogen-induced pulmonary inflammation reveal divergent roles for Th1 and Th2 responses in tissue repair. J Immunol. 2003;171(7):3655-67.
191. Butti E, Bergami A, Recchia A, Brambilla E, Del Carro U, Amadio S, et al. IL4 gene delivery to the CNS recruits regulatory T cells and induces clinical recovery in mouse models of multiple sclerosis. Gene Ther. 2008;15(7):504-15.
192. Gobbo OL, O'Mara SM. Exercise, but not environmental enrichment, improves learning after kainic acid-induced hippocampal neurodegeneration in association with an increase in brain-derived neurotrophic factor. Behav Brain Res. 2005;159(1):21-6.
193. Kerschensteiner M, Gallmeier E, Behrens L, Leal VV, Misgeld T, Klinkert WE, et al. Activated human T cells, B cells, and monocytes produce brain-derived neurotrophic factor in vitro and in inflammatory brain lesions: a neuroprotective role of inflammation? J Exp Med. 1999;189(5):865-70.
194. Kerschensteiner M, Stadelmann C, Dechant G, Wekerle H, Hohlfeld R. Neurotrophic cross-talk between the nervous and immune systems: implications for neurological diseases. Ann Neurol. 2003;53(3):292-304.
195. Elenkov IJ, Chrousos GP. Stress hormones, proinflammatory and antiinflammatory cytokines, and autoimmunity. Ann N Y Acad Sci. 2002;966:290-303.
196. Tan KS, Nackley AG, Satterfield K, Maixner W, Diatchenko L, Flood PM. Beta2 adrenergic receptor activation stimulates pro-inflammatory cytokine production in macrophages via PKA- and NF-kappaB-independent mechanisms. Cell Signal. 2007;19(2):251-60.
197. Hanke ML, Powell ND, Stiner LM, Bailey MT, Sheridan JF. Beta adrenergic blockade decreases the immunomodulatory effects of social disruption stress. Brain Behav Immun. 2012;26(7):1150-9.
198. Stark JL, Avitsur R, Padgett DA, Campbell KA, Beck FM, Sheridan JF. Social stress induces glucocorticoid resistance in macrophages. Am J Physiol Regul Integr Comp Physiol. 2001;280(6):R1799-805.
199. Kinsey SG, Bailey MT, Sheridan JF, Padgett DA, Avitsur R. Repeated social defeat causes increased anxiety-like behavior and alters

splenocyte function in C57BL/6 and CD-1 mice. Brain Behav Immun. 2007;21(4):458-66.
200. Kavelaars A, van de Pol M, Zijlstra J, Heijnen CJ. Beta 2-adrenergic activation enhances interleukin-8 production by human monocytes. J Neuroimmunol. 1997;77(2):211-6.
201. Elenkov IJ, Papanicolaou DA, Wilder RL, Chrousos GP. Modulatory effects of glucocorticoids and catecholamines on human interleukin-12 and interleukin-10 production: clinical implications. Proc Assoc Am Physicians. 1996;108(5):374-81.
202. Chelmicka-Schorr E, Kwasniewski MN, Thomas BE, Arnason BG. The beta-adrenergic agonist isoproterenol suppresses experimental allergic encephalomyelitis in Lewis rats. J Neuroimmunol. 1989;25(2-3):203-7.
203. Malfait AM, Malik AS, Marinova-Mutafchieva L, Butler DM, Maini RN, Feldmann M. The beta2-adrenergic agonist salbutamol is a potent suppressor of established collagen-induced arthritis: mechanisms of action. J Immunol. 1999;162(10):6278-83.
204. Chrousos GP. The hypothalamic-pituitary-adrenal axis and immune-mediated inflammation. N Engl J Med. 1995;332(20):1351-62.
205. Boumpas DT, Chrousos GP, Wilder RL, Cupps TR, Balow JE. Glucocorticoid therapy for immune-mediated diseases: basic and clinical correlates. Ann Intern Med. 1993;119(12):1198-208.
206. Besedovsky H, del Rey A, Sorkin E, Dinarello CA. Immunoregulatory feedback between interleukin-1 and glucocorticoid hormones. Science. 1986;233(4764):652-4.
207. Wu CY, Wang K, McDyer JF, Seder RA. Prostaglandin E2 and dexamethasone inhibit IL-12 receptor expression and IL-12 responsiveness. J Immunol. 1998;161(6):2723-30.
208. Ramírez F, Fowell DJ, Puklavec M, Simmonds S, Mason D. Glucocorticoids promote a TH2 cytokine response by CD4+ T cells in vitro. J Immunol. 1996;156(7):2406-12.
209. Gayo A, Mozo L, Suárez A, Tuñon A, Lahoz C, Gutiérrez C. Glucocorticoids increase IL-10 expression in multiple sclerosis patients with acute relapse. J Neuroimmunol. 1998;85(2):122-30.
210. Strelzyk F, Hermes M, Naumann E, Oitzl M, Walter C, Busch HP, et al. Tune it down to live it up? Rapid, nongenomic effects of cortisol on the human brain. J Neurosci. 2012;32(2):616-25.
211. John CD, Christian HC, Morris JF, Flower RJ, Solito E, Buckingham JC. Annexin 1 and the regulation of endocrine function. Trends Endocrinol Metab. 2004;15(3):103-9.
212. Davies E, Omer S, Buckingham JC, Morris JF, Christian HC. Expression and externalization of annexin 1 in the adrenal gland:

structure and function of the adrenal gland in annexin 1-null mutant mice. Endocrinology. 2007;148(3):1030-8.
213. Taylor AD, Cowell AM, Flower J, Buckingham JC. Lipocortin 1 mediates an early inhibitory action of glucocorticoids on the secretion of ACTH by the rat anterior pituitary gland in vitro. Neuroendocrinology. 1993;58(4):430-9.
214. Taylor AD, Loxley HD, Flower RJ, Buckingham JC. Immunoneutralization of lipocortin 1 reverses the acute inhibitory effects of dexamethasone on the hypothalamo-pituitary-adrenocortical responses to cytokines in the rat in vitro and in vivo. Neuroendocrinology. 1995;62(1):19-31.
215. Taylor AD, Christian HC, Morris JF, Flower RJ, Buckingham JC. An antisense oligodeoxynucleotide to lipocortin 1 reverses the inhibitory actions of dexamethasone on the release of adrenocorticotropin from rat pituitary tissue in vitro. Endocrinology. 1997;138(7):2909-18.
216. Eberhard DA, Brown MD, VandenBerg SR. Alterations of annexin expression in pathological neuronal and glial reactions. Immunohistochemical localization of annexins I, II (p36 and p11 subunits), IV, and VI in the human hippocampus. Am J Pathol. 1994;145(3):640-9.
217. Cunningham C, Campion S, Lunnon K, Murray CL, Woods JF, Deacon RM, et al. Systemic inflammation induces acute behavioral and cognitive changes and accelerates neurodegenerative disease. Biol Psychiatry. 2009;65(4):304-12.
218. Rook GA, Lowry CA. The hygiene hypothesis and psychiatric disorders. Trends Immunol. 2008;29(4):150-8.
219. Raison CL, Rutherford RE, Woolwine BJ, Shuo C, Schettler P, Drake DF, et al. A randomized controlled trial of the tumor necrosis factor antagonist infliximab for treatment-resistant depression: the role of baseline inflammatory biomarkers. JAMA Psychiatry. 2013;70(1):31-41.
220. Maes M, Scharpé S, Meltzer HY, Okayli G, Bosmans E, D'Hondt P, et al. Increased neopterin and interferon-gamma secretion and lower availability of L-tryptophan in major depression: further evidence for an immune response. Psychiatry Res. 1994;54(2):143-60.
221. Seidel A, Arolt V, Hunstiger M, Rink L, Behnisch A, Kirchner H. Increased CD56+ natural killer cells and related cytokines in major depression. Clin Immunol Immunopathol. 1996;78(1):83-5.
222. Eaton WW, Byrne M, Ewald H, Mors O, Chen CY, Agerbo E, et al. Association of schizophrenia and autoimmune diseases: linkage of Danish national registers. Am J Psychiatry. 2006;163(3):521-8.
223. Zorrilla EP, Luborsky L, McKay JR, Rosenthal R, Houldin A, Tax A, et al. The relationship of depression and stressors to immunological

assays: a meta-analytic review. Brain Behav Immun. 2001;15(3):199-226.
224. Ivanova SA, Semke VY, Vetlugina TP, Rakitina NM, Kudyakova TA, Simutkin GG. Signs of apoptosis of immunocompetent cells in patients with depression. Neurosci Behav Physiol. 2007;37(5):527-30.
225. Segerstrom SC, Taylor SE, Kemeny ME, Fahey JL. Optimism is associated with mood, coping, and immune change in response to stress. J Pers Soc Psychol. 1998;74(6):1646-55.
226. Miller AH. Depression and immunity: a role for T cells? Brain Behav Immun. 2010;24(1):1-8.
227. Sperner-Unterweger B, Whitworth A, Kemmler G, Hilbe W, Thaler J, Weiss G, et al. T-cell subsets in schizophrenia: a comparison between drug-naive first episode patients and chronic schizophrenic patients. Schizophr Res. 1999;38(1):61-70.
228. Cosentino M, Fietta A, Caldiroli E, Marino F, Rispoli L, Comelli M, et al. Assessment of lymphocyte subsets and neutrophil leukocyte function in chronic psychiatric patients on long-term drug therapy. Prog Neuropsychopharmacol Biol Psychiatry. 1996;20(7):1117-29.
229. Kubera M, Van Bockstaele D, Maes M. Leukocyte subsets in treatment-resistant major depression. Pol J Pharmacol. 1999;51(6):547-9.
230. Boscarino JA, Chang J. Higher abnormal leukocyte and lymphocyte counts 20 years after exposure to severe stress: research and clinical implications. Psychosom Med. 1999;61(3):378-86.
231. Olff M. Stress, depression and immunity: the role of defense and coping styles. Psychiatry Res. 1999;85(1):7-15.
232. Gladkevich A, Kauffman HF, Korf J. Lymphocytes as a neural probe: potential for studying psychiatric disorders. Prog Neuropsychopharmacol Biol Psychiatry. 2004;28(3):559-76.
233. Herbert TB, Cohen S. Stress and immunity in humans: a meta-analytic review. Psychosom Med. 1993;55(4):364-79.
234. Harpaz I, Abutbul S, Nemirovsky A, Gal R, Cohen H, Monsonego A. Chronic exposure to stress predisposes to higher autoimmune susceptibility in C57BL/6 mice: glucocorticoids as a double-edged sword. Eur J Immunol. 2013;43(3):758-69.
235. Gladkevich A, Nelemans SA, Kauffman HF, Korf J. Microarray profiling of lymphocytes in internal diseases with an altered immune response: potential and methodology. Mediators Inflamm. 2005;2005(6):317-30.
236. Zhumabekov T, Corbella P, Tolaini M, Kioussis D. Improved version of a human CD2 minigene based vector for T cell-specific expression in transgenic mice. J Immunol Methods. 1995;185(1):133-40.

237. Schreiner B, Heppner FL, Becher B. Modeling multiple sclerosis in laboratory animals. Semin Immunopathol. 2009;31(4):479-95.
238. Korn T, Reddy J, Gao W, Bettelli E, Awasthi A, Petersen TR, et al. Myelin-specific regulatory T cells accumulate in the CNS but fail to control autoimmune inflammation. Nat Med. 2007;13(4):423-31.
239. Odoardi F, Sie C, Streyl K, Ulaganathan VK, Schläger C, Lodygin D, et al. T cells become licensed in the lung to enter the central nervous system. Nature. 2012;488(7413):675-9.
240. Barker TT, Lee PY, Kelly-Scumpia KM, Weinstein JS, Nacionales DC, Kumagai Y, et al. Pathogenic role of B cells in the development of diffuse alveolar hemorrhage induced by pristane. Lab Invest. 2011;91(10):1540-50.
241. Reeves WH, Lee PY, Weinstein JS, Satoh M, Lu L. Induction of autoimmunity by pristane and other naturally occurring hydrocarbons. Trends Immunol. 2009;30(9):455-64.
242. Xu Y, Lee PY, Li Y, Liu C, Zhuang H, Han S, et al. Pleiotropic IFN-dependent and -independent effects of IRF5 on the pathogenesis of experimental lupus. J Immunol. 2012;188(8):4113-21.
243. Aharoni R, Vainshtein A, Stock A, Eilam R, From R, Shinder V, et al. Distinct pathological patterns in relapsing-remitting and chronic models of experimental autoimmune enchephalomyelitis and the neuroprotective effect of glatiramer acetate. J Autoimmun. 2011;37(3):228-41.
244. Weber MS, Prod'homme T, Youssef S, Dunn SE, Rundle CD, Lee L, et al. Type II monocytes modulate T cell-mediated central nervous system autoimmune disease. Nat Med. 2007;13(8):935-43.
245. Livak KJ, Schmittgen TD. Analysis of relative gene expression data using real-time quantitative PCR and the 2(-Delta Delta C(T)) Method. Methods. 2001;25(4):402-8.
246. Deacon RM. Digging and marble burying in mice: simple methods for in vivo identification of biological impacts. Nat Protoc. 2006;1(1):122-4.
247. Deacon RM. Housing, husbandry and handling of rodents for behavioral experiments. Nat Protoc. 2006;1(2):936-46.
248. Bourin M, Hascoët M. The mouse light/dark box test. Eur J Pharmacol. 2003;463(1-3):55-65.
249. Deacon RM, Rawlins JN. Hippocampal lesions, species-typical behaviours and anxiety in mice. Behav Brain Res. 2005;156(2):241-9.
250. Protais P, Costentin J, Schwartz JC. Climbing behavior induced by apomorphine in mice: a simple test for the study of dopamine receptors in striatum. Psychopharmacology (Berl). 1976;50(1):1-6.

251. D'Acquisto F, Piras G, Rattazzi L. Pro-inflammatory and pathogenic properties of Annexin-A1: the whole is greater than the sum of its parts. Biochem Pharmacol. 2013;85(9):1213-8.
252. Rattazzi L, Piras G, Ono M, Deacon R, Pariante CM, D'Acquisto F. $CD4^+$ but not $CD8^+$ T cells revert the impaired emotional behavior of immunocompromised RAG-1-deficient mice. Transl Psychiatry. 2013;3:e280.
253. Lalive PH, Molnarfi N, Benkhoucha M, Weber MS, Santiago-Raber ML. Antibody response in MOG(35-55) induced EAE. J Neuroimmunol. 2011;240-241:28-33.
254. Drappa J, Kamen LA, Chan E, Georgiev M, Ashany D, Marti F, et al. Impaired T cell death and lupus-like autoimmunity in T cell-specific adapter protein-deficient mice. J Exp Med. 2003;198(5):809-21.
255. Langrish CL, Chen Y, Blumenschein WM, Mattson J, Basham B, Sedgwick JD, et al. IL-23 drives a pathogenic T cell population that induces autoimmune inflammation. J Exp Med. 2005;201(2):233-40.
256. O'Connor RA, Prendergast CT, Sabatos CA, Lau CW, Leech MD, Wraith DC, et al. Cutting edge: Th1 cells facilitate the entry of Th17 cells to the central nervous system during experimental autoimmune encephalomyelitis. J Immunol. 2008;181(6):3750-4.
257. Domingues HS, Mues M, Lassmann H, Wekerle H, Krishnamoorthy G. Functional and pathogenic differences of Th1 and Th17 cells in experimental autoimmune encephalomyelitis. PLoS One. 2010;5(11):e15531.
258. Buccafusco JJ, Buccafusco JJMobain. Methods of behavioral analysis in neuroscience. 2nd ed. ed. Boca Raton ; London: CRC Press; 2009.
259. Cryan JF, Holmes A. The ascent of mouse: advances in modelling human depression and anxiety. Nat Rev Drug Discov. 2005;4(9):775-90.
260. Witkin JM. Animal models of obsessive-compulsive disorder. Curr Protoc Neurosci. 2008;Chapter 9:Unit 9.30.
261. Rodgers RJ, Cao BJ, Dalvi A, Holmes A. Animal models of anxiety: an ethological perspective. Braz J Med Biol Res. 1997;30(3):289-304.
262. Walsh RN, Cummins RA. The Open-Field Test: a critical review. Psychol Bull. 1976;83(3):482-504.
263. Lever C, Burton S, O'Keefe J. Rearing on hind legs, environmental novelty, and the hippocampal formation. Rev Neurosci. 2006;17(1-2):111-33.
264. Radjavi A, Smirnov I, Kipnis J. Brain antigen-reactive CD4(+) T cells are sufficient to support learning behavior in mice with limited T cell repertoire. Brain Behav Immun. 2014;35:58-63.

265. Hess K, Yang Y, Golech S, Sharov A, Becker KG, Weng NP. Kinetic assessment of general gene expression changes during human naive CD4+ T cell activation. Int Immunol. 2004;16(12):1711-21.
266. Jaremka LM, Glaser R, Loving TJ, Malarkey WB, Stowell JR, Kiecolt-Glaser JK. Attachment anxiety is linked to alterations in cortisol production and cellular immunity. Psychol Sci. 2013;24(3):272-9.
267. Czibere L, Baur LA, Wittmann A, Gemmeke K, Steiner A, Weber P, et al. Profiling trait anxiety: transcriptome analysis reveals cathepsin B (Ctsb) as a novel candidate gene for emotionality in mice. PLoS One. 2011;6(8):e23604.
268. Jean-Christophe C SB, Jorge O. CIS (multiple sclerosis) (case-control) (time-series). 2008.
269. Huggins A, Paschalidis N, Flower RJ, Perretti M, D'Acquisto F. Annexin-1-deficient dendritic cells acquire a mature phenotype during differentiation. FASEB J. 2009;23(4):985-96.
270. Cohen S, Janicki-Deverts D, Doyle WJ, Miller GE, Frank E, Rabin BS, et al. Chronic stress, glucocorticoid receptor resistance, inflammation, and disease risk. Proc Natl Acad Sci U S A. 2012;109(16):5995-9.
271. Ackerman KD, Heyman R, Rabin BS, Anderson BP, Houck PR, Frank E, et al. Stressful life events precede exacerbations of multiple sclerosis. Psychosom Med. 2002;64(6):916-20.
272. Evers AW, Verhoeven EW, Kraaimaat FW, de Jong EM, de Brouwer SJ, Schalkwijk J, et al. How stress gets under the skin: cortisol and stress reactivity in psoriasis. Br J Dermatol. 2010;163(5):986-91.

6. Appendix

frontiers in
IMMUNOLOGY

ORIGINAL RESEARCH ARTICLE
published: 21 November 2013
doi: 10.3389/fimmu.2013.00400

Emotional change-associated T cell mobilization at the early stage of a mouse model of multiple sclerosis

Giuseppa Piras[1], Lorenza Rattazzi[1], Adam McDermott[1], Robert Deacon[2] and Fulvio D'Acquisto[1]*

[1] *William Harvey Research Institute, Barts and The London School of Medicine, Queen Mary University of London, London, UK*
[2] *Department of Experimental Psychology, University of Oxford, Oxford, UK*

Edited by:
Oreste Gualillo, Santiago University Clinical Hospital, Spain

Reviewed by:
Andrey Ivanov Tchorbanov, Bulgarian Academy of Sciences, Bulgaria
Angela Ianaro, Università di Napoli Federico II, Italy

***Correspondence:**
Fulvio D'Acquisto, William Harvey Research Institute, Barts and The London School of Medicine, Queen Mary University of London, Charterhouse Square, London EC1M 6BQ, UK
e-mail: f.dacquisto@qmul.ac.uk

Autoimmune diseases like multiple sclerosis (MS) are known to be associated with debilitating emotional disorders that manifest long before the flaring of motor dysfunctions. Given the emerging role of T cells in controlling both emotions and autoimmunity, in this study we explored possible correlation between T cell activation and changes in emotional behavior in a mouse model of MS. Our results showed a significant increase in blood circulating T cells as soon as at day 4 post immunization. This lymphocytosis remained stable with time and preceded the infiltration of T cell in the CNS. The kinetic of T cell entry in the blood matched the kinetic of changes in behavior measured using the open field test. Treatment with glatiramer acetate, a well-known immunomodulatory drug for MS, suppressed behavioral changes while retaining the T cells in the draining lymph nodes. Together these results provide evidence of a positive correlation between the emigration of T cells in circulation and changes in emotions during chronic inflammatory diseases. The validation of these findings in the clinic might help to better understand the cause of the emotional and psychological burden of patients suffering MS or other autoimmune diseases. Most importantly our study suggests novel therapeutic venues for the treatment of the emotional changes associated with autoimmunity.

Keywords: T cells, multiple sclerosis, immunomodulation, mood disorders, behavior

INTRODUCTION

A wealth of studies in the literature has indicated a significant increase in emotional changes in patients suffering from multiple sclerosis (MS) (1–3) as well as from other autoimmune diseases (4). Major depression (5–7), bipolar depression (2, 8), anxiety (9–11), alcohol abuse (12, 13), and other substance abuses (14) are all at an increased prevalence in MS population. These emotional dysfunctions are not simply a reactive psychological response to the impact of this pathology on the patient's life style and have been correlated with the development of MS and other autoimmune diseases. Indeed, the depression and anxiety rates are higher in MS than in those patients experiencing other chronic diseases (15). It is in fact estimated that between 40 and 50% of patients with MS will experience a type of depression within their lifetime. As consequence of this, MS patients show a higher rate of suicides when compared to a normal population with most occurring within 5 years of diagnosis (16, 17).

One of the most unexpected aspects of the correlation between emotional disorders and MS is their association in time. Recent evidence suggests that depression usually presents before the onset of MS symptoms or even before diagnosis (9, 18) and with over a third of MS patients having a family history of depression (19, 20). Indeed, looking at MS patient blogs[1,2] as well as at systematic epidemiological studies, it is clear that patients often lament of having suffered panic attack or anxiety over limited period of time. In other words, patients suffered from unexpected attacks of anxiety that did not necessarily correlated with any manifestation of the disease. In other cases, it seems that these "bouts" of anxiety and panic attack precede or follow the same pattern of MS. Most intriguingly, MS and mental disorders like depression show a large degree of similarities. Indeed, both can provoke cognitive impairment, muscle weakness, or tiredness (21–23).

Previous studies, summarized in **Table 1**, addressed the behavioral modifications occurring in mouse models of MS, the experimental autoimmune encephalomyelitis (EAE). These studies reported either no changes (24) or an inverse correlation between social exploration and the rise of inflammatory mediators including IL-1, TNF-α, and PGE_2 (25). Conversely, Peruga et al. demonstrated that mice immunized with a suboptimal dose of $MOG_{35–55}$ (50 μg) showed the manifestation of motor impairment at day 60 after immunization and had an increase anxiety-like behavior that correlated with an increase in the level of TNF-α and with neuronal loss in the hippocampus (26). This was also associated with a doubled depressive-like behavior in the learned helplessness paradigm. In a more recent study, Haji et al. assessed the behavior of mice subjected to EAE before locomotor defects started to show (27). Their results suggested firstly that high anxiety indexes in EAE mice precede the appearance of motor defects and secondly that TNF-α has a pivotal role in the high anxiety response because of the ability of this cytokine to cause striatum inflammation and microglia activation. In addition, intracerebroventricular administration of etanercept, an inhibitor of TNF-α signaling, resulted in anxiolytic-like effects in EAE mice.

[1] http://www.mssociety.org.uk/forum/everyday-living
[2] http://www.thisisms.com/forum/

Table 1 | Previous studies characterizing behavioral changes in mouse models of EAE.

	Pollak et al. (25)	Peruga et al. (26)	Rodrigues et al. (24)	Haji et al. (27)	Acharjee et al. (28)
Animals	Female SJL/J mice	Female C57BL/6 mice	Female C57BL/6 mice	Female C57BL/6 mice	Female C57BL/6 mice
EAE protocol	150 μg of $PLP_{139–151}$ 15–20 × 10^6 activated lymph node cells i.p.	50 μg of $MOG_{35–55}$ 100 ng of PTX i.p.	100 μg of $MOG_{35–55}$ 300 ng of PTX i.p.	200 μg of $MOG_{35–55}$ 500 ng of PTX i.p.	100 μg of $MOG_{35–55}$ 800 ng of PTX i.p.
Onset of motor deficits (days)	Not specified	Signs of tail weakness at 60 dpi	Clinical signs of disease at 11 dpi	Expected at 10–11 dpi [according to Ref. (29)]	Limp tails at 9–13 dpi
Behavioral parameters/ paradigms	Food and sucrose intake; social exploration	Open field; rotarod; light/dark box; startle response and pre-pulse inhibition; learned helplessness paradigm	Elevated plus maze; inhibitory avoidance task; object recognition task	Open field; elevated plus maze	Open field; elevated plus maze; forced swim test; tail suspension; sociability test; fear conditioning
Cytokine levels	IL-1β expression/level (RT-PCR/ELISA) and TNF-α expression (RT-PCR); PGE2 production (RIA assay); brain (cerebellum, hypothalamus, hippocampus, brain stem)	IL-6 and TNF-α expression (RT-PCR); brain (hippocampus); 15, 29, 41, 59 dpi	–	TNF-α levels (ELISA); Brain (striatum); 10 dpi	IL-1β and TNF-α expression (RT-PCR); brain (hippocampus, hypothalamus, amygdala) 7 dpi
Main results	Transient sickness behavior episodes associated with EAE attacks; Increased pro-inflammatory cytokine levels before the onset of motor impairment; decrease in pro-inflammatory cytokines at the peak of the neurological symptoms	Anxiety- and depression-like behavior before the occurrence of motor deficits; Increased TNF-α and neuronal loss in the hippocampus	No differences in anxiety-like behavior and memory in animals induced with EAE	Anxiety-like behavior before the occurrence of motor deficits; Increased TNF-α levels and activated microglia in the striatum	Anxiety- and depression-like behavior, memory loss and conditioned learning deficits in early stage of EAE; elevated levels of IL-1β and TNF-α in the hypothalamus and increased basal plasma corticosterone levels

All these studies focused on the biochemical and cellular changes occurring in the CNS while very little has been explored in terms of possible changes occurring in the periphery such as in the blood. Indeed, a great deal of studies, including our own in RAG-$1^{-/-}$ (30), have shown that T cells plays a pivotal role in regulating emotion in mice (31–34) as well as in humans (35, 36) besides being the main drive of autoimmune diseases.

In this study we set to investigate the correlation between emotional changes and T cell activation during the very early stages of the EAE. Consistent with the already published experimental and clinical studies mentioned before, our results confirmed that emotional changes occur long before the manifestation of motor dysfunction and within the first days after the immunization. In addition, we provide evidence of a direct correlation between changes in behavior and the time-dependent activation and expansion of T cells, thus confirming a very tight crosstalk between immunity and mental health during the development of chronic inflammatory diseases.

MATERIALS AND METHODS

MICE

We used 6-week-old male mice for all the experiments. Mice were housed in groups of six per cage under specific-pathogen-free conditions and with free access to food and water. Mice were housed for at least 7 days prior to testing. Wild type C57BL/6 mice purchased from Charles River. All experiments were performed during the light phase of the light-dark cycle and no more than two tests per day were performed. All tests were conducted under license from the Home Office and according to the UK Animals (Scientific Procedures) Act, 1986.

$MOG_{35–55}$-INDUCED EXPERIMENTAL AUTOIMMUNE ENCEPHALOMYELITIS

This model of autoimmunity is mainly driven by T cells and has been extensively used to investigate the early events that characterized the development of MS including the activation of the immune response that precedes the neuronal damage caused by inflammatory cells (37). Male C57BL/6 mice received

an intradermal injection of $MOG_{35–55}$ (300 μg) emulsified in Complete Freund's adjuvant (CFA) and two doses of pertussis toxin (PTX) at day zero and day 2 as previously reported (38). The $MOG_{35–55}$/CFA emulsion was prepared by dissolving 300 μg of $MOG_{35–55}$ peptide (MEVGWYRSPFSRVVHLYRNGK, synthesized by Cambridge Research Biochemicals, Cleveland, UK) in 150 μl of PBS and then mixed with 150 μl of CFA (Complete Freud's Adjuvant, Sigma-Aldrich). The resulting suspension was emulsified using a high-pressure polytron homogenizer. The severity of the disease was scored on a scale of 0–6 with 0 = no neurological signs, 1 = tail weakness, 2 = tail paralysis, 3 = loss of righting reflex (the mouse can no longer right themselves after being laid on their back), 4 = hind leg paralysis, 5 = quadriplegia, and 6 = death. In some experiments, mice were immunized with CFA only or with the antigenic ovalbumin peptide $OVA_{323–339}$ (100 μg) and received the two doses of PTX at day 0 and 2. For the treatment with glatiramer acetate (GA; Poly Ala, Glu, Lys, Tyr [6:2:5:1], Sigma), mice were subcutaneously immunized with GA (150 μg/100 μl of PBS) every day for 7 days before the immunization with $MOG_{35–55}$/CFA. Control mice were administered the same volume of PBS vehicle.

LEUKOCYTES ISOLATION FROM CENTRAL NERVOUS SYSTEM

Vertebral columns were dissected from the lumbar to the cervical region and washed several times in PBS to remove blood trace. Spinal cords were extracted by hydro pressure in the spinal canal by using a 2-ml syringe and 19-gage needle. Subsequently, tissues were torn apart in sterile PBS by mechanical pressure through a 70-μm mesh cell strainer (Falcon). Mononuclear cells and lymphocytes were isolated by density gradient centrifugation in Percoll (GE Healthcare). In detail, cells were pelleted at 400 g for 5 min and suspended in a 30% Percoll solution. The 30% Percoll solution was carefully layered onto a 70% Percoll solution in a ratio 2:1 and centrifuged at 500 *g* for 30 min. In this density gradient mononuclear cells sediment at the interface between 30 and 70% Percoll layers. About 2–3 ml of interface solution was collected only after the fatty layer at the top of the centrifuge tube was carefully removed. The purified mononuclear cells were washed twice in RPMI supplemented with 100 U/ml of penicillin and streptomycin and 10% of FCS (Invitrogen).

FLOW CYTOMETRIC ANALYSIS

Lymphocytes were stained in 100 μl of FACS buffer (PBS containing 5% FCS and 0.02% of NaN_3) containing the following antibodies: anti-CD3 PE-Cy5 (clone 145-2C11, eBioscience), anti-CD4 FITC (clone GK 1.5, eBioscience), anti-CD8 PE (clone 53-6.7, eBioscience) as previously reported (39). Cells were labeled with the appropriate concentration of conjugated antibodies for 1 h at 4°C as previously described. Samples were acquired with FACSCalibur and analyzed using FlowJo™ software (Tree Star, Inc., Oregon Corporation). Peripheral blood leukocytes were collected at different time points after immunization. Briefly, blood samples were collected by intracardiac puncture performed under anesthesia in syringes containing sodium citrate 3.2% (w/v). Cells were pellet at 300 g and resuspended in FACS buffer containing 1:500 Fc blocking antibody (anti-mouse CD16/32) and then stained with anti-CD3 (clone 145-2C11). Red blood cells were lysed with RBC Lysis Buffer according to the manufacturer's instruction (eBioscience).

PLASMA CYTOKINE MEASUREMENT

Blood was collected by intracardiac puncture performed under anesthesia. Plasma was obtained from the clotted blood by centrifugation (8000 rpm, 5 min) and stored at −80°C before the assay. Cytokine levels in the same samples were measured (dil. 1:500) using Mouse Th1/Th2/Th17/Th22 16plex Kit FlowCytomix and according to the manufacturer's instructions (eBioscience).

OPEN FIELD ACTIVITY TEST

The open field is a test commonly used to assess locomotor, exploratory, and anxiety-like behavior in laboratory animals. It is based on the conflict between the spontaneous aversion that rodents have of the central area of a novel or brightly lit open field versus their desire to explore new environments (40). The test was performed as previously described with some modifications (41). The open field consisted of a white PVC arena (i.e., a plastic rectangular container size 50 cm × 30 cm) divided into 10 cm × 10 cm squares ($n = 15$). Mice were brought into the experimental room 15 min before testing. Each mouse was placed in one of the corner squares facing the wall. A mouse was observed and recorded for 5 min. The total number of squares crossed, latency to the first rear and the total number of rears were assessed. After each test the arena was cleaned with water to attenuate and homogenize olfactory traces.

DATA ANALYSIS

Pairwise comparisons were made by *t*-test and comparisons of more than two groups were analyzed using one-way ANOVA. The differences in behavior between control and immunized mice were determined using two-way repeated measure ANOVA and day-by-day Bonferroni post-test. The results were expressed as mean ± SEM. Fit linear regressions and 95% confidence bands to the means of parameters over time were calculated by Prism (GraphPad software).

RESULTS

PHASES OF DISEASE IN $MOG_{35–55}$-INDUCED EAE

Immunization of C57BL/6 mice with $MOG_{35–55}$/CFA causes a neurodegenerative inflammatory disease that resembles the primary progressive form of MS (42, 43). Although the manifestations of the disease are not always synchronous in all the mice, it is possible to distinguish three main phases: the pre-onset, the onset, and the disease phase (**Figure 1A**). During the pre-onset (day 0–10), mice do not show any visible motor defects while behavioral changes are readily visible since day 2 post immunization. At the onset of the disease (day 10–12), mice develop a weak or flaccid tail and start to show signs of motor dysfunction. During the disease phase (day 12–22) mice progressively loose the ability to move the hind legs and a significant weight loss (up to 10%) occurs. Mice were tested starting from day 2 (before PTX injection) and every other day till day 10, i.e., before the occurrence of any motor defect (**Figure 1B**).

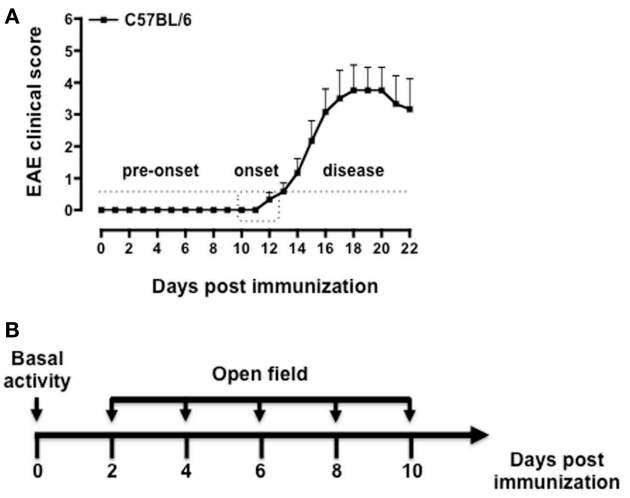

FIGURE 1 | Phases of the disease in MOG_{35-55}-induced EAE and behavioral assessment protocol. The graph in **(A)** shows a typical pattern of development of the EAE clinical score with the three main phases of the disease while the scheme in **(B)** shows a schematic of the behavioral test protocol used in the study. The results in **(A)** are from a single experiment with $n = 10$ mice and are representative of $N = 5$–6 separate experiments.

CHANGES IN BEHAVIOR IN THE OPEN FIELD TEST

The open field test has been previously used in the majority of studies assessing anxiety behavior during EAE (see **Table 1**). We used this test as read-out system for the behavioral changes at the early stages of the EAE. The convenience of this test is that it provides easy and simultaneous measure of multiple parameters including locomotion, exploration, and anxiety.

As shown in **Figure 2**, both $MOG_{35–55}$/CFA immunized mice and PBS-treated control group showed a gradual and time-dependent decrease in locomotor activity (between 50 and 35%, respectively) that became almost stable from day 4 onward ($p < 0.05$; **Figure 2A**). The number of passages through the central square is considered a measure of anxiety and exploratory activity in this test. Control mice showed a variable but overall stable number of central square visits throughout the 8-days of testing. In contrast, immunized mice showed a significant reduction by day 2 and a further decrease at day 4. This value also remained constant for the next 4 days ($p < 0.01$; **Figure 2B**).

Rearing in mice and other rodent is an emotional and protective response to the stress of a new environment; this is a typical vertical activity that consists in the standing completely erect on the hind legs. This "risk-assessment" behavior indicates that the animal is hesitant to move from its present location to a new position. In the open field test, the latency to the first rear is considered a measure of depression and associated anxiety (40, 44). Control mice did not show any significant changes in the number of rearing (data not shown) or in the latency to the first rear throughout the time of the experiment. Conversely, immunized mice showed a steep increase in latency to rearing until day 4 and then a decline to almost basal level from day 8 (**Figure 2C**). When we compared the fold changes versus baseline values of all the parameters we have measured (**Figure A1** in Appendix), the latency to rearing showed the highest fold change (about fivefold). Most interestingly, this followed a linear correlation from day 0 to 4 with a slope that was significantly different from zero [$b = 20.51$, $F(1,15) = 16.26$, $p < 0.01$; **Figure 2D**].

BEHAVIORAL CHANGES AT THE EARLY STAGE OF EAE MIRROR THE EXPANSION AND MOBILIZATION OF T CELLS

To test if the changes in behavior observed in immunized mice were correlated to early cellular and molecular events that are important for the development of EAE, we sacrificed mice at day 0, 2 and 4, and 8 and collected peripheral blood and spleens. As shown in **Figure 3**, the total number of $CD3^+$ cells in the spleen peaked at day 4 and then returned to basal level at day 8. No changes in the percentages of CD4 or CD8 T cell subsets profile were observed (**Figure A2** in Appendix). Similarly, the percentages and total number of $CD3^+$ cells in peripheral blood increased until day 4 while starting to decline at day 8. This decline of peripheral T cell number was even more evident if the mice started to show signs of disease at day 8.

The reduction of circulating T cells at day 10 coincided with the expected infiltration in the CNS. Indeed, consistent with other previously published studies, very few T cells were detected in the spinal cord of control mice while a significant increase (fourfold) were found in the same tissues of the EAE mice at day 8 (**Figure A3** in Appendix). The percentage of T cells further increased as the EAE progressed and was directly correlated to the severity of the disease (data not shown).

T CELL MOBILIZATION AT THE EARLY STAGE OF EAE IS INDEPENDENT OF PERIPHERAL INFLAMMATORY CYTOKINES AND NOT RELATED TO IMMUNIZATION WITH CFA

We next investigated whether the time dependent emigration of T cells in circulation and the changes in behavior we observed were due to changes in circulating inflammatory cytokines. When we scanned serum samples for inflammatory or classical T cell cytokines, only IL-1, IL-18, and GM-CSF could be detected. However, none of these mediators was differentially modulated over time (**Figure 4**) ruling out the possibility that none of cytokines we have measured (IL-2, IFN-γ, IL-4, IL-5, IL-6, TNF-α, and IL-17) are released in circulation upon immunization and could be associated with the changes of rearing latency.

To further demonstrate that the changes in behavior we observed over time were associated with T cell activation and not just the effects of CFA, we tested mice immunized with CFA only or with the immunogenic peptide $OVA_{323–339}$. We used the change in latency as this was the parameter that gave us the highest fold changes and hence most suitable to appreciate any modulatory effect. This parameter shows the lapse in time to the first "reactive and solution-seeking" event and suggests a delay to react to unexpected and novel conditions (the open field) – a response that is typical of anxious state. As shown in **Figure 5**, CFA only immunized mice showed no difference compared to vehicle-injected mice while $OVA_{323–339}$ immunized mice showed a significant ($p < 0.05$) increase in latency (**Figure 5A**).

Immunization with CFA only caused a significant increase in the percentage of $CD3^+$ T cells that was associated with the expected leukocytosis induced by this treatment. However, mice

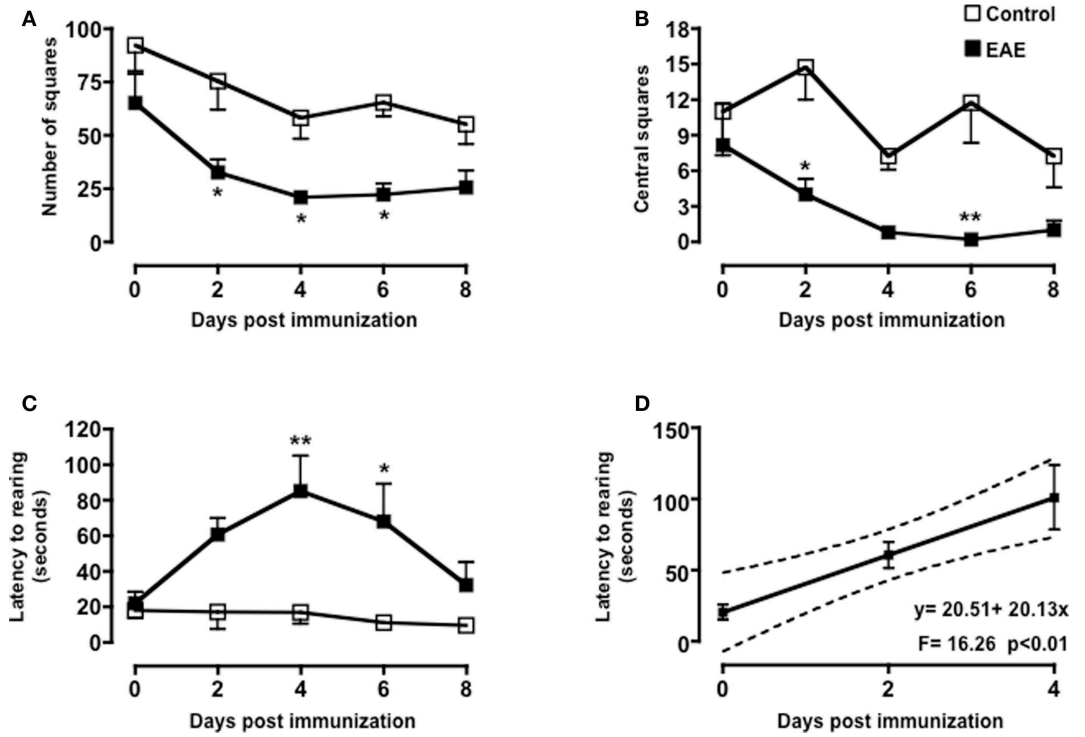

FIGURE 2 | Behavior of MOG_{35-55}-immunized mice in the open field test. The graphs show the total number of squares crossed **(A)**, number of central squares entries **(B)**, latency to rearing, and the relative linear regression **(C,D)** of control or MOG_{35-55}-immunized mice assessed during a 5-min test. Values are expressed as mean ± SEM for six to eight mice and are representative of $N = 5$–6 separate experiments. $^{*}p < 0.05$, $^{**}p < 0.01$ indicate significant values compared to control mice.

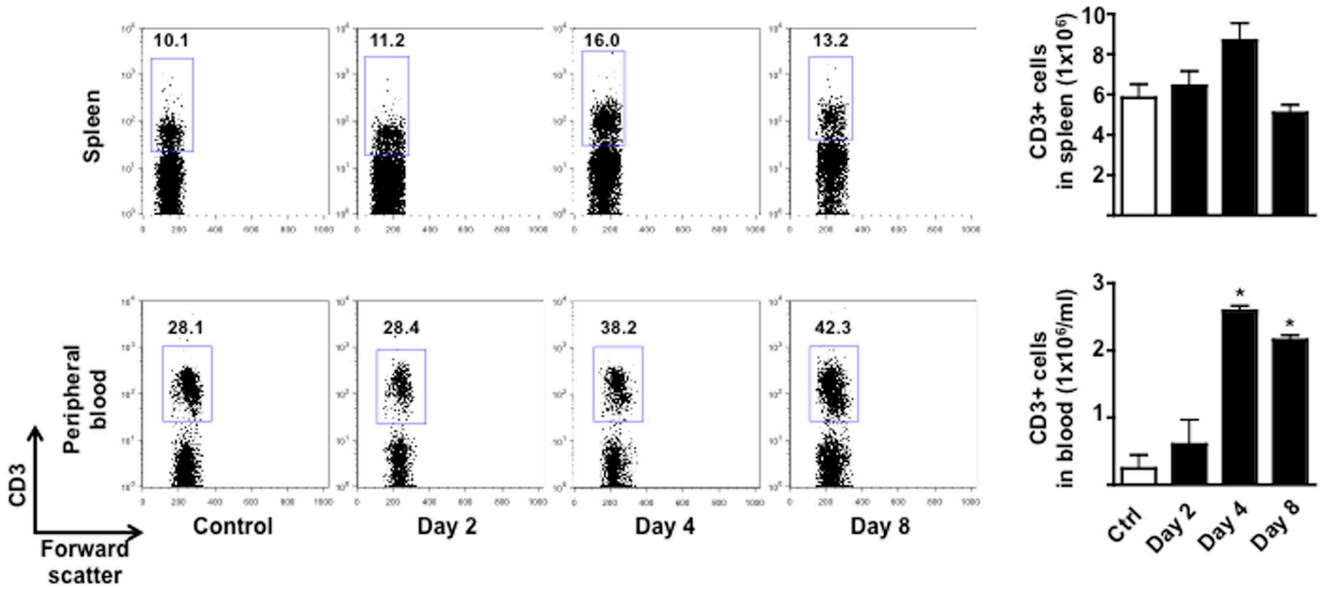

FIGURE 3 | Expansion and mobilization of T cells during the early stages of MOG_{35-55}-induced EAE. The dot plots show the percentages of $CD3^{+}$ T cells while the bar graphs show the comparison of the total number of $CD3^{+}$ T cells in spleen (*top panels*) or peripheral blood (*bottom panels*) of control or MOG_{35-55}-immunized mice. Values are expressed as mean ± SEM for three to four mice. $^{*}p < 0.05$ indicates significant values compared to control mice.

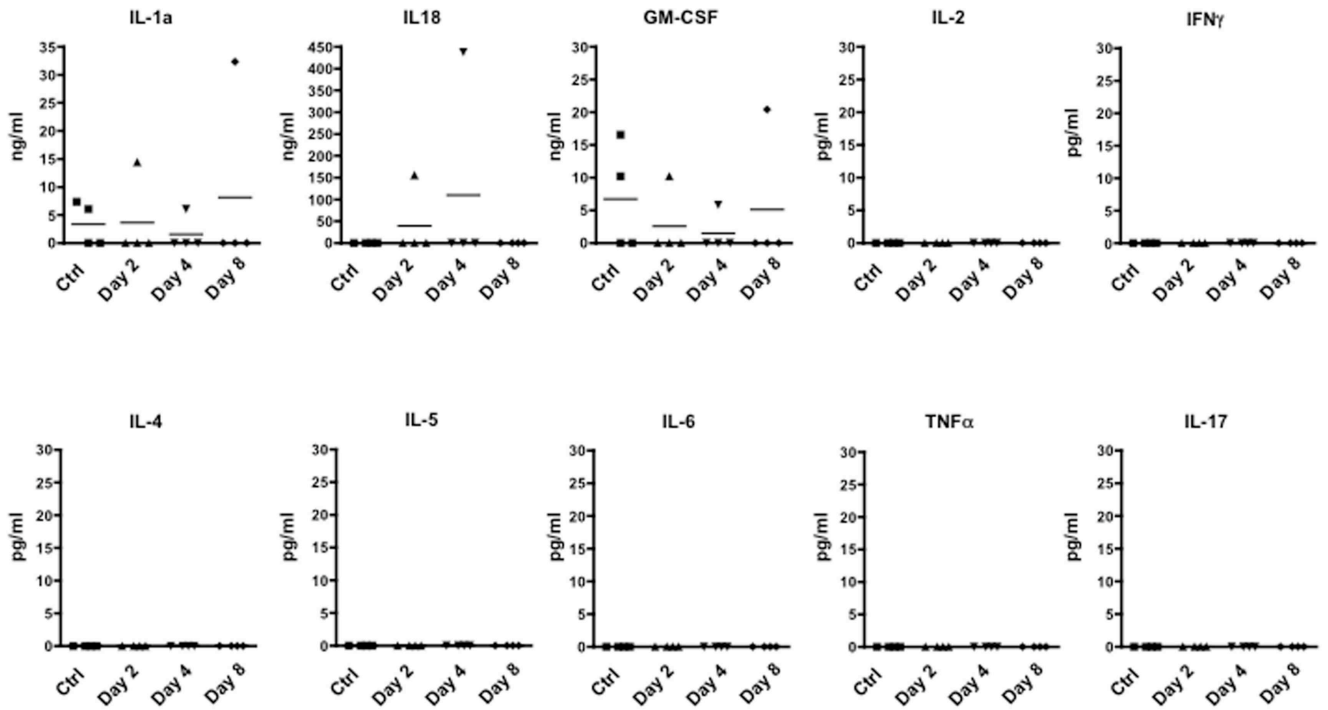

FIGURE 4 | Levels of inflammatory cytokine in the plasma of MOG_{35-55}-immunized mice. The graphs show the level of the indicated cytokines in the plasma of control or MOG_{35-55}-immunized mice sacrificed at the indicated time points. The results are representative of $n = 4$ mice.

treated in the same condition but immunized with $OVA_{323–339}$ showed a further and significant increment in the percentages and number of circulating T cells (**Figures 5B,C**, respectively). Together these results provide a further link between antigenic stimulation of T cells and emotional response in mice.

GLATIRAMER ACETATE ATTENUATES THE INCREASED DIGGING LATENCY OF $MOG_{35–55}$-IMMUNIZED MICE

To further confirm the link between T cell emigration and increased latency to rearing, we pre-treated mice with a known immunomodulatory drug that is effective in the treatment of MS. As shown in **Figure 6A**, administration of dose of GA that inhibits the development of EAE (45) (data not shown) caused a significant reduction in the latency to rearing ($p < 0.01$). Most importantly, when we counted the number of T cells in the draining lymph nodes, we could observed a significant increase in cell number in mice treated with GA compared to those receiving PBS control (**Figure 6B**). This result further suggested that the retaining of T cells from the circulation significantly influence and mirror the changes in behavior.

DISCUSSION

Emerging evidences have shown that T cells contribute to functions other than those related to the immune response (30, 33, 46–50). The aim of this study was to explore a possible correlation between T cell activation and behavioral changes that occur at the early stage of the $MOG_{35–55}$-induced EAE. Consistent with previous observations (24, 25, 27, 28, 40) and the results obtained by Haji et al. (27), immunized mice showed a reduced number of crossed central squares in the open field and an overall decrease in exploratory activity as indicated by the reduced number of squares.

The EAE is a classical model of autoimmune diseases where mice are immunized with an antigen that resembles a tissue component of the target organ. Activated antigen presenting cells present the antigenic $MOG_{35–55}$ to T cells in the local draining lymph nodes (37, 42). Clonally activated T cells expand and then move first into the blood stream and thereafter into "homing licensing organs" like the lung (51). Here, their membrane make-up and gene profile change to acquire a "pathogenic" phenotype. These "licensed" cells are in fact capable of infiltrating the target organs (spinal cord and brain in this case) and initiate a cascade of events that ultimately lead to chronic inflammation and tissue damage (52).

Consistent with this model, our results show that the number of T cells increases in the spleen of immunized mice and this is followed by their migration into the bloodstream (time when the changes in emotional behavior occur) and ultimately into the CNS (time when the emotional behaviors come back to basal level). In light of these findings, it is possible to hypothesize that the two stages of T cell movement, i.e., first in the bloodstream and then into the CNS, mirror the two stages of MS development: mood changes first and motor dysfunction later. These events are not antigen specific (in this case neuronal antigen specific) or a specific feature of MS. Indeed, the results obtained using another non-endogenous antigen such as $OVA_{323–339}$ provided us with the same findings obtained with the $MOG_{35–55}$. This highlights

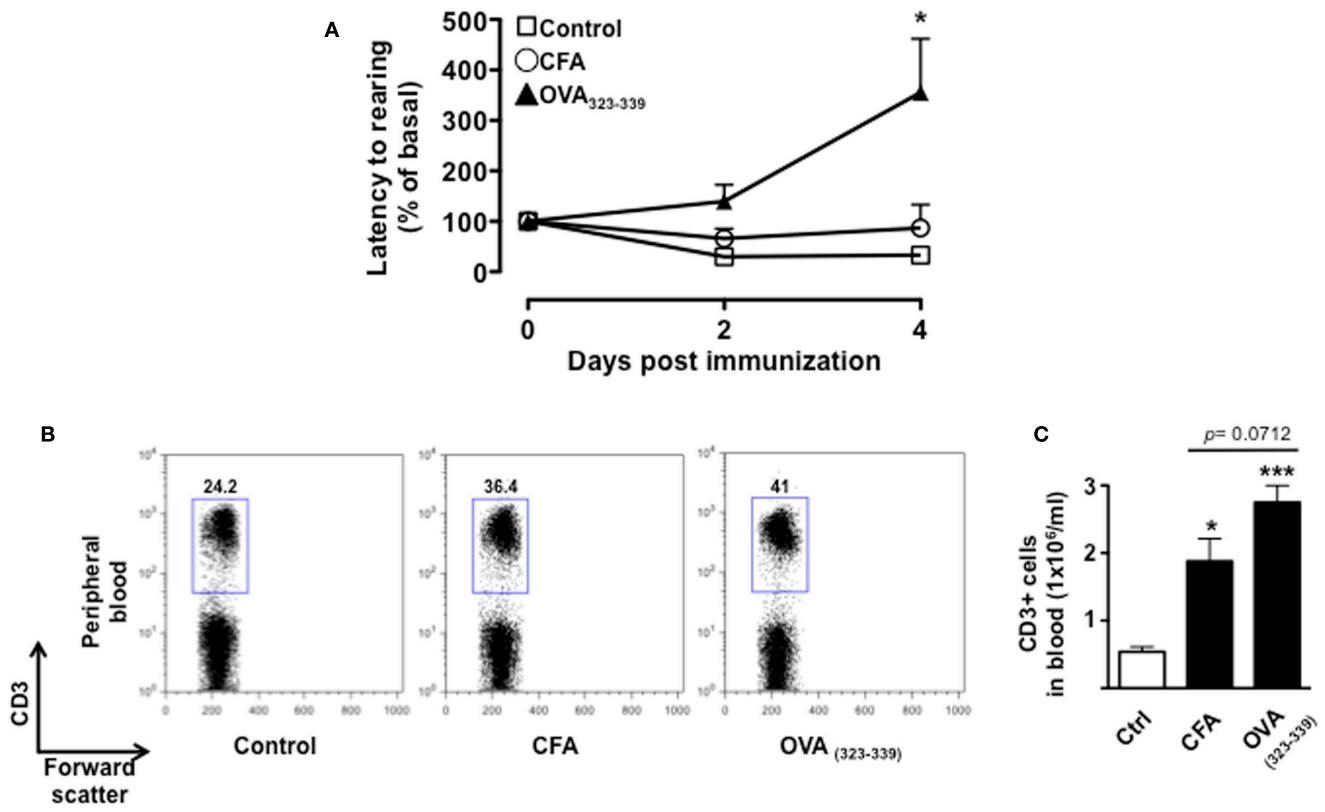

FIGURE 5 | The increase in latency to rearing relies on T cell antigenic stimulation. The graph in **(A)** shows the percentage of latency to rearing of control, CFA only or $OVA_{323-339}$-immunized mice. Values are expressed as mean percentage ± SEM of the basal activity for eight to nine mice. The dot plots **(B)** show the percentages of $CD3^+$ T cells while the bar graph **(C)** shows the comparison of the total number of $CD3^+$ T cells in peripheral blood of control, CFA only or $OVA_{323-339}$-immunized mice at day 4. The results are representative of $n = 6–8$ mice.

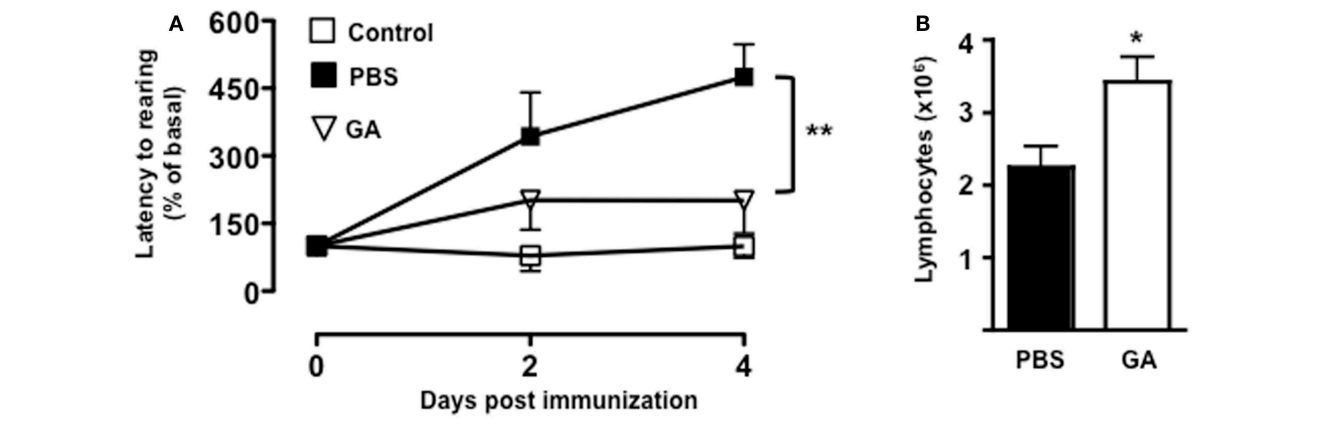

FIGURE 6 | Glatiramer acetate inhibits the emotional changes of MOG_{35-55}-immunized mice. The graph in **(A)** shows the percentage of latency to rearing of vehicle-treated non-immunized mice, glatiramer acetate-(GA), or control PBS-treated mice subjected to MOG_{35-55}-induced EAE and assessed during the 5-min test. The values are expressed as mean percentage ± SEM of the basal activity for six to eight. $^{**}p < 0.01$ indicates significant values compared to control mice. The bar graph in **(B)** shows the total number of T cells in the draining lymph nodes of glatiramer acetate-(GA) or control PBS-treated mice subjected to MOG_{35-55}-induced EAE at day 4. The results are representative of $n = 6–8$ mice.

the importance of T cell priming and expansion rather than a general inflammation for the emotional changes. Indeed, the lack of any significant changes in circulating cytokines suggests that these events are not part of the classical sickness behavior observed during acute inflammation (53). Further studies, now in progress in the lab, will verify this hypothesis in other models of

autoimmune disease such as the collagen-induced arthritis or double strand DNA/peptide-induced lupus. The validation of these findings might indeed explain or provide a "consensus hypothesis" for the high incidence of mood disorders as a common feature of autoimmune pathologies.

Although we have not explored the passage of T cells through the lungs in our system, there are some indications that this might be a likely event. Several studies have already shown that trafficking of T lymphocytes to specific organs, such as the skin and lungs, is part of the body's defense mechanism following acute psychological stress (35, 36, 54). It is interesting to note at this regard that patients suffering panic and anxiety attack often declare to be "out of breath" and that problems get "under our skin" when there is something that we cannot be rid of.

On a more scientific ground, seminal investigations from Schwartz's group have recently shown that T lymphocytes migrate to the brain in response to psychological stress and that their function there is to alleviate its negative behavioral consequences. In addition to this, the authors also showed that immunization of T cells with a CNS-related peptide reduced the stress-induced anxiety and restored levels of BDNF, shown to be important for stress resilience (55, 56). In light of these findings, it is feasible to hypothesize that the drop in latency we have observed in our study might be due to the infiltration of T cells in the CNS and concomitant induction of a protective "resilient response."

Further studies by Kipnis's team have provided further insights on the multiple roles of T cells as homeostatic keepers of CNS functions. The authors were the first to describe a critical role for T cell derived IL-4 as key cytokine involved in learning and memory through regulation of myeloid cells present in the meningeal space (32, 57). This intriguing new concept has been recently confirmed by showing improved learning and memory in T cell deficient SCID mice adoptively transferred with M2 macrophages (58). Considering the well-known crosstalk between cognition and emotion regulation (31), it would be interesting to explore the possible changes in myeloid cell phenotype during the early stages of the EAE.

Glatiramer acetate, known in the clinic as copaxone, is one of the most common disease-modifying drugs together with interferon beta. Although its mechanisms of action have not been fully defined, a great deal of evidence suggests that it acts directly or indirectly on T cell activation (59–62). When we tested it in our system, we could clearly see a significant reduction of latency to rearing (**Figure 6**). Most interestingly, we also observed that GA pre-treatment caused a significant retention of T cells in the periphery compared to control mice. In light of these findings, it is tempting to speculate that the reduced activation of T cells, while reducing the signs of motor dysfunctions and the progression of the disease, it also reduces emotional changes.

In conclusion, the results of this study suggest a further mechanism (besides CNS inflammation) for the link between the neuronal and immune systems – more specifically the emotional state and immune response – during the course of autoimmune diseases like MS. The validation of these results in the clinic, together with further exploration of the mechanism by which T cells cause debilitating mood changes during the early stage of MS, might help to identify alternative immunomodulatory treatments with reduced impact on the mental well being of these patients.

ACKNOWLEDGMENTS

We would like to thank Dr. Lucy Norling for carefully reading the manuscript.

REFERENCES

1. Paparrigopoulos T, Ferentinos P, Kouzoupis A, Koutsis G, Papadimitriou GN. The neuropsychiatry of multiple sclerosis: focus on disorders of mood, affect and behaviour. *Int Rev Psychiatry* (2010) **22**:14–21. doi:10.3109/09540261003589323
2. Iacovides A, Andreoulakis E. Bipolar disorder and resembling special psychopathological manifestations in multiple sclerosis: a review. *Curr Opin Psychiatry* (2011) **24**:336–40. doi:10.1097/YCO.0b013e328347341d
3. Labuz-Roszak B, Kubicka-Baczyk K, Pierzchala K, Machowska-Majchrzak A, Skrzypek M. Fatigue and its association with sleep disorders, depressive symptoms and anxiety in patients with multiple sclerosis. *Neurol Neurochir Pol* (2012) **46**:309–17. doi:10.5114/ninp.2012.30261
4. Stojanovich L. Stress and autoimmunity. *Autoimmun Rev* (2010) **9**:A271–6. doi:10.1016/j.autrev.2009.11.014
5. Wang JL, Reimer MA, Metz LM, Patten SB. Major depression and quality of life in individuals with multiple sclerosis. *Int J Psychiatry Med* (2000) **30**:309–17. doi:10.2190/PGWT-UXJ0-7UEH-LGRY
6. Benedetti F, Campori E, Colombo C, Smeraldi E. Fluvoxamine treatment of major depression associated with multiple sclerosis. *J Neuropsychiatry Clin Neurosci* (2004) **16**:364–6. doi:10.1176/appi.neuropsych.16.3.364
7. Feinstein A, Roy P, Lobaugh N, Feinstein K, O'Connor P, Black S. Structural brain abnormalities in multiple sclerosis patients with major depression. *Neurology* (2004) **62**:586–90. doi:10.1212/01.WNL.0000110316.12086.0C
8. Ybarra MI, Moreira MA, Araujo CR, Lana-Peixoto MA, Teixeira AL. Bipolar disorder and multiple sclerosis. *Arq Neuropsiquiatr* (2007) **65**:1177–80. doi:10.1590/S0004-282X2007000700016
9. Korostil M, Feinstein A. Anxiety disorders and their clinical correlates in multiple sclerosis patients. *Mult Scler* (2007) **13**:67–72. doi:10.1177/1352458506071161
10. Poder K, Ghatavi K, Fisk JD, Campbell TL, Kisely S, Sarty I, et al. Social anxiety in a multiple sclerosis clinic population. *Mult Scler* (2009) **15**:393–8. doi:10.1177/1352458508099143
11. Giordano A, Granella F, Lugaresi A, Martinelli V, Trojano M, Confalonieri P, et al. Anxiety and depression in multiple sclerosis patients around diagnosis. *J Neurol Sci* (2011) **307**:86–91. doi:10.1016/j.jns.2011.05.008
12. Quesnel S, Feinstein A. Multiple sclerosis and alcohol: a study of problem drinking. *Mult Scler* (2004) **10**:197–201. doi:10.1191/1352458504ms992oa
13. Sammarco CL. A case study: identifying alcohol abuse in multiple sclerosis. *J Neurosci Nurs* (2007) **39**:373–6. doi:10.1097/01376517-200712000-00008
14. Hawkes CH. Are multiple sclerosis patients risk-takers? *QJM* (2005) **98**:895–911. doi:10.1093/qjmed/hci135
15. Chwastiak L, Ehde DM, Gibbons LE, Sullivan M, Bowen JD, Kraft GH. Depressive symptoms and severity of illness in multiple sclerosis: epidemiologic study of a large community sample. *Am J Psychiatry* (2002) **159**:1862–8. doi:10.1176/appi.ajp.159.11.1862
16. Gaskill A, Foley FW, Kolzet J, Picone MA. Suicidal thinking in multiple sclerosis. *Disabil Rehabil* (2011) **33**:1528–36. doi:10.3109/09638288.2010.533813
17. Pompili M, Forte A, Palermo M, Stefani H, Lamis DA, Serafini G, et al. Suicide risk in multiple sclerosis: a systematic review of current literature. *J Psychosom Res* (2012) **73**:411–7. doi:10.1016/j.jpsychores.2012.09.011
18. Zabad RK, Patten SB, Metz LM. The association of depression with disease course in multiple sclerosis. *Neurology* (2005) **64**:359–60. doi:10.1212/01.WNL.0000149760.64921.AA
19. Sullivan MJ, Weinshenker B, Mikail S, Bishop SR. Screening for major depression in the early stages of multiple sclerosis. *Can J Neurol Sci* (1995) **22**:228–31.
20. Sullivan MJ, Weinshenker B, Mikail S, Edgley K. Depression before and after diagnosis of multiple sclerosis. *Mult Scler* (1995) **1**:104–8.
21. Schwid SR, Covington M, Segal BM, Goodman AD. Fatigue in multiple sclerosis: current understanding and future directions. *J Rehabil Res Dev* (2002) **39**:211–24.
22. Gupta RK. Major depression: an illness with objective physical signs. *World J Biol Psychiatry* (2009) **10**:196–201. doi:10.1080/15622970902812072
23. Maes M. An intriguing and hitherto unexplained co-occurrence: depression and chronic fatigue syndrome are manifestations of shared inflammatory, oxidative and nitrosative (IO&NS) pathways. *Prog Neuropsychopharmacol Biol Psychiatry* (2011) **35**:784–94. doi:10.1016/j.pnpbp.2010.06.023

24. Rodrigues DH, Vilela Mde C, Lacerda-Queiroz N, Miranda AS, Sousa LF, Reis HJ, et al. Behavioral investigation of mice with experimental autoimmune encephalomyelitis. *Arq Neuropsiquiatr* (2011) **69**:938–42. doi:10.1590/S0004-282X2011000700018
25. Pollak Y, Ovadia H, Orion E, Weidenfeld J, Yirmiya R. The EAE-associated behavioral syndrome: I. Temporal correlation with inflammatory mediators. *J Neuroimmunol* (2003) **137**:94–9. doi:10.1016/S0165-5728(03)00075-4
26. Peruga I, Hartwig S, Thone J, Hovemann B, Gold R, Juckel G, et al. Inflammation modulates anxiety in an animal model of multiple sclerosis. *Behav Brain Res* (2011) **220**:20–9. doi:10.1016/j.bbr.2011.01.018
27. Haji N, Mandolesi G, Gentile A, Sacchetti L, Fresegna D, Rossi S, et al. TNF-alpha-mediated anxiety in a mouse model of multiple sclerosis. *Exp Neurol* (2012) **237**:296–303. doi:10.1016/j.expneurol.2012.07.010
28. Acharjee S, Nayani N, Tsutsui M, Hill MN, Ousman SS, Pittman QJ. Altered cognitive-emotional behavior in early experimental autoimmune encephalitis – cytokine and hormonal correlates. *Brain Behav Immun* (2013) **33**:164–72. doi:10.1016/j.bbi.2013.07.003
29. Centonze D, Muzio L, Rossi S, Cavasinni F, De Chiara V, Bergami A, et al. Inflammation triggers synaptic alteration and degeneration in experimental autoimmune encephalomyelitis. *J Neurosci* (2009) **29**:3442–52. doi:10.1523/JNEUROSCI.5804-08.2009
30. Rattazzi L, Piras G, Ono M, Deacon R, Pariante CM, D'Acquisto F. CD4(+) but not CD8(+) T cells revert the impaired emotional behavior of immunocompromised RAG-1-deficient mice. *Transl Psychiatry* (2013) **3**:e280. doi:10.1038/tp.2013.54
31. Dolan RJ. Emotion, cognition, and behavior. *Science* (2002) **298**:1191–4. doi:10.1126/science.1076358
32. Gadani SP, Cronk JC, Norris GT, Kipnis J. IL-4 in the brain: a cytokine to remember. *J Immunol* (2012) **189**:4213–9. doi:10.4049/jimmunol.1202246
33. Kipnis J, Gadani S, Derecki NC. Pro-cognitive properties of T cells. *Nat Rev Immunol* (2012) **12**:663–9. doi:10.1038/nri3280
34. Damasio A, Carvalho GB. The nature of feelings: evolutionary and neurobiological origins. *Nat Rev Neurosci* (2013) **14**:143–52. doi:10.1038/nrn3403
35. Stefanski V, Peschel A, Reber S. Social stress affects migration of blood T cells into lymphoid organs. *J Neuroimmunol* (2003) **138**:17–24. doi:10.1016/S0165-5728(03)00076-6
36. Dhabhar FS. Psychological stress and immunoprotection versus immunopathology in the skin. *Clin Dermatol* (2013) **31**:18–30. doi:10.1016/j.clindermatol.2011.11.003
37. Fletcher JM, Lalor SJ, Sweeney CM, Tubridy N, Mills KH. T cells in multiple sclerosis and experimental autoimmune encephalomyelitis. *Clin Exp Immunol* (2010) **162**:1–11. doi:10.1111/j.1365-2249.2010.04143.x
38. Paschalidis N, Iqbal AJ, Maione F, Wood EG, Perretti M, Flower RJ, et al. Modulation of experimental autoimmune encephalomyelitis by endogenous annexin A1. *J Neuroinflammation* (2009) **6**:33. doi:10.1186/1742-2094-6-33
39. Paschalidis N, Huggins A, Rowbotham NJ, Furmanski AL, Crompton T, Flower RJ, et al. Role of endogenous annexin-A1 in the regulation of thymocyte positive and negative selection. *Cell Cycle* (2010) **9**:784–93. doi:10.4161/cc.9.4.10673
40. Walsh RN, Cummins RA. The open-field test: a critical review. *Psychol Bull* (1976) **83**:482–504. doi:10.1037/0033-2909.83.3.482
41. Deacon RM, Croucher A, Rawlins JN. Hippocampal cytotoxic lesion effects on species-typical behaviours in mice. *Behav Brain Res* (2002) **132**:203–13. doi:10.1016/S0166-4328(01)00401-6
42. Constantinescu CS, Farooqi N, O'Brien K, Gran B. Experimental autoimmune encephalomyelitis (EAE) as a model for multiple sclerosis (MS). *Br J Pharmacol* (2011) **164**:1079–106. doi:10.1111/j.1476-5381.2011.01302.x
43. Denic A, Johnson AJ, Bieber AJ, Warrington AE, Rodriguez M, Pirko I. The relevance of animal models in multiple sclerosis research. *Pathophysiology* (2011) **18**:21–9. doi:10.1016/j.pathophys.2010.04.004
44. Prut L, Belzung C. The open field as a paradigm to measure the effects of drugs on anxiety-like behaviors: a review. *Eur J Pharmacol* (2003) **463**:3–33. doi:10.1016/S0014-2999(03)01272-X
45. Smirnov I, Walsh JT, Kipnis J. Chronic mild stress eliminates the neuroprotective effect of Copaxone after CNS injury. *Brain Behav Immun* (2013) **31**:177–82. doi:10.1016/j.bbi.2012.12.015
46. Kipnis J, Cohen H, Cardon M, Ziv Y, Schwartz M. T cell deficiency leads to cognitive dysfunction: implications for therapeutic vaccination for schizophrenia and other psychiatric conditions. *Proc Natl Acad Sci U S A* (2004) **101**:8180–5. doi:10.1073/pnas.0402268101
47. Ziv Y, Ron N, Butovsky O, Landa G, Sudai E, Greenberg N, et al. Immune cells contribute to the maintenance of neurogenesis and spatial learning abilities in adulthood. *Nat Neurosci* (2006) **9**:268–75. doi:10.1038/nn1629
48. Brynskikh A, Warren T, Zhu J, Kipnis J. Adaptive immunity affects learning behavior in mice. *Brain Behav Immun* (2008) **22**:861–9. doi:10.1016/j.bbi.2007.12.008
49. Garg SK, Banerjee R, Kipnis J. Neuroprotective immunity: T cell-derived glutamate endows astrocytes with a neuroprotective phenotype. *J Immunol* (2008) **180**:3866–73.
50. Rook GA, Lowry CA, Raison CL. Lymphocytes in neuroprotection, cognition and emotion: is intolerance really the answer? *Brain Behav Immun* (2011) **25**:591–601. doi:10.1016/j.bbi.2010.12.005
51. Odoardi F, Sie C, Streyl K, Ulaganathan VK, Schlager C, Lodygin D, et al. T cells become licensed in the lung to enter the central nervous system. *Nature* (2012) **488**:675–9. doi:10.1038/nature11337
52. Kawakami N, Lassmann S, Li Z, Odoardi F, Ritter T, Ziemssen T, et al. The activation status of neuroantigen-specific T cells in the target organ determines the clinical outcome of autoimmune encephalomyelitis. *J Exp Med* (2004) **199**:185–97. doi:10.1084/jem.20031064
53. Dantzer R. Cytokine-induced sickness behaviour: a neuroimmune response to activation of innate immunity. *Eur J Pharmacol* (2004) **500**:399–411. doi:10.1016/j.ejphar.2004.07.040
54. Viswanathan K, Dhabhar FS. Stress-induced enhancement of leukocyte trafficking into sites of surgery or immune activation. *Proc Natl Acad Sci U S A* (2005) **102**:5808–13. doi:10.1073/pnas.0501650102
55. Lewitus GM, Cohen H, Schwartz M. Reducing post-traumatic anxiety by immunization. *Brain Behav Immun* (2008) **22**:1108–14. doi:10.1016/j.bbi.2008.05.002
56. Lewitus GM, Schwartz M. Behavioral immunization: immunity to self-antigens contributes to psychological stress resilience. *Mol Psychiatry* (2009) **14**:532–6. doi:10.1038/mp.2008.103
57. Derecki NC, Cardani AN, Yang CH, Quinnies KM, Crihfield A, Lynch KR, et al. Regulation of learning and memory by meningeal immunity: a key role for IL-4. *J Exp Med* (2010) **207**:1067–80. doi:10.1084/jem.20091419
58. Derecki NC, Quinnies KM, Kipnis J. Alternatively activated myeloid (M2) cells enhance cognitive function in immune compromised mice. *Brain Behav Immun* (2011) **25**:379–85. doi:10.1016/j.bbi.2010.11.009
59. Kala M, Miravalle A, Vollmer T. Recent insights into the mechanism of action of glatiramer acetate. *J Neuroimmunol* (2011) **235**:9–17. doi:10.1016/j.jneuroim.2011.01.009
60. Racke MK, Lovett-Racke AE. Glatiramer acetate treatment of multiple sclerosis: an immunological perspective. *J Immunol* (2011) **186**:1887–90. doi:10.4049/jimmunol.1090138
61. Oreja-Guevara C, Ramos-Cejudo J, Aroeira LS, Chamorro B, Diez-Tejedor E. TH1/TH2 cytokine profile in relapsing-remitting multiple sclerosis patients treated with glatiramer acetate or natalizumab. *BMC Neurol* (2012) **12**:95. doi:10.1186/1471-2377-12-95
62. Aharoni R. The mechanism of action of glatiramer acetate in multiple sclerosis and beyond. *Autoimmun Rev* (2013) **12**:543–53. doi:10.1016/j.autrev.2012.09.005

Conflict of Interest Statement: The authors declare that the research was conducted in the absence of any commercial or financial relationships that could be construed as a potential conflict of interest.

Received: 22 October 2013; accepted: 08 November 2013; published online: 21 November 2013.

*Citation: Piras G, Rattazzi L, McDermott A, Deacon R and D'Acquisto F (2013) Emotional change-associated T cell mobilization at the early stage of a mouse model of multiple sclerosis. Front. Immunol. **4**:400. doi: 10.3389/fimmu.2013.00400*

This article was submitted to Inflammation, a section of the journal Frontiers in Immunology.

APPENDIX

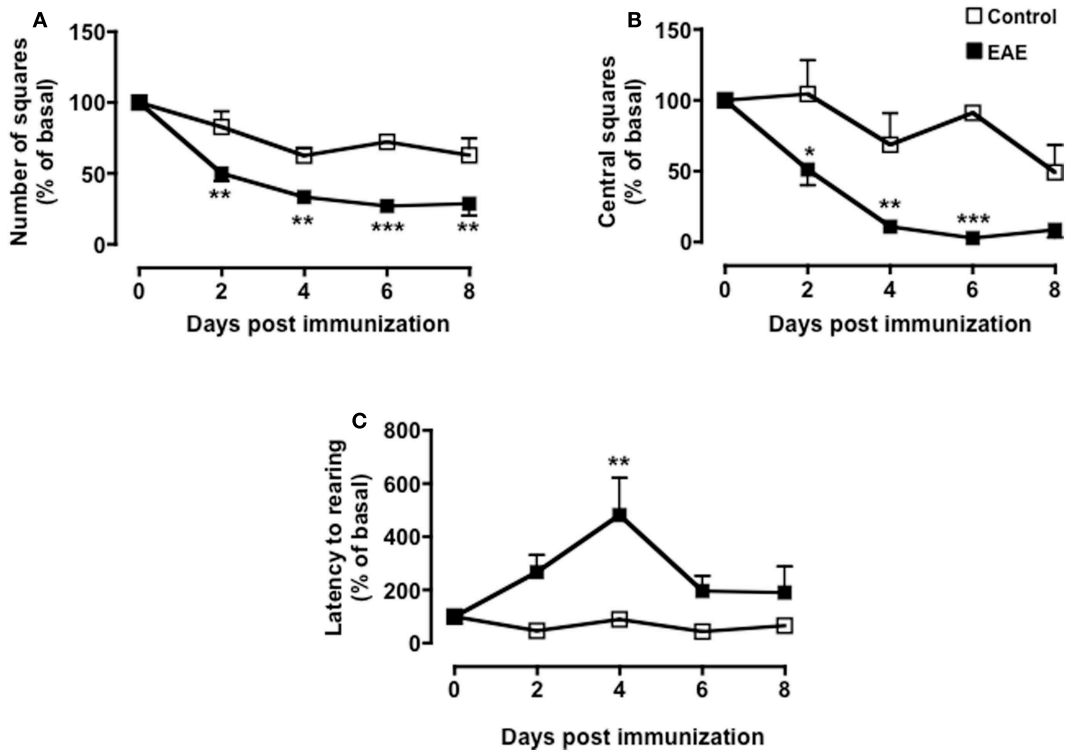

FIGURE A1 | Behavior of MOG_{35-55}-immunized mice in the open field test. The graphs show the percentage of total number of squares crossed **(A)**, number of central squares entries **(B)**, and latency to rearing **(C)** of control or MOG_{35-55}-immunized mice compared to their baseline levels assessed during a 5-min test. Values are expressed as mean percentage ± SEM for six to eight mice and are representative of $N = 5–6$ separate experiments. $*p < 0.05$, $**p < 0.01$, $***p < 0.001$ indicate significant values compared to control mice.

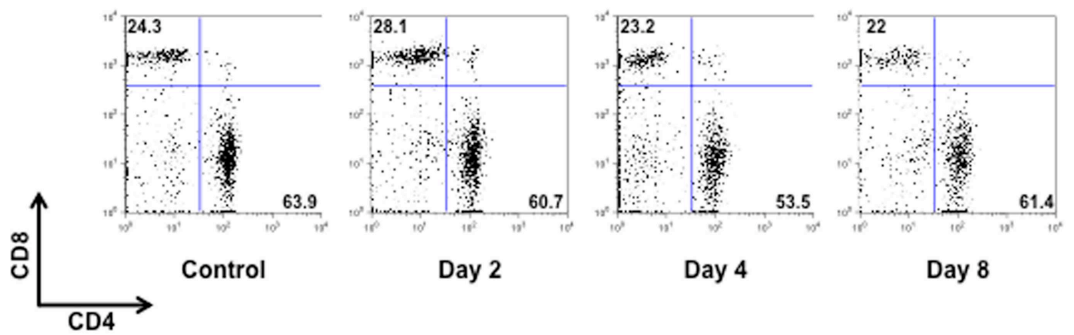

FIGURE A2 | CD4/CD8 T cell profile of MOG_{35-55}-immunized mice. The dot plots show the percentages of $CD4^+$ and $CD8^+$ T cells in the spleen of control or MOG_{35-55}-immunized mice sacrificed at the indicated time points. The results are representative of $n = 6–8$ mice.

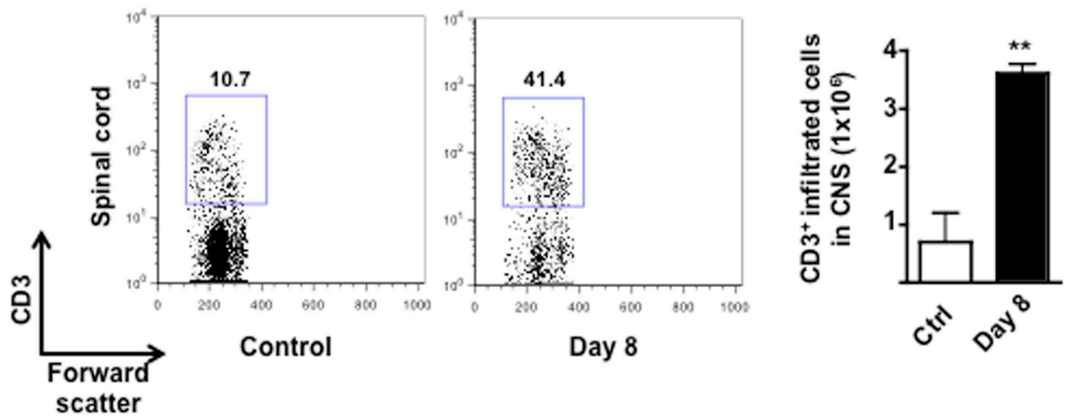

FIGURE A3 | Infiltration of T cells in the CNS of MOG_{35-55}-immunized mice. The dot plots and bar graph show the comparison of the percentages and total number of $CD3^+$ T cells infiltrated in the spinal cord of control or MOG_{33-55}-immunized mice. Values are expressed as mean ± SEM for three mice and are representative of $N = 3$ separate experiments. $^{**}p < 0.01$ indicates significant values compared to control mice.